



AUTHOR:

TITLE:

YEAR:

OpenAIR citation:

This work was submitted to- and approved by Robert Gordon University in partial fulfilment of the following degree:

OpenAIR takedown statement:

Section 6 of the “Repository policy for OpenAIR @ RGU” (available from <http://www.rgu.ac.uk/staff-and-current-students/library/library-policies/repository-policies>) provides guidance on the criteria under which RGU will consider withdrawing material from OpenAIR. If you believe that this item is subject to any of these criteria, or for any other reason should not be held on OpenAIR, then please contact openair-help@rgu.ac.uk with the details of the item and the nature of your complaint.

This is distributed under a CC _____ license.

PROPERTIES OF A HIGH-CURRENT DISCHARGE

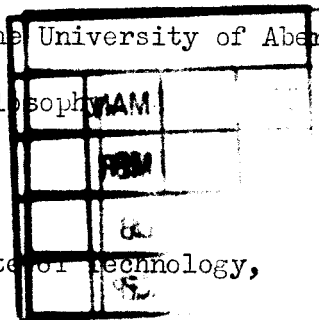
IN ALKALI-METAL-SEEDED RARE GASES

BY

HENRY I. ELLINGTON, B.Sc., A.INST.P.

A thesis submitted to the University of Aberdeen for the
Degree of Doctor of Philosophy

School of Physics,
Robert Gordon's Institute of Technology,
Aberdeen.

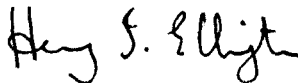


April, 1969.

DECLARATION.

I began my experimental work on gas discharges at A.E.R.E. Harwell, where I joined the Magnetohydrodynamics Section of the Direct Conversion Group in 1963, after graduating from Aberdeen University with a B.Sc. in Natural Philosophy. In 1965, I left Harwell in order to take a teacher training course at Aberdeen College of Education. I resumed my research in 1966, when I took up my present post as a lecturer in physics at Robert Gordon's Institute of Technology, and enrolled as a part-time research student in the Department of Natural Philosophy of Aberdeen University. At Aberdeen, I continued with my experimental work, and also carried out a detailed theoretical analysis of my experimental results; the latter task has occupied most of my time during the last three years.

This thesis is an account of the above work, and is presented in conformity with the regulations for the Degree of Doctor of Philosophy of Aberdeen University. It was written by myself, describes work that was carried out by myself, is entirely original (except where due reference is made), and has not been submitted previously for a higher degree. All quotations have been indicated by quotation marks, and all sources of information by specific references.


Henry I. Ellington.

April, 1969.

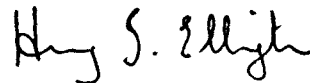
ACKNOWLEDGEMENTS.

First of all, I wish to acknowledge the help, advice and encouragement that I have continually received from my three supervisors, Professor P.D. Dunn of the University of Reading, Professor R.V. Jones of the University of Aberdeen, and Dr. N.H. Langton of Robert Gordon's Institute of Technology.

Secondly, I wish to thank the members of the former Direct Conversion Group of A.E.R.E. Harwell (especially J.C. Ralph, L.G. Sanders and M. Sakuntala) for their many helpful discussions, and to thank D.R. Appleby and H. Jones for their technical assistance.

Thirdly, I wish to thank the Governors of Robert Gordon's Institute of Technology for providing me with the facilities for my research, and for their financial support. I am also extremely grateful for the encouragement that I have received from Dr. G. Bulmer, the Director of the Institute. I wish to thank W. Reeves, A. Middleton, G. Stephen and the late J. Pirie for their technical help, and to thank Miss C. Pirie for typing and duplicating this thesis, and for all the other work that she has done in connection with my research.

Finally, I wish to thank the Faculty of Science of the University of Aberdeen for accepting me as a research student.



Henry I. Ellington.

ABSTRACT.

This thesis is an account of a detailed investigation of the properties of a recently-discovered gas discharge - a discharge that operates at a few volts or tens of volts, and which carries a current of the order of amps through a mixture consisting of a hot, atmospheric-pressure rare gas (the "diluent") to which a small amount of alkali metal vapour has been added as an easily-ionised "seed".

Part I of the thesis is an account of the author's experimental work. It opens with a short description of the different types of conventional gas discharge, and then gives a broad introduction to the author's research program, showing how it arose out of the search for a suitable working fluid for a reactor-powered MHD generator, stating its aims, and giving a review of related work. A detailed description of the apparatus is then given. This is shown to consist basically of two ovens, mounted one above the other, the thermostatically-controlled lower oven containing the seeding trap, and the upper oven containing the thermostatically-controlled high-temperature furnace that heated the electrode system to the required temperature; the diluent gas first flowed through the seeding trap, where it became saturated with the required amount of alkali metal vapour, and then passed slowly through the electrode system before being discharged into the atmosphere. The electrode system consisted of two plane-parallel stainless-steel electrodes, whose separation could be varied up to 30 mm.

The experimental procedure is then described, and it is shown that two basic experiments were carried out. In the first of these, the breakdown voltage of the gas was measured at different electrode spacings, and in the second, plots of electrode voltage against electrode spacing were made at different discharge currents. The latter were always found to be straight lines, the slope of the line giving the value of the electric field in the positive column, and the voltage intercept giving the value of the voltage drop at the cathode (the cathode fall). It is shown that the author's experimental research program consisted basically of carrying out the above measurements at different ambient gas temperatures (range studied - 500 to 950°C) and seed pressures (range studied - 7×10^{-3} torr to 60 torr) in a variety of seed-diluent mixtures, sodium, potassium and caesium being used as seeds, and helium, neon and argon as diluents.

Part I of the thesis concludes by giving the results of the above experiments. It is shown that the establishment of the discharge under study is brought about by the breakdown of the gas, which occurs at a breakdown voltage that depends mainly on the electrode spacing, seed pressure, and choice of diluent gas. The discharge itself is shown to consist of two main regions, namely, a constricted, cylindrical positive column that extends from the anode to within a short distance of the cathode, and a thin, glowing sheath that covers the entire cathode surface; the two regions are separated by a dark space. The positive

column is shown to expand as the current increases, while the value of its electric field is shown to depend mainly on the discharge current, seed pressure, and choice of diluent gas, and hardly at all on the gas temperature or choice of seed metal. The cathode fall is shown to depend mainly on the discharge current, seed pressure, and choice of seed metal. The breakdown of the gas, the positive column of the discharge, and the cathode regions of the discharge are discussed in successive chapters.

Part II of the thesis is an attempt to explain the experimental results, and is subdivided into three parts. Part IIA deals with the breakdown of the gas. It begins with a detailed examination of the breakdown process, and a semi-empirical formula for the breakdown voltage is then derived. The formula is then applied to the experimental breakdown voltage results, and is shown to be capable of giving a fairly satisfactory explanation of most features of these results.

Part IIB deals with the positive column of the discharge. It begins by classifying the column, and then shows that four equations, dealing respectively with the energy balance, electron energy balance, ion balance, and current continuity, are necessary and sufficient to describe the column. These four equations are then discussed in some detail, a separate chapter being devoted to the development of each. The resulting theory is then applied to the author's experimental results. It is shown that the theory is capable of giving a satisfactory explanation of the basic properties of the column and of their dependence on the

discharge current, and that the theory is also capable of explaining the observed effects of changing the nature and pressure of the seed metal, and the effects of changing the diluent gas. Part IIB concludes with a theoretical discussion of the effect on the column properties of varying the diluent pressure.

Part IIC deals with the cathode regions of the discharge under study. It begins by classifying the cathode mechanism and setting up a rough model of the cathode regions of the discharge, and follows with a detailed discussion of the emission process, and of the processes that occur in the cathode fall space.

Part IIC ends by using the theory that has been developed to explain several features of the experimental cathode fall results.

TABLE OF CONTENTS.

	Page
<u>INTRODUCTION</u> -----	15
 <u>PART I. THE EXPERIMENTAL WORK.</u>	
<u>Chapter 1. Electric discharges in gases.</u>	
1.1 The different types of gas discharge -----	19
1.2 Dark discharges -----	21
1.3 The glow discharge -----	22
1.4 The arc discharge -----	26
 <u>Chapter 2. The author's research program, and a review of related work.</u>	
2.1 The early history of MHD -----	30
2.2 Work on MHD in Britain -----	32
2.3 The search for a low-temperature gaseous conductor, and the work of Ralph -----	35
2.4 The research program of the author -----	39
2.5 A review of related work -----	42
 <u>Chapter 3. The apparatus used.</u>	
3.1 General description of the apparatus -----	51
3.2 The lower oven and seeding trap -----	56
3.3 The upper oven and inner furnace -----	64
3.4 The electrode system and its associated circuitry -	68
3.5 The materials used in the experiments -----	76

	Page
<u>Chapter 4. The experimental procedure.</u>	
4.1 The preparation and warming up of the apparatus ---	77
4.2 The experimental measurements-----	80
4.3 The shutting down of the apparatus -----	87
4.4 High speed photographic work -----	88
4.5 Spectroscopic work -----	89
<u>Chapter 5. The breakdown of the gas.</u>	
5.1 The events leading up to breakdown -----	91
5.2 The dependence of the breakdown voltage on the electrode spacing -----	93
5.3 The dependence of the breakdown voltage on the seed pressure -----	93
5.4 The dependence of the breakdown voltage on the ambient temperature -----	98
5.5 The dependence of the breakdown voltage on the choice of seed metal -----	101
5.6 The dependence of the breakdown voltage on the choice of diluent gas -----	101
5.7 The effect of added molecular impurities on the breakdown voltage -----	101
<u>Chapter 6. The positive column of the discharge</u>	
6.1 The dependence of the column properties on the discharge current -----	104
6.2 The dependence of the column properties on the seed pressure -----	112
6.3 The dependence of the column properties on the ambient gas temperature -----	116
6.4 The effect on the column properties of changing the diluent gas -----	119

	Page
6.5 The effect on the column properties of changing the seed metal -----	121
6.6 The effect on the column properties of added molecular impurities -----	122
 <u>Chapter 7. The cathode regions of the discharge.</u>	
7.1 The two modes of the cathode mechanism -----	126
7.2 The transition between the modes and the stability of the diffuse mode -----	131
7.3 The value of the cathode fall of the diffuse mode; its dependence on the discharge current -----	136
7.4 The dependence of the cathode fall on the seed pressure -----	138
7.5 The dependence of the cathode fall on the ambient temperature -----	142
7.6 The dependence of the cathode fall on the choice of diluent -----	147
7.7 The dependence of the cathode fall on the choice of seed -----	148
7.8 The effect of added molecular impurities on the cathode fall -----	149

PART II. DISCUSSION OF THE RESULTS.

IIA. THE BREAKDOWN OF THE GAS.

Chapter 8. Analysis of the breakdown process.

8.1 The low-current equilibrium discharge -----	153
8.2 The approach to breakdown -----	155
8.3 The classical derivation of the First Townsend Coefficient -----	159
8.4 Von Engel's derivation of the First Townsend Coefficient -----	161
8.5 Calculation of the breakdown voltage -----	162

	Page
8.6 The limitations of the theory -----	163
8.7 Comparison of the breakdown process with the conventional spark breakdown of a gas -----	166

Chapter 9. Discussion of the breakdown voltage
results.

9.1 Introduction -----	171
9.2 Dependence on electrode spacing -----	172
9.3 Dependence on seed pressure -----	174
9.4 Dependence on temperature -----	180
9.5 The effect of changing the diluent gas -----	184
9.6 The effect of changing the seed -----	185
9.7 The effect of added molecular impurities -----	186

IIB. THE POSITIVE COLUMN OF THE DISCHARGE.

Chapter 10. Preliminary discussion of the positive
column properties.

10.1 Classification of the column -----	189
10.2 The Tonks-Langmuir theory of the low-pressure arc column -----	194
10.3 Extension of the Tonks-Langmuir theory to the high-pressure column -----	196
10.4 Modification of the theory to describe the column under study -----	199

Chapter 11. The energy balance equation.

11.1 General discussion of the energy balance process --	202
11.2 The radiation losses from the column -----	205
11.3 The external energy balance equation -----	208
11.4 The internal energy balance equation -----	213

	Page
<u>Chapter 12. The electron energy balance equation.</u>	
12.1 General discussion of the electron energy balance process -----	215
12.2 The value of the electron temperature -----	217
12.3 The conditions for the electron energy distribution to be Maxwellian -----	222
12.4 The value of the ion temperature in the plasma ---	226
<u>Chapter 13. The ion balance equation.</u>	
13.1 The degree of ionisation in equilibrium plasmas - the Saha equation -----	229
13.2 The degree of ionisation of the seed in non- equilibrium plasmas -----	232
13.3 Evidence for the validity of the ion balance equation in the column under study -----	235
13.4 Justification for ignoring radial ion losses in the column under study -----	237
<u>Chapter 14. The arc current equation.</u>	
14.1 The conduction of electricity through a gas -----	243
14.2 The value of the electronic mobility -----	246
<u>Chapter 15. The basic properties of the column.</u>	
15.1 The constriction of the column - magnetic constriction -----	251
15.2 The constriction of the column - thermal constriction -----	254
15.3 The boundary of the column -----	258
15.4 Analysis of the current-dependent experimental results: preliminary considerations -----	260
15.5 Application of the "channel model" to the column -	264

	Page
15.6 The temperature profile of the column -----	269
15.7 The electron temperature profile of the column ---	281
15.8 The value of the degree of elevation of the electron temperature -----	287

Chapter 16. The dependence of the column properties
on the nature and pressure of the seed

16.1 The effect on the column properties of changing the seed -----	292
16.2 The optimum seeding fraction in equilibrium plasmas -----	298
16.3 The optimum seeding fraction in nonequilibrium plasmas -----	301
16.4 The effects on the column properties of varying the seed pressure -----	305

Chapter 17. The dependence of the column properties
on the nature and pressure of the
diluent gas.

17.1 The effect of the choice of diluent on the column properties: preliminary discussion -----	313
17.2 The effect on the electron energy balance process of changing the diluent -----	315
17.3 The dependence of $\frac{X_{He}}{X_{Ar}}$ on the seed pressure -----	319
17.4 The effect on the column properties of changing the diluent pressure -----	323

IIC. THE CATHODE REGIONS OF THE DISCHARGE

Chapter 18. Analysis of the diffuse cathode mechanism.

18.1 Classification of the diffuse cathode mechanism --	335
18.2 Development of a theory to describe the diffuse mode of the discharge -----	338

	Page
18.3 The emission process of the diffuse mode -----	343
18.4 The theory of space-charge-restricted current flow -----	348
18.5 Application of the theory to the cathode fall region of the diffuse mode -----	355
18.6 A model of the cathode fall region of the diffuse mode -----	361
18.7 Discussion of the experimental cathode fall results -----	365
CONCLUSION -----	371
REFERENCES -----	377

In order to facilitate cross-referencing within the thesis, all figures, photographs, tables and equations have been assigned a decimal number, the figures before the point indicating the chapter, and those after the point showing the number of the section, figure, etc., within the chapter (e.g. equation 11.14).

All specific references are indicated in the text by giving the surname(s) of the author(s), followed by the date of publication (e.g. Smith 1940). The references are listed alphabetically at the end of the thesis under the name of the first author, and take the following form: name(s) of author(s); date of publication; name of journal or book; publisher (if a book); volume; first and last pages.

INTRODUCTION.

This thesis is an account of a detailed investigation of the properties of a type of gas discharge that was first reported by Ralph in 1963. The discharge is produced when a sufficiently high voltage is applied across a hot, atmospheric-pressure rare gas to which a small amount of alkali metal vapour has been added as an easily-ionised "seed", and has several interesting and unusual properties. In addition to its intrinsic scientific interest, it has potential applications in the field of closed-cycle magnetohydrodynamic power generation, and for this reason, the electrical properties of the type of plasma that exists in its positive column have been extensively studied in recent years.

The thesis is divided into two parts, Part I being a description of the experimental work, and Part II, which is considerably longer than Part I, being an analysis of the experimental results. Part I opens with a brief description of the different types of conventional gas discharge (Chapter 1), and then gives a broad introduction to the author's research program, including a review of related work (Chapter 2). Chapter 3 then gives a detailed description of the apparatus, while Chapter 4 describes the procedure that was employed in the different experiments that were carried out. The next three chapters give the results of these experiments, Chapter 5 dealing with the breakdown of the gas that leads to the establishment of the discharge under study, Chapter 6 with the properties of the

the positive column of the discharge, and Chapter 7 with the cathode regions of the discharge.

Part II of the thesis is itself subdivided into three sections; Part IIA (Chapters 8 and 9) deals with the breakdown of the gas, Part IIB (Chapters 10 - 17) with the positive column of the discharge, and Part IIC (Chapter 18) with the cathode regions of the discharge. Each of the subsections of Part II is preceded by a short summary of its contents.

Much of the work that is described in this thesis has already been published, and a list of the relevant publications is given below. The list includes four U.K.A.E.A. research memoranda, (Ellington 1964, 1965 A,B,C), which deal with the part of the author's work that was carried out at Harwell, a conference paper (Ellington and Ralph 1966), which summarises the Harwell work, and five journal papers (Ellington 1967, 1968 A,B,C, 1969), which deal almost entirely with the part of the work that was carried out in Aberdeen, and consist mainly of theoretical discussions of the author's experimental results.

LIST OF AUTHOR'S PUBLICATIONS

1. "Electrical conductivity of inert gas - alkali metal plasmas with elevated electron temperatures", by H.I. Ellington; U.K.A.E.A. Res. Grp. Memo. no. AERE - M1474 (1964).
2. "Low-voltage diffuse discharge in atmospheric-pressure argon with small additions of potassium", by H.I. Ellington; U.K.A.E.A. Res. Grp. Memo. no. AERE - M1545 (1965A).
3. "Low-voltage diffuse discharge in atmospheric-pressure helium with small additions of potassium", by H.I. Ellington; U.K.A.E.A. Res. Grp. Memo. no. AERE - M1597 (1965B).

4. "Low-voltage diffuse discharge in atmospheric pressure helium and argon, seeded with small amounts of caesium, potassium and sodium", by H.I. Ellington; U.K.A.E.A. Res. Grp. Memo. no. AERE - M1616 (1965C).
5. "Atmospheric pressure discharges in inert gases seeded with alkali metal vapour", by H.I. Ellington and J.C. Ralph; "Electricity from MHD", vol. 2, (Vienna: I.A.E.A.) pp. 17-27 (1966).
6. "The constricted positive column of a nonequilibrium electric discharge in alkali-metal-seeded rare gases", by H.I. Ellington; Brit. J. Appl. Phys., vol. 18, pp. 931-37 (1967).
7. "Breakdown voltage measurements in alkali-metal-seeded rare gases at elevated temperatures and atmospheric pressure", by H.I. Ellington; Brit. J. Appl. Phys. (J. Phys. D), ser. 2, vol. 1, pp. 49-53 (1968A).
8. "The effect of the bulk gas on the electrical conductivity of potassium-seeded nonequilibrium plasmas", by H.I. Ellington; Brit. J. Appl. Phys. (J. Phys. D), ser. 2, vol. 1, pp. 189-192 (1968B).
9. "The value of the breakdown voltage in hot alkali-metal-seeded rare gases", by H.I. Ellington; Brit. J. Appl. Phys. (J. Phys. D), ser. 2, vol. 1, pp. 1082-84 (1968C).
10. "Development of a theory to describe constricted positive columns in alkali-metal-seeded rare gases", by H.I. Ellington; Brit. J. Appl. Phys. (J. Phys. D), ser. 2, vol. 2, pp. 65-69 (1969).

PART I

THE EXPERIMENTAL WORK

CHAPTER 1

ELECTRIC DISCHARGES IN GASES.

1.1 THE DIFFERENT TYPES OF GAS DISCHARGE.

Any flow of electric charge through a gaseous medium is termed a gas discharge. Gases are normally excellent insulators, but if some of the atoms can be ionised, the gas becomes capable of supporting a current. There are three main classes of steady-state gas discharge. These are

1. Townsend or dark discharges, which carry very low currents (generally from 10^{-12} to 10^{-6} amps) and are usually not self-sustaining,
2. glow discharges, which generally carry currents in the range from 10^{-6} to 1 amp, and are self-sustaining,
3. arc discharges, which generally carry currents of over 10^{-1} amps, and are also self-sustaining.

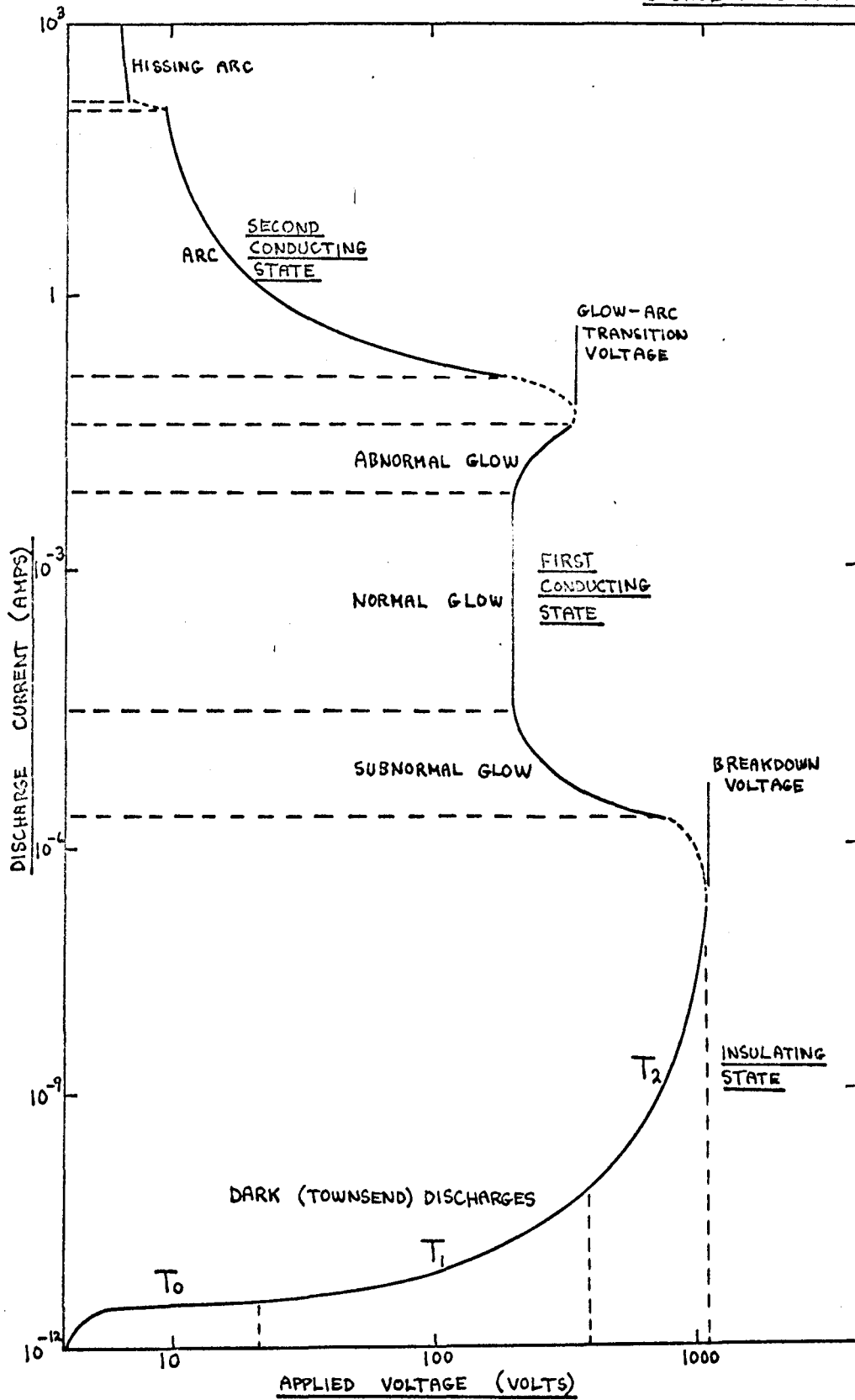
If the voltage between two electrodes immersed in a gas is steadily increased, all three types of discharge will normally be observed. Figure 1.1 gives an idealised current /voltage characteristic for a typical gas, and illustrates this progressive breakdown process.

The dark discharge is seen to give way to a glow discharge at a certain critical applied voltage termed the breakdown voltage, and the glow makes the transition to an arc discharge at a second breakdown voltage. Transitions between the three types are generally reversible. Let us examine the three types of gas discharge in more detail.

FIGURE 1.1

IDEALISED CURRENT/VOLTAGE CHARACTERISTIC FOR A GAS

SOURCE : COBINE (1958)



1.2 DARK DISCHARGES.

Dark discharges, sometimes called Townsend discharges after J. S. Townsend, who carried out early and extensive investigations in the field, are usually not self-sustaining, and the gas is still, generally speaking, in the insulating state. The dark discharges (so named because they give out no apparent light) owe their existence to some external source of ionisation of the gas, and if this source is removed, the discharge can no longer exist. Normally, this primary ionisation is caused by subjecting the gas to some form of ionising radiation, or by producing electrons from a photo-cathode, but, as we shall see later, intrinsic ionisation of the gas can be produced by raising its temperature to a sufficiently high value. The dark discharges can be subdivided into three main types, shown as T_0 , T_1 and T_2 in figure 1.1. If the applied voltage is sufficiently low, only the ions produced by the external source are available to carry current, and once these have all been brought into use, the current is saturated, and does not increase with a further rise in the applied voltage. This is region T_0 in figure 1.1. If the applied voltage is increased steadily, we eventually enter the first Townsend discharge, shown as T_1 in figure 1.1, and the current begins to rise once more. Here, the electrons produced by the external source are accelerated in the now-high electric field, so that they produce secondary electrons by means of electron-atom collisions. The original current is multiplied by a factor that depends on the applied voltage, the properties of the gas, and the geometry of the system.

The number of ionising collisions undergone by an electron per cm. of path length is known as the first Townsend coefficient. The discharge current is proportional to the strength of the original ionising source, and if the latter is removed, the discharge collapses. If the applied voltage is further increased, the current begins to rise even more rapidly, and the second Townsend discharge is encountered - region T_2 of figure 1.1. In this region, the electric field is high enough to produce ion pairs by processes other than direct electron-atom collisions. These secondary processes may be ionisation by positive ions, or production of electron emission by the impact of photons or positive ions on the cathode surface. Whatever the actual process involved, it is represented in the mathematical theory of the discharge by the second Townsend coefficient, which is defined as the number of ion pairs produced by a positive ion per cm. of its path. The rate of ion-pair multiplication eventually becomes so great that the slope of the current/voltage plot becomes infinite, whereupon the gas breaks down, and enters the region of self-sustained discharges.

1.3 THE GLOW DISCHARGE.

The glow discharge, or first conducting state, is encountered when the voltage across a gas is increased beyond a critical value, and breakdown occurs. Figure 1.1 shows the three main subdivisions of the glow region. These are, in order of increasing current, the subnormal glow, where the electrode voltage falls as

the current rises, the normal glow, where the voltage is independent of the current over several orders of magnitude of current, and finally, the abnormal glow, where the voltage rises as the current increases. If the current is raised to a sufficiently high level, the gas undergoes a further breakdown, and the discharge changes to an arc.

The glow discharge is normally encountered in low-pressure gases or vapours, and is usefully employed in fluorescent tubes and neon signs. There are a large number of types of glow, their nature depending on the gas, the pressure, and the geometry of the system. The structure of a typical glow is somewhat complicated, as is shown by figure 1.2, which illustrates the various regions that extend from the cathode to the anode. The structure of the discharge can be divided into two main regions, namely the cathode regions, comprising the various glows and dark spaces that extend from in front of the cathode surface to the boundary of the positive column, and the positive column itself, which makes up the bulk of most glow discharges. Figure 1.3 shows how the electric potential varies from the cathode to the anode. It is seen that there is a large voltage drop across the cathode regions (generally between 100 and 400 volts), and a much more gradual voltage drop along the length of the positive column (generally between 1 and 500 volts per cm. per torr gas pressure). As the gas pressure is reduced, the cathode regions are found to expand at the expense of the positive column, and if the pressure

FIGURE 1.2 THE STRUCTURE OF THE GLOW DISCHARGE

SOURCE : COBINE (1958)

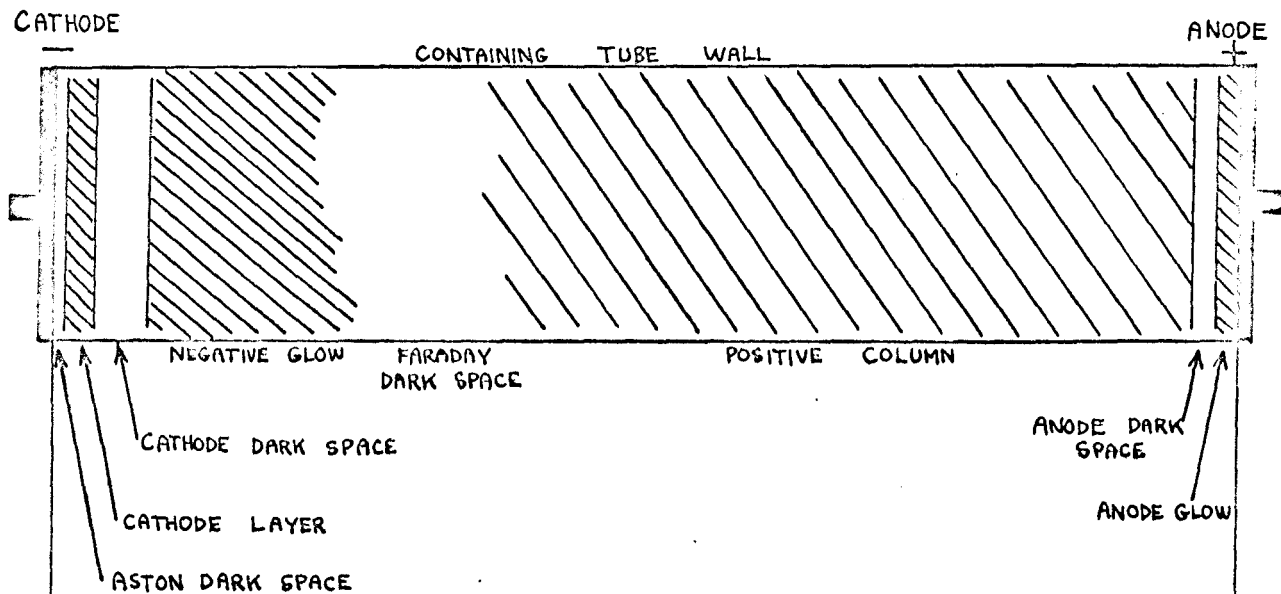
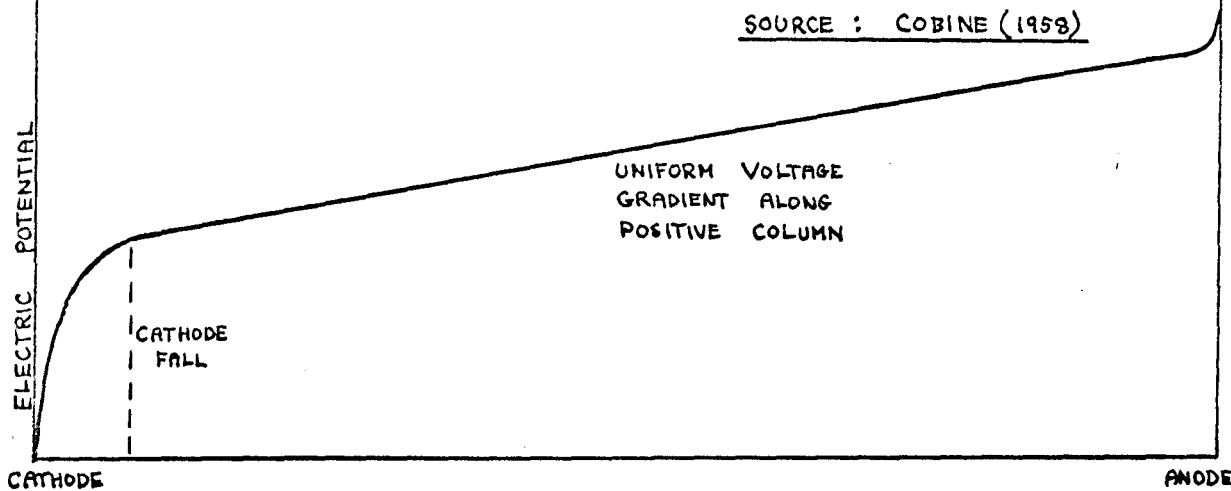


FIGURE 1.3 THE VOLTAGE PROFILE OF THE GLOW DISCHARGE

SOURCE : COBINE (1958)



is increased, they contract towards the cathode surface until eventually only the negative glow and Faraday dark space are distinguishable. The positive column fills the remainder of the available space, extending to the walls of the containing tube unless these are very remote or the gas pressure is high. As the gas pressure is increased, the positive column constricts laterally until it is apparently no different from that of an arc discharge carrying a similar current. If the inter-electrode distance is altered, the positive column adjusts its length to accommodate the change, whereas the cathode regions do not alter in extent. All these facts indicate that the phenomena near the cathode are essential to the discharge, whereas the positive column merely serves as a conducting path for the current.

The mechanisms that support the glow appear to be roughly as follows. In the neighbourhood of the cathode, electrons are accelerated in the high electric field and produce ion pairs by colliding with the atoms. The electrons pass into the positive column, and the ions fall onto the cathode surface, where they produce emission of electrons. To obtain a steady-state discharge, each electron produced from the cathode must undergo ionising collisions sufficient to bring about the emission of one more electron from the cathode. The positive column is an example of a plasma, a partly-ionised gas where the electron number density equals the ion number density, so that the net space charge is zero. In the positive column of a low-pressure glow, the electrons have a considerably higher mean energy than the gas atoms, so that the

electron temperature is higher than the gas temperature (which is very rarely higher than 100°C). An elevated electron temperature is vital for the maintenance of a glow positive column, since the ionisation of the gas in the column is brought about by collisions between high-energy electrons and gas atoms. The positive ions and electrons move in opposite directions through the plasma under the influence of the column field, but nearly all the discharge current is carried by the electrons, since these have a much greater mobility than the positive ions.

1.4 THE ARC DISCHARGE.

The arc discharge, or second conducting state, is the third main class of gas discharge. The differences between a glow and an arc lie mainly in their respective cathode phenomena. The cathode fall region of a glow has a high voltage drop - generally several hundred volts - and has a low current density, whereas that of an arc "has a voltage drop of the order of the minimum ionising potential of the gas or vapour involved" (Compton 1927), and a very high current density. Another important distinction between the two is that thermal effects do not play an important part in the cathode mechanism of the glow discharge (which operates at room temperature or slightly above), whereas the cathode mechanism of an arc relies entirely on thermal effects, and operates at a very high temperature. Largely because of this, the spectrum of the cathode fall region of an arc contains the characteristic lines of the vapour of the cathode material, whereas

that of a glow contains only the characteristic lines of the gas. The positive column of an arc can be very similar to that of a glow under similar conditions of current and pressure, but the arc column is generally distinguished by being constricted near the two electrodes.

A typical arc voltage/current characteristic is shown in figure 1.1. The arc voltage falls steadily as the current rises, and at very high currents, the arc may give way to a hissing arc, with a sudden drop in voltage. For a given current, the voltage rises with increasing electrode separation, and above very close spacings, does so linearly, indicating a uniform voltage drop along the positive column.

The structure of a typical arc is simpler than that of a glow, and is shown in figure 1.4. It consists essentially of a positive column connecting the cathode arc spot to the anode arc spot. The core of the arc is intensely luminous, and is surrounded by a cooler region called the aureole. A typical voltage profile is shown in figure 1.5. There is a sharp drop at the cathode (generally under 20 volts), a uniform drop along the positive column (generally of the order of tens or hundreds of volts/cm), and another sudden drop at the anode, usually smaller than that at the cathode.

The arc mechanism is also simpler than that of a glow. Its temperature is much higher, and both the electrode arc spots are generally at the boiling point of the material used. At the cathode, heavy bombardment of the surface by positive ions keeps

FIGURE 1.4 THE STRUCTURE OF THE ARC DISCHARGE

SOURCE : COBINE (1958)

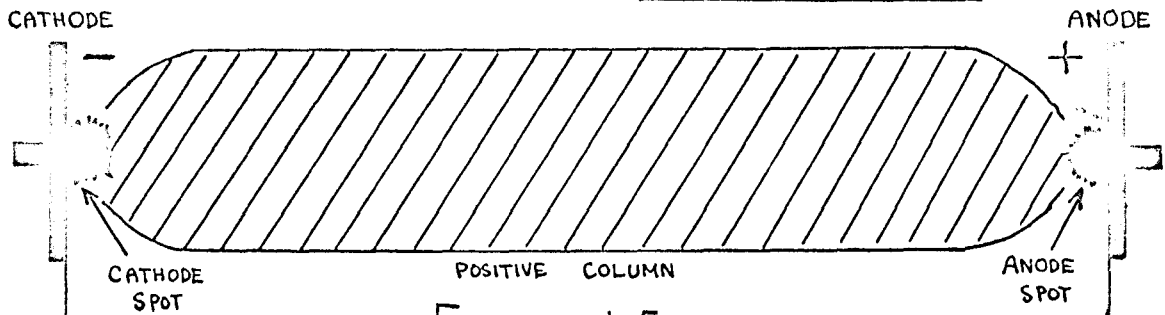


FIGURE 1.5

THE VOLTAGE PROFILE OF THE ARC DISCHARGE

SOURCE : COBINE (1958)

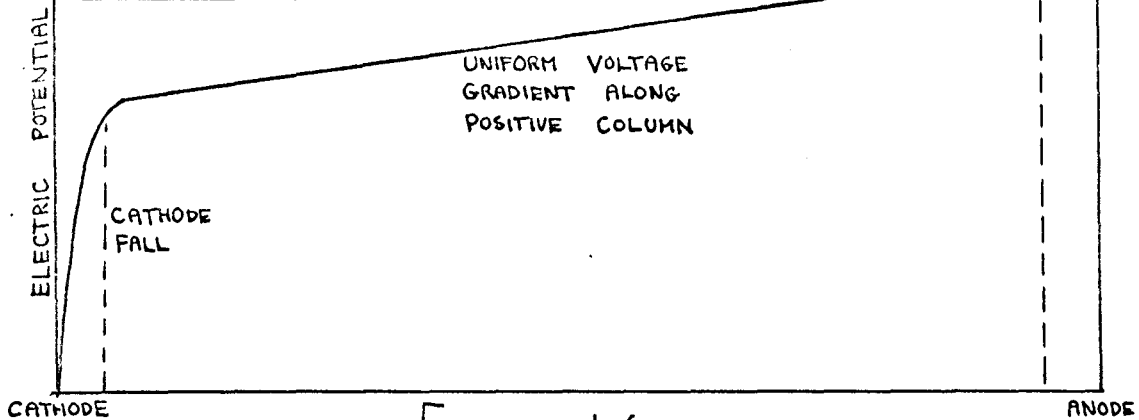
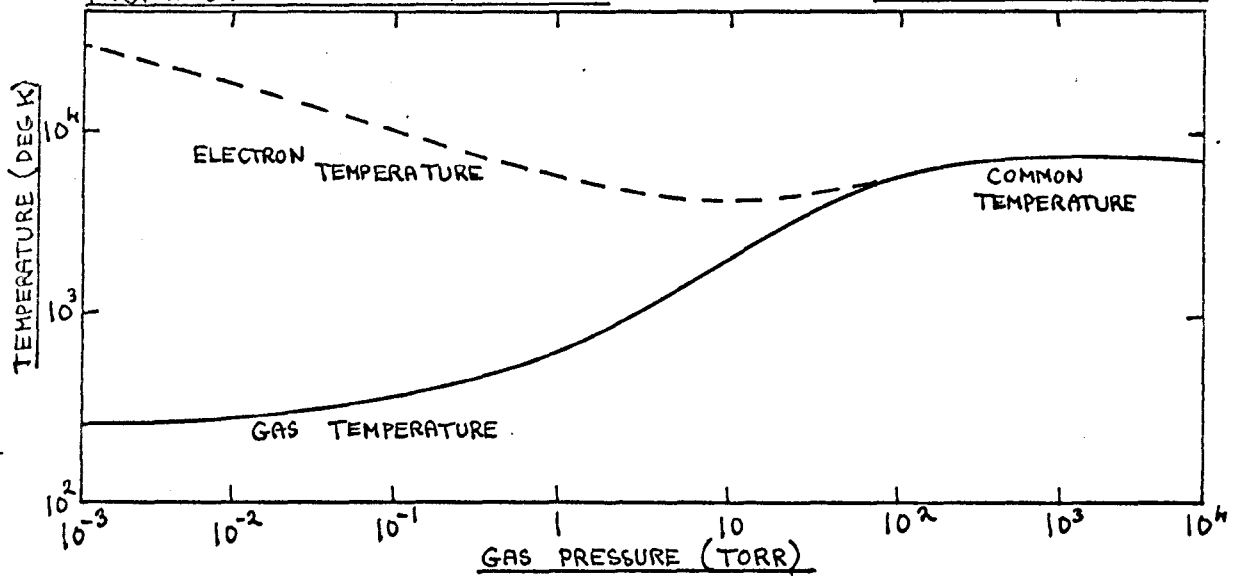


FIGURE 1.6

PLOTS OF ELECTRON TEMPERATURE AND GAS TEMPERATURE AGAINST GAS PRESSURE

SOURCE : COBINE (1958)



the temperature high, and copious thermionic emission of electrons occurs. As the current density at the spot is extremely high, the power is concentrated in a small region. This thermionic spot tends to move quite rapidly over the cathode surface. If the cathode is externally heated, the arc is called a hot cathode arc, and the cathode fall is generally less than that of a conventional, unheated arc. As in the glow, the arc positive column generally constitutes the largest part of the discharge, and merely serves as a conducting path for the flow of current between the electrodes, since it is not essential for the existence of the discharge. At low pressures, the arc positive column is very similar to that of a glow, the gas being fairly cool, and the electron temperature high, but as the pressure increases, the gas temperature rises and the electron temperature falls, until at high pressures the two are equal. This is illustrated in figure 1.6. High-pressure arc positive columns are generally constricted, and operate at extremely high temperatures - often of the order of 6000°K or more. These high temperatures are necessary to provide the high degree of ionisation that exists in such columns, since the ionisation is not produced by high-energy electrons, but by collisions between the gas atoms themselves. As in the case of the glow positive column, the ion number density equals the electron number density, but nearly all of the discharge current is carried by the electrons because of their greater mobility.

CHAPTER 2.

THE AUTHOR'S RESEARCH PROGRAM, AND A REVIEW OF RELATED WORK.

2.1 THE EARLY HISTORY OF MHD.

As the author's work on seeded rare gases was originally undertaken as part of the British MHD research program, we will begin this chapter by giving a brief discussion of magneto-hydrodynamic power generation. We will describe the principle on which it is based, trace its early development, and give reasons for the vast interest that has been shown in the subject during the last decade. We will then show how the author's research program arose out of the need to find a gaseous mixture suitable for use as the working fluid in a reactor-driven MHD generator.

The principle of MHD power generation is a simple one, being a direct application of Faraday's discovery that an e.m.f. is induced within a conducting body that moves through a magnetic field. In a conventional electricity generator, the conductor is a metal, but in an MHD generator, it is a partly-ionised gas: this is passed at high velocity through a duct situated in a powerful transverse magnetic field, and the resulting current, which is induced at right angles to both the direction of flow and the magnetic field, is drawn off by means of electrodes situated along the sides of the duct. A comprehensive account of the basic physics of the MHD duct and of the different

possible duct geometries has been given by several authors, including Rosa (1961) and Ralph (1964).

Although the principle of using an ionised gas as the conductor in a generator has been known for over a century, it was not until the late 1950's that the practical application of the principle became feasible. Many experiments were carried out before this, culminating in the work of Karlowitz in the late 1930's (Karlowitz et. al. 1940), but these all failed to produce significant power because of the inadequate electrical conductivity of the gases employed (Coombe 1964). A conductivity of at least 10 mhos/metre was required, and while it was known that pure gases could be made to exhibit this order of conductivity by heating them to temperatures of the order of 6000°K, such temperatures were (and, indeed, still are) well beyond the range that could be withstood by any known duct or electrode material. After the failure of Karlowitz's experiment, no serious work on MHD was carried out for over 20 years, initially because of the intervention of the war, and latterly because of the domination of post-war work on electricity generation by the development of nuclear power, and, in particular, by the seemingly imminent prospect of cheap thermonuclear power (Coombe 1964). When it eventually became evident that several decades of fundamental research into the physics of thermonuclear plasmas were likely to be required before a fusion generator became a practical possibility, however, the search for alternative methods of generating electricity was resumed. **MHD** now appeared to be one

of the most promising of these methods, mainly due to the fact that the American space program had led to the development of suitable high-temperature duct materials, and had also made available high-velocity, high-temperature gas streams (Coombe 1964). These technological advances, combined with the development of the concept of increasing the electrical conductivity of a gas by seeding it with a small amount of easily-ionised material, meant that the highest temperatures that could be withstood by potential duct materials now overlapped with the lowest temperatures that could be used to obtain an adequate electrical conductivity in the gas (2000 - 3000°K), so that MHD had now become a practical possibility. This fact was first realised by Sporn and Kantrowitz (1959), whose design study for a 500 MW power station aroused world-wide interest in MHD, and marked the start of the vast theoretical and experimental effort that was subsequently devoted to the subject during the early 1960's, mainly in America, Britain, France and Russia. This work was reviewed by Thring in 1965.

2.2 WORK ON MHD IN BRITAIN.

In Britain, the main motivation for the development of MHD has come from the fact that the demand for electricity is doubling every decade or so, a rate of increase that led Herbert to predict in 1962 that over 50% of Britain's fuel requirements would have to be imported by 1980. The overall efficiency of the conventional boiler-turboalternator method of generating power has risen by an average of 0.5% per annum during the last 20 years, mainly

because of the steady increase in the Carnot efficiency of the steam cycle that has been made possible by raising the inlet temperature of the system (Dunn et. al. 1962, Dunn 1964), but such a rate of increase does not even begin to cope with the rising demand for electricity in this country. The situation is made worse by the fact that there is known to be a practical limit to the overall efficiency that is likely to be attained by the turbo-alternator system - thought to be of the order of 40 - 45% (Dunn et. al. 1962). One method that has been suggested for surpassing this limiting efficiency is the use of a thermodynamic topping device (Dunn et. al. 1962). This would be used in conjunction with a conventional turboalternator system, and would operate at a much higher temperature than the latter, passing on its exhaust gases to the boiler of the turboalternator. If the efficiency of the conventional plant is E_1 and that of the topping device E_2 then it can be shown that the overall station efficiency would be $E_1 + (1 - E_1)E_2$ (Dunn 1964). With the maximum possible E_1 as 0.4, the presence of the topper would add $0.6 E_2$ to the overall station efficiency, so that topper efficiencies of the order of 10-30% are of considerable interest. Because of their high operational temperature, it is hoped to use MHD generators as the topping devices in such systems (Dunn et. al. 1962, Dunn 1964, Coombe 1964). In particular, it is hoped to use MHD generators in conjunction with the new generation of high-temperature advance gas reactors that are being developed by the United Kingdom Atomic Energy Authority for the Central Electricity

Generating Board. Such reactors, driving conventional power stations, and using MHD generators as toppers, appear to offer a very cheap and efficient source of electricity, with overall station efficiencies of the order of 60% being a distinct possibility (Dunn et. al. 1962, Dunn 1964).

After the appearance of Sporn and Kantrowitz's paper had shown that MHD was a practical possibility, several MHD research teams were set up in Britain in the early 1960's (Thring 1965). The main effort was concentrated at three centres, the first being at C.E.R.L. Leatherhead, the main research establishment of the Central Electricity Generating Board, where the prospects of using an open-cycle, combustion-product generator as the topper for a fossil-fuelled station was explored by a team led by J. K. Wright (Thring 1965). The second was at Newcastle, where the International Research and Development Company set up a research team led by B. C. Lindley to investigate the possibility of constructing a closed-cycle generator using caesium-seeded helium as the working fluid (Thring 1965). The third was at A.E.R.E., Harwell, where the Direct Conversion group (led by P. D. Dunn, one of the men responsible for arousing widespread interest in MHD in this country) established a section to investigate the possibility of building a reactor-powered generator using an alkali-metal-seeded rare gas as the working fluid (Thring 1965, Ralph and Bainton 1966). This last group was led by J. C. Ralph, whose work on seeded rare gases will now be described in detail, as it represented the starting point of the author's research program.

2.3 THE SEARCH FOR A LOW-TEMPERATURE GASEOUS CONDUCTOR, AND THE WORK OF RALPH.

In order to make MHD practicable at the temperatures that appeared likely to be attained by nuclear reactors in the foreseeable future, Ralph and the other workers investigating the possibility of building a reactor-powered MHD generator had to find a gas with an electrical conductivity of at least 10 mhos/metre at a pressure of one or more atmospheres and a temperature of the order of 1000 - 1500°K. When the search for such a gas was started in the early 1960's, it was a well-established fact that conductivities of this order could be produced by seeding a high-pressure gas with a percent-or-so of alkali metal vapour and heating it to a temperature high enough to produce roughly 1% ionisation of the seed (Rosa 1961), but the temperature that was required to produce such a degree of ionisation was well over 2000°K; at 1500°K, the degree of seed ionisation that could be produced by purely thermal ionisation processes could be shown to be several orders of magnitude too low to be of any practical use. Despite this fact, Ralph and several other workers set up experimental facilities to measure the electrical conductivity of atmospheric-pressure alkali-metal-seeded rare gases in the temperature range 1500 - 2000°C, as such mixtures appeared to be the most promising from an MHD point of view. These experiments all produced the totally unexpected result that such mixtures broke down electrically when very moderate electric fields were applied across them, and then exhibited electrical conductivities

that were several orders of magnitude greater than the expected values (Westendorp et. al. 1961, Ralph 1962, 1963, Kerrebrock 1962, Robben 1962, Ben Daniel and Bishop 1963). It was realised that the mechanism responsible for this anomalously - high conductivity was the occurrence of field-induced electron heating, resulting in a plasma in which the electron temperature was higher than the gas temperature and in which the seed atoms were ionised by the high-energy electrons. A theoretical description of the mechanism was given by Kerrebrock (1962), and the significance of the discovery was discussed by Hurwitz et. al. (1962) and by Ben Daniel and Tamor (1962), who showed that it was theoretically possible to produce nonequilibrium ionisation in an MHD duct by means of the induced electric field that is produced by the interaction of the gas with the magnetic field. This represented a possible method of producing a working fluid for a reactor-driven generator, a method that was subsequently investigated by a large number of research groups (see Thring 1965).

The process by which nonequilibrium ionisation can be produced in a seeded rare gas will be discussed in detail in Chapters 12 and 13, but a short explanation of the phenomenon will now be given. When an electric field is applied across a gas, any free electrons present in the gas acquire energy from the field, and pass this energy on to the gas molecules during the collisions that occur between the electrons and the molecules. Provided that the value of the electronic mean free path in the gas is high, and the electron number density is high enough for the

electrons to interact among themselves more strongly than with the gas molecules, the free electrons are capable of adopting a separate Maxwellian energy distribution that corresponds to a higher temperature than that of the gas molecules. Such conditions, which prevail in the positive columns of low-pressure glow and arc discharges, and which bring about the ionisation of the gas that is necessary for the maintenance of these columns, can only be produced in molecular gases if the pressure is very low; the ability of such gases to support nonequilibrium conditions decreases rapidly as the pressure rises, because of the fall in the electronic mean free path (see figure 1.6), and by the time atmospheric pressure is reached, no significant elevation of the electron temperature is possible. In the rare gases, on the other hand, the value of the electronic mean free path is high even at atmospheric pressure, because of the extremely low electron collision cross sections of the rare gas molecules, and this fact, taken along with the fact that these molecules are monatomic, means that the rate of energy transfer from the free electrons to the gas atoms is very low. This enables an atmospheric-pressure rare gas to behave like a low-pressure gas when it comes to supporting nonequilibrium conditions. The presence of a percent-or-so of alkali metal vapour does not greatly reduce the ability of the rare gas to support an elevated electron temperature, and greatly enhances the electrical conductivity of the gas, since the alkali metal atoms have the lowest ionisation potentials of all the elements, and are therefore

much more easily ionised by the fast electrons that are present in the high-energy tail of the electron energy distribution than are the rare gas atoms. Thus, we see that an alkali-metal-seeded rare gas has the electrical properties of a low-pressure alkali metal vapour, but retains all the other properties of a high-pressure gas, thus making it an ideal working fluid for a reactor-driven MHD generator, in which the gas pressure has to be high in order to satisfy heat transfer requirements.

Let us now examine Ralph's work on seeded rare gases in a little more detail. As we have already seen, his experimental facility was designed to study the electrical properties of thermally-ionised alkali-metal-seeded rare gases in the temperature range 1500 - 2000°C (Ralph 1962, 1963). It consisted basically of two ovens, mounted one above the other. The lower oven held the seeding trap, this being a stainless-steel cylinder containing molten alkali metal through which the rare gas was slowly bubbled, thus causing it to become saturated with alkali metal vapour at a pressure that was determined by the temperature of the trap (see section 3.2). The upper oven contained the high-temperature furnace that was used to raise the electrode system to the required temperature. This furnace consisted of six tantalum cylinders, connected in series, through which a current of up to 500 amps could be passed. The electrode system was situated at the centre of this heater, and consisted of two horizontal tantalum discs 2 cm in diameter whose separation could be varied from 1 - 4 mm; the electrodes could be viewed through a 1 cm diameter viewing hole.

Using this apparatus, Ralph found that atmospheric-pressure rare gases seeded with a torr-or-so of caesium or potassium and heated to temperatures as low as 750°C broke down under electric fields of the order of a few tens of volts/cm, and then supported a steady-state discharge that was capable of carrying currents of the order of amps at electrode voltages of only a few volts. He found that this discharge had a constricted positive column, and that the cathode was covered by a thin, luminous sheath. The presence of the latter, combined with the fact that all the discharges studied by Ralph had rising voltage/current characteristics, led Ralph to describe the discharge as an abnormal glow. He also found that the properties of the discharge were insensitive to changes in the ambient temperature (range studied - 750 to 1000°C), and that the voltages needed to produce and maintain the discharge were somewhat higher in helium than in neon or argon. Having obtained these results, Ralph started work on an MHD generator, leaving the basic work on the electrical properties of seeded rare gases to be continued by M. Sakuntala (a Research Fellow on leave from Banares University) and the author, who both joined Ralph's group in the summer of 1963.

2.4 THE RESEARCH PROGRAM OF THE AUTHOR.

The experimental research program. The original aim of the author's research program was to obtain experimental data on the properties of the high-current discharge that had been discovered and studied by Ralph (1962, 1963), data that was needed for the Harwell MHD generator project. The work was to be carried out

in two stages, the first consisting of a thorough investigation of the basic properties of the discharge, and of the dependence of these properties on the discharge current, seed pressure and ambient temperature. The mixture to be studied during this stage of the work was potassium-seeded argon, as this was the mixture that was to be used as the working fluid in the Harwell generator. The specific aims of this part of the work were as follows:

1. to measure the voltage drops at the electrodes, the voltage gradient along the positive column, the diameter of the positive column, and the current density and electrical conductivity in the column plasma,
2. to find how these properties depended on the discharge current, and determine the current range through which the discharge was stable,
3. to study the discharge throughout as wide a seed pressure range as possible in order to determine the most suitable seed pressure for use in the generator,
4. to study the discharge throughout as wide an ambient temperature range as possible, and determine the lowest temperature at which the discharge could be supported.

In addition to studying the actual high-current discharge, the author was to carry out systematic measurements of the breakdown voltage at different electrode spacings, seed pressures and ambient temperatures, as this information was also of considerable interest in the MHD field.

Once the properties of the potassium-argon discharge had been thoroughly investigated, it was intended to move on to the second stage of the work, in which the investigations were to be extended to other seed-diluent mixtures. The effects on the discharge properties of changing the diluent gas from argon to helium or neon were to be investigated, as were the effects of changing the seed metal from potassium to caesium or sodium. The effect of these changes on the value of the breakdown voltage was also to be investigated during this stage of the work. Finally, the effects on the discharge properties of adding known amounts of molecular impurity to the seed-diluent mixture were to be investigated, in order to obtain some idea of the maximum level of impurity that could be tolerated in the generator duct.

In order to carry out this research program, the author constructed two experimental facilities, the first being used at Harwell from 1963 - 1965, and the second at Aberdeen from 1966 - 1969 (see Chapter 3). Using these two rigs, all the aims of the author's experimental program have been achieved, as will be shown in the remaining chapters of Part I of this thesis. Excellent agreement was obtained between the results that were produced by the two rigs, the Aberdeen rig being used first to check and then to extend the results that were obtained at Harwell.

The theoretical research program. The aims of the present thesis go far beyond those of the experimental research program given above, as the author has also set himself the task of explaining the experimental results that he has obtained. The specific

objectives of this part of the work, which has occupied most of the author's time during the last three years, can be stated as follows:

1. to derive a theoretical expression for the value of the breakdown voltage in seeded gases, and see whether the results of the author's breakdown voltage measurements are consistent with this expression,
2. to give a reasonably-complete description of the physical processes that are active in the positive column of the high-current discharge, set up the equations that are necessary and sufficient to describe the column, and determine whether the results of the author's measurements of the column field, diameter, current density etc., are consistent with these equations,
3. to give a reasonably-complete description of the physical processes that occur in the two cathode mechanisms of the high-current discharge.

Most of these objectives have now been achieved, as will be shown in Part II of this thesis.

2.5 A REVIEW OF RELATED WORK.

Since 1960, a great deal of work has been carried out on the electrical properties of seeded rare gases, and much of this is highly germane to the work of the author. We will now give a brief survey of this work, and also of related work on unseeded rare gases. The survey will be carried out under the following six headings:

1. Experimental work on equilibrium plasmas,
2. Experimental work on moving nonequilibrium plasmas,
3. Experimental work on pulsed nonequilibrium discharges,
4. Experimental work on inhomogeneous nonequilibrium plasmas,
5. Theoretical work on seeded rare gases,
6. Work on unseeded rare gases.

1. Experimental work on equilibrium plasmas. Since the discovery of field-induced nonequilibrium ionisation in high-pressure plasmas, comparatively little work has been carried out on the physics of thermally-ionised plasmas. Harris (1963, A, B) has carried out extensive work on such plasmas, however, measuring the electrical conductivity of a number of atmospheric-pressure mixtures in the temperature range 1500 - 2000°K; he used caesium and potassium as seed metals, and helium, neon and argon as diluent gases. In the course of this work, he succeeded in measuring the equilibrium optimum seeding fractions of several seed-diluent mixtures, results that proved to be in excellent agreement with the theoretical values for these mixtures.

2. Experimental work on moving nonequilibrium plasmas. As pointed out by Kerrebrock (1965), "it is impossible to maintain nonequilibrium conditions in a steady, homogeneous, stagnant gas, since the energy that is transferred from the electrons to the gas atoms must somehow be disposed of if the difference between the electron and gas temperatures is to be maintained". A number of workers have succeeded in studying the electrical

properties of homogeneous nonequilibrium plasmas, however, and these have all employed one or other of the following experimental techniques to prevent the gas temperature from rising above the ambient value. In the first method, originally developed by Kerrebrock (1962), a rapidly-moving stream of hot, seeded gas is produced by means of an arc heater, and is made to pass through a test duct, convection within the stream being relied upon to keep the gas temperature nearly constant as the gas passes through this duct. In the second method, originally used by Westendorp et. al. (1961), an electric field is suddenly applied to a stagnant gas, and the nonequilibrium ionisation is studied in the short interval after the electron temperature has risen, but before the gas temperature has risen. Let us now examine the work that has been carried out using the first of these techniques.

The moving gas technique was first used by Kerrebrock in 1962. He studied atmospheric-pressure potassium-argon in the temperature range 1000 - 2500°K, and succeeded in amassing a great deal of information about the dependence of the electrical conductivity of such plasmas on the current density (Kerrebrock and Hoffman 1964). He also measured the electron temperature in the plasma by means of the line reversal technique, and showed that this was considerably higher than the gas temperature.

The work of Robben (1962), who also used the moving gas technique, was very similar to that of Kerrebrock, and produced similar results.

Other workers who employed this technique were Sheindlin, Batenin and Asinovsky (1964), who also studied an atmospheric-pressure potassium-argon system. They measured the electrical conductivity of the plasma throughout a wide temperature range, and also measured the temperatures of the components of the plasma. They found the electron temperature to be considerably higher than the gas temperature, and also found that the measured value of the electron temperature was in good agreement with the value that could be deduced from the electrical conductivity results using the Saha equation.

Pinchak and Zukoski (1963) and Zukoski, Cool and Gibson (1963) carried out similar work to this, also working with potassium-argon at atmospheric pressure. They measured the electrical conductivity of the mixture, and showed that the variation in the electron temperature (obtained by a spectroscopic method) agreed with the variation predicted by the Saha equation. More recently, Cool and Zukoski (1966) reported direct measurements of the gas temperature, electron temperature and electrical conductivity, quantities that were also measured by Chu and Gottschlich (1968).

3. Experimental work on pulsed nonequilibrium discharges. The pulse technique has been used by a large number of workers. In 1961, Westendorp et. al. studied static caesium-seeded helium at 200°C and $\frac{1}{5}$ atmosphere, and observed extremely high conductivity values. In 1963, Ben Daniel and Bishop, who studied a static caesium-helium mixture at pressures of $\frac{1}{5}$ and $\frac{1}{10}$ atmosphere,

obtained similar results, observing electron temperatures in the range 2000 - 4000 °K while the gas temperature remained in the range 400 - 500°K.

Extensive work on pulsed discharges in low-pressure caesium-helium, potassium-helium, caesium-argon and potassium argon plasmas has been carried out by Morgulis and Polushkin (1966). They used a diluent pressure of 60 torr and a seed pressure of 0.01 - 0.5 torr, and measured the electrical conductivity throughout the current density range 4 - 70 amps/cm². Their results proved to be in excellent agreement with those of the author (Chapter 6), since they found that (a) the field needed to support a given current density was considerably higher with helium as the diluent gas than with argon as diluent, (b) the differences between the properties of caesium- and potassium-seeded plasmas were small, caesium-seeded plasmas having a slightly higher conductivity. The author has found that the results of Morgulis and Polushkin are in good agreement with the theory that is developed in Chapters 12 - 14.

The work of Labois and Lemaire (1964), Labois and Ricateau (1965) and Bernard et. al. (1966) at C.E.A. Saclay also employed a pulse technique. Using a double oven system similar to that used by Ralph and the author, these workers studied an atmospheric-pressure caesium-argon discharge under a wide range of experimental conditions. They also measured the optimum seeding fraction of a nonequilibrium caesium-argon plasma, and obtained a value that proved to be in excellent agreement with that obtained by the author (see Chapter 16).

4. Experimental work on inhomogeneous nonequilibrium plasmas.

Although most of the workers investigating the nonequilibrium properties of seeded rare gases confined their studies to homogeneous plasmas, a certain amount of work has been done on the properties of the inhomogeneous plasmas that are found in the positive columns of steady-state nonequilibrium discharges in static gases. Ralph's work was concerned with such discharges, (Ralph 1962, 1963), as was the extension of his work that was carried out by Sakuntala and the author. Sakuntala began her work by studying a steady-state high-current discharge in potassium-argon, paying particular attention to the processes active at the cathode of the discharge (Sakuntala 1964). She then studied the low-current discharge that precedes the breakdown of the gas, and gave a comprehensive account of the events that led up to breakdown (Sakuntala 1965). After this, she measured the electron temperature in the pre-breakdown discharge by means of a double-probe technique, and showed that the electron temperature in the plasma rose steadily as the discharge current rose to the value at which the transition to the high-current discharge took place (Sakuntala 1966).

Another worker who carried out extensive work on steady-state nonequilibrium discharges is Evans. He studied the discharge that is the subject of the present thesis, using the author's early experimental results (Ellington 1965 A, B, C) as a starting point. The object of his original experiments was to extend the author's work on caesium-argon (the mixture shown by the

author to be the most promising from an MHD point of view) to a moving gas stream, and in the course of the work, (Evans 1967) he obtained results that were in good qualitative and quantitative agreement with those of the author. He then extended the work to the duct of an MHD generator, and became the first man to extract significant power from a generator that relied on field-induced nonequilibrium ionisation for the production of a highly-conducting working fluid (Evans 1968).

5. Theoretical work on seeded rare gases. A great deal of theoretical work on the nonequilibrium properties of seeded rare gases has been carried out during the past decade, so the following survey has been confined to work that is particularly relevant to that of the author.

Several workers have attempted to determine the optimum seeding fraction of seeded plasmas (the ratio of seed pressure to diluent pressure that produces the maximum plasma conductivity). The problem was solved fairly easily for the case of equilibrium plasmas, in which the electron temperature equals the gas temperature (Zimin and Popov 1964), and it was then thought by many workers that the formula derived by Zimin and Popov (see Chapter 16) would also be valid for nonequilibrium plasmas (Kerrebrock and Hoffman 1964). This hypothesis was incompatible with the theoretical work of Shair (1963, 1964) on the physics of the MHD duct, however, and was soon disproved experimentally (Ellington 1965 A, B, C, Ellington and Ralph 1966, Labois and Ricateau 1965). All of the above workers showed that the

seeding fraction appeared to be roughly an order of magnitude lower under nonequilibrium conditions than under equilibrium conditions, a conclusion that was also reached by Rice and Parsons (1966) and Rice (1967) in their theoretical work on nonequilibrium conductivity. In 1966, a general formula for the value of the optimum seeding fraction in nonequilibrium plasmas was developed by Smith and Shair, who showed that the author's experimental optimum seeding fraction results (Ellington and Ralph 1966) were in good agreement with their new theory (see Chapter 16).

Other theoretical work that is relevant to the present thesis is the work of Monti and Napolitano (1964, A, B) on the validity of the Saha equation in describing nonequilibrium plasmas (see Chapter 13), and the work of Lutz (1963, 1967) and Kerrebrock (1965) on the value of the radiation losses from seeded plasmas (see Chapter 11).

6. Work on unseeded rare gases. Recent work on unseeded rare gases that has been carried out by Massey and Cannon is closely related to the work of the author (Massey and Cannon 1965), (Massey 1965). They have found that unseeded argon and neon at pressures up to 600 torr and low ambient temperatures are capable of supporting a type of constricted nonequilibrium discharge that has properties intermediate between those of the nonequilibrium discharge that is the subject of this thesis and those of conventional thermal arcs in high-pressure rare gases of the type studied by Suits in the 1930's (Suits 1939 A, B, C). This type of discharge has many properties in common with the discharge

studied by the author (see Chapter 10). A similar discharge has been studied by Sugawara (1967).

Other related work on pure rare gases is that of George (1963, 1964), who has studied a high-current arc discharge in unseeded rare gases. He employed an electrode system consisting of two concentric graphite cylinders, and studied the electrical properties of argon and helium throughout a wide temperature and pressure range. In the course of this work, he obtained a great deal of information about the dependence of the breakdown properties of high-pressure argon and helium on the ambient gas temperature. He later extended his work to seeded rare gases (George 1965).

CHAPTER 3THE APPARATUS USED3.1 GENERAL DESCRIPTION OF THE APPARATUS.

In order to carry out the experimental part of the research program described in the last chapter, the author had to construct an experimental facility in which the electrical properties of static, atmospheric-pressure, alkali-metal-seeded rare gases could be studied under carefully-controlled conditions. The apparatus had to meet the following specifications.

1. The electrode separation had to be easily variable in the course of an experiment in order to allow the positive column voltage gradient and cathode fall of the high-current discharge to be measured.
2. The electrode system had to be clearly visible so that the discharge could be studied visually, photographically and spectroscopically.
3. The electrode system had to be capable of being heated up to 950°C, and its temperature had to be accurately known and easily controlled.
4. The seed pressure in the electrode area had to be accurately known and easily controlled throughout the pressure range 10^{-2} - 40 torr.
5. The apparatus had to be easily dismantled, cleaned and maintained to enable rapid turn about between experiments. A versatile apparatus that could accommodate a variety of electrode systems was desirable.

6. The power requirements of the apparatus were to be as simple as possible, with all the circuits operating directly from the single-phase mains supply if possible.

7. A power pack capable of producing a continuously-variable D.C. voltage up to 100 volts and capable of supplying a current of 20 amps was required to power the discharge.

With these requirements in mind, the author decided to build a greatly-modified version of the experimental lay-out that had been used by Ralph and Sakuntala, a lay-out that consisted essentially of two ovens, one mounted immediately above the other; the lower oven contained the seeding trap, and the upper oven the electrode system. As was mentioned in the last chapter, two experimental facilities were in fact built by the author, the first being used at Harwell from 1963-1965, and the second at Aberdeen from 1966-1969. These were identical in their basic design, differing only in a few minor details.

A block diagram of the apparatus used by the author is given in figure 3.1, while the actual physical lay-out is shown in figure 3.2, which shows the front elevation of the apparatus. The apparatus was mounted in two Dexion racks, one containing the two ovens, and the other containing the various ancillary circuits and control panels. The two ovens were mounted in a framework roughly 3 feet high, the upper oven resting on a one-inch-thick Sindanyo sheet which formed the top of the framework, and the lower oven resting on two rails so that it was situated just below the upper oven. This was found to be the most convenient

FIGURE 3.1

BLOCK DIAGRAM OF APPARATUS

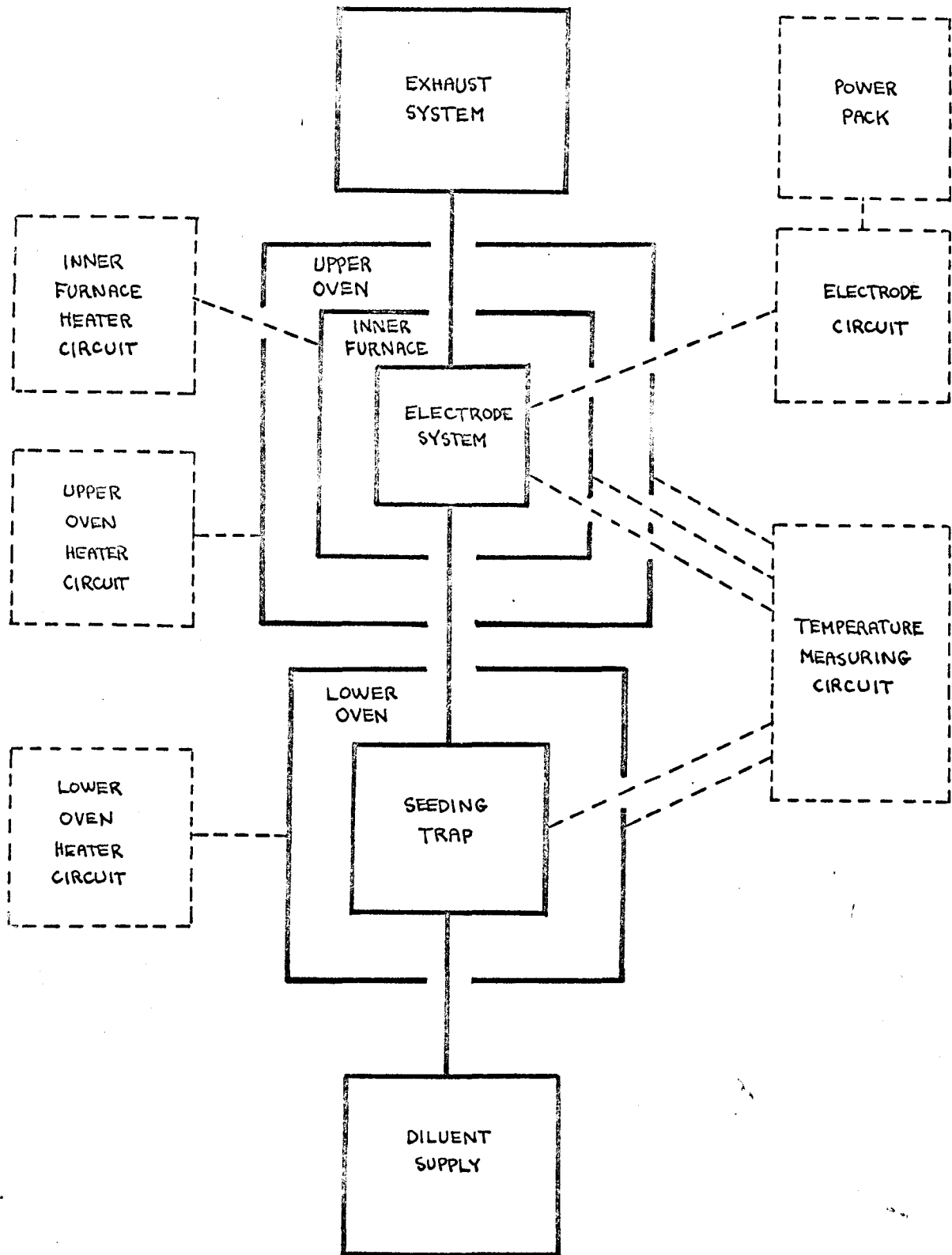
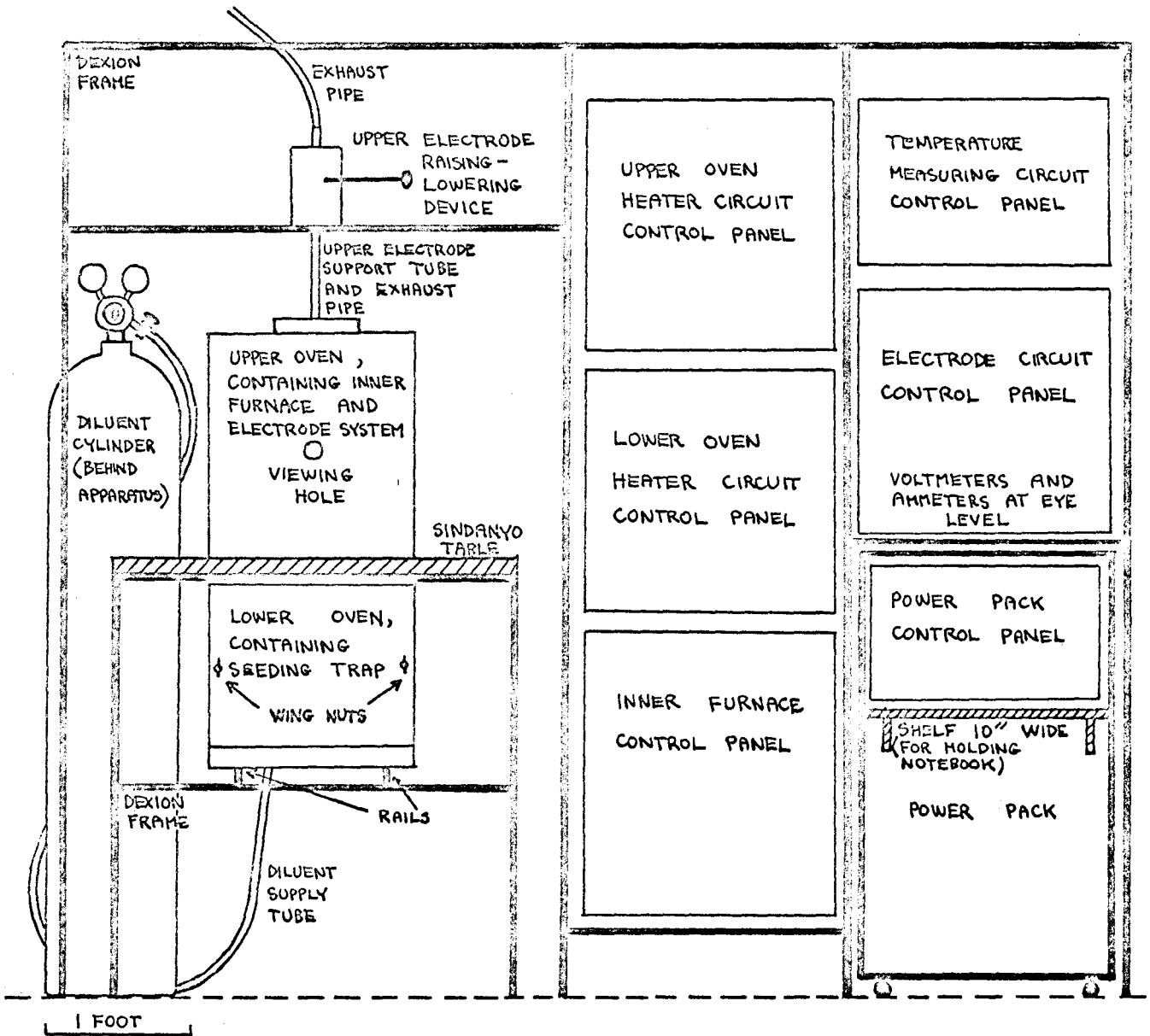


FIGURE 3.2
PHYSICAL LAY-OUT OF APPARATUS
 (FRONT ELEVATION)



arrangement of the ovens, as the upper oven and electrode system were at a convenient height, while the lower oven could be slid backwards to allow easy access to the seeding trap, which was bolted to a pipe that projected downwards from the upper oven. The diluent supply consisted of a cylinder of rare gas fitted with a two-stage regulator and a 0-10 litre-per-minute rotameter flowmeter, and was connected to the copper pipe that led to the seeding trap by means of a P.V.C. tube. After passing through the seeding trap, where it became saturated with alkali metal vapour at the required pressure, the gas flowed up into the electrode area, and eventually passed into the exhaust system. In all the author's experiments, the latter consisted of a P.V.C. tube which passed out through a convenient window and discharged into the atmosphere, where immediate oxidation of the alkali metal vapour occurred.

The rack containing the various circuits and control panels extended over and round the rack that contained the two ovens, thus allowing the many wires and thermocouples that connected the ovens to the control panels to be kept tidy. The control panels were arranged so that the apparatus could be conveniently operated from a sitting position, the ammeters and voltmeters that were used in the measurement of the discharge properties being situated at eye level, immediately above the wheel that controlled the output voltage of the electrode circuit power pack (and hence the discharge current). Detailed descriptions of the different parts of the apparatus will now be given.

3.2 THE LOWER OVEN AND SEEDING TRAP

The method by which the diluent gas was seeded with the required amount of alkali metal vapour was essentially that which had been successfully developed by Ralph. The rare gas was made to pass slowly through a trap containing molten alkali metal at a temperature corresponding to the required vapour pressure, so that the gas was saturated with alkali metal vapour on emerging from the trap. The detailed construction of the seeding trap and the oven that contained it is shown in figure 3.3. The oven was roughly cubic in shape, having an interior 12" deep by 12" broad by 13" high, each of its walls consisting of two $\frac{1}{2}$ inch Sindanyo sheets separated by a $\frac{1}{2}$ inch air space. The heater elements consisted of armoured heater cables fixed to the oven walls in the case of the Harwell rig, and electric fire elements mounted on the oven floor in the case of the Aberdeen rig. The circuit that was used to control the oven temperature is shown in figure 3.4. A base-load heater of 1 KW was employed, together with a thermostatically-controlled 0 - 2 KW heater whose power rating could be altered by means of a variac. The thermostat controller operated in two stages, the dropper resistors being switched in and out of the heater circuit by a high-current relay that was itself opened and closed by the relay of the Honeywell potentiometer controller to which the actual control thermocouple was attached. The hot junction of this thermocouple was situated inside the seeding trap, thus ensuring that the temperature indicated on the potentiometer controller corresponded to that of the seed. All the thermocouples used by the author were

FIGURE 3.3
LOWER OVEN AND SEEDING TRAP
(SIDE CROSS SECTION)

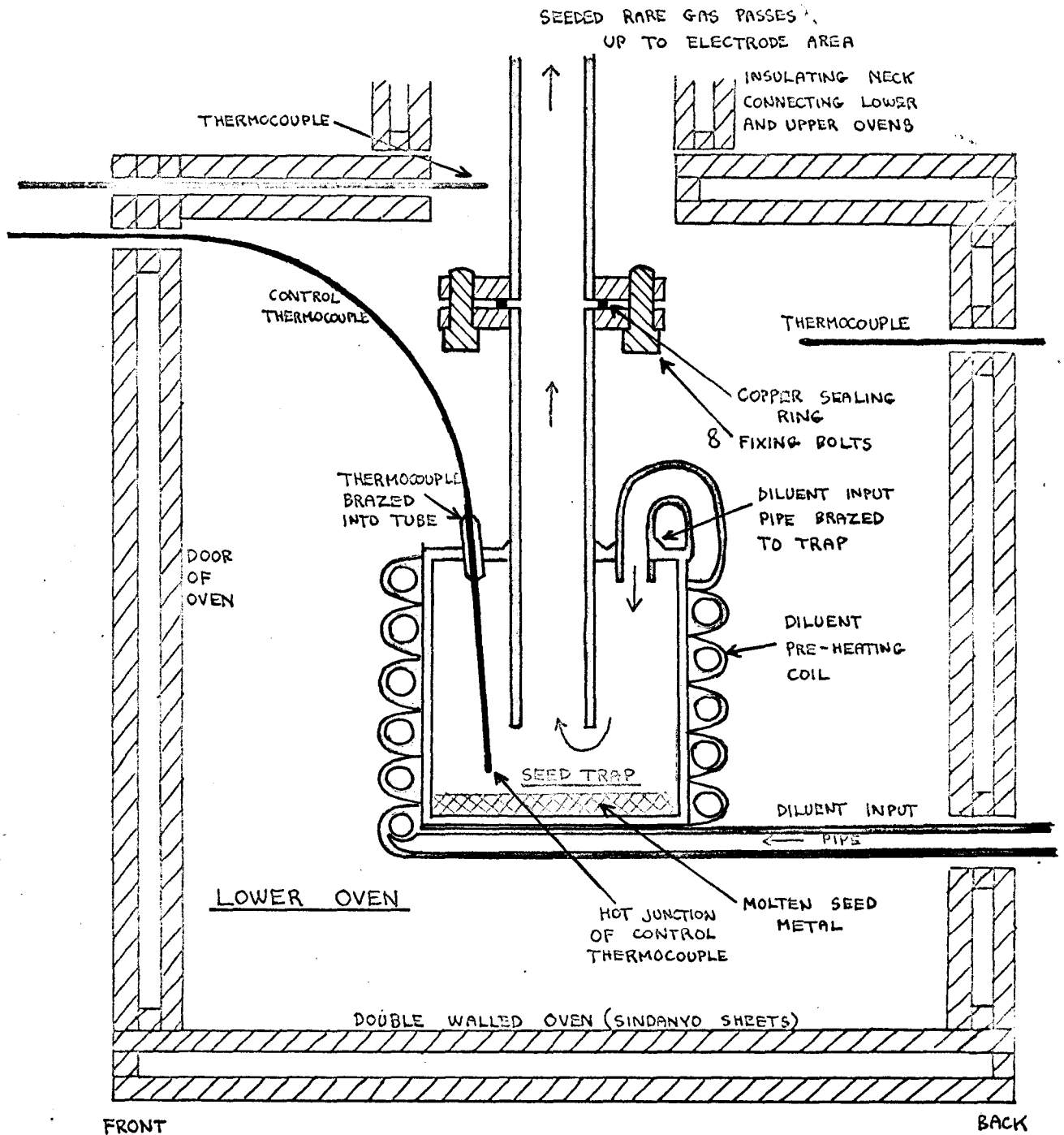
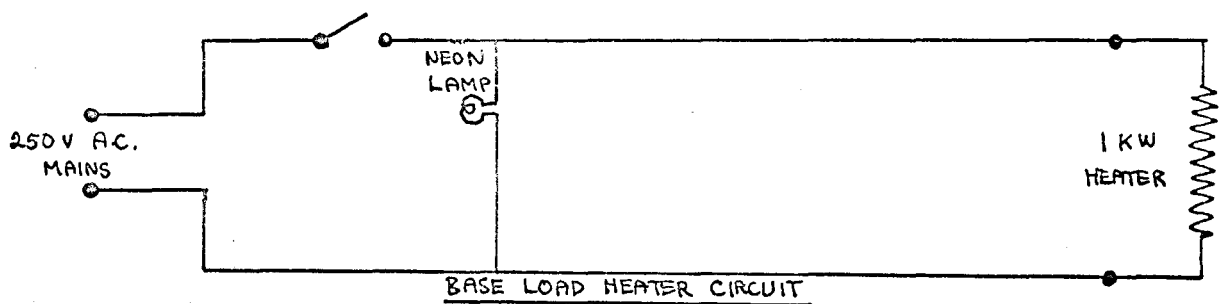
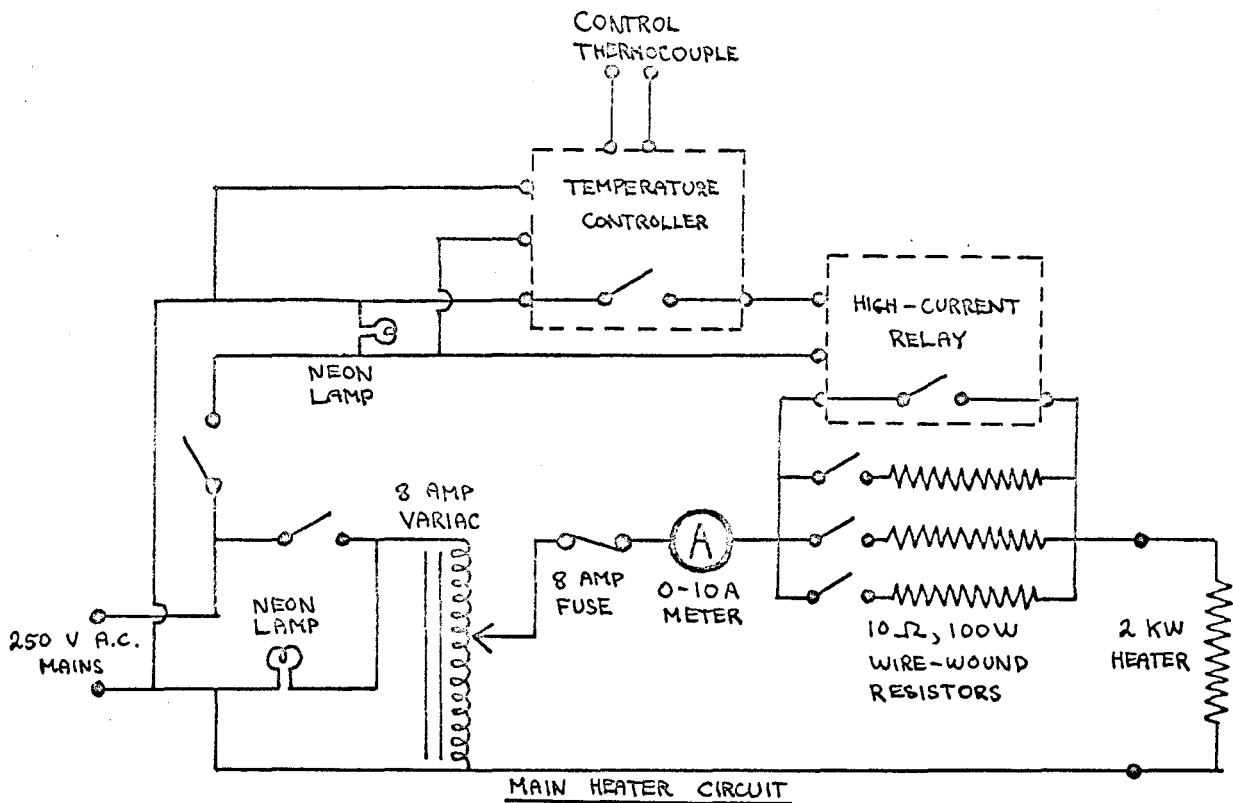


FIGURE 3.4

LOWER OVEN HEATER CIRCUIT



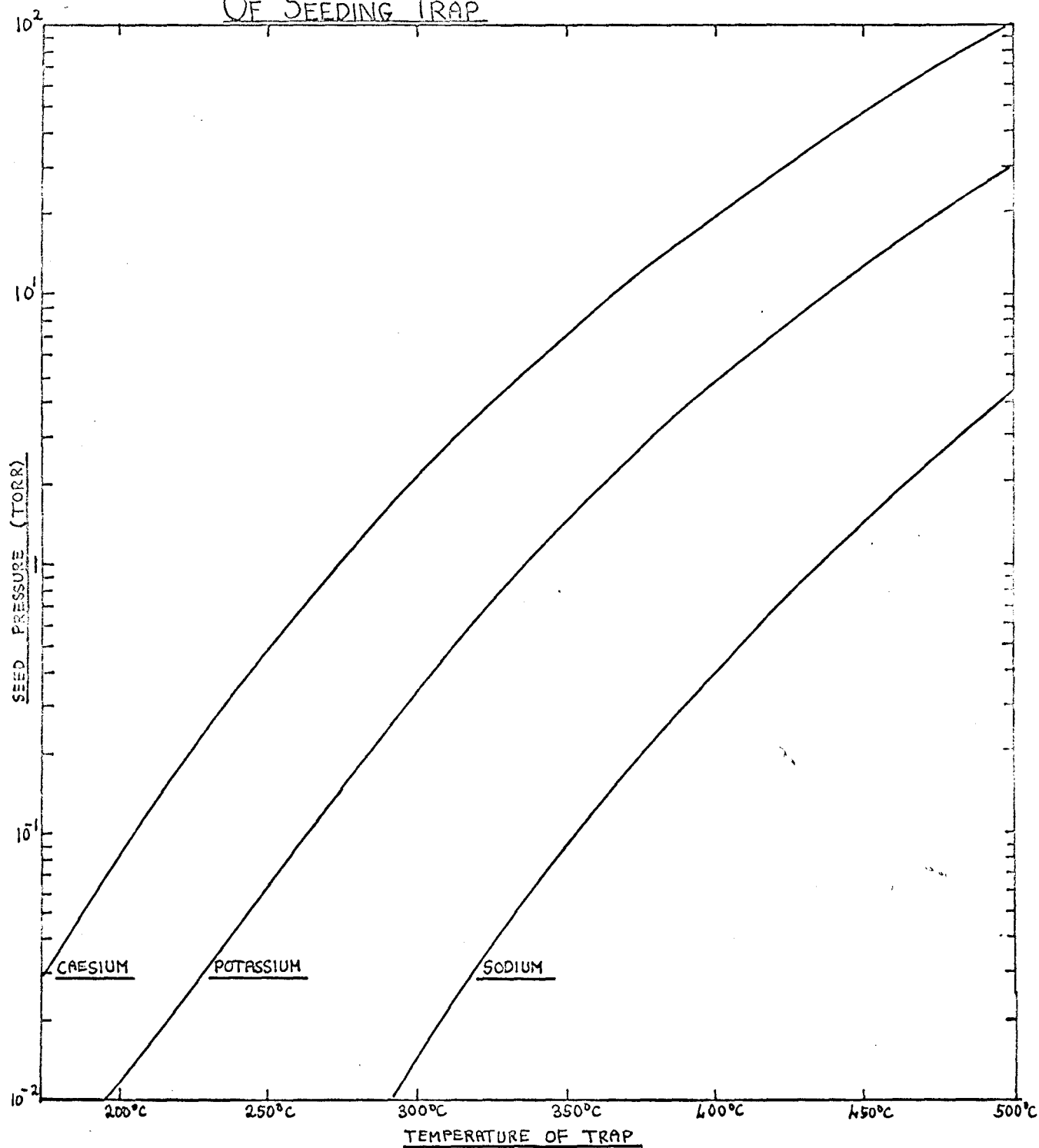
$\frac{1}{16}$ inch e.d. stainless-steel-sheathed mineral-insulated chrome-alumel thermocouples, and could be purchased complete with compensating cables.

The seeding trap itself consisted of a stainless steel cylinder 4 inches high and 4 inches in diameter. The diluent gas entered the top of the trap by passing through a six foot length of $\frac{1}{4}$ inch bore copper tubing wound into a helical coil which surrounded the trap and acted as a preheater for the gas. It then flowed through the body of the trap, eventually passing into the upper oven through the one-inch-bore stainless steel tube that connected the trap to the electrode area (see figures 3.3 and 3.7). The design of the trap ensured that the diluent gas spent a reasonably long time in the vicinity of the alkali metal, and was found to give better results than the original trap that was used by Ralph. In the latter, the rare gas was simply bubbled through a quantity of molten seed metal contained in a one-inch-bore tube, no preheating coil being used.

The method of seeding described above depended on the fact that the seeding trap was (relatively speaking) the coldest part of the apparatus, and therefore determined the vapour pressure throughout the apparatus. The temperature was carefully monitored throughout the rest of the apparatus to ensure that this was the case, as the presence of a cold spot would ruin the seeding process. The relationship between the saturated vapour pressures of the seeds employed in the author's experiments (sodium, potassium and caesium) and the temperature is shown in figure 3.5. It is seen that a given seed pressure can be obtained at a much lower

FIGURE 3.5

PLOTS OF SEED PRESSURE AGAINST TEMPERATURE
OF SEEDING TRAP

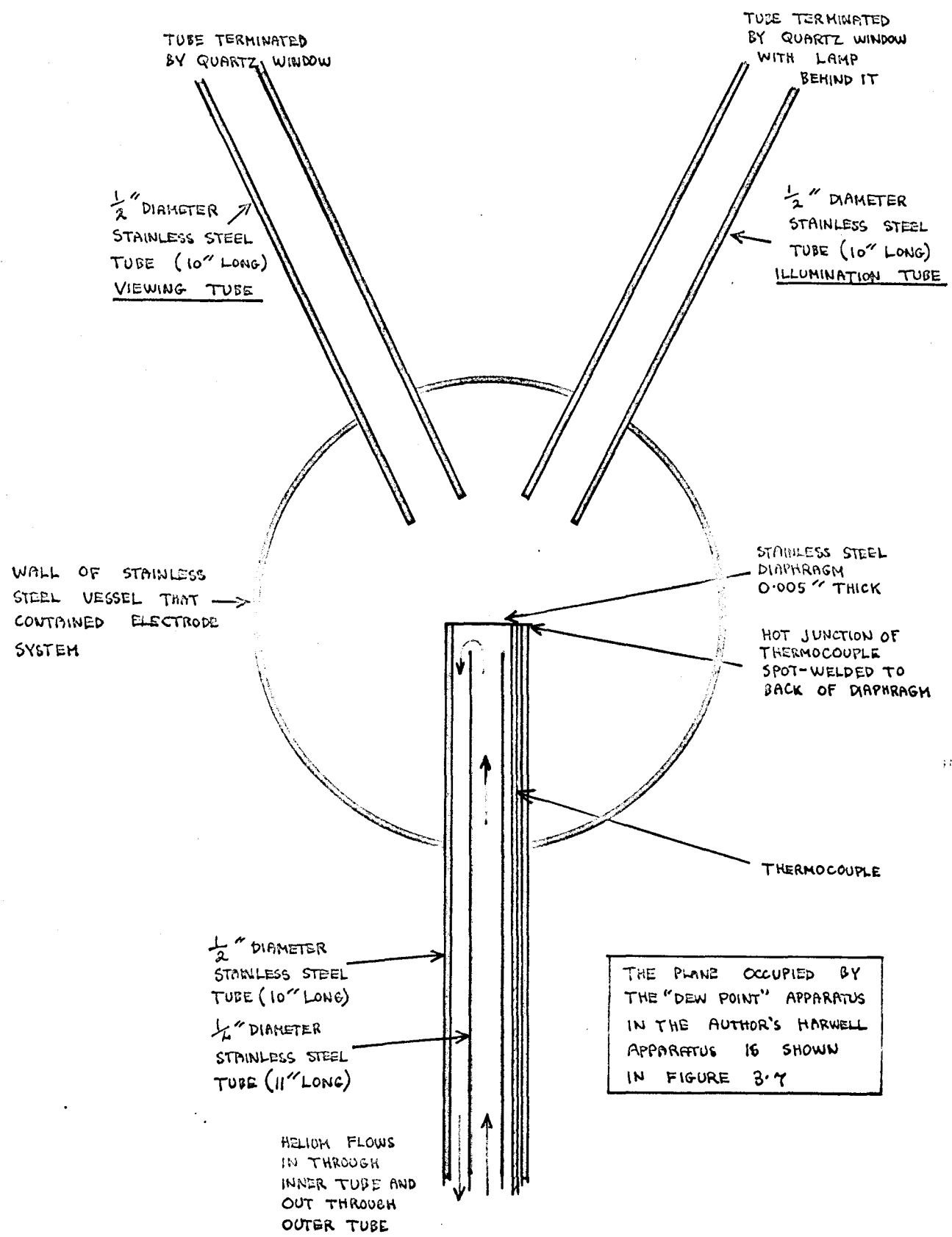


temperature with caesium as seed than with sodium as seed, with potassium occupying an intermediate position. It is also seen that a small change in the temperature leads to a comparatively large change in the seed pressure, a fact which meant that the trap temperature had to be measured extremely accurately in order to minimise the error in the seed pressure. The highest temperature that could be reached by the seeding oven was 540°C , a fact that limited the sodium seed pressure to 10 torr, but allowed seed pressures of over 40 torr to be reached with potassium and caesium.

The dew point apparatus. When experimental work on seeded gases was started at Harwell, there was some doubt about the efficiency of the method of seeding that is described above, since it was not known for certain that the vapour pressure throughout the apparatus was in fact determined by the temperature of the seeding trap. In order to determine whether or not the seeding process was reliable, Ralph devised a diagnostic technique based on the measurement of the dew point in the vicinity of the electrodes. The method consisted of cooling a metal diaphragm, and observing the temperature at which the alkali metal started to condense on it; if this temperature equalled the trap temperature, the seed pressure in the vicinity of the electrodes was equal to the saturated vapour pressure corresponding to the temperature of the trap. The dew point apparatus is shown in **figure 3.6**, and consisted essentially of three tubes arranged in the form of a Y. A stainless steel diaphragm 0.005 inches thick

FIGURE 3.6

THE "DEW POINT" APPARATUS
(HORIZONTAL CROSS-SECTION)



THE PLANE OCCUPIED BY THE "DEW POINT" APPARATUS IN THE AUTHOR'S HARWELL APPARATUS IS SHOWN IN FIGURE 3.7

was welded to the end of one of these tubes, and was situated just below the electrode system; the diaphragm was cooled by passing helium across its back, its temperature being measured by means of a thermocouple whose hot junction was spot welded to its back. The front of the diaphragm was illuminated by a small lamp situated at the end of one of the other two tubes, while the onset of the condensation process was observed by looking down the third tube. Both of these tubes were terminated by a quartz window. The dew point apparatus was first tested by constructing a pilot model, and was subsequently incorporated in the author's Harwell facility. It was found that the seed pressure throughout the apparatus was effectively controlled by the temperature of the seeding trap provided that the rest of the apparatus was kept at a higher temperature than the trap and the diluent flow rate was kept low. A flow rate of $\frac{1}{2}$ litre/min. was found to produce satisfactory results, and was used in all the author's subsequent experiments. When the author had satisfied himself as to the efficiency of the seeding process, having found that the seed pressure in the electrode area could be determined with an accuracy of at least $\pm 25\%$, the dew point apparatus was removed from the Harwell apparatus for reasons that will be given in the next section. It was not deemed necessary to incorporate it in the Aberdeen apparatus.

3.3 THE UPPER OVEN AND INNER FURNACE.

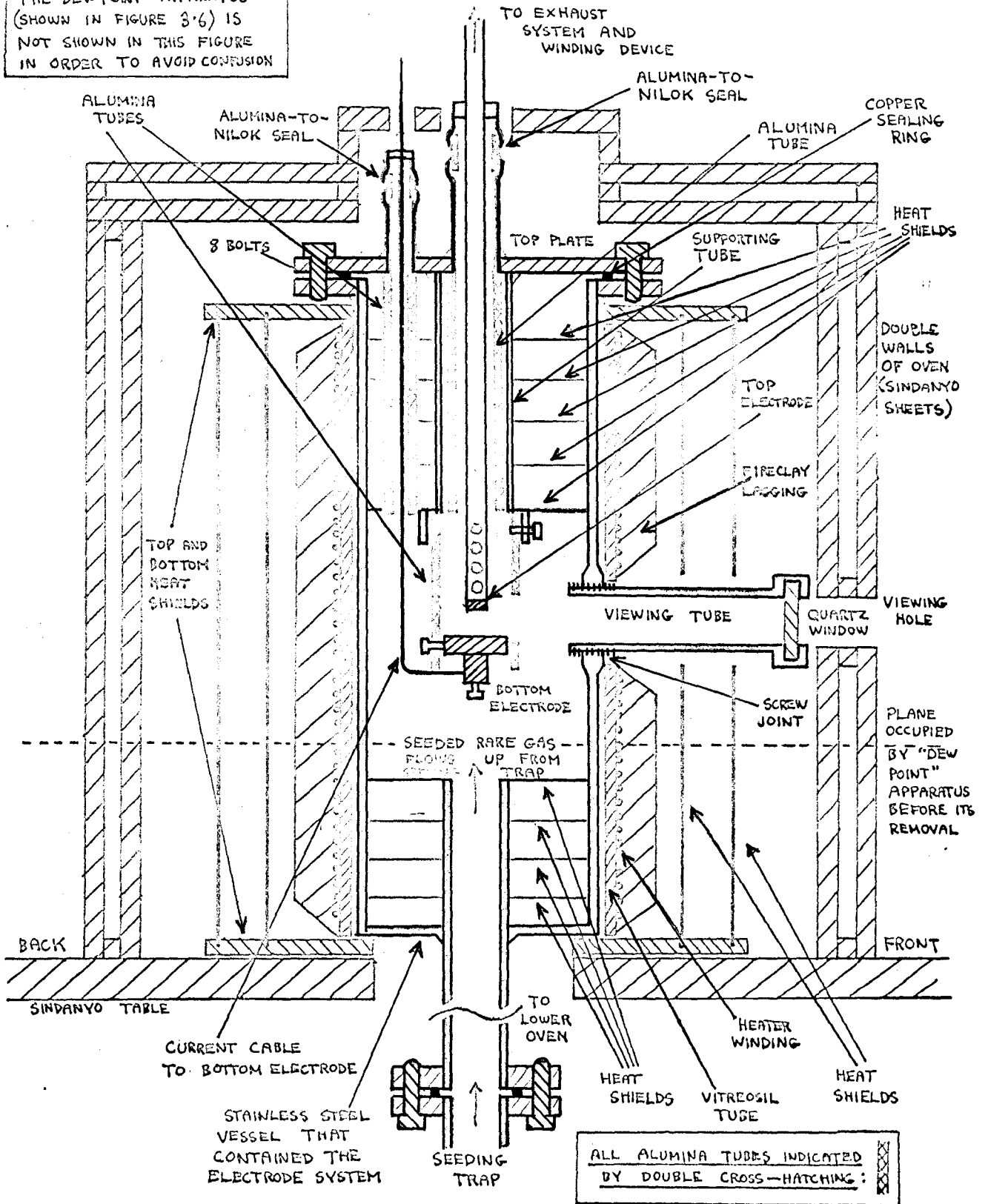
The lay-out of the upper oven and inner furnace is shown in figure 3.7. The upper oven was very similar to the lower oven, both in size and construction, the main difference being that its heaters were not thermostatically controlled. The main purpose of the oven was to keep the whole of the upper part of the apparatus at a higher temperature than the seeding trap in order to ensure the correct functioning of the seeding process, but it also served as a first stage in the process of raising the electrode system to the high temperature that was necessary for the production of the type of discharge under study. The temperature of the upper oven was generally kept in the range 450 - 500°C.

It was in the design of the inner furnace that the apparatus built by the author differed most from the original apparatus of Ralph. Ralph's heater was designed to operate at much higher temperatures than that of the author (1500 - 2000°C), and consisted of six concentric tantalum cylinders connected in series, the electrode system being situated inside the innermost cylinder. This type of heater had several operational drawbacks. Firstly, the fact that the heater was located in an alkali metal vapour atmosphere meant that it had to operate at a very low voltage in order to avoid arcing, so that the heater current had to be very large (100 - 400 amps); this necessitated the use of a large transformer and cumbersome bus bars. Secondly, the fact that the heater operated at a very large current meant that it did not

FIGURE 3.7 UPPER OVEN AND INNER FURNACE

(SIDE CROSS SECTION)

THE "DEW POINT" APPARATUS (SHOWN IN FIGURE 3.6) IS NOT SHOWN IN THIS FIGURE IN ORDER TO AVOID CONFUSION



easily lend itself to thermostatic control; the heater current was simply controlled by a large variac, a fact that made accurate preselection of the electrode temperature difficult. Thirdly, the volume available for housing the electrode system was severely limited in extent, since the innermost cylinder of the heater had a bore of only $1\frac{3}{4}$ inches. This meant that the electrode size was limited, and also meant that the lower electrode had to be attached to the bottom of the apparatus rather than to the top plate. Fourthly, the fact that the temperature difference between the electrode area and the outside of the outermost heater cylinder was very large meant that the size of the hole that could be cut through the cylinder to allow visual observation of the electrode area was limited by heat loss considerations. In practice, a hole 1 cm in diameter was employed, and this proved to be much too small to allow the discharge to be clearly seen, or to allow photographic or spectroscopic work to be easily carried out.

The furnace design that was adopted by the author had none of the above disadvantages, and satisfied all the design requirements listed at the beginning of this chapter. Instead of being situated inside the vessel that contained the seeded rare gas, the heater completely surrounded it, thus greatly increasing the space that was available for housing the electrode system to a cylinder $3\frac{1}{2}$ inches in diameter and roughly 5 inches in length.

The fact that the heater **no** longer had to operate in an alkali metal atmosphere meant that it could operate at a much higher voltage, and hence at a lower current. This enabled it to operate straight from a variac, and also enabled the furnace to be thermostatically controlled. The furnace consisted of a vitreosil cylinder 12 inches long and 4 inches in bore on which was wound a 16 ohm coil of 18 s.w.g. **nichrome** wire. The heater was lagged by an inch of fireclay, and was surrounded by two stainless steel cylinders which acted as heat shields. Stainless steel top and bottom plates were also employed. The vessel that contained the electrode system consisted of a stainless steel cylinder 12 inches long and $3\frac{1}{2}$ inches in bore. The pipe that led from the seeding trap was welded to the bottom of this cylinder, while the plate to which the electrode assembly was attached was bolted to the flange that formed the upper rim of the vessel. Vertical heat losses from the electrode area (which was at a higher temperature than the upper and lower extremities of the electrode vessel) were reduced by the presence of horizontal heat shields inside the vessel. The one-inch-bore viewing tube that enabled the electrode system to be clearly seen was screwed into the electrode vessel through a hole in the heater, as were the three tubes of the dew point apparatus (not shown in figure 3.7). When Ralph constructed his original apparatus, there was some doubt about whether the presence of tubes leading from the electrode area to outside the apparatus would interfere with the seeding process by causing the seed to condense at their cold outer extremities.

In practice, it was found that the presence of such tubes had no measurable effect on the seed pressure inside the apparatus, and it was concluded that the static conditions prevailing in the tubes kept the rate of loss of alkali metal vapour by diffusion along the tubes to a level that was considerably below the rate of supply of alkali metal vapour from the seeding trap. As was mentioned in the last section, the three tubes of the dew point apparatus were eventually removed from the apparatus, as they proved to be practically impossible to unscrew from the electrode vessel when the apparatus had to be dismantled because of a heater breakdown. Such breakdowns were common when the apparatus was first operated, but were later obviated by changing the material of the heater winding from kanthal to nichrome.

The circuit that controlled the heater current is shown in figure 3.8, and was very similar to that employed to control the lower oven heaters. The thermocouple that operated the thermostat was situated just outside the alumina cylinder that contained the electrodes. This circuit was found to give excellent control over the ambient temperature in the electrode area, the variation from the selected temperature being less than $\pm 5^{\circ}\text{C}$.

3.4 THE ELECTRODE SYSTEM AND ITS ASSOCIATED CIRCUITRY.

The lay-out of the electrode system that was employed in the great majority of the author's experiments is shown in figure 3.9. The entire electrode assembly was attached to a circular plate that was bolted to the top of the electrode vessel, and could therefore be easily removed for cleaning, maintenance and alteration.

FIGURE 3.8

INNER FURNACE HEATER CIRCUIT

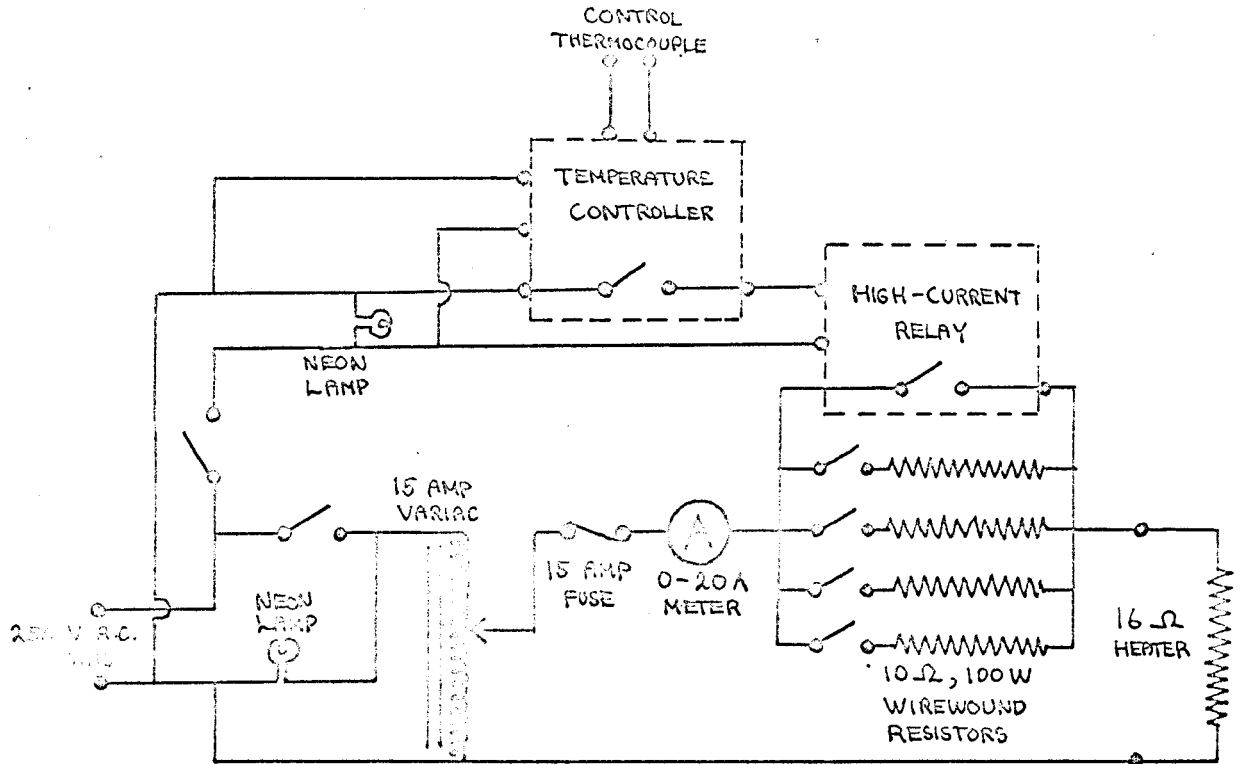
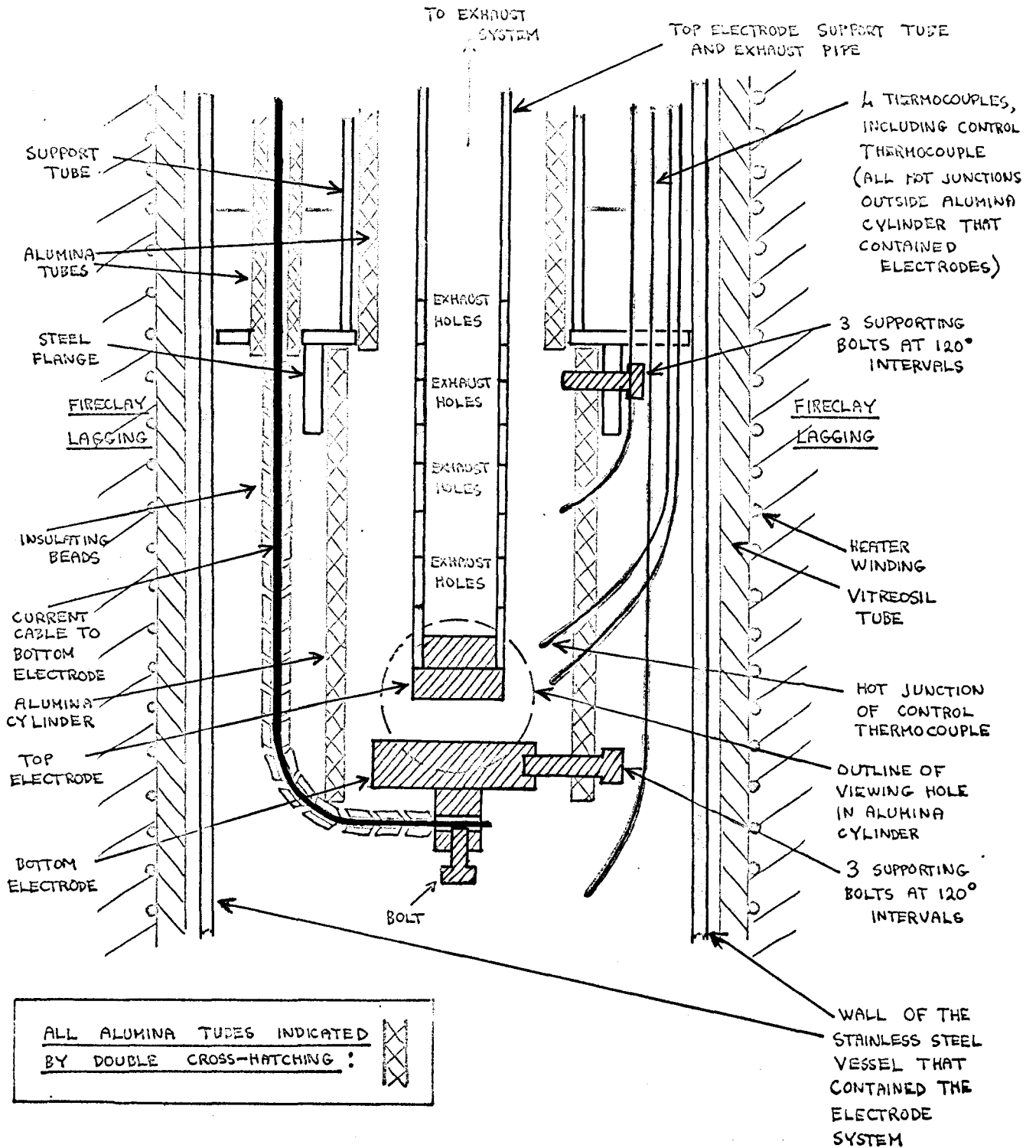


FIGURE 3.9

THE ELECTRODE SYSTEM

(FRONT CROSS SECTION)



The actual electrodes were contained in an alumina cylinder 7 cm long and 37 mm in bore. This was attached to the bottom heat shield by means of three screws. The lower electrode, which was generally $1\frac{1}{4}$ inches in diameter, was supported at the bottom of this cylinder by three screws, the current cable to the electrode being insulated by alumina beads and being led through the top plate by means of a ceramic-to-metal seal. All the ceramic-to-metal seals used by Ralph and the author were of a special type, consisting of an alumina insulator brazed to nielok tubes by pure copper braze (ordinary braze was found to be attacked by the alkali metal). The moveable top electrode, which was $\frac{1}{2}$ inch in diameter, was attached to the end of a $\frac{1}{2}$ inch-diameter stainless steel tube which served not only as a support for the electrode and a conductor for the discharge current, but also as an exhaust pipe for the seed-diluent mixture, several holes being drilled near its lower end to enable it to fulfil the latter purpose. The location of the entrance to the exhaust pipe just above the upper electrode helped to ensure that the seeded gas flowed through the electrode system. The upper electrode support tube passed through the top plate by means of a sliding joint in a ceramic-to-metal seal, and was connected to the rack-and-pinion device that was used to raise and lower the electrode. The latter was situated immediately above the upper oven.

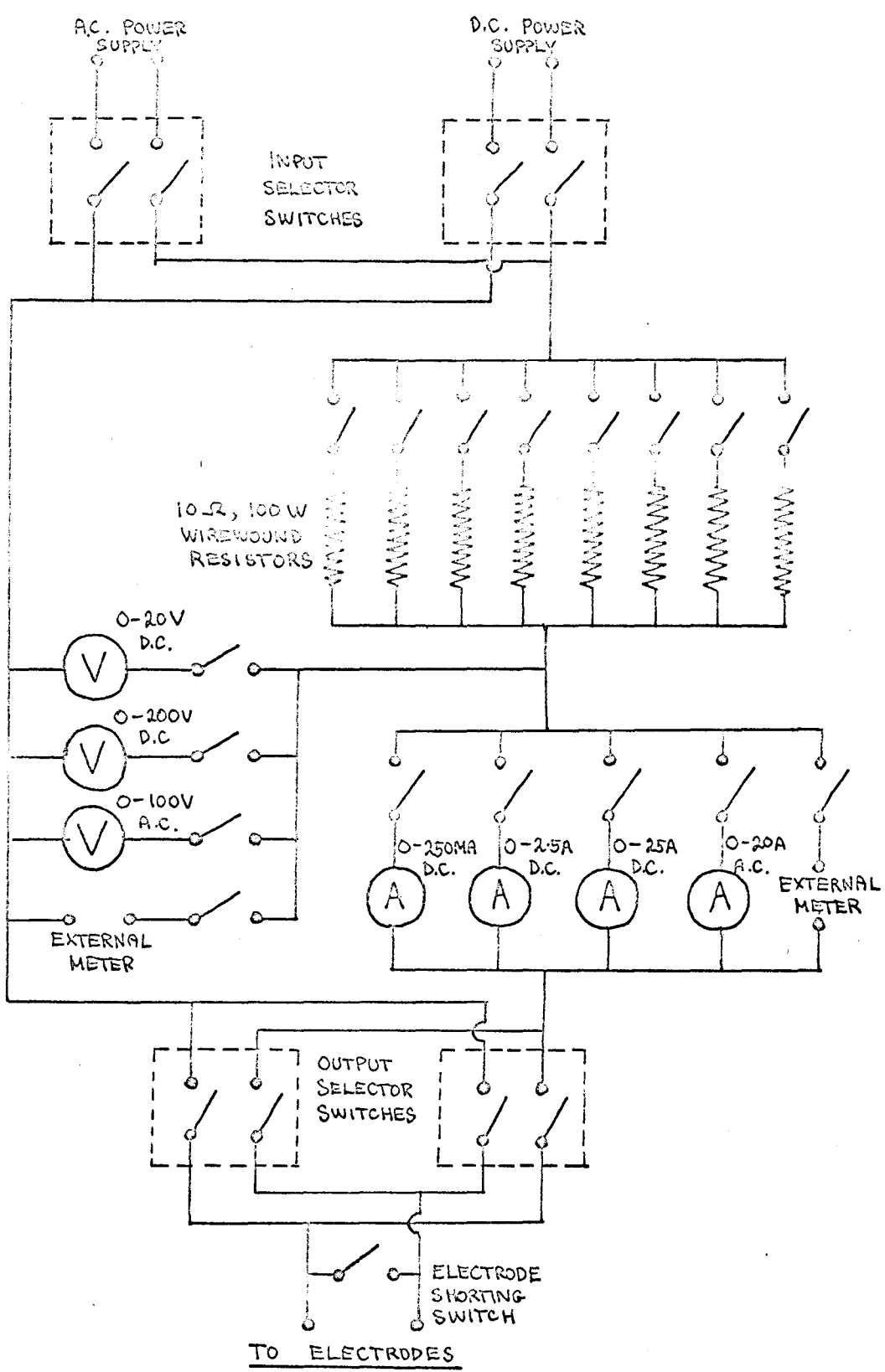
The ambient temperature in the electrode area was measured by four thermocouples, one of which was connected to the inner furnace thermostat. The other thermocouples were connected to

the temperature measuring circuit, as were all the other thermocouples that were not connected directly to thermostats. In the case of the Harwell apparatus, the temperature measuring circuit consisted of a 16 channel Kent recorder, which gave a continuous record of the temperatures of the different parts of the apparatus. In the case of the Aberdeen apparatus, the thermocouples were connected to a series of selector switches, which enabled any given thermocouple to be connected to a Honeywell potentiometer indicator.

In some of the author's experiments (notably the high-speed photographic work to be described in the next chapter) a fixed electrode facility was used. This was similar to the system shown in figure 3.9 except that the electrodes were mounted horizontally on the sides of the alumina cylinder in such a way that they were clearly visible through the viewing tube.

The circuit that was used to control the discharge current is shown in figure 3.10. The input selector switches were used to choose either the A.C. or the D.C. supply. The current control resistors were required to limit the discharge current, which, like that of a conventional arc, would otherwise have become uncontrollable. In general, only one resistor was used, but when a very high current was required, more were added in parallel. The various ammeters and voltmeters that were employed in the study of the discharge covered the current and voltage ranges of interest, and the fact that they were connected into the circuit through individual switches meant that the full current range could

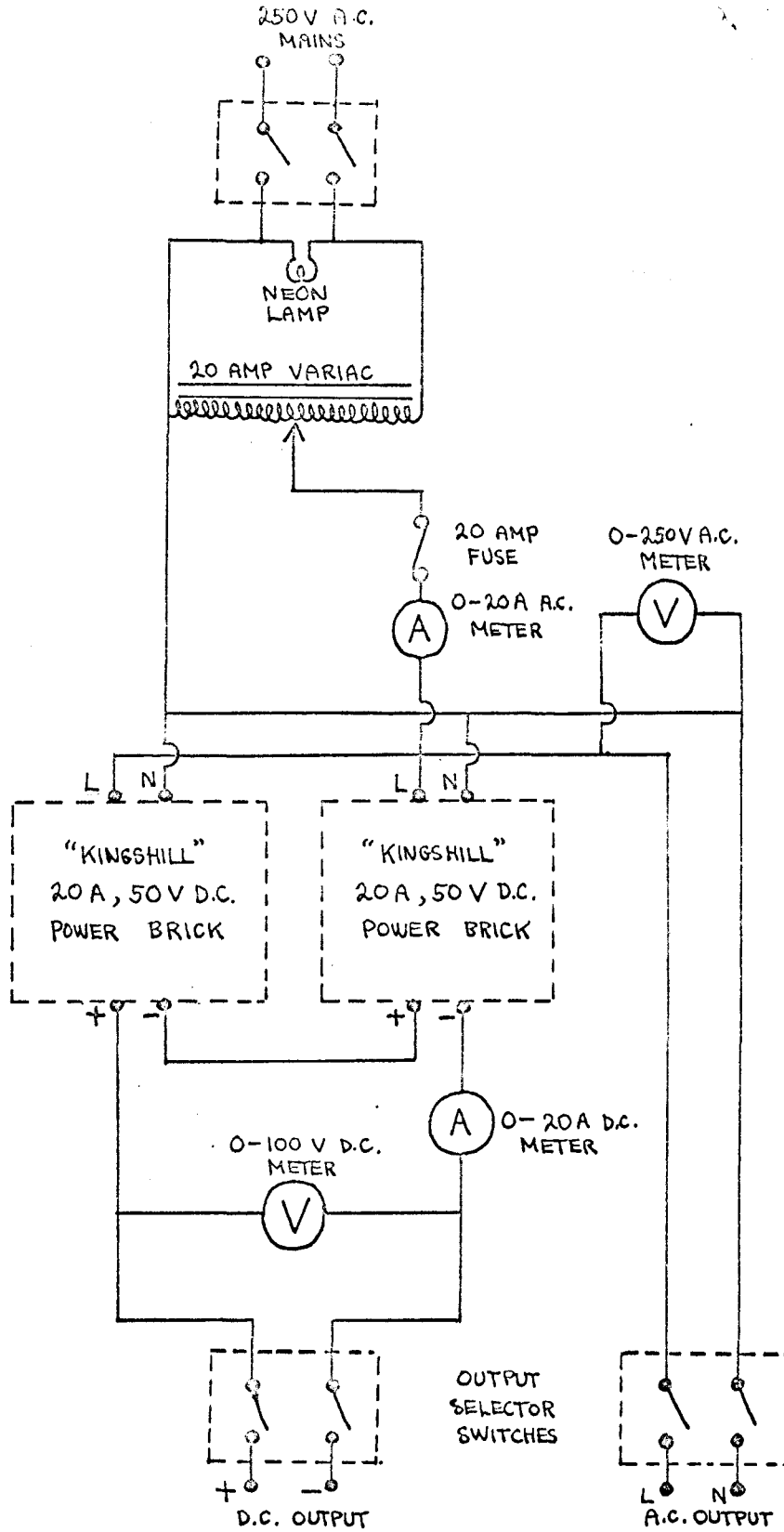
FIGURE 3.10 THE ELECTRODE CIRCUIT



be studied without breaking the electrode circuit and interrupting the discharge. This represented a great improvement over Ralph's original apparatus, in which two avometers were used to measure the discharge current and voltage. The presence of the output selector switches enabled the polarity of the electrodes to be rapidly reversed in the course of an experiment. The electrode shorting switch was used for testing the circuit for continuity.

In Ralph's apparatus, the current of the D.C. discharge was drawn from a battery of 40 lead accumulators connected in series. The main drawbacks of this system were that the voltage could only be varied by two volt steps, and could not be varied while the discharge was actually operating. To overcome these deficiencies, which greatly limited the extent to which the discharge could be studied, the author built a power pack capable of supplying direct currents of up to 20 amps, a power pack whose output voltage could be varied continuously throughout the range 0 - 100 volts. The circuit for this power pack is shown in figure 3.11. Its main components were two Kingshill power bricks, each capable of supplying 20 amps D.C. at an output voltage of 50 volts when connected to the 250 volt mains. These had their inputs connected in parallel to the output of the 20 amp variac that was used to control the discharge current, and had their outputs connected in series, thus doubling the maximum output voltage that could be obtained from a single power brick. The power pack was also capable of supplying alternating current, this being taken straight from the output of the control

THE A.C.-D.C. POWER PACK CIRCUIT



variac; the A.C. voltage could therefore be continuously varied from 0 - 250 volts, and the maximum current that could be drawn was 20 amps.

3.5 THE MATERIALS USED IN THE EXPERIMENTS

The three diluent gases that were used by the author were helium, neon and argon, all three gases being available in cylinders from the British Oxygen Company. The gases were all of the highest available purity, the impurity levels being as follows:

- helium - less than 20 parts per million
- neon - less than 100 parts per million
- argon - less than 50 parts per million

The three seed metals used were sodium, potassium and caesium, all being of ordinary laboratory reagent quality. The sodium and potassium were supplied in the form of slugs, and were delivered in oil-filled aluminium cylinders, each containing 100 gm of the metal. The caesium, on the other hand, was supplied in glass ampoules, each containing 5 gm of the metal, and was considerably more expensive than either potassium or sodium. For this reason, most of the author's work was carried out using potassium as the seed metal.

CHAPTER 4THE EXPERIMENTAL PROCEDURE4.1 THE PREPARATION AND WARMING UP OF THE APPARATUS

In all the experiments carried out by the author, the same basic procedure was adopted. This consisted of three main processes, namely (1) the preparation and warming up of the apparatus, (2) the experimental measurements, and (3) the shutting down of the apparatus. These will now be described in turn.

The day before an experimental run was to be carried out, the electrode assembly was removed from the apparatus, dismantled, and cleaned. The electrodes had to have their working surfaces renewed after every experiment, since they became coated with a thin layer of greenish-coloured contamination, probably caused by a reaction between the alkali metal and one of the constituents of the stainless steel. This contamination was removed using a file, and the surface was then polished to a mirror finish using a draw file and chalk. The electrode system was assembled, care being taken to ensure that all the wires and thermocouples were correctly positioned. The top plate of the apparatus, with the electrode system attached, was then bolted into position, and the outer insulation that surrounded the various tubes and wires that emerged from the top of the upper oven arranged in position. When the top electrode had been connected to its winding mechanism, and the latter had been checked for smooth working, the electrode system was tested for continuity and for possible shorts to earth using

an avometer. The p.v.c. tube that served as an exhaust pipe for the seeded rare gas was now checked for possible blockages, since quite large pieces of alkali metal were sometimes found to accumulate inside it in the course of a long experimental run; the tube was then attached to the apparatus.

The interior of the seeding trap was now rinsed with acetone to ensure that none of the water which had previously been used to dissolve the unused alkali metal remained in the trap, and was then thoroughly rinsed with sodium-dried diethyl ether. A protective face mask was worn during the next operation - the loading of the trap with alkali metal. The loading procedure depended on which seed was being used. In the case of sodium and potassium, which were supplied in cylindrical slugs, two or three slugs (weighing approximately 20 gm) were removed from their oil-filled container and were thoroughly washed in a beaker of ether. The slugs were then transferred to a clean beaker of ether, and were cut up into small pieces, using a scalpel. The pieces were dropped into the trap, which was partly filled with ether in order to prevent the seed metal from oxidising. The trap was then bolted into position, and the lower oven slid forward, the upper tube that led to the trap being passed through a hole in the back of the oven; the p.v.c. diluent supply tube was then attached to this tube.

In the case of caesium, which ignites spontaneously on contact with air, a different loading procedure was adopted. In this case, the diluent supply pipe was attached to the trap after

the latter had been rinsed with ether, and the trap was filled with argon. The caesium was supplied in 5 gm ampoules, two of which were used per run. The tops of the ampoules were nipped off with pliers, and the ampoules quickly inverted and dropped into the trap, which was then bolted into position as before, the diluent supply pipe only being disconnected from the trap for the short time necessary to slide the lower oven into position.

When the seeding trap had been loaded and bolted into position and the oven door closed, the diluent flow rate was set at $\frac{1}{2}$ litre per minute. The oven heaters were switched on, the lower oven thermostat being set at 100°C, and the upper oven inner furnace thermostat at 200°C. The apparatus was now left overnight to allow all the air and ether vapour to be removed from the seeding trap and electrode vessel by the flow of rare gas.

Next morning, with the apparatus filled with pure rare gas, the apparatus was ready to be taken up to its operational temperature. The lower oven thermostat was set at the temperature corresponding to the required seed pressure (see figure 3.5), and the inner furnace thermostat at the required electrode temperature. In order to reach an electrode temperature of 950°C and a trap temperature of between 300 and 400°C, the heating process took roughly two hours, the diluent flow rate being kept at $\frac{1}{2}$ litre/min. throughout. When the electrode system and seeding trap had reached their required temperatures, the following checks were carried out.

- (1) The electrode system was checked for short circuits and leaks to earth.

- (2) The top electrode winding device was checked for smooth running.
- (3) The electrodes were touched together, and the pointer on the winding device set at zero.
- (4) The electrode circuit was set up and tested.

The experiment could now proceed.

4.2 THE EXPERIMENTAL MEASUREMENTS

In nearly all the author's experiments, the following basic measurements were carried out. (a) The breakdown voltage was measured at different electrode spacings. (b) Plots of electrode voltage against electrode spacing were made at different discharge currents. (c) The positive column diameter was measured at different discharge currents. Let us discuss how these measurements were carried out, and show how further information about the discharge could be obtained from them.

(a) The measurement of the breakdown voltage.

The breakdown voltage was measured using a moving coil voltmeter connected across the electrodes (see figure 3.10). The electrode separation was set at the required spacing, and the output voltage of the D.C. power supply increased steadily until the gas broke down, i.e., underwent the transition from a low-current dark discharge to the high-current discharge under study. The voltage was then immediately lowered, so that the discharge reverted to the low-current state, and the system was left for a few moments to allow the effects of any heating that might have occurred to disappear. The voltage was then raised to a few volts below the point at which breakdown had occurred, and the last part

of the approach to breakdown carried out very slowly so that an accurate measurement of the breakdown voltage could be obtained. If there was any doubt about the result, the measurement was repeated. The breakdown voltage was generally measured at set electrode spacings (1, 5, 10, 15, 20 and 25 mm with argon as diluent, and 1, 2, 3, 4, 5 and 6 mm with helium as diluent), and a plot of breakdown voltage against spacing made as the results were obtained, so that any dubious results could be checked at once. The results of the author's breakdown voltage measurements are given in Chapter 5.

(b) The electrode voltage/electrode spacing plots.

All the information about the dependence of the positive column field and cathode fall of the high current D.C. discharge on the experimental conditions was obtained by plotting electrode voltage against electrode spacing at different currents. This required two people, one to operate the electrode winding mechanism, and the other to control the discharge current. The electrode spacing was set at 1 mm, and the applied voltage increased until breakdown occurred. The discharge current was set at the required value, and the electrode voltage noted. With argon as the diluent gas, the winding mechanism operator then increased the electrode spacing to 5 mm, the current being kept constant by increasing the applied voltage, and the new electrode voltage was noted. The process was repeated for spacings of 10, 15, 20 and 25 mm. With helium as diluent, the spacings at which the measurement was carried out were 1, 2, 3, 4, 5 and 6 mm. In both cases, the results were plotted on graph paper as they were obtained, a method that enabled immediate repetition of any dubious result to be carried out.

The plot was made at currents of $\frac{1}{8}$, $\frac{1}{4}$, $\frac{1}{2}$, 1, 2, 4, 8 and 16 amps, or at as many of these currents as the conditions allowed. Typical results are given in figures 4.1 and 4.2, the first set being for 3.5 torr of potassium in argon at an ambient temperature of 950°C, and the second set being for 3.5 torr of potassium in helium at an ambient temperature of 950°C.

In all cases, it was found that the plots were straight lines that had a positive slope and a positive intercept on the voltage axis. Measurement of the slope thus enabled the value of the positive column field to be deduced, and the fact that the plots were straight lines showed that this field was independent of the electrode spacing. In deducing the value of the column field in this way, it was assumed that the column field was uniform throughout the inter-electrode space, an assumption that was shown to be correct by the work of Evans (1967), who extended the author's work to a moving gas system, and obtained probe profiles of the discharge which showed that the positive column field was indeed uniform. The results of the author's measurements of the column field are given in Chapter 6.

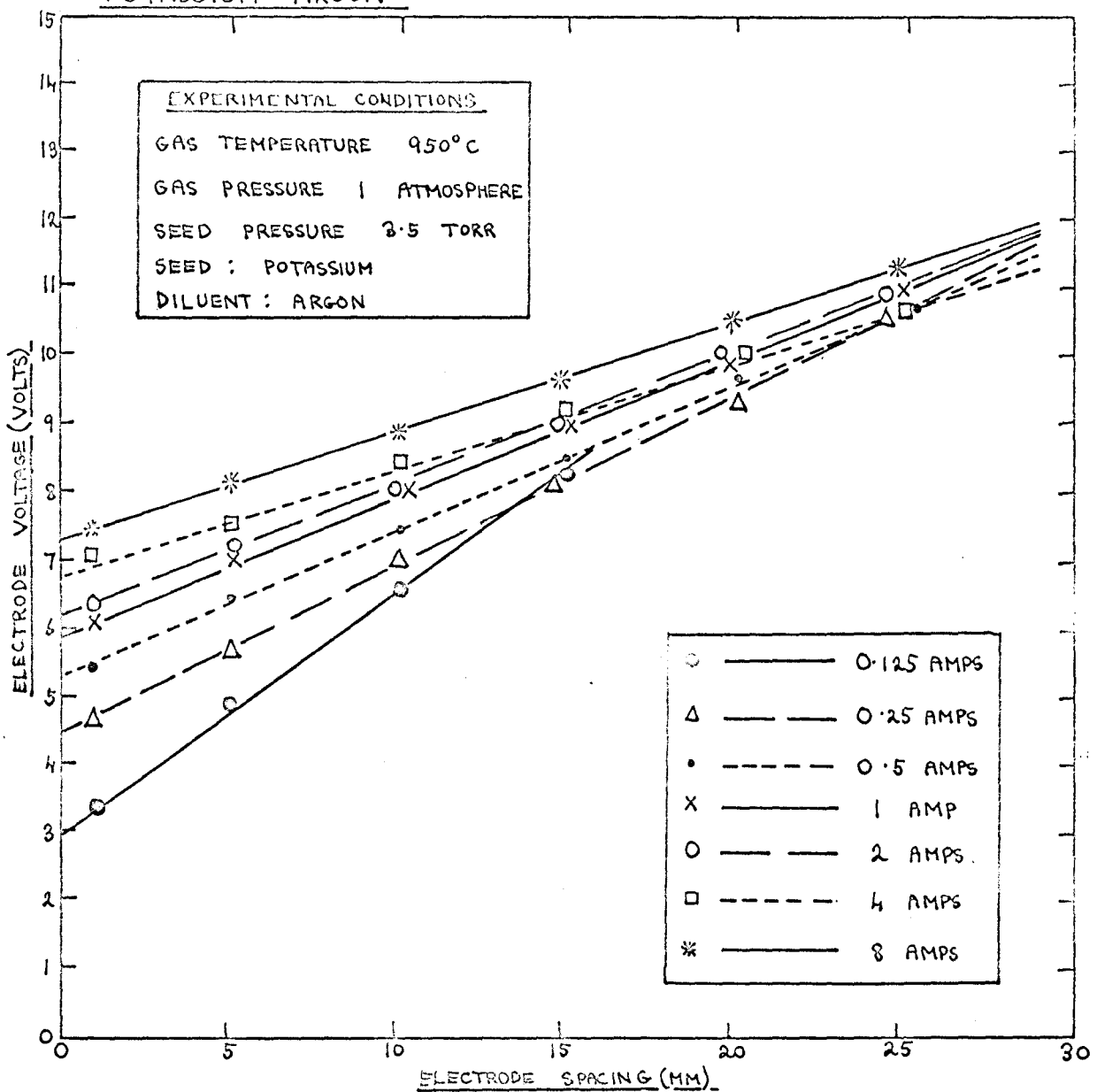
The second property of the discharge that could be deduced from the voltage/spacing plots was the total electrode voltage drop. When the author started work on the discharge, this was thought to occur almost entirely at the cathode, and the author subsequently carried out probe measurements which confirmed that this was the case. The results of the author's measurements of the cathode fall are given in Chapter 7.

(c) The measurement of the positive column diameter.

The diameter of the positive column of the high-current discharge

FIGURE 4.1

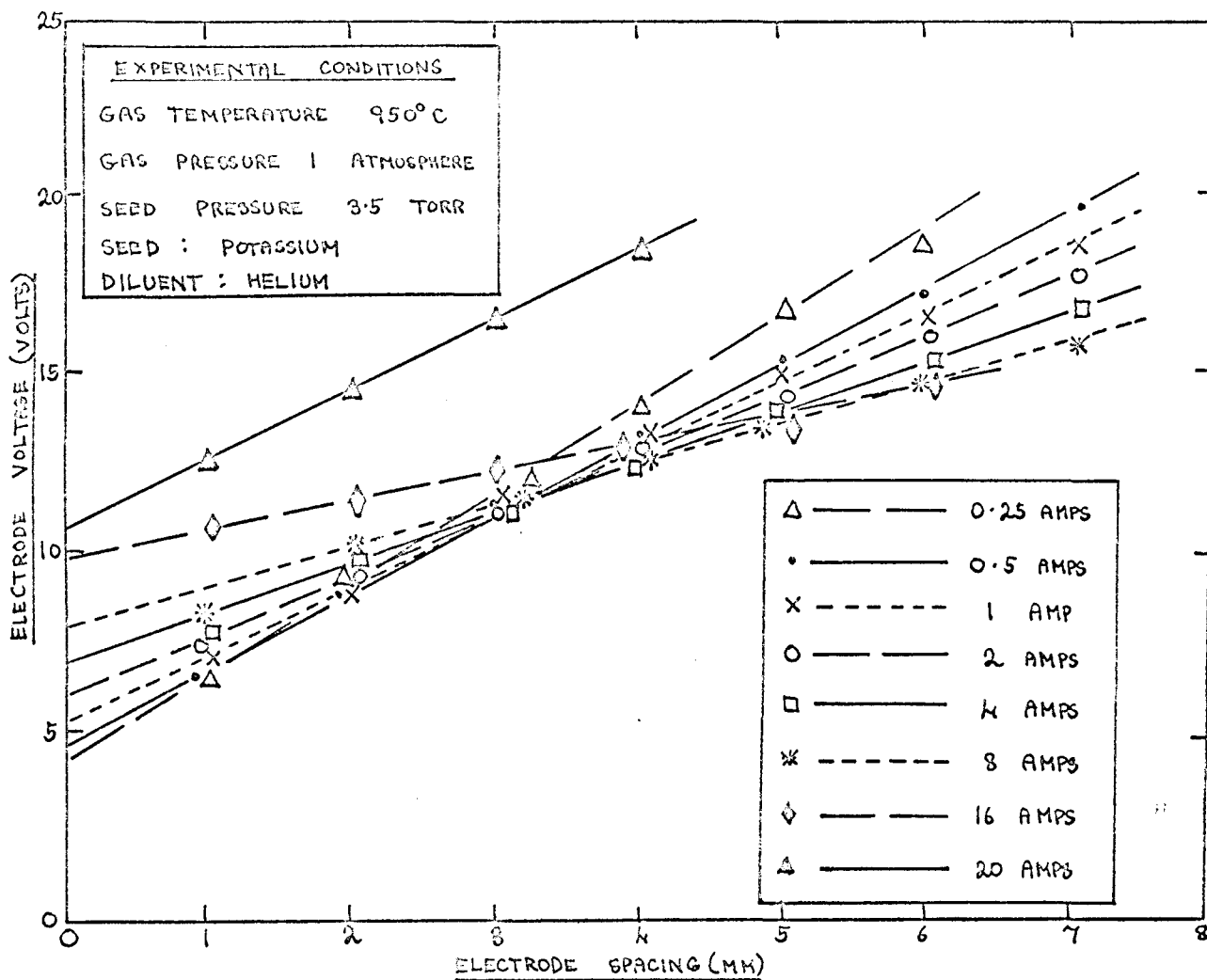
A TYPICAL SET OF PRIMARY EXPERIMENTAL RESULTS FOR POTASSIUM-ARGON



DISCHARGE CURRENT	POSITIVE COLUMN DIAMETER
0.125 AMPS	2 MM
0.25 AMPS	2.5 MM
0.5 AMPS	3.5 MM
1 AMP	5 MM
2 AMPS	7 MM
4 AMPS	9 MM
8 AMPS	10 MM

ELECTRODE SPACING	BREAKDOWN VOLTAGE
1 MM	11 V
5 MM	24 V
10 MM	40 V
15 MM	55 V
20 MM	70 V
25 MM	85 V

A TYPICAL SET OF PRIMARY EXPERIMENTAL RESULTS FOR
POTASSIUM-HELIUM



DISCHARGE CURRENT	POSITIVE COLUMN DIAMETER
0.25 AMPS	2 MM
0.5 AMPS	3 MM
1 AMP	4 MM
2 AMPS	6 MM
4 AMPS	8.5 MM
8 AMPS	10 MM
16 AMPS	10 MM
20 AMPS	10 MM

ELECTRODE SPACING	BREAKDOWN VOLTAGE
1 MM	12V
2 MM	28V
3 MM	43V
4 MM	51V
5 MM	78V

was measured by the following technique. A scale was constructed, showing the top electrode (which was $\frac{1}{2}$ inch in diameter) calibrated in mm, and the diameter of the column was compared visually with the diameter of the top electrode, using the scale as a guide. This measurement was made possible by the fact that the top electrode and positive column were both clearly visible through the viewing tube provided that the electrode separation was not too great. Several observers carried out independent measurements of the same column diameters using this technique, and the results indicated that the absolute value of the visible diameter of the positive column could be measured to within an accuracy of $\pm 10\%$ for currents up to 5 amps. At currents greater than 5 amps, the column boundary became much less well-defined, and the error in the value of the column diameter became considerably greater. The results of the author's measurements of the column diameter are given in Chapter 6.

Once a complete set of the above measurements had been taken, the value of the quantity which was being varied on that particular day (either the ambient gas temperature or the seed pressure) was altered, and the system allowed to re-settle before the measurements were repeated. This procedure was repeated until the desired range of gas temperature or seed pressure had been investigated.

When the gas temperature was being varied, the measurements were first carried out at the highest temperature to be studied (950°C in all cases), and the temperature was then taken down by 50 degree steps until results became unobtainable.

When the seed pressure was being varied, on the other hand,

the opposite procedure was adopted, the measurements being first carried out at the lowest seed pressure to be studied, and the seed pressure being increased throughout the day. When very low seed pressures were to be studied, the apparatus had to be thoroughly outgassed to ensure that no alkali metal remained in the electrode area from previous experiments. This was done by loading the seeding trap two days before the experimental run was to be carried out, taking the upper oven up to its operating temperature, and passing pure rare gas through the hot apparatus for roughly 36 hours.

With potassium as seed, it was possible to extend an experimental run through several successive days, provided that the seed pressure employed was not too high. At a seed pressure of 3.5 torr, for example, the mass flow rate of potassium from the seeding trap was only of the order of 0.1 gm per hour, so that the 20 gm of potassium originally placed in the trap allowed the experiment to continue for approximately 200 hours. At higher seed pressures, the seed lasted for a correspondingly shorter time, and when very high seed pressures were being investigated, care had to be taken to ensure that the supply of seed did not run out in the course of the experiment. With caesium as seed, it was not generally possible to extend an experimental run to longer than a single day, because the seed was used up much more quickly than in the case of potassium. This was partly due to the fact that a smaller quantity of metal was used (mainly because of the extremely high cost of caesium), and partly due to the high atomic weight of caesium, which meant that the mass flow rate needed to maintain a

given seed pressure was over three times as high as for potassium. When working at high caesium pressures, particular care had to be taken to ensure that the supply of caesium would last long enough to allow the experiment to be completed.

4.3 THE SHUTTING DOWN OF THE APPARATUS

When a day's experimental work had been completed, the procedure that was adopted depended on whether or not the run was to be continued on the following day. If it was, the seeding oven was allowed to cool to 100°C, the electrode area to 200°C, and the system left overnight, the diluent flow rate being kept at $\frac{1}{2}$ litre/min. If the apparatus was to be dismantled and cleaned, on the other hand, it was allowed to cool down to room temperature, the gas flow being stopped once the temperature in the electrode area had fallen below 500°C, as there was then no danger of the stainless steel oxidising. The apparatus was generally allowed to cool down overnight.

Next day, the lower oven was opened and slid back, and the seeding trap unbolted. The trap was taken to an open space outside the building, well away from cars, trees or other buildings, and water was carefully sprinkled onto it from a safe distance by means of a hose pipe in order to dissolve the unused seed metal. If the operation was performed extremely carefully, loud explosions could generally be avoided, but if an appreciable amount of alkali metal remained in the trap, a vigorous reaction was inevitable. When the smoke and flames had stopped emanating from the trap, it was thoroughly soaked both internally and externally, emptied,

and dried, a hot air hose being used to speed up the latter process. A protective face mask was worn throughout the entire operation of removing and cleaning the trap.

4.4 HIGH SPEED PHOTOGRAPHIC WORK

In September 1963, the author attempted to obtain high-speed films of the potassium-argon discharge, the photographic work being carried out by the Photographic Group of A.E.R.E., Harwell. The apparatus of Ralph was used, and although films were obtained, they were in black-and-white and were of poor quality. This was partly due to the fact that the supporting framework of the apparatus prevented the camera lens from being placed close to the viewing window, and partly because the viewing hole was only 1 cm in diameter, thus greatly restricting visibility. Shortly afterwards, the author started to build the apparatus described in the last chapter, and one of the design requirements was that the apparatus had to be capable of producing good quality colour films of the discharge. Accordingly, the apparatus was provided with a one-inch-bore viewing tube, and the supporting framework was designed so that the camera could have its lens hard up against the window of the tube. Using the new apparatus, two sets of colour films were taken of AC and DC discharges in potassium-seeded argon. One set was taken at 150 frames/sec., and the other at 2500 frames/sec., using an ultra-high-speed camera. These films provided a great deal of information about the discharge, particularly about the nature of the two cathode mechanisms

(see Chapter 7), and about the build-up of the cathode sheath that precedes the breakdown of the gas (see Chapter 9).

The electrode system that was used in the photographic work consisted of two $\frac{3}{4}$ inch diameter stainless steel electrodes mounted 1 cm apart in the fixed electrode facility described in section 3.4. The current was led to the electrodes by 12 s.w.g. platinum wire, as it was desired to pass very large currents, and copper wires had been found to melt during extended, high-current runs with the fixed electrode facility.

4.5 SPECTROSCOPIC WORK

In an attempt to obtain information about the nature of the discharge under study, the author carried out a spectroscopic investigation of the potassium-argon discharge. A standard Hilger-Watt constant deviation prism spectrometer fitted with a plate camera was used in the work, the plates being Ilford H.P.3. Spectra of both the diffuse and constricted forms of the discharge were taken, the exposure times in the two cases being respectively $1\frac{1}{2}$ hours and 1 minute. Neon, argon and mercury spectra were taken on the same plate in order to calibrate it. The positions of the lines were measured by means of a travelling microscope, and a calibration curve relating wavelength to position was drawn using the lines of the three known spectra; this enabled the wavelengths of the unknown lines to be determined. The identification of the unknown spectra was facilitated by assigning to each line a number corresponding to its apparent intensity, as shown by

the degree of blackening of the plate. The intensities were given on a 0 - 10 scale, 0 corresponding to a line that was only just visible, and 10 to the brightest line present. The Handbook of Physics and Chemistry, which gives the wavelengths and relative intensities of the lines of the various elements, was used in the identification.

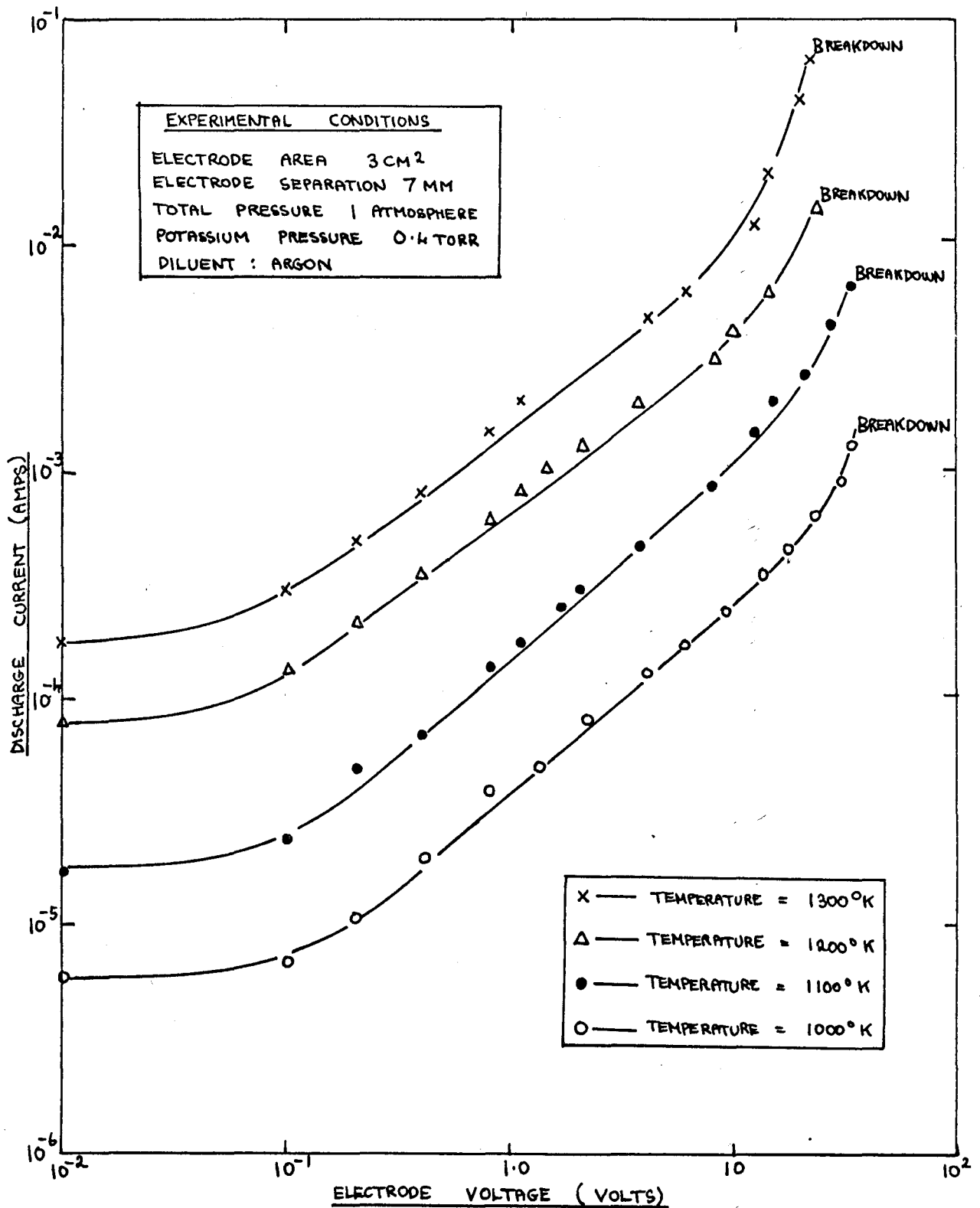
Using the technique described above, it was shown that the main lines that were present in the spectrum of the form of the discharge with the diffuse cathode sheath were those of the seed metal. The lines of the diluent gas could not be detected, thus confirming that the diluent gas took no active part in the conduction of electricity, since it showed that the diluent atoms were not even excited, let alone ionised.

The spectrum of the form of the discharge with the constricted arc spot was completely different. In this case, the main lines were those of chromium and manganese, two metals that were present in the stainless steel of which the electrodes were made. The lines of the seed metal were also present, but the lines of the diluent gas could not be detected. The presence of strong chromium and manganese lines confirmed that the constricted form of the cathode mechanism was a conventional thermionic arc spot (see Chapter 7).

CHAPTER 5THE BREAKDOWN OF THE GAS5.1 THE EVENTS LEADING UP TO BREAKDOWN

When a small voltage is applied between two electrodes immersed in a hot rare gas-alkali metal vapour mixture, a small current (generally in the microamp or milliamp range) is found to flow. As the applied voltage is increased, the current rises, until at a certain critical voltage, the gas breaks down, and the discharge changes from a low-current dark discharge to the high-current discharge that is the subject of this thesis. Typical pre-breakdown current/voltage characteristics are shown in figure 5.1, which shows results obtained by Sakuntala (1965) at different temperatures in argon seeded with 0.4 torr of potassium. The current is seen to be linearly dependent on the applied voltage through about two orders of magnitude of current, with the linear region of each plot eventually giving way to a region in which the slope increases steadily, becoming infinite at the actual point of breakdown. Similar pre-breakdown current/voltage results have been obtained by the author, and these have proved to be in good agreement with Sakuntala's work, but the main part of the author's work on the breakdown of the gas consisted of measurements of the actual breakdown voltage at different electrode spacings, seed pressures and ambient temperatures in a variety of seed-diluent mixtures. The remainder of this chapter deals exclusively with the results of these measurements.

PLOTS OF PRE-BREAKDOWN CURRENT AGAINST APPLIED VOLTAGE
AT DIFFERENT TEMPERATURES IN POTASSIUM-ARGON (SAKUNTALA 1965)



5.2 THE DEPENDENCE OF THE BREAKDOWN VOLTAGE ON THE ELECTRODE SPACING

It was found that for all the mixtures studied under all experimental conditions, the breakdown voltage was linearly dependent on the electrode spacing over a wide spacing range. This is illustrated in figures 5.2 - 5.4. Figure 5.2 shows plots of breakdown voltage against electrode spacing for a number of seed-diluent mixtures, the ambient gas temperature and seed pressure being 950°C and 3.5 torr in all cases. Figure 5.3 shows plots of breakdown voltage against electrode spacing for potassium-argon at different temperatures, the seed pressure being 3.5 torr throughout, while figure 5.4 shows plots of breakdown voltage against electrode spacing for different potassium pressures in argon, the ambient temperature being 950°C throughout. All the plots in these three figures are seen to be straight lines. An interesting point is that the plots do not pass through the origin, but cut the breakdown voltage axis at a small positive value that depends on the mixture and conditions. This will be discussed in Part II.

5.3 THE DEPENDENCE OF THE BREAKDOWN VOLTAGE ON THE SEED PRESSURE

The dependence of the breakdown voltage on the seed pressure is shown in figure 5.5, which shows plots of breakdown voltage against seed pressure for potassium in argon and helium, the electrode spacing and ambient temperature being 5 mm and 950°C.

FIGURE 5.2

LOTS OF BREAKDOWN VOLTAGE AGAINST ELECTRODE SPACING
FOR DIFFERENT MIXTURES

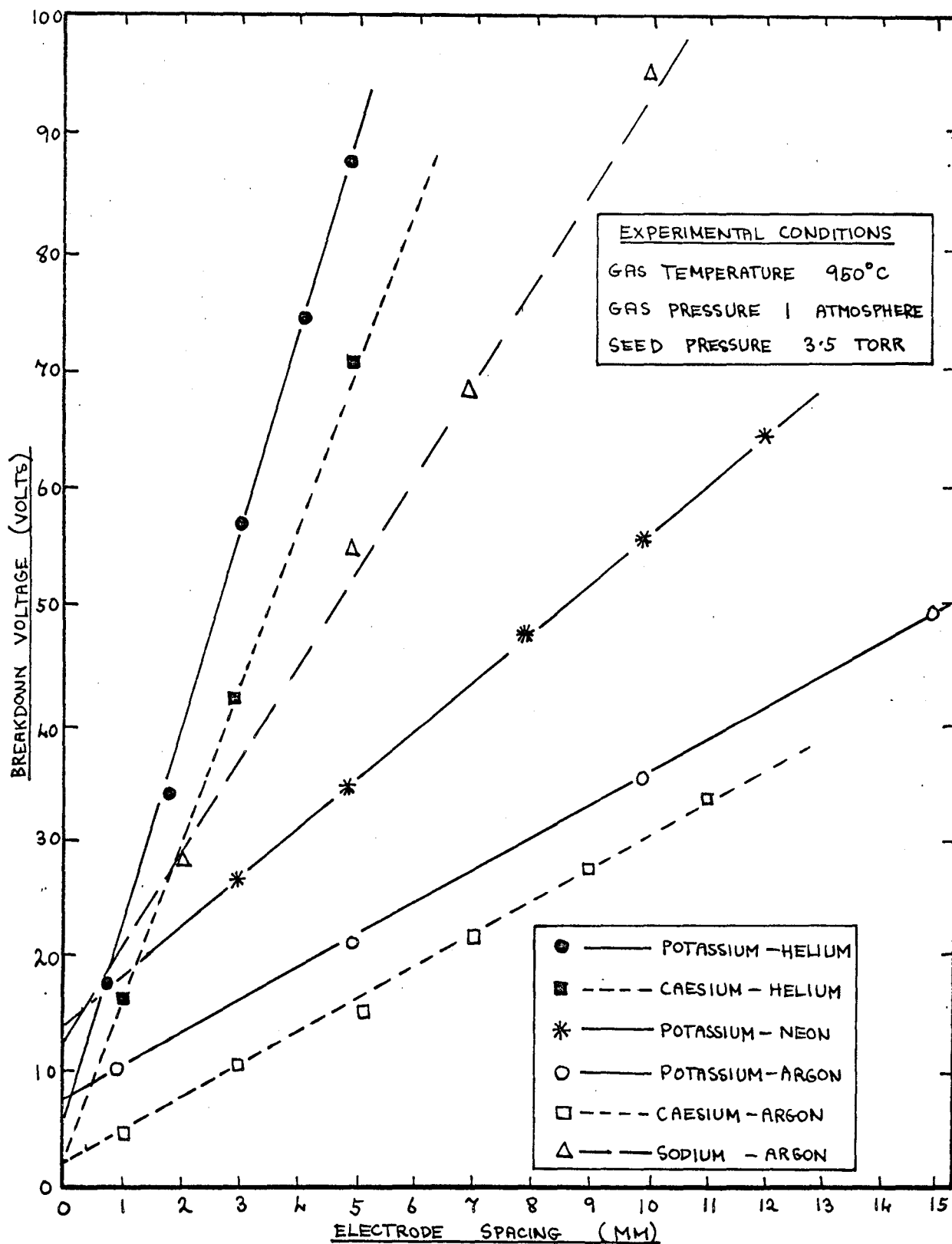


FIGURE 5.3

LOTS OF BREAKDOWN VOLTAGE AGAINST ELECTRODE SPACING
FOR POTASSIUM-ARGON AT DIFFERENT TEMPERATURES

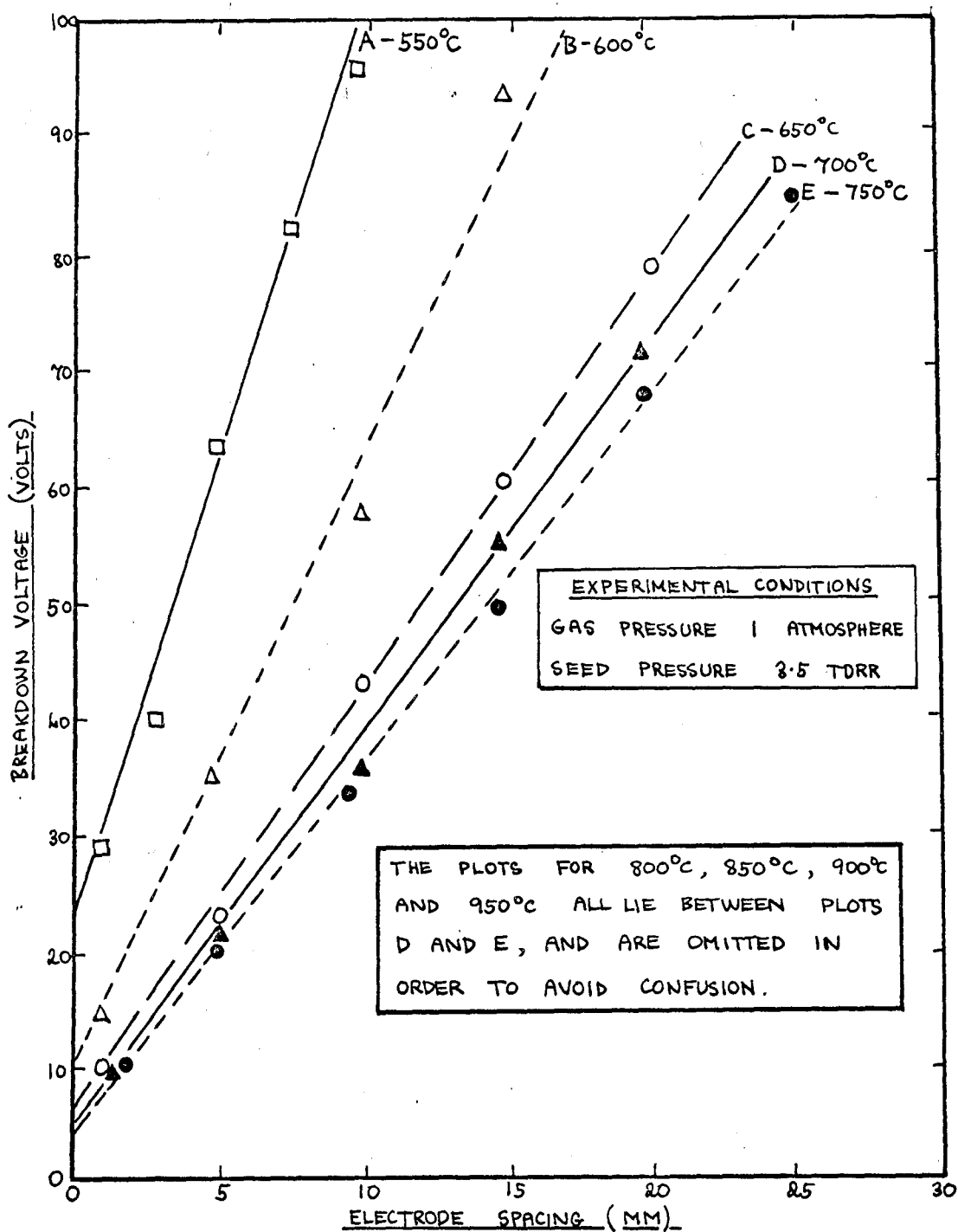
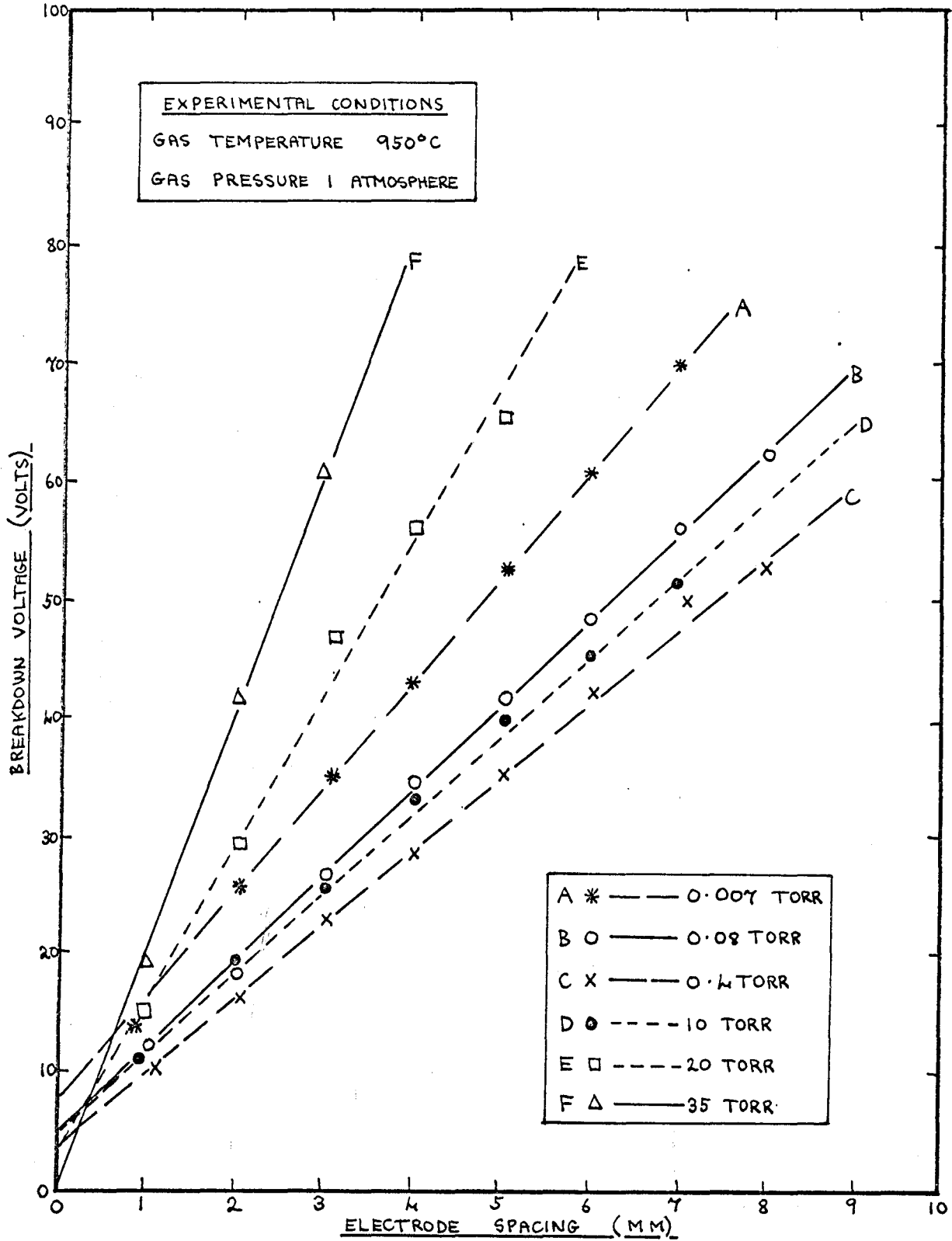
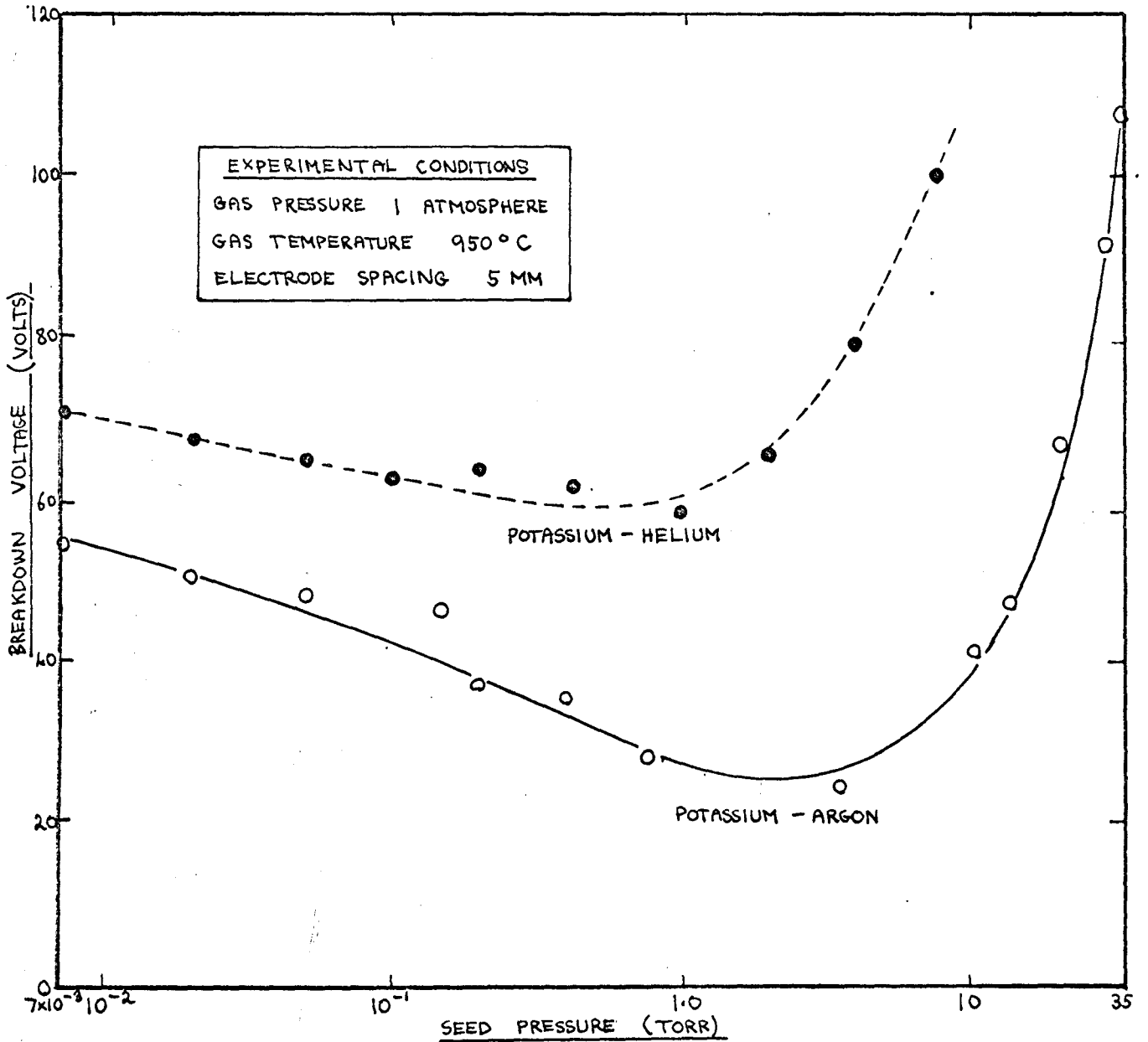


FIGURE 5.4

PLOTS OF BREAKDOWN VOLTAGE AGAINST ELECTRODE SPACING
FOR DIFFERENT POTASSIUM PRESSURES IN ARGON



PLOTS OF BREAKDOWN VOLTAGE AGAINST SEED PRESSURE FOR DIFFERENT MIXTURES



As the seed pressure rises from very low values, the breakdown voltage is seen to fall gradually, pass through a broad minimum, and then rise, eventually becoming linearly-dependent on the seed pressure (see figure 9.2).

5.4 THE DEPENDENCE OF THE BREAKDOWN VOLTAGE ON THE AMBIENT TEMPERATURE.

For all the seed-diluent mixtures studied, it was found that the breakdown voltage was practically independent of the gas temperature over a wide temperature range. This is illustrated in figures 5.6 and 5.7, the first of which shows plots of breakdown voltage against gas temperature for different electrode spacings in potassium-argon, the seed pressure being 3.5 torr throughout. It is seen that the breakdown voltage for a given spacing is practically constant down to a temperature of about 700 or 650°C, below which it begins to increase sharply, the rate of increase becoming greater as the temperature falls. In figure 5.7, plots of breakdown voltage against gas temperature are given for caesium- and potassium-argon and caesium- and potassium-helium, the electrode spacing and seed pressure being 5 mm and 3.5 torr. It is seen that the breakdown voltage is practically constant over a wide temperature range for all four mixtures, and that the increase in the breakdown voltage below 650°C that is observed with potassium as seed is not evident with caesium as seed.

PLOTS OF BREAKDOWN VOLTAGE AGAINST GAS TEMPERATURE
FOR DIFFERENT ELECTRODE SPACINGS IN POTASSIUM-ARGON

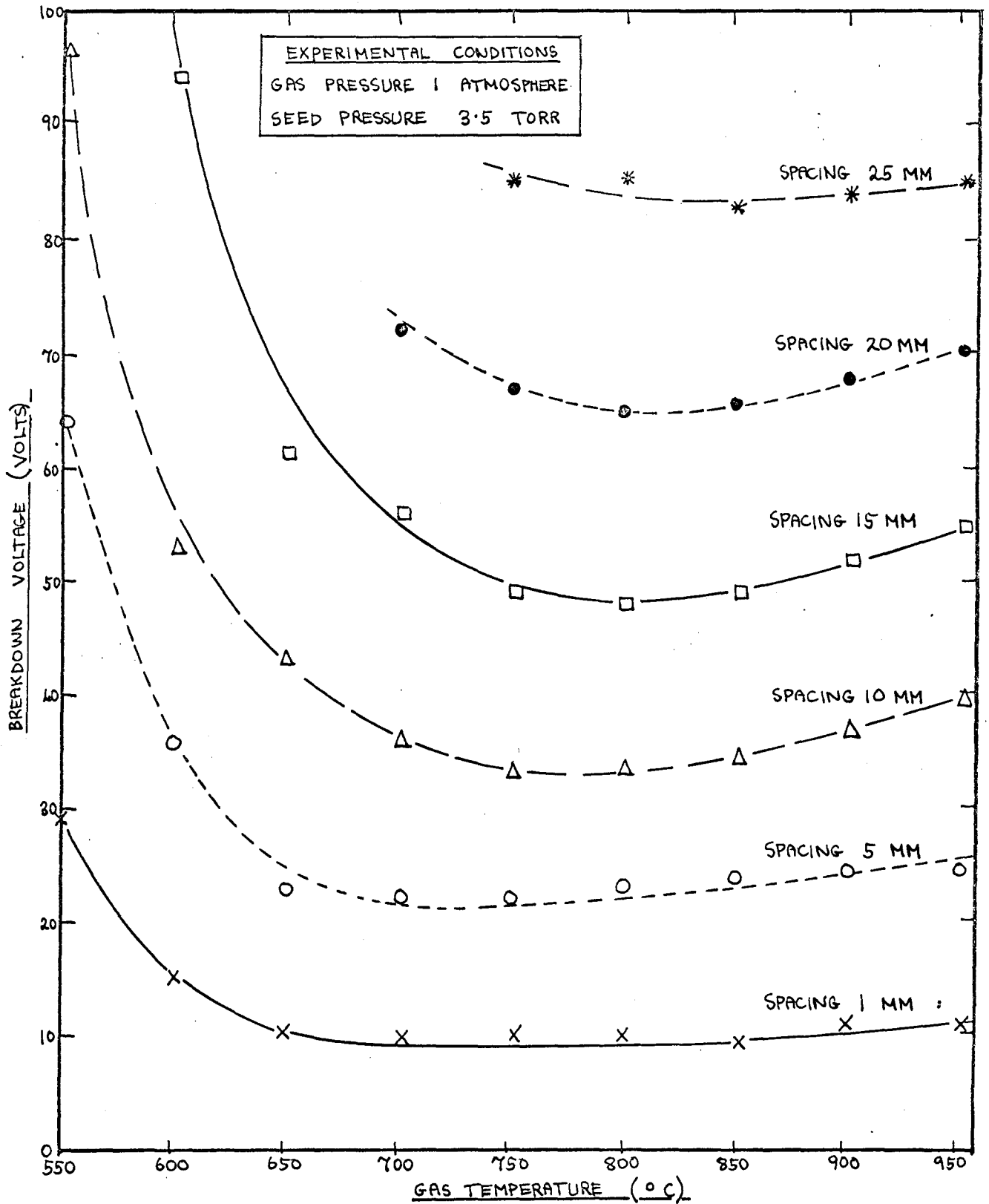
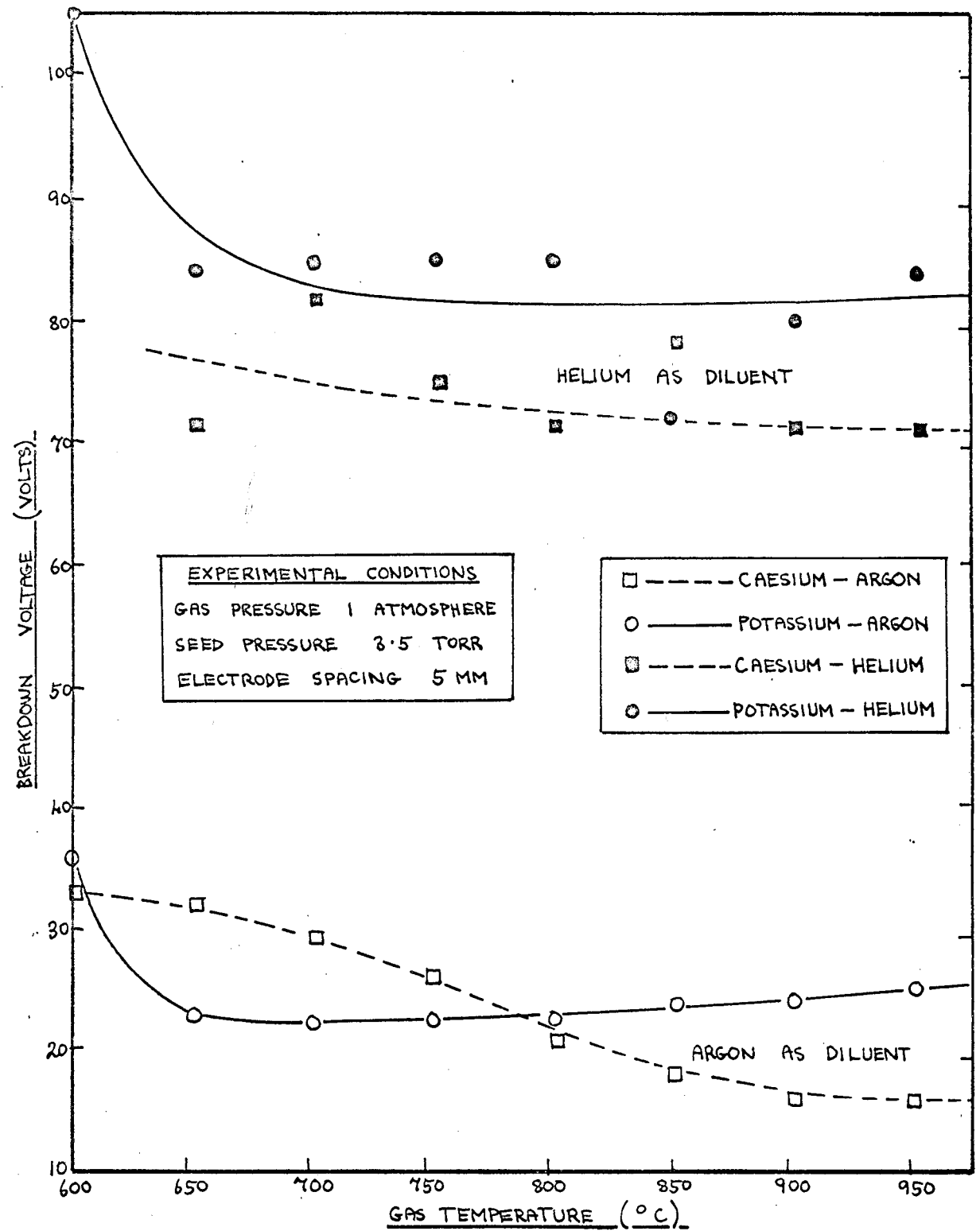


FIGURE 5.7

PLOTS OF BREAKDOWN VOLTAGE AGAINST GAS TEMPERATURE
FOR DIFFERENT MIXTURES



5.5 THE DEPENDENCE OF THE BREAKDOWN VOLTAGE ON THE CHOICE OF SEED METAL

For a given diluent, the breakdown voltage values with potassium as seed do not differ greatly from those with caesium as seed, the former generally being slightly higher, as is illustrated in figures 5.2 and 5.7. With sodium as seed, on the other hand, the breakdown voltage values appear to be two or three times higher than for caesium or potassium (see figure 5.2).

5.6 THE DEPENDENCE OF THE BREAKDOWN VOLTAGE ON THE CHOICE OF DILUENT GAS

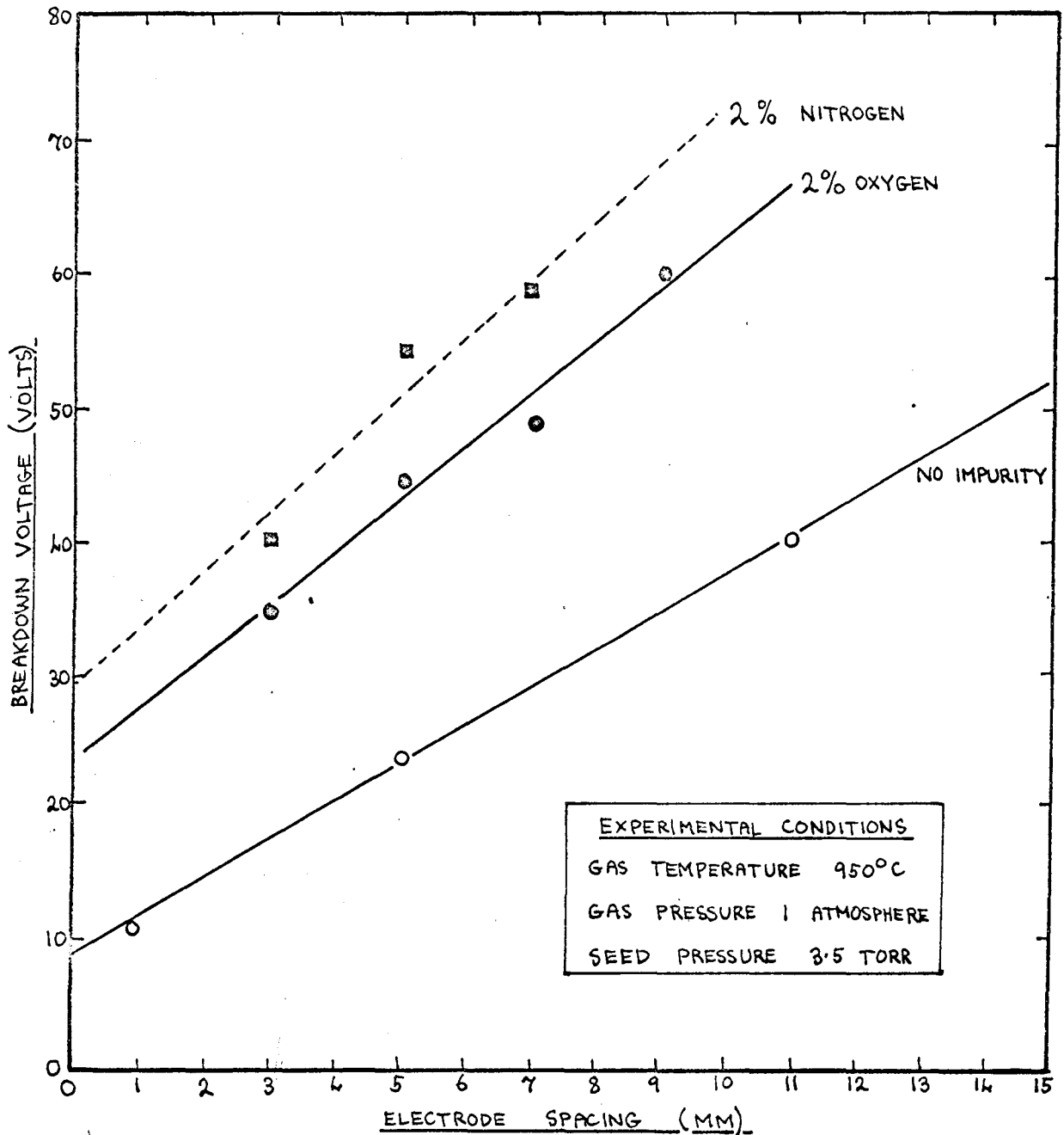
The choice of diluent appears to be a very important factor in determining the breakdown voltage, as is shown in figures 5.2, 5.5 and 5.7. For a given seed and constant experimental conditions, the breakdown voltage with helium as diluent is considerably higher than with argon as diluent, a result that agrees with the observations of Ralph (1962). Neon occupies an intermediate place between argon and helium.

5.7 THE EFFECT OF ADDED MOLECULAR IMPURITIES ON THE BREAKDOWN VOLTAGE

The effect of added molecular impurities on the electrical properties of alkali-metal-seeded rare gases was investigated by adding small, controlled amounts of oxygen and nitrogen to potassium-seeded argon (see section 6.6), and it was found that comparatively large amounts of impurity had to be added before any significant change in the breakdown voltage values occurred.

FIGURE 5.8

PLOTS OF BREAKDOWN VOLTAGE AGAINST ELECTRODE SPACING
FOR DIFFERENT MOLECULAR IMPURITIES IN POTASSIUM-ARGON



In figure 5.8, plots of breakdown voltage against electrode spacing are given for a 2 percent-by-volume impurity of oxygen and nitrogen, the plot obtained in the pure potassium-argon mixture being given for comparison. It is seen that both the slopes of the lines and the zero-spacing voltage intercepts are increased by the addition of the impurities. Nitrogen appears to have a somewhat greater effect than oxygen.

CHAPTER 6THE POSITIVE COLUMN OF THE DISCHARGE6.1 THE DEPENDENCE OF THE COLUMN PROPERTIES ON THE DISCHARGE CURRENT

We have seen in Chapter 2 that the cathode regions of the discharge under study are connected to the anode by a cylindrical positive column. The properties of this column and their dependence on the experimental conditions and choice of seed and diluent will now be described in detail.

The properties of the column are strongly dependent on the value of the discharge current. There appears to be a minimum current below which the column cannot exist, the value of this current depending mainly on the nature of the mixture through which the discharge propagates. Table 6.1 shows how this minimum current varies from mixture to mixture, the seed pressure and ambient temperature being 3.5 torr and 950°C in all cases. The diameter of the positive column at the minimum current is also given in the table, and is seen to have roughly the same value for all the mixtures studied. No corresponding upper limit to the column current was observed in any of the mixtures studied; indeed, the column appears to become progressively more stable as the current increases.

TABLE 6.1

MIXTURE	MINIMUM STABLE CURRENT	COLUMN DIAMETER AT MINIMUM CURRENT
SODIUM-ARGON	$\frac{1}{8}$ AMP	3 mm
POTASSIUM-ARGON	$\frac{1}{8}$ AMP	2 mm
CAESIUM-ARGON	$\frac{1}{4}$ AMP	2 mm
POTASSIUM-HELIUM	$\frac{1}{4}$ AMP	2 mm
CAESIUM-HELIUM	$\frac{1}{2}$ AMP	2 mm
POTASSIUM-NEON	$\frac{1}{4}$ AMP	2 mm

As the discharge current increases, the column properties are observed to change in the following manner.

- (1) The column expands steadily, its cross sectional area being roughly proportional to the discharge current over a wide current range.
- (2) The column core becomes steadily brighter, its luminosity increasing from a dull glow at low currents to an intense glow at the higher currents studied, and eventually becoming painful to look at.
- (3) The column electric field falls.

Figure 6.1 shows how the positive column field in the various mixtures studied depends on the discharge current. With potassium as seed, (curves B, E and F), the field falls steadily as the current increases, appears to reach a minimum value somewhere between 8 amps and 16 amps, and then begins to rise again.

PLOTS OF POSITIVE COLUMN FIELD AGAINST DISCHARGE CURRENT FOR DIFFERENT MIXTURES

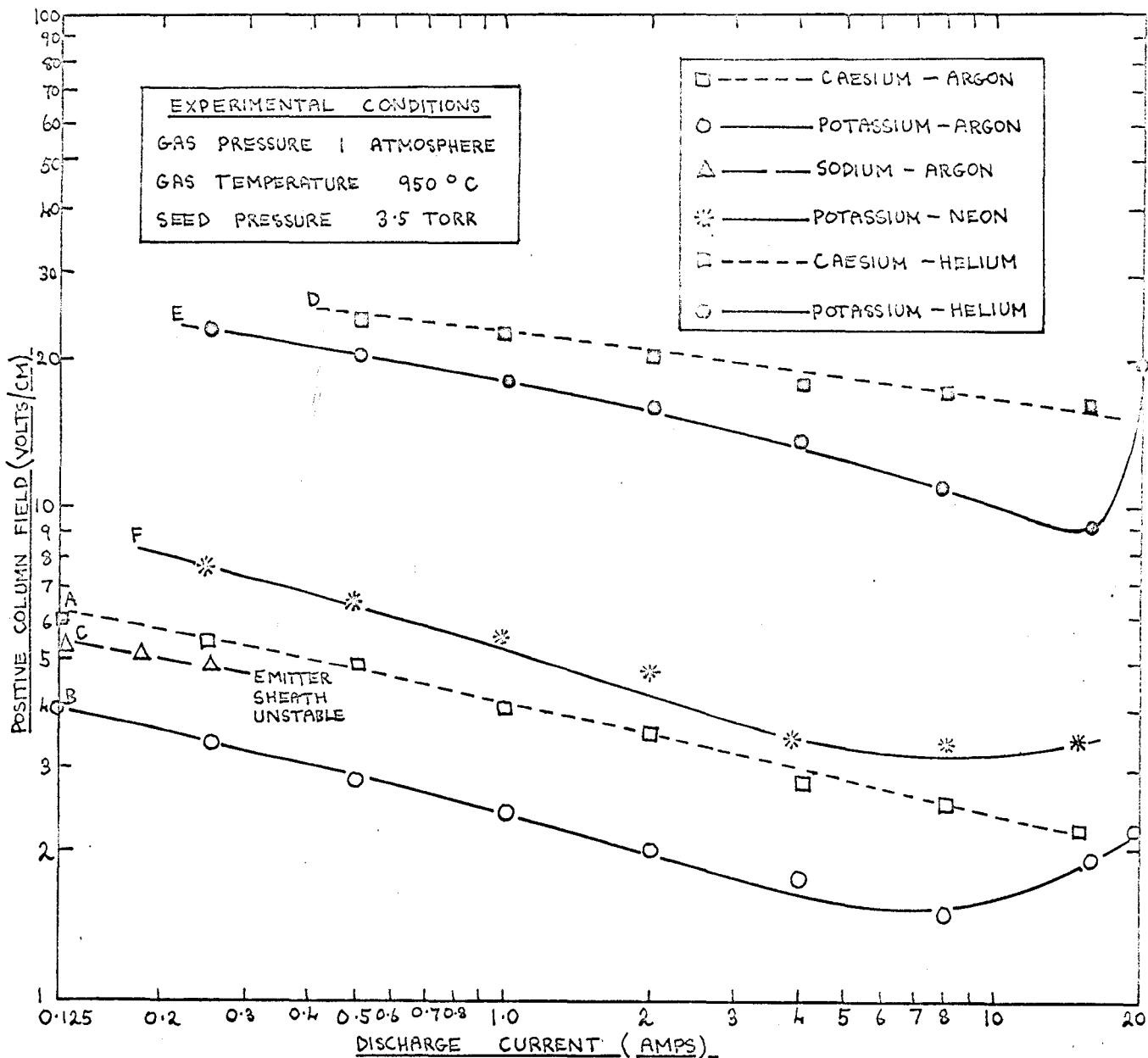


FIGURE 6.2

PLOTS OF SQUARE OF POSITIVE COLUMN DIAMETER AGAINST
DISCHARGE CURRENT FOR DIFFERENT MIXTURES

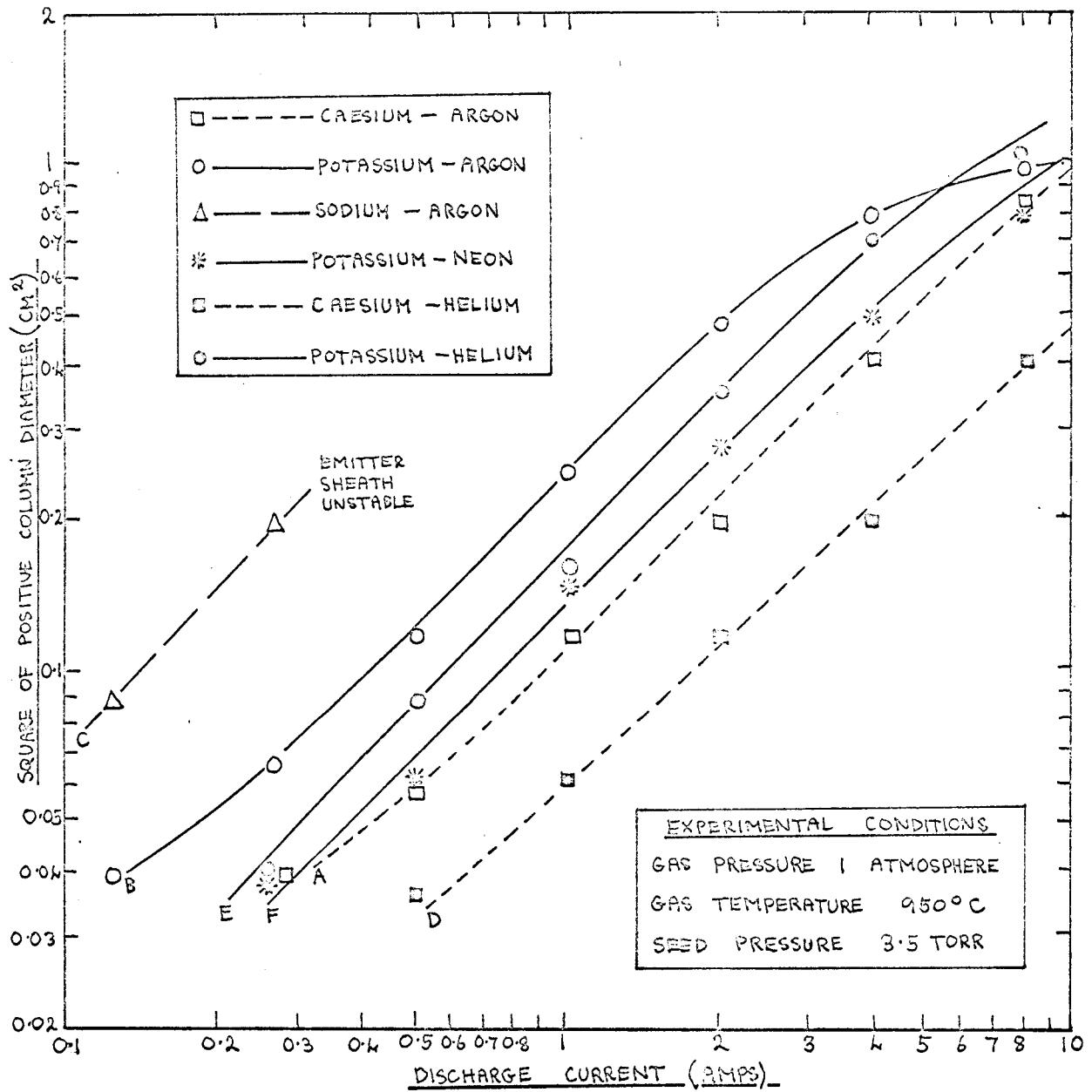
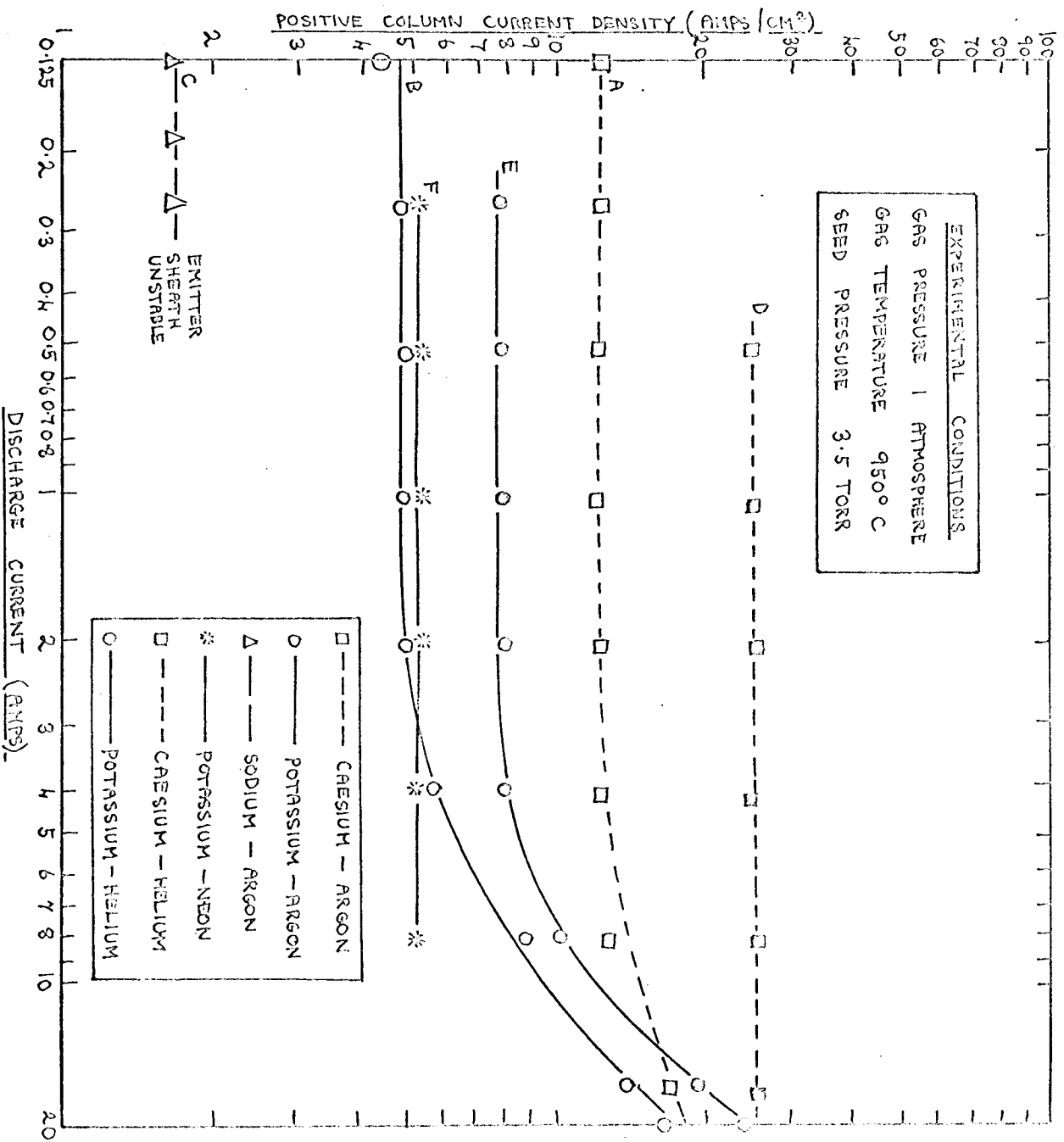
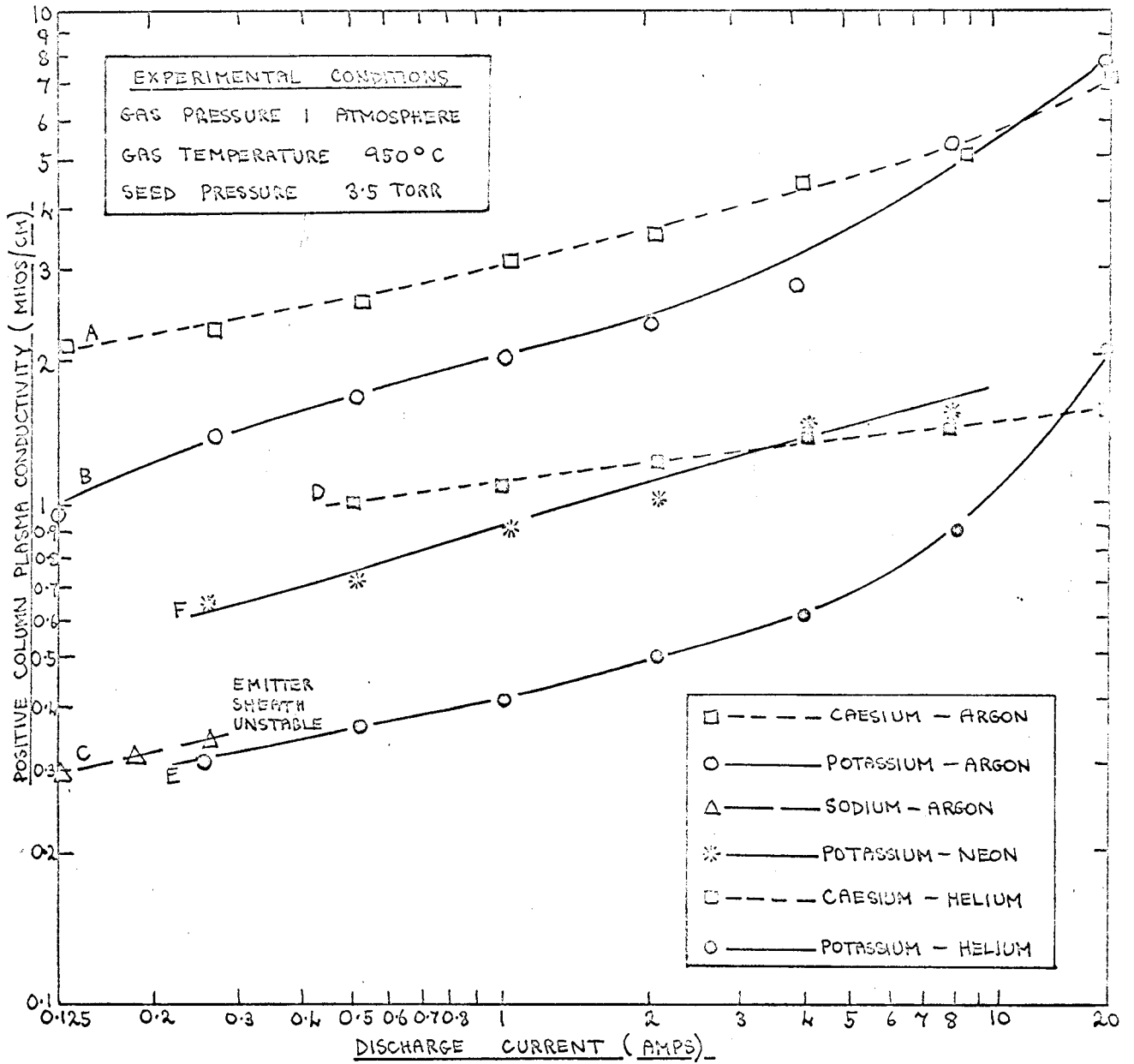


Figure 6.3

LOTS OF POSITIVE COLUMN CURRENT DENSITY AGAINST DISCHARGE CURRENT FOR DIFFERENT MIXTURES



PLOTS OF POSITIVE COLUMN PLASMA CONDUCTIVITY AGAINST DISCHARGE CURRENT FOR DIFFERENT MIXTURES



With caesium as seed, on the other hand, (curves A and D), no such minimum field is observed, the column field falling steadily throughout the current range investigated. The sodium-argon results, (curve C), were restricted by the fact that the cathode mechanism of the discharge proved to be incapable of supporting a current greater than $\frac{1}{2}$ amp without changing to a constricted arc spot. Von Engel (priv. comm.) suggests that the rise in the column field that is observed at very high currents in potassium-seeded mixtures may be due to the fact that the column has begun to interact with the walls of the containing tube (this had a bore of 37 mm). This theory is supported by the fact that the two mixtures for which the field is not observed to rise have higher current densities and smaller column diameters than the various potassium-seeded columns. The experimental error in the results shown in Figure 6.1 is estimated to be of the order of $\pm 5\%$.

Figure 6.2 shows how the column expands as the current rises, the square of the column diameter being plotted against the current. It is seen that the resulting plot is a straight line throughout a fairly wide current range for all the mixtures studied, indicating that the column cross sectional area is roughly proportional to the current. We can therefore conclude that the column diameter is approximately equal to $A\sqrt{i}$ over this linear region, i being the current, and A being an empirical constant that depends on the mixture and experimental conditions. The values of A for the columns described in figure 6.2 are given in Table 6.2.

TABLE 6.2

MIXTURE	EMPIRICAL VALUE OF A (CM.AMF ^{-1/2})
CAESIUM-ARGON	0.32 ± 10%
POTASSIUM-ARGON	0.50 ± 10%
SODIUM-ARGON	0.86 ± 10%
CAESIUM-HELIUM	0.22 ± 10%
POTASSIUM-HELIUM	0.42 ± 10%
POTASSIUM-NEON	0.42 ± 10%

The experimental error in the absolute values of the column diameter is estimated to be of the order of ± 10%, so that the corresponding error in the column area is ± 20%. The error in the column diameter becomes considerably greater than 10% when the current rises above a value of about 5 amps, however, since the column boundary becomes progressively less well-defined as the current reaches very high values. For this reason, the quantitative analysis of the column properties that will be carried out in Part II will be limited to columns carrying currents of 4 amps and under.

Figure 6.3 shows how the mean value of the current density in the various columns studied depends on the discharge current. It is seen that the mean current density remains roughly constant over a wide current range, this being a consequence of the fact that the column cross sectional area is proportional to the current. The absolute error in the current density values shown in figure 6.3 is the same as for the results shown in figure 6.2, namely, ± 20%.

Figure 6.4 shows the dependence of the mean plasma electrical conductivity on the discharge current, the values being obtained from the current density and electric field values given in figures 6.3 and 6.1. It is seen that the conductivity rises steadily as the current increases for all the mixtures studied. The absolute error in the conductivity values is the sum of the absolute errors in the current density and field values, i.e. roughly $\pm 25\%$.

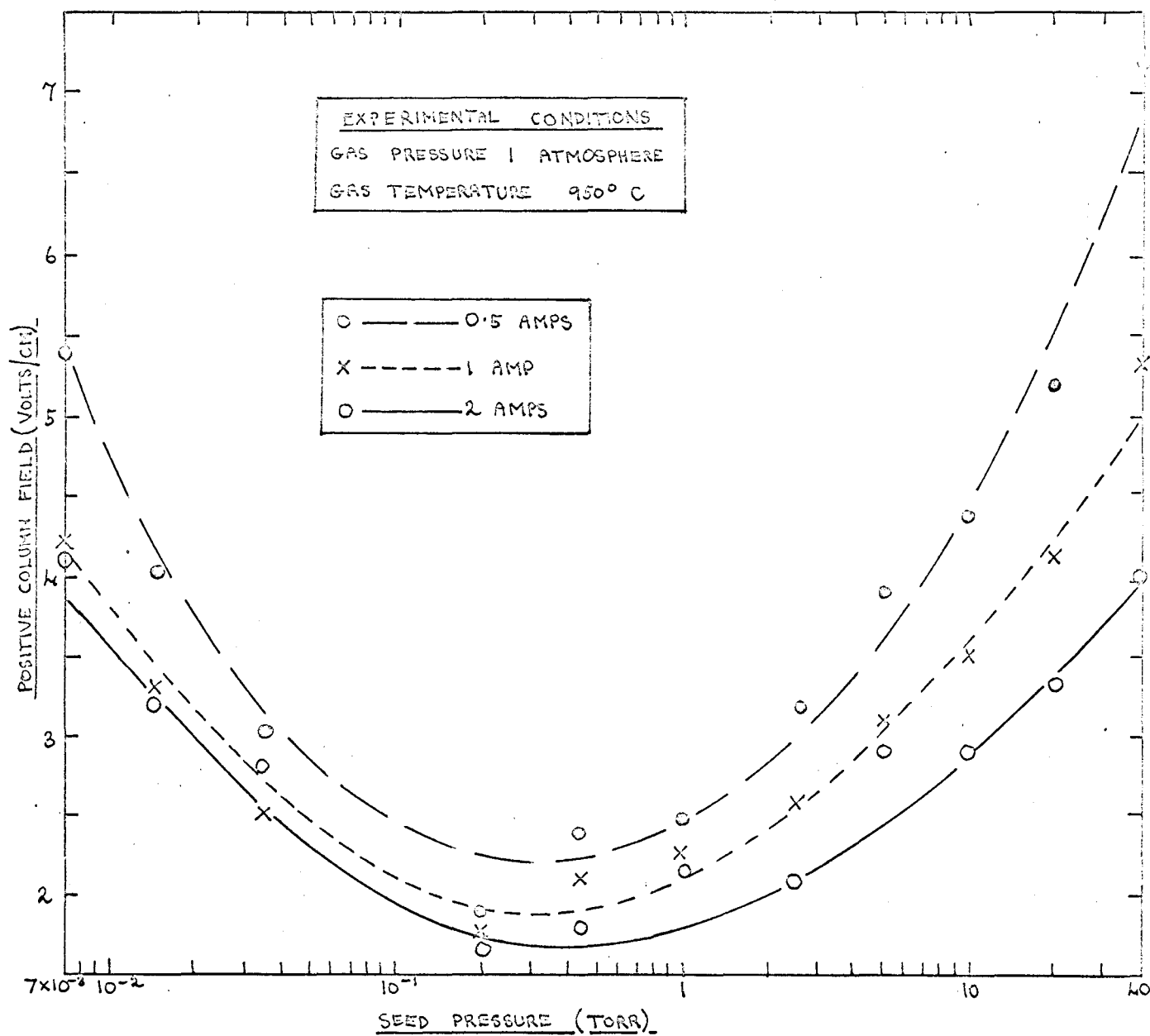
6.2 THE DEPENDENCE OF THE COLUMN PROPERTIES ON THE SEED PRESSURE

In figure 6.5, the dependence of the positive column field on the seed pressure is shown for different currents in potassium-argon. It is seen that the field values increase sharply as the seed pressure reaches very high or very low values, passing through a broad minimum in the neighbourhood of 0.2 torr. It is also seen that the column field decreases as the discharge current rises throughout the seed pressure range investigated. The positive column diameter at a given current was not found to vary greatly throughout the seed pressure range investigated, so that the minimum value of the column field corresponds to a maximum value of the mean plasma conductivity.

In figure 6.6, plots of positive column field against seed pressure are shown for a current of $\frac{1}{2}$ amp in potassium- and caesium-helium and potassium- and caesium-argon. It is seen that the two argon curves (A and B) lie very close together, as do the two helium curves (C and D), and that all four curves pass through a broad minimum.

FIGURE 3-3

PLOTS OF POSITIVE COLUMN FIELD AGAINST SEED PRESSURE FOR
DIFFERENT CURRENTS IN POTASSIUM-ARGON



Plots Of Positive Column Field Against Seed Pressure For Different Mixtures

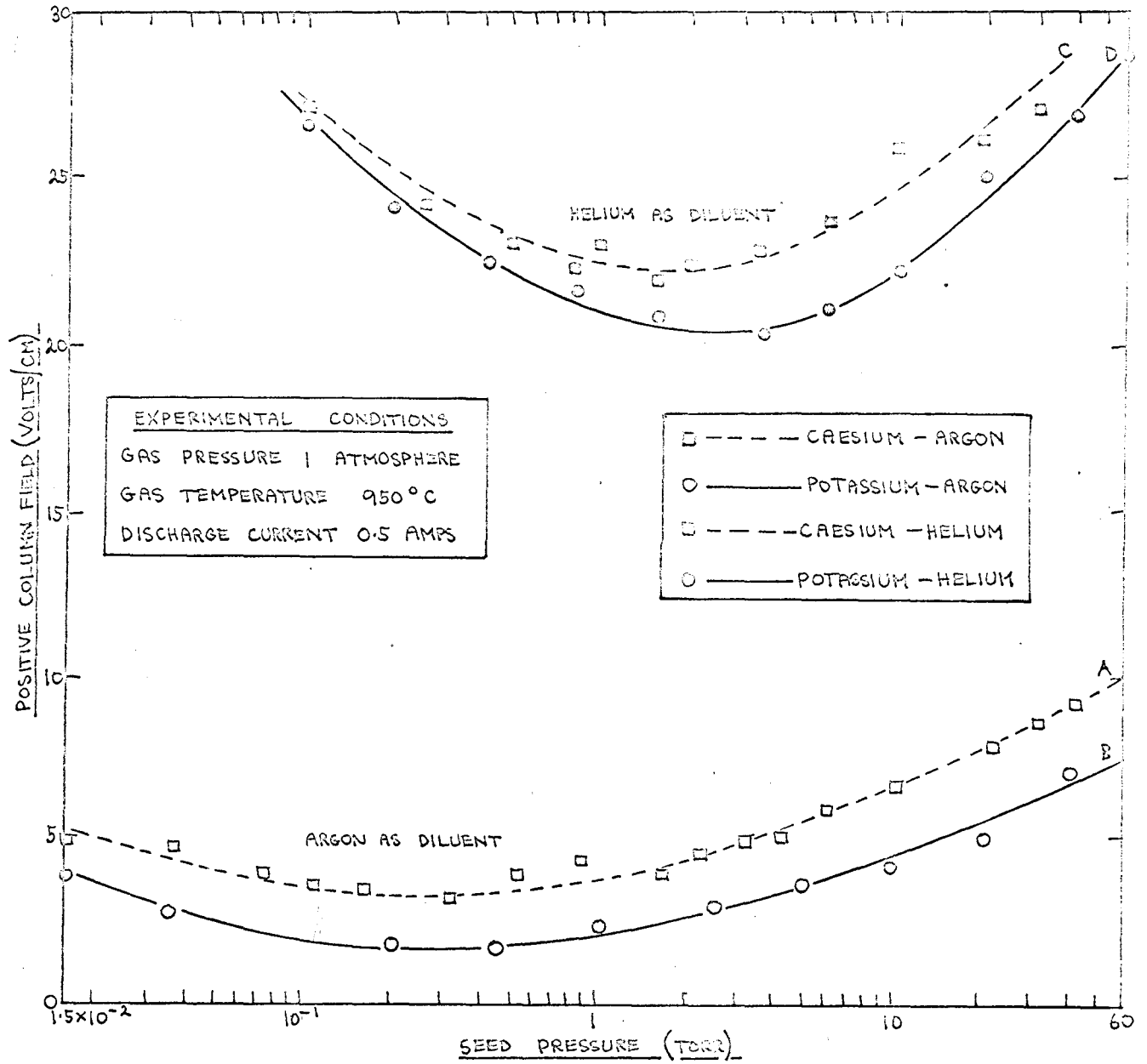
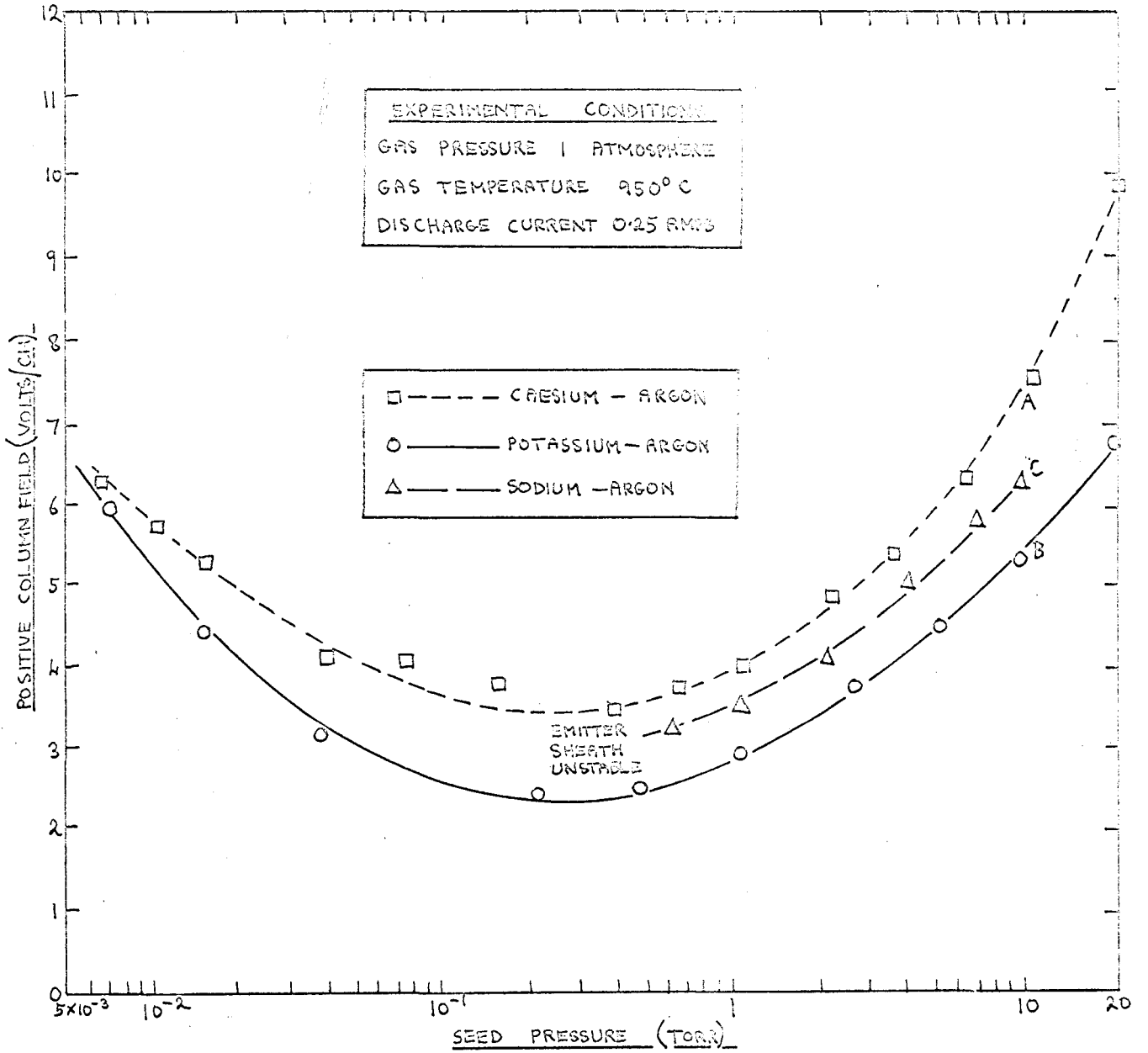


FIGURE 6.7

PLOTS OF POSITIVE COLUMN FIELD AGAINST SEED PRESSURE FOR DIFFERENT SEEDS IN ARGON



In figure 6.7, plots of column field against seed pressure are shown for sodium, potassium and caesium in argon, the discharge current being $\frac{1}{4}$ amp in all cases. The three curves are seen to have the same shape, and to lie very close together. Sodium-argon results could only be obtained between seed pressures of 6.6 and 10 torr, the lower limit being determined by the fact the cathode sheath was unstable at low seed pressures, and the upper limit corresponding to the highest temperature that could be reached by the seeding oven.

6.3 THE DEPENDENCE OF THE COLUMN PROPERTIES ON THE AMBIENT GAS TEMPERATURE

The properties of the positive column under study appear to be virtually independent of the ambient gas temperature. This was first reported by Ralph (1962), who showed that the total electrode voltage required to support a given current in potassium- and caesium-argon was roughly constant throughout the temperature range 750 - 1000°C. The author greatly extended these investigations, and studied the temperature dependence of the positive column field and cathode fall throughout the range 550 - 950°C. The somewhat unexpected result obtained was that the positive column field required to support a given current was virtually unaffected by changes in the ambient gas temperature. This is illustrated by figures 6.8 and 6.9. In the former, positive column field is plotted against ambient temperature for a number of different currents in potassium-argon and potassium-helium, while in the latter, the positive column field required to support a current of 1 amp is plotted against temperature for

LOTS OF POSITIVE COLUMN FIELD AGAINST AMBIENT GAS TEMPERATURE FOR DIFFERENT CURRENTS IN POTASSIUM-ARGON AND POTASSIUM-HELIUM

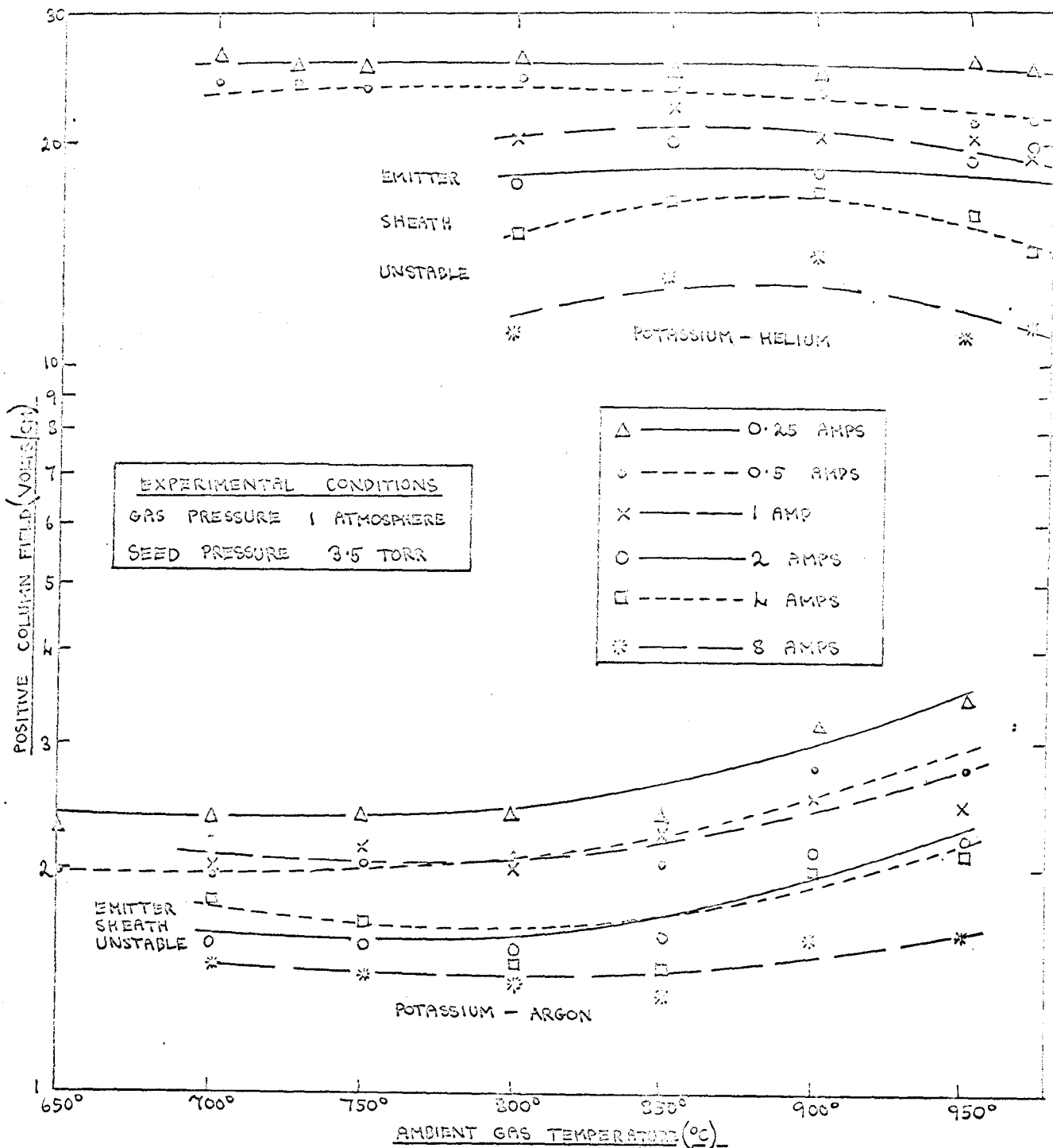
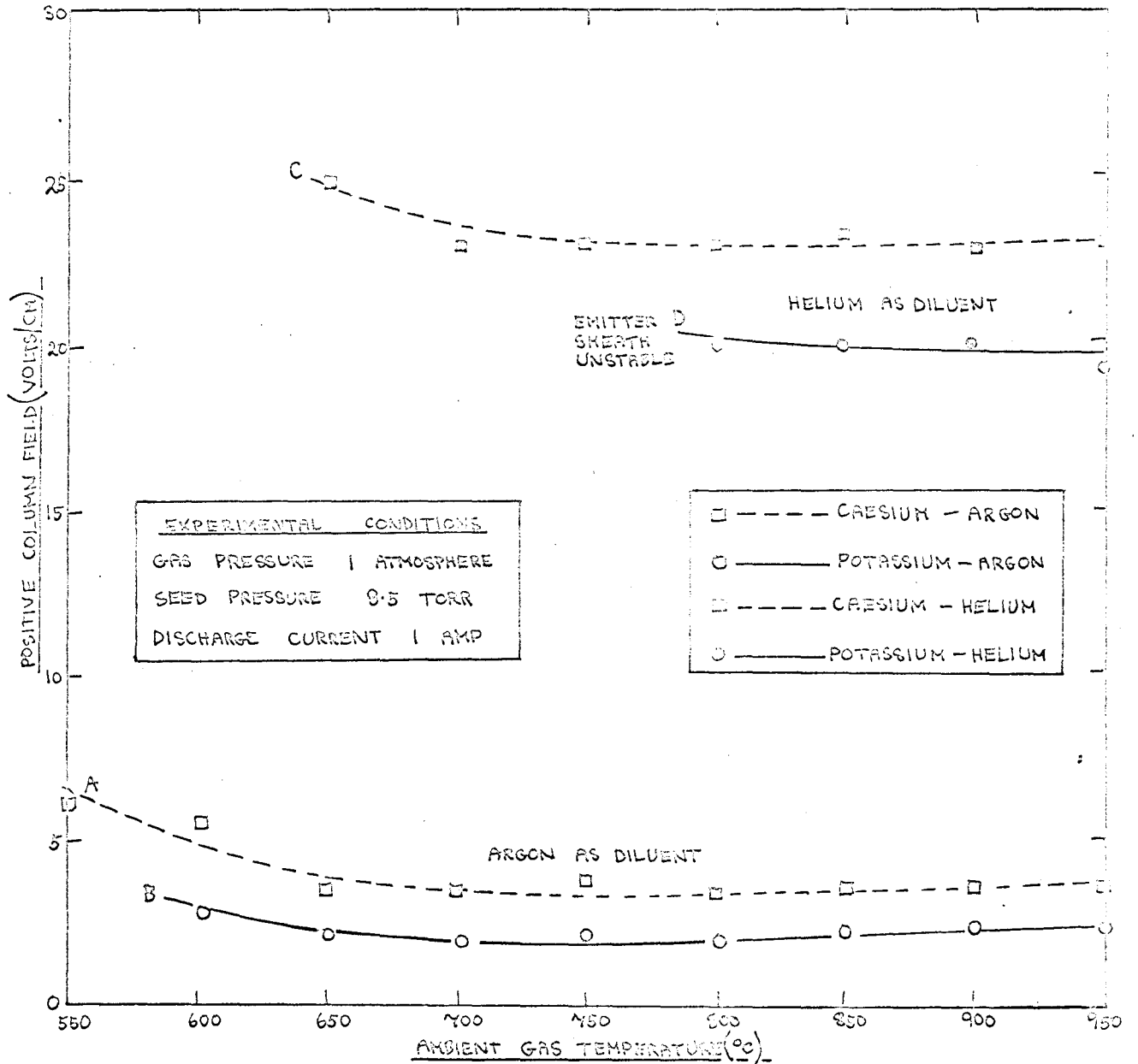


FIGURE 6.9

Plots of Positive Column Field vs Ambient Gas Temperature for Different Mixtures



caesium- and potassium-argon and caesium- and potassium-helium. Three results are evident from the data given in these figures. Firstly, the positive column field required to support a given current shows no sign of changing as the ambient temperature falls, remaining roughly constant even when the lowest temperatures at which the cathode sheath is stable are approached. Secondly, the result that the column field falls as the discharge current rises appears to be true throughout the temperature range studied. Thirdly, the field values for helium-diluted mixtures are seen to be considerably higher than the corresponding values for argon-diluted mixtures throughout the temperature range investigated. It must be stressed that the temperature being varied in the experiments discussed in this section is the ambient gas temperature and not the actual column gas temperature; it will be shown in Part II that the latter is determined by the energy balance processes active in the column, and is generally considerably higher than the ambient temperature.

6.4 THE EFFECT ON THE COLUMN PROPERTIES OF CHANGING THE DILUENT GAS

One of the most pronounced features of the experimental data given in this chapter is the result that the column electric field (X) required to support a given current is strongly dependent on the choice of diluent gas. This is illustrated by figure 6.1, which shows plots of column field against discharge current for various mixtures. Curve E (potassium-helium) is seen to lie at

far higher field values than curve F (potassium-neon), the latter, in turn, lying at higher field values than curve B (potassium-argon). Furthermore, the ratios $\frac{X_{He}}{X_{Ar}}$ and $\frac{X_{Ne}}{X_{Ar}}$ appear to remain roughly constant throughout the current range investigated. The same features are shown by curve D (caesium-helium) and curve A (caesium-argon), the helium field values being considerably higher than the argon values, and the ratio $\frac{X_{He}}{X_{Ar}}$ remaining roughly constant throughout the current range investigated.

Figure 6.9 also illustrates the strong dependence of the column field on the choice of diluent, and shows that the results given in the last paragraph appear to be true throughout the temperature range investigated. In this figure, which shows plots of column field against ambient temperature for a current of 1 amp in caesium- and potassium-argon and caesium- and potassium-helium, the two helium curves (C and D) lie close together, as do the two argon curves (A and B), the former being at considerably higher field values than the latter; in addition, the ratio $\frac{X_{He}}{X_{Ar}}$ for a given seed remains roughly constant throughout the temperature range investigated.

Essentially the same features are shown by the curves of figure 6.6, these being plots of column field against seed pressure for a current of $\frac{1}{2}$ amp in caesium- and potassium-argon and caesium- and potassium-helium. It is seen that the two helium curves (C and D) again lie close together, and have their minima in roughly the same place, as do the two argon curves (A and B), and it is also seen that the two argon curves have their minima at

seed pressures roughly an order of magnitude below the two helium curves. In this case, however, the ratio $\frac{X_{He}}{X_{Ar}}$ for a given seed does not remain constant throughout the seed pressure range investigated, but falls steadily as the seed pressure rises.

6.5 THE EFFECT ON THE COLUMN PROPERTIES OF CHANGING THE SEED METAL

Somewhat surprisingly, the value of the positive column field that is required to support a given current appears to depend only slightly on the choice of seed metal, a result also obtained by Morgulis and Polushkin (1966) for the low-pressure discharge studied by them. This result is clearly illustrated by figures 6.6 and 6.7, which show plots of column field against seed pressure for a variety of mixtures, and also by figure 6.9, which shows plots of column field against ambient temperature for different mixtures. In all three figures, the field value required to support a given current in a given diluent does not depend strongly on the choice of seed. Furthermore, any differences that do exist between potassium-seeded mixtures and caesium-seeded mixtures appear to become negligible at very low seed pressures, as is shown by curves C and D of figure 6.6, and curves A and B of figure 6.7.

The property of the positive column which does seem to depend fairly strongly on the choice of seed is the positive column diameter (see Table 6.2), so that the mean current density and mean plasma conductivity also depend fairly strongly on the choice of seed. Figure 6.3 shows that sodium-argon (curve C) has a much

lower current density at a given current than potassium-argon (curve B), which, in turn, has a lower current density than caesium-argon (curve A). The same is true with helium as diluent, curve E (for potassium) lying well below curve D (for caesium).

6.6 THE EFFECT ON THE COLUMN PROPERTIES OF ADDED MOLECULAR IMPURITIES

The effects of added molecular impurities on the properties of the discharge under study were investigated by adding controlled amounts of oxygen and nitrogen to a potassium-argon mixture. A cylinder of the molecular gas was connected via a two-stage regulator to a needle valve, and the system was calibrated for low flow rates by varying the needle setting, and collecting the gas over water in a measuring cylinder, the regulator pressure being kept constant throughout. Known, controlled flow rates of the order of a few cm^3 per minute could be obtained in this way. The impurity was added to the argon flow, and the percentage volume impurity was determined by taking the ratio of the impurity and argon flow rates. It was found that impurity levels of the order of 1% were needed before any significant change in the discharge properties occurred - a much higher level than that which had been thought tolerable by some workers on the M.H.D. applications of the nonequilibrium discharge.

Figure 6.10 shows the effect of oxygen on the potassium-argon discharge, electrode voltage being plotted against electrode spacing for a discharge current of 1 amp, while figure 6.11 shows the effect of nitrogen on the same discharge. It is seen that the

PLOTS OF ELECTRODE VOLTAGE AGAINST ELECTRODE SPACING FOR DIFFERENT AMOUNTS OF OXYGEN IN FETTERILL-ARGON

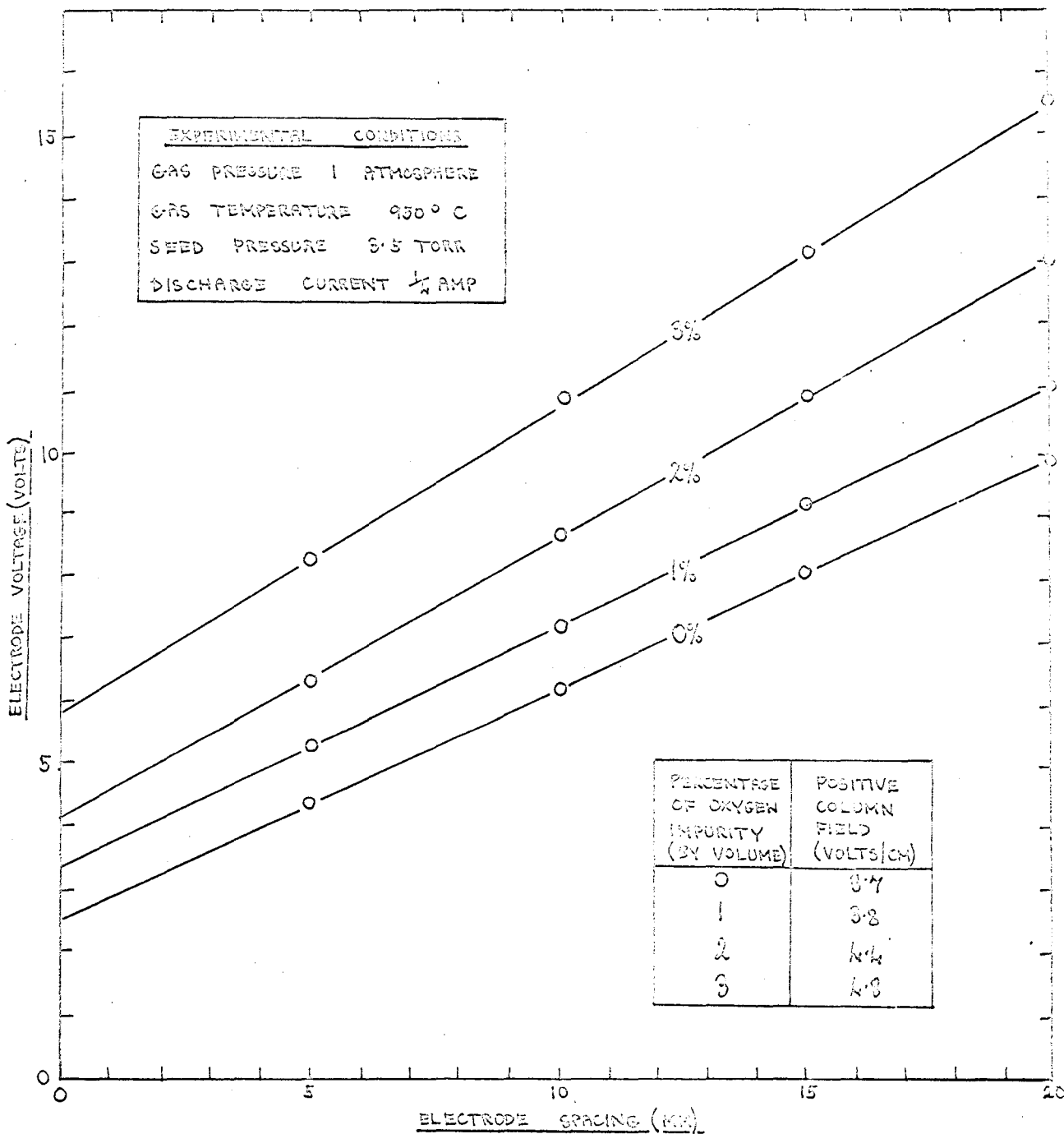
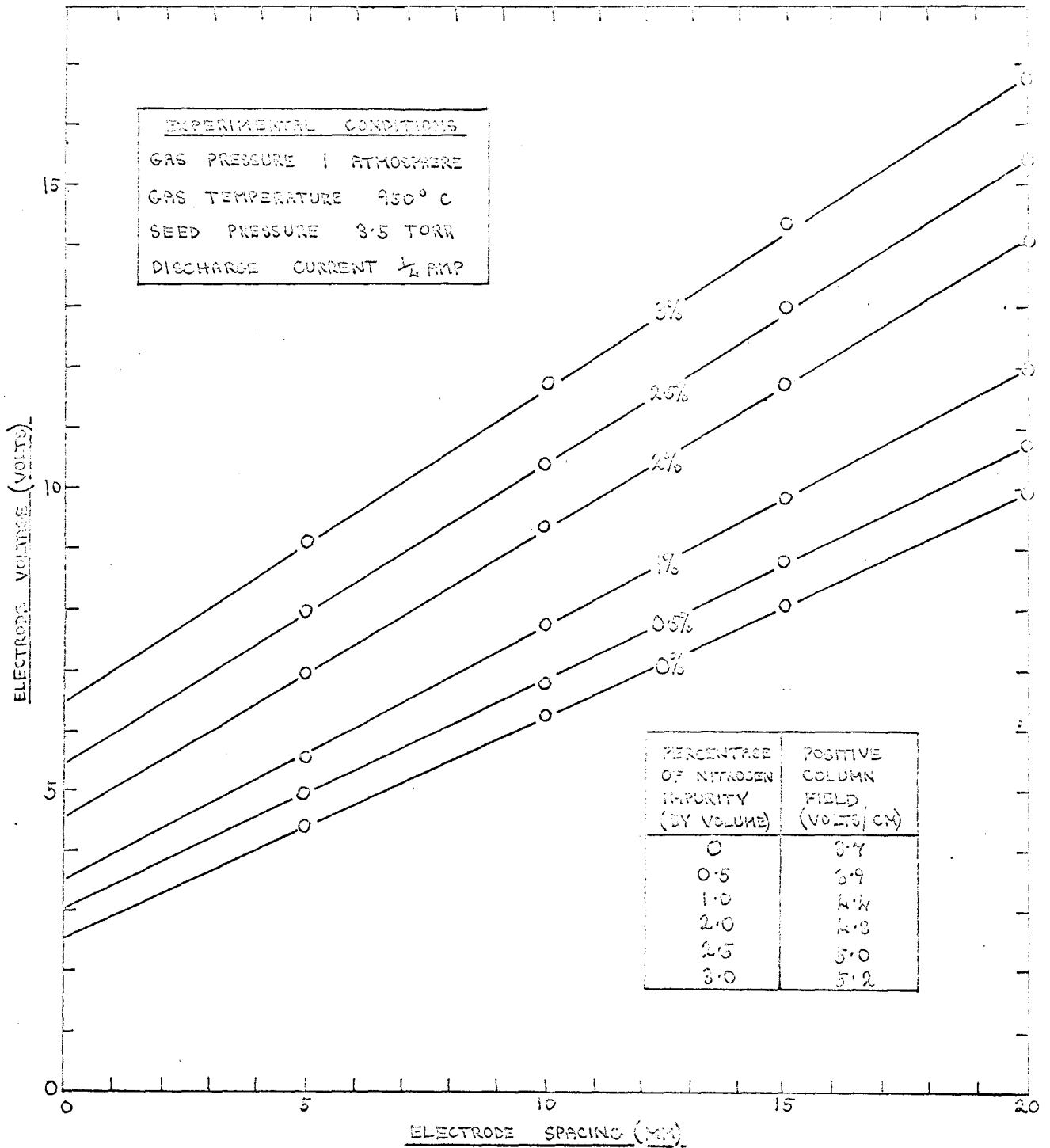


FIGURE 6.11

PLOTS OF ELECTRODE VOLTAGE AGAINST ELECTRODE SPACING FOR
DIFFERENT AMOUNTS OF NITROGEN IN PETROLIUM-ARGON

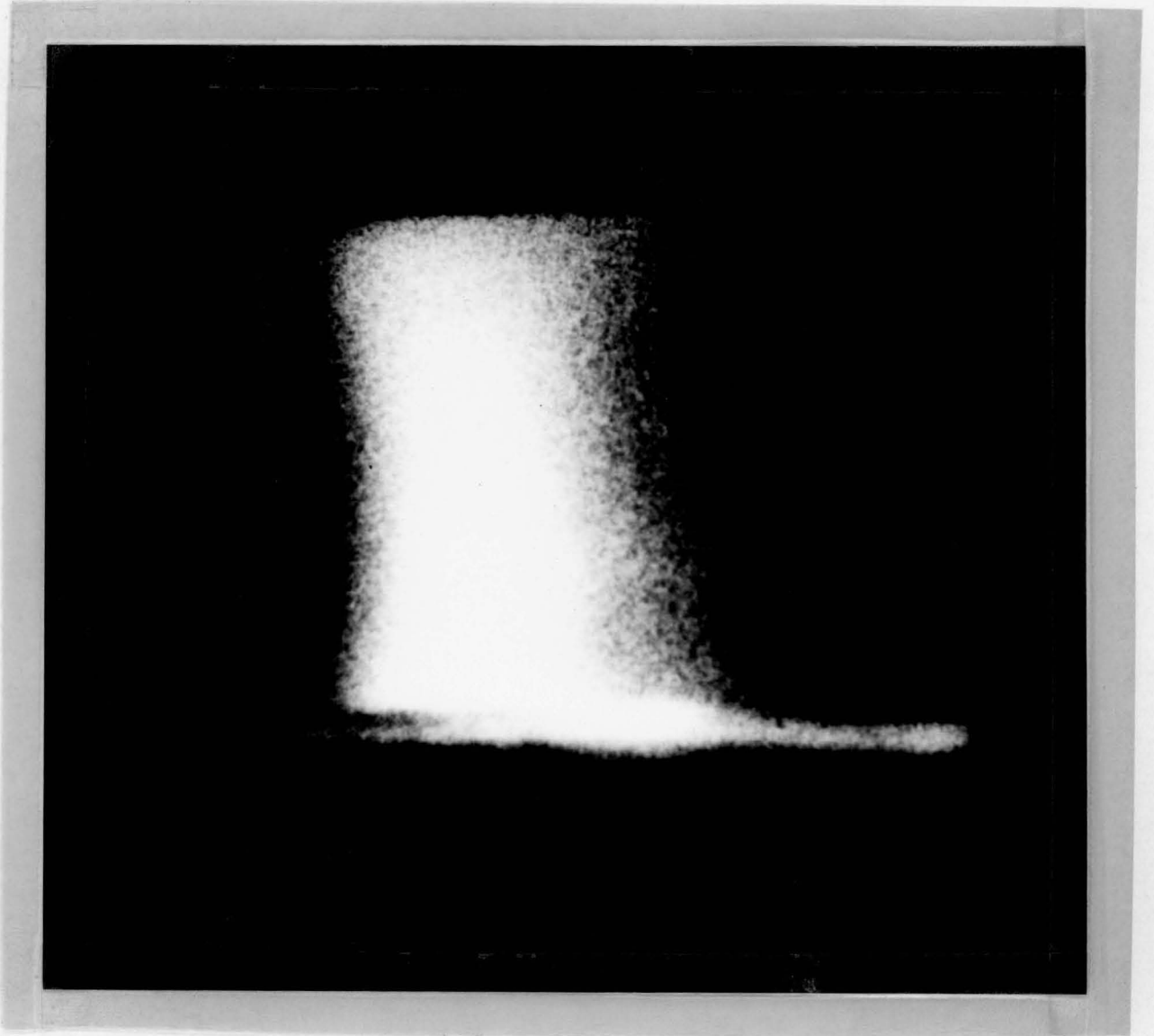


electrode voltage at a given spacing rises as the percentage impurity increases, partly because the column field (voltage gradient) increases, and partly because the cathode fall (zero spacing voltage intercept) rises. Nitrogen appears to have a slightly greater effect on the discharge than oxygen. The author was the first person ~~to~~ obtain experimental results which showed the effect on the properties of a nonequilibrium discharge of added molecular impurities (Ellington and Ralph 1966).

CHAPTER 7THE CATHODE REGIONS OF THE DISCHARGE7.1 THE TWO MODES OF THE CATHODE MECHANISM

As mentioned in Chapter 2, the cathode mechanism of the discharge under study can adopt two distinct forms, which the author has termed the diffuse and constricted modes. Let us examine them in turn.

THE DIFFUSE MODE In the diffuse mode, the entire cathode surface is covered by a thin glowing sheath of the order of 1 mm thick. This sheath, which sometimes extends round the sides of the electrode, appears to be of uniform thickness and intensity when the current is low, but when the current is high, the region immediately under the positive column is somewhat brighter than the rest, indicating that most of the electron emission takes place from this part of the electrode. The sheath has the colour of the flame of the seed material, indicating that the decay of excited seed atoms is responsible for its light output, a conclusion that is supported by the study of the spectrum of the cathode regions of the discharge. The voltage drop across the sheath has a value of several volts or tens of volts, the exact value depending on the discharge current, the experimental conditions, and the nature of the seed-diluent mixture. Extensive data on the value of this voltage drop will be given later in this chapter. The diffuse mode of the cathode mechanism is clearly illustrated in Photograph 7.1, which shows a potassium-argon discharge carrying a current of

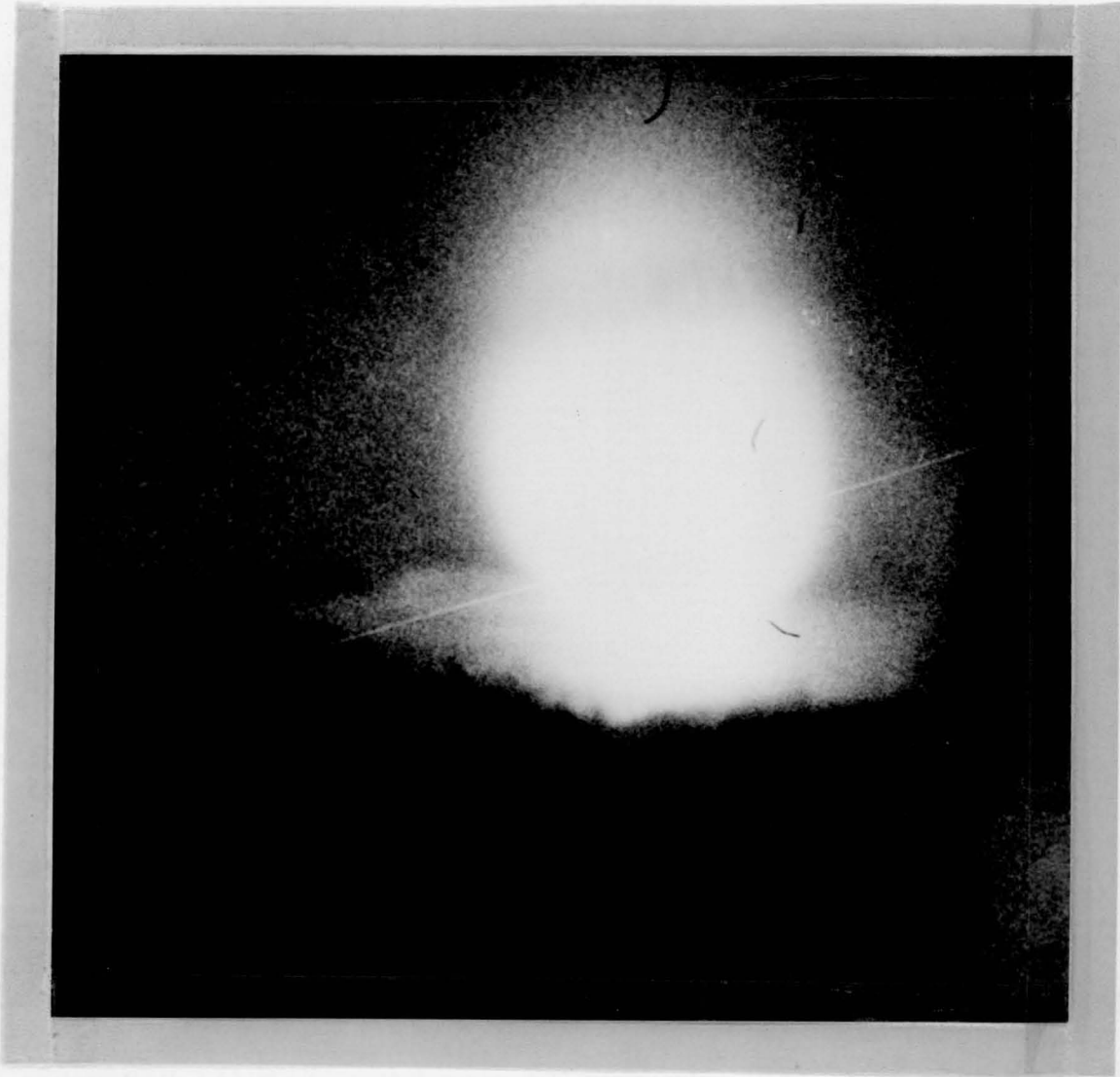
PHOTOGRAPH 7.1THE DIFFUSE FORM OF THE CATHODE MECHANISM

1 amp. The glowing sheath that covers the cathode surface is clearly seen, as is the dark space that exists between the sheath and the positive column.

THE CONSTRICTED MODE The constricted mode of the cathode mechanism appears to be a thermionic arc spot that has all the properties that are associated with the cathode spot of a conventional arc discharge. In this mode, no cathode sheath is present, and the emission of electrons takes place from a localised arc spot that generally moves rapidly about the electrode surface. This spot and its surrounding aureole give out an intense blue light which cannot be directly viewed without the use of a welding mask or similar protective device. Spectroscopic examination of the spot shows that lines of the seed metal are present, but that the dominant lines are those of chromium and manganese, two metals which are present in the electrode material (18/8/1 stainless steel). This supports our classification of the constricted mode as a thermionic arc spot (see Chapter 1). The cathode fall associated with the constricted mode is usually less than that associated with the diffuse mode, and generally has a value of a few volts. The constricted mode is illustrated in Photograph 7.2, which shows a potassium-argon discharge carrying a current of about 3 amps. The localised nature of the arc spot is clearly seen, as is its enormous light output, which clearly illuminates the entire electrode area, and swamps the relatively-feeble light output of the positive column.

PHOTOGRAPH 7.2

THE CONSTRICTED FORM OF THE CATHODE MECHANISM



It appears that the nature of the arc spot of the constricted mode undergoes a gradual change as the discharge current rises to very high values, a fact that was revealed by the high-speed photographic work described in Chapter 4. In one of these films, the constricted mode of a discharge in potassium-argon was photographed in colour at 2500 frames/sec. as the current was slowly raised from a few amps to over 20 amps, and the following observations were made. At low currents (under 5 amps) the arc spot had all the properties that were described in the last paragraph, having a bright blue colour, and moving rapidly over the electrode surface, but as the current rose above 5 amps, the spot gradually settled down to one place, and then began to spread out over the cathode surface. As the current rose above 10 amps, the appearance of the cathode regions was totally different from when constriction first occurred. The spot appeared to be fairly stable, and was spread out over a quite large area of the electrode surface, which was seen to bulge and glow white hot (it was afterwards discovered to have melted). The spot no longer had its characteristic blue colour, but was yellow-white in appearance. As the current rose to 20 amps, the cathode "spot" was now of considerable extent, covering almost half the electrode, and appeared to be covered by an intensely bright sheath, not unlike that associated with the diffuse mode at similar currents.

The constricted cathode mechanism was found to be capable of supporting very large currents throughout an extremely wide range of temperatures and seed pressures - a far wider range than that

through which the diffuse mode was stable. If the arc spot was allowed to persist for any length of time, however, extensive damage to the cathode surface was liable to result, large sections being melted or eaten away. For this reason, only the diffuse mode of the cathode mechanism was studied in detail by the author, and the bulk of this chapter is concerned with the properties of this mode.

7.2 THE TRANSITION BETWEEN THE MODES AND THE STABILITY OF THE DIFFUSE MODE

Transition from the diffuse mode of the cathode mechanism to the constricted mode is thought by the author to occur when the cathode surface becomes incapable of emitting enough electrons to maintain the discharge without forming a thermionic arc spot. For given experimental conditions, the transition occurs when the discharge current reaches a certain critical value. As the current rises, the cathode fall of the diffuse mode increases steadily, until at the critical current, the sheath that covers the cathode surface suddenly collapses, and the constricted arc spot appears. The transition is generally accompanied by a jump in the value of the discharge current and a fall in the electrode voltage, since the cathode fall associated with the thermionic arc spot is generally smaller than that associated with the diffuse mode. The current at which the transition occurs depends not only on the nature of the seed-diluent mixture and on the experimental conditions, but also on the way in which the current is increased. If the discharge current is raised quickly, the transition is often found to take

place at a considerably lower current than that at which it takes place if the current is increased gradually; any sudden increase in the current generally results in immediate constriction. The transition to the constricted mode is generally found to be reversible, as the discharge can usually be restored to the diffuse mode by lowering the discharge current to below the value at which constriction occurred.

The degree of stability of the diffuse mode depends on several factors, namely, the ambient temperature, the seed pressure, the choice of seed material, and the choice of diluent gas. Let us consider these in turn.

DEPENDENCE ON TEMPERATURE The lower the ambient temperature, the lower is the current that can be carried without constriction of the cathode mechanism taking place. Below a certain critical temperature that depends on the nature of the mixture and on the experimental conditions, only the constricted mode is stable.

When studying the potassium-argon discharge, the author carried out a series of experiments using a hollow cathode which could be cooled below the ambient temperature by passing helium through it. A thermocouple was spot welded to the inside of the emitting surface of the electrode in order to measure its temperature, and this showed that the temperature of the cathode surface was higher than the ambient gas temperature, with the difference between the two increasing steadily as the discharge current rose. The actual surface temperature could not be measured, but the results obtained with the internal thermocouple indicated that the surface

temperature of the cathode was several hundred degrees higher than the ambient gas temperature for currents of 1 amp and over. The effect on the stability of the diffuse mode of the cathode mechanism of cooling the cathode was determined, and was found to depend on whether the cooling was carried out while the discharge was running, or before the discharge was struck. In the former case, it was found that the cathode could be cooled to several hundred degrees below the ambient gas temperature (which was about 950°C) without constriction occurring, provided that the cooling was carried out gradually, and the current was not too high. If the cathode was cooled to the same temperature when no current was being passed, however, and the discharge was then struck, immediate constriction generally occurred, although transition to the diffuse mode could generally be brought about by lowering the current. The effect on the discharge of cooling the anode was also investigated, and the cooling was found to have no noticeable effect.

DEPENDENCE ON SEED PRESSURE The lower the seed pressure, the less stable is the diffuse mode of the cathode mechanism, and the lower is the current that can be carried without constriction occurring. At very low seed pressures, the diffuse mode can only be supported with difficulty, and any sudden increase in the current tends to produce constriction. Conversely, the diffuse mechanism is found to be extremely stable at very high seed pressures.

DEPENDENCE ON SEED MATERIAL The stability of the diffuse mode depends strongly on the choice of seed. Caesium can support it at seed pressures as low as 7×10^{-3} torr (the lowest seed pressure

reached in the author's experiments), and temperatures as low as 500°C (the lowest temperature at which the discharge was studied), and potassium is almost as good. Sodium, on the other hand, can support the diffuse form only at seed pressures above 0.6 torr and temperatures above 850°C, and even then is only capable of supporting currents up to $\frac{1}{2}$ amp. If a small amount of potassium is added to the sodium, however, the stability of the diffuse mode is greatly enhanced, and it can exist at much lower temperatures and seed pressures, and support much higher currents. This fact was discovered by accident when the author began to study the sodium-argon discharge. The author had failed to anticipate the necessity of thoroughly outgassing the apparatus before changing from potassium-argon to sodium-argon, and when the sodium-seeded discharge was first observed, it was found to be stable over a fairly wide current and temperature range. This was later inferred to be due to the fact that a small amount of potassium remained in the apparatus, for when the apparatus was held at the operating temperature (950°C) for two days, the discharge was found to become progressively less stable, until it settled down to steady behaviour, and the sodium-argon results quoted in this thesis were obtained.

DEPENDENCE ON DILUENT GAS Generally speaking, the diffuse mode is more stable with argon as diluent than with helium as diluent, as is clearly seen in figures 7.3 and 7.7. The diffuse mode is stable down to considerably lower ambient temperatures with argon as diluent than with helium, and is also stable down to lower seed pressures with the former gas.

A comparison of the stability of the diffuse mode in the different mixtures studied by the author is given in Table 7.1. The first column gives the maximum current that can be supported by the diffuse mode at a seed pressure of 3.5 torr and an ambient temperature of 950°C. The second column gives the lowest ambient temperature at which a current of $\frac{1}{4}$ amp could be supported at a seed pressure of 3.5 torr. The third column gives the lowest seed pressure at which a current of $\frac{1}{4}$ amp could be supported when the ambient temperature was 950°C. It is seen that the best mixtures from the point of view of the stability of the diffuse cathode mechanism are caesium-argon and potassium-argon, with caesium-helium not far behind. The least stable mixture studied was sodium-argon. Sodium-helium was not studied by the author, as it was thought that results would be virtually unobtainable with this mixture.

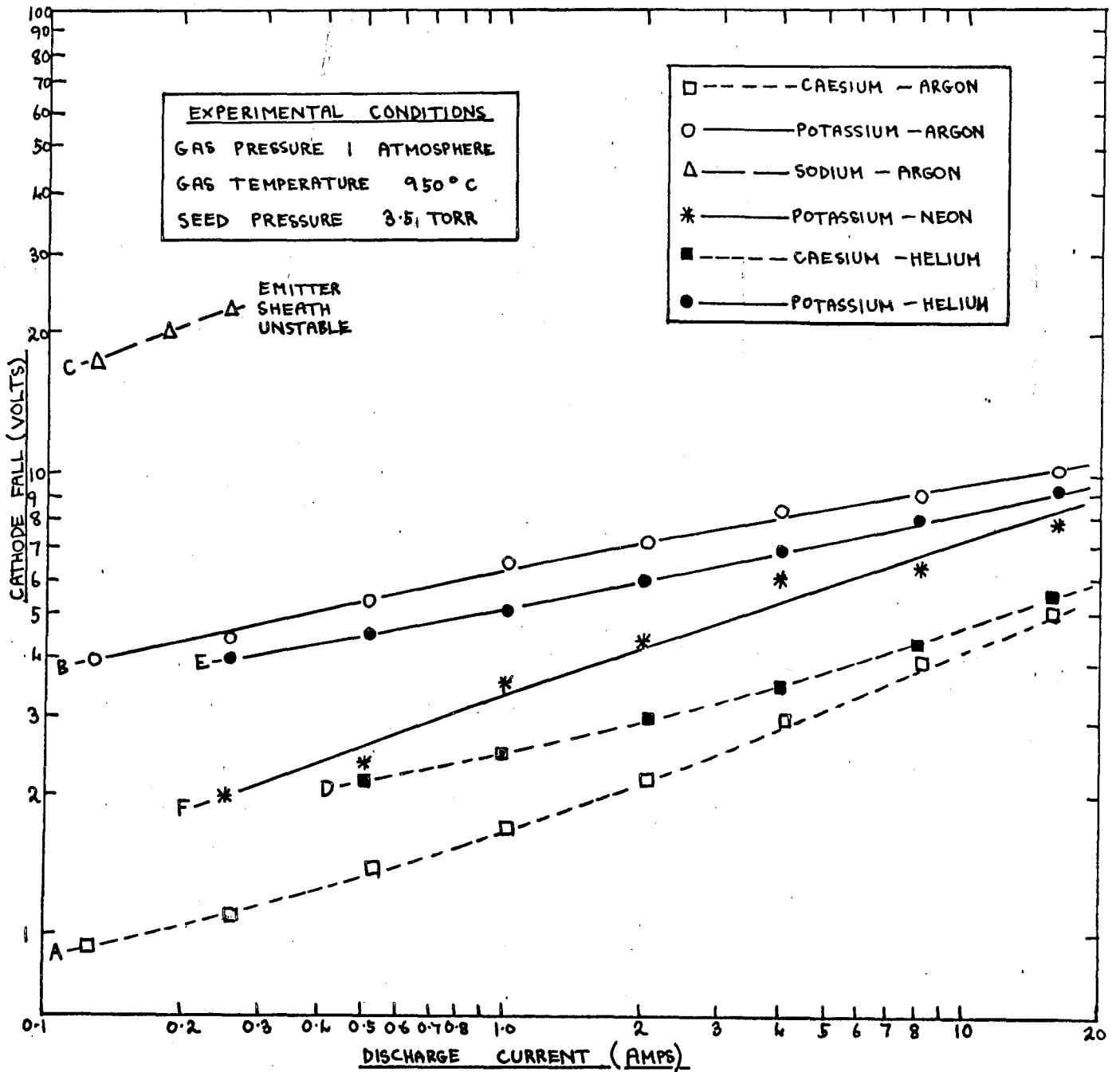
TABLE 7.1

MIXTURE	HIGHEST CURRENT POSSIBLE AT 3.5 TORR AND 950°C	LOWEST TEMPERATURE POSSIBLE AT $\frac{1}{4}$ AMP AND 3.5 TORR ⁴	LOWEST SEED PRESSURE POSSIBLE AT $\frac{1}{4}$ AMP AND 950°C
SODIUM-ARGON	$\frac{1}{4}$ AMP	850°C	0.6 TORR
POTASSIUM-ARGON	No limiting current	600°C	7×10^{-3} TORR
CAESIUM-ARGON	observed	500°C	7×10^{-3} TORR
POTASSIUM-HELIUM	(currents up to 20 amps reached)	700°C	10^{-1} TORR
CAESIUM-HELIUM		Below 700°C	Below 10^{-1} TORR

7.3 THE VALUE OF THE CATHODE FALL OF THE DIFFUSE MODE; ITS DEPENDENCE ON THE DISCHARGE CURRENT

The remainder of this chapter deals exclusively with the diffuse mode of the cathode mechanism, and gives a detailed account of the dependence of its cathode fall on the different experimental variables. It was found that the value of the cathode fall for a given current in a given mixture under fixed experimental conditions varied slightly from experiment to experiment, probably due to slight differences in the condition of the electrode surface. If the discharge was studied using newly-polished electrodes, for example, the cathode fall values were sometimes found to be slightly lower than the values that were obtained when the cathode had been in use for some time (in some of the author's experimental runs, the apparatus was used on several successive days without dismantling it and cleaning the electrodes). Because of these variations, the experimental error in the absolute cathode fall values quoted in this thesis is quite large, and is estimated to be of the order of $\pm 15\%$. The cathode fall did not appear to depend on the actual size of the cathode. Most of the author's work was carried out using a top electrode $\frac{1}{2}$ inch in diameter, and a bottom electrode $1\frac{1}{4}$ inches in diameter, and the results obtained with the former as cathode showed no systematic difference from those obtained when the polarity of the electrodes was reversed. One rather interesting observation was that the cathode fall appeared to be higher when the discharge was first struck than it was after the discharge had been allowed to settle down, a

PLOTS OF CATHODE FALL AGAINST DISCHARGE CURRENT FOR DIFFERENT MIXTURES



difference of a few volts being sometimes noted. All the results given in this chapter were taken after the discharge had reached a steady state.

We have already mentioned that the value of the cathode fall increases as the discharge current rises. This result was found to be true for all the mixtures studied under all the experimental conditions for which the diffuse mode was stable, and is illustrated in figure 7.1, which shows plots of cathode fall against discharge current for the different mixtures studied, the seed pressure and ambient temperature being 3.5 torr and 950°C in all cases.

7.4 THE DEPENDENCE OF THE CATHODE FALL ON THE SEED PRESSURE

The cathode fall of the diffuse mode depends strongly on the seed pressure in some mixtures, and hardly at all in others. Figure 7.2 shows plots of cathode fall against seed pressure for different currents in potassium-argon, the ambient temperature being 950°C. It is seen that the cathode fall is very high at low seed pressures, falls to a minimum of a few volts at about 8 torr, and then rises slightly.

In figure 7.3, cathode fall is plotted against seed pressure for a current of $\frac{1}{2}$ amp in caesium- and potassium-helium and caesium- and potassium-argon, the ambient temperature being 950°C in all cases. The two curves with potassium as seed (B and D) have roughly the same shape, both showing the minimum mentioned above,

PLOTS OF CATHODE FALL AGAINST SEED PRESSURE FOR DIFFERENT CURRENTS IN POTASSIUM-ARGON

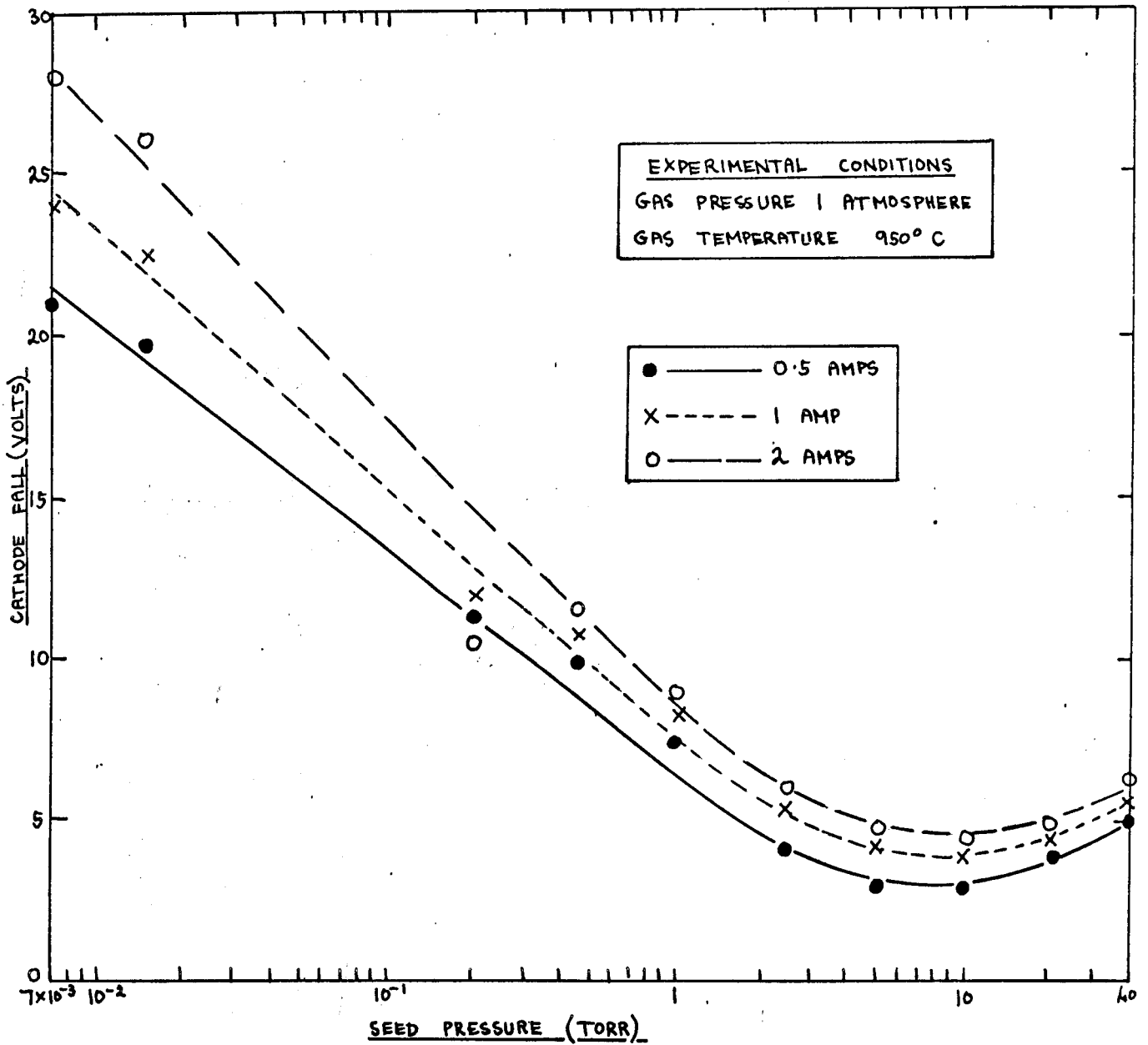
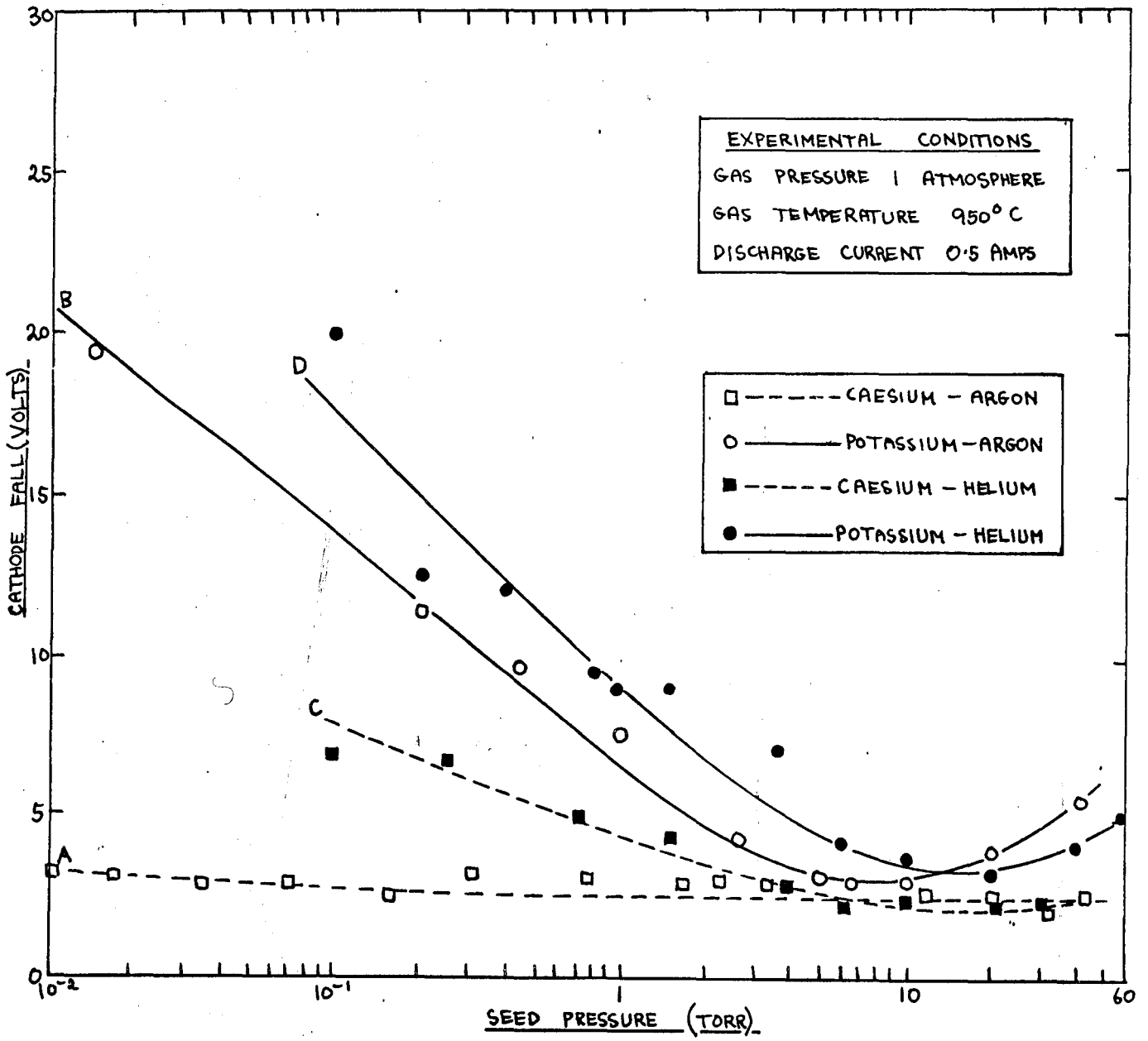
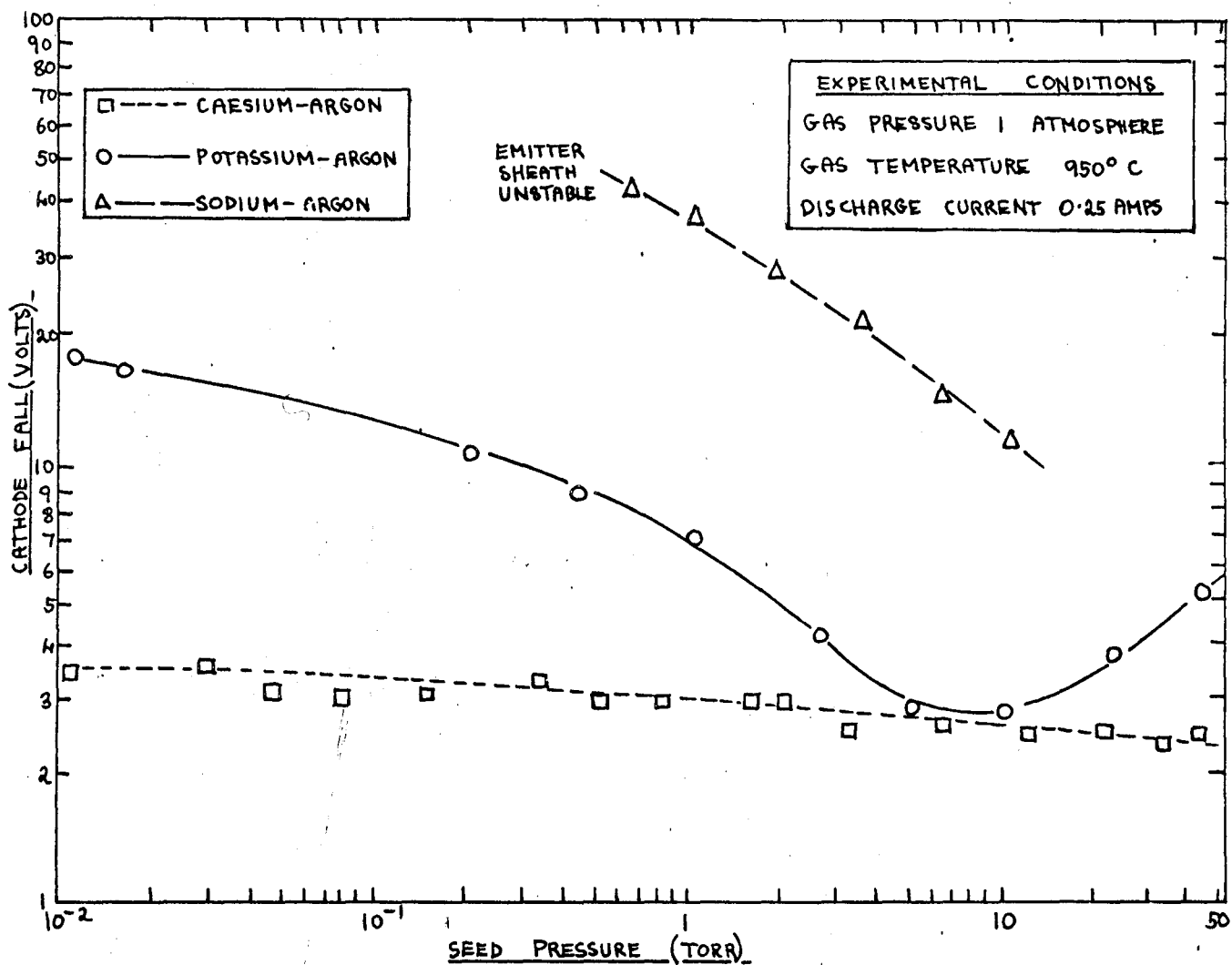


FIGURE 7.3

PLOTS OF CATHODE FALL AGAINST SEED PRESSURE FOR DIFFERENT MIXTURES



PLOTS OF CATHODE FALL AGAINST SEED PRESSURE FOR DIFFERENT SEEDS IN ARGON



but the minimum is seen to occur at a seed pressure of 20 torr in the potassium-helium case. The caesium-seeded curves (A and C) have no minima, the cathode fall remaining roughly constant above a seed pressure of 5 torr, and do not rise to such high values at low seed pressures as do the potassium curves. Between seed pressures of roughly 2 and 20 torr, all four curves are seen to lie fairly close together.

Figure 7.4 shows plots of cathode fall against seed pressure for a current of $\frac{1}{4}$ amp in caesium-, potassium- and sodium-argon, the ambient temperature being 950°C in all cases. The lower limit of the sodium-argon results was determined by the fact that the diffuse cathode mechanism could not exist below 0.6 torr, while the upper limit was set by the fact that a seed pressure of 10 torr corresponded to the highest temperature that could be attained by the seeding oven. With sodium as seed, the cathode fall is seen to fall steadily as the seed pressure rises.

7.5 THE DEPENDENCE OF THE CATHODE FALL ON THE AMBIENT TEMPERATURE

As in the case of the breakdown voltage and the positive column field, the cathode fall is found to be practically independent of the ambient gas temperature over a fairly wide temperature range. This is illustrated in figures 7.5 and 7.6, which show cathode fall plotted against ambient temperature for different currents in potassium-argon and potassium-helium, the seed pressure being 3.5 torr in both cases. In the potassium-argon case, the cathode fall is seen to remain roughly constant throughout the

FIGURE 7.5

PLOTS OF CATHODE FALL AGAINST AMBIENT GAS TEMPERATURE
FOR DIFFERENT CURRENTS IN POTASSIUM-ARGON

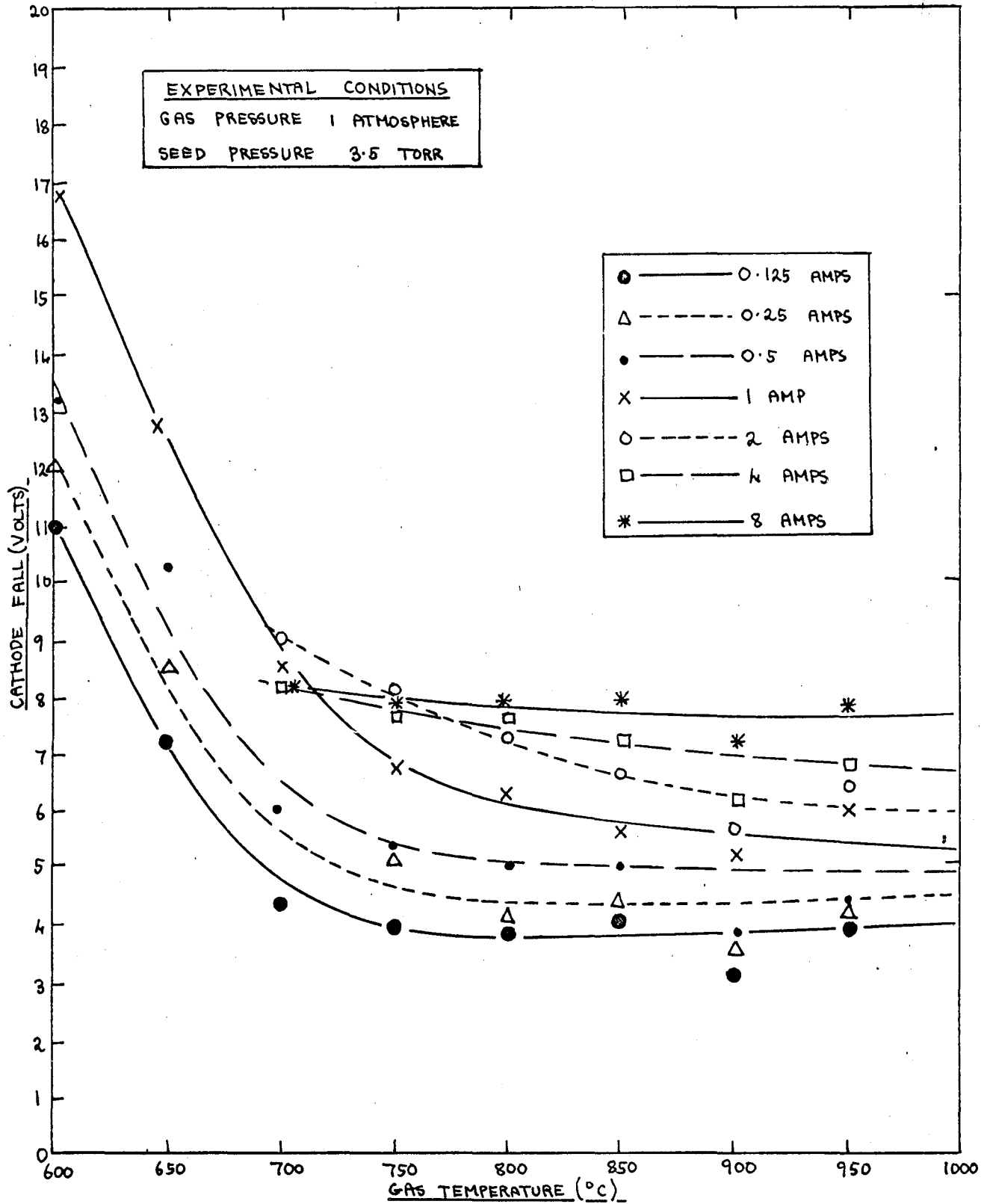


FIGURE 7.6

PLOTS OF CATHODE FALL AGAINST AMBIENT GAS TEMPERATURE
FOR DIFFERENT CURRENTS IN POTASSIUM-HELIUM

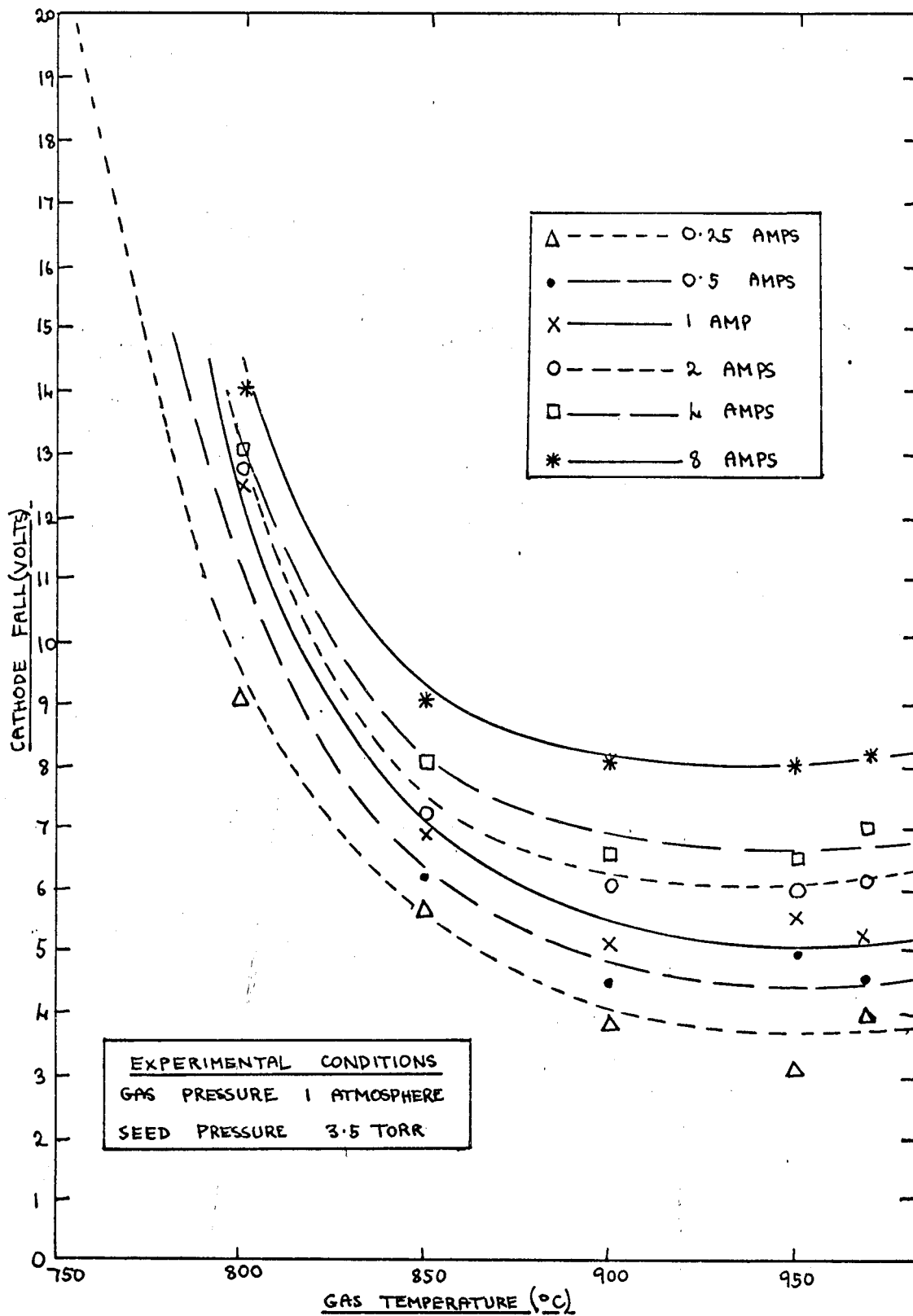


FIGURE 7.7

PLOTS OF CATHODE FALL AGAINST AMBIENT GAS TEMPERATURE FOR DIFFERENT MIXTURES

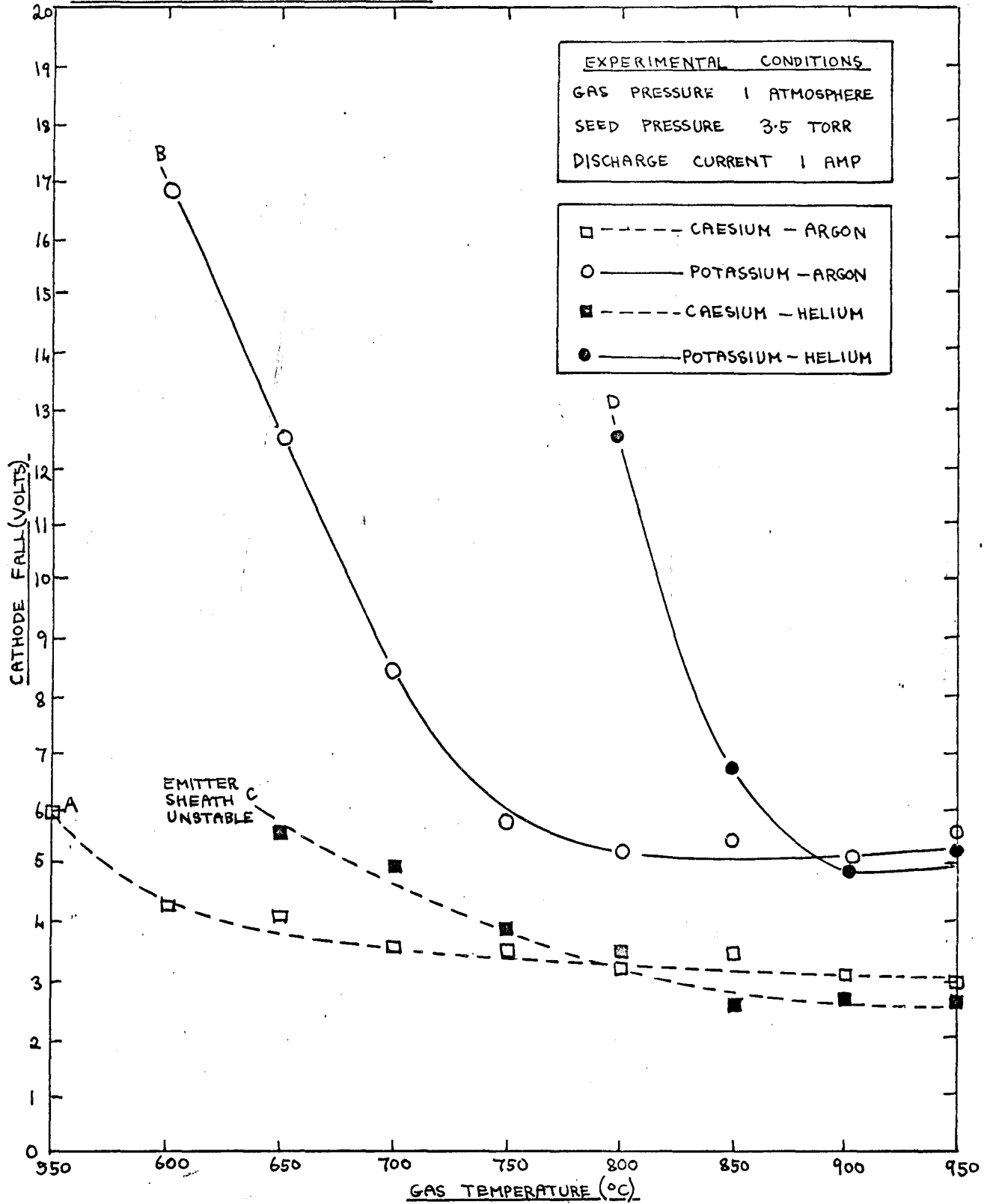
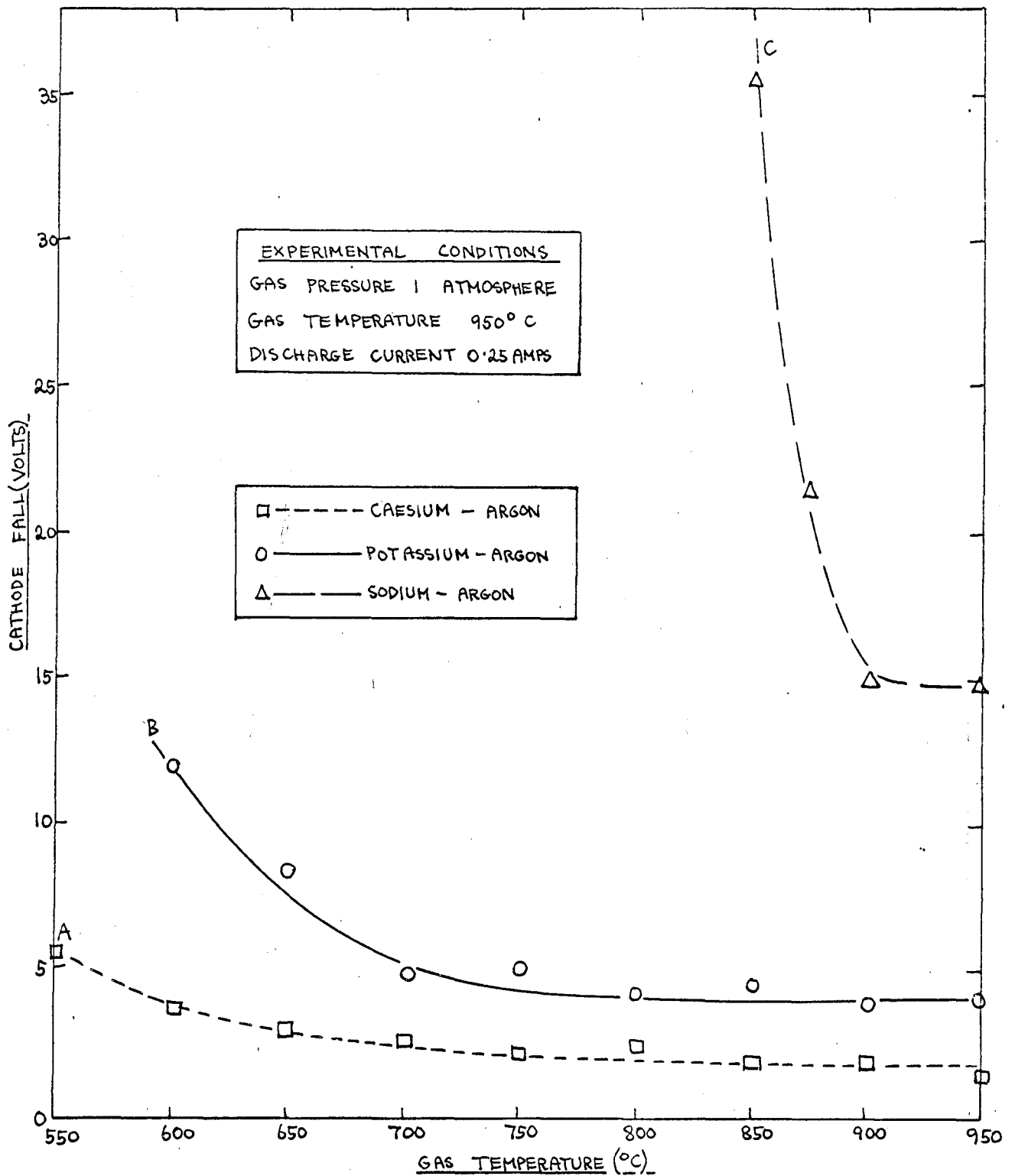


FIGURE 4.8

PLOTS OF CATHODE FALL AGAINST AMBIENT GAS TEMPERATURE
FOR DIFFERENT SEEDS IN ARGON



temperature range $950^{\circ}\text{C} - 750^{\circ}\text{C}$, rising rapidly when the temperature falls below the latter value. The potassium-helium results are qualitatively similar, though in this case the cathode fall begins to rise when the temperature falls below 875°C .

In figure 7.7, plots of cathode fall against ambient temperature are given for a current of $\frac{1}{2}$ amp in caesium- and potassium-argon and caesium- and potassium-helium, the seed pressure being 3.5 torr throughout. Figure 7.8 shows plots of cathode fall against ambient temperature for a current of $\frac{1}{4}$ amp in caesium-, potassium- and sodium-argon, the seed pressure being 3.5 torr in all cases. All the curves in these two figures have a region through which the cathode fall remains roughly constant, the extent of the region varying from mixture to mixture, and all the curves begin to rise when the temperature falls below the lower limit of this region.

It must again be stressed that the temperature being varied in figures 7.5 - 7.8 is the ambient temperature, and not the actual temperature of the cathode surface, which, as we have seen, appears to be higher than the ambient temperature.

7.6 THE DEPENDENCE OF THE CATHODE FALL ON THE CHOICE OF DILUENT

In figures 7.3 and 7.7, it is seen that the value of the diffuse mode cathode fall at a given current is practically the same in a mixture with helium as the diluent gas as in a similar mixture with argon as the diluent gas provided that the seed pressure and ambient temperature are high. At low seed pressures and low

temperatures, however, the helium values tend to be higher than the argon values.

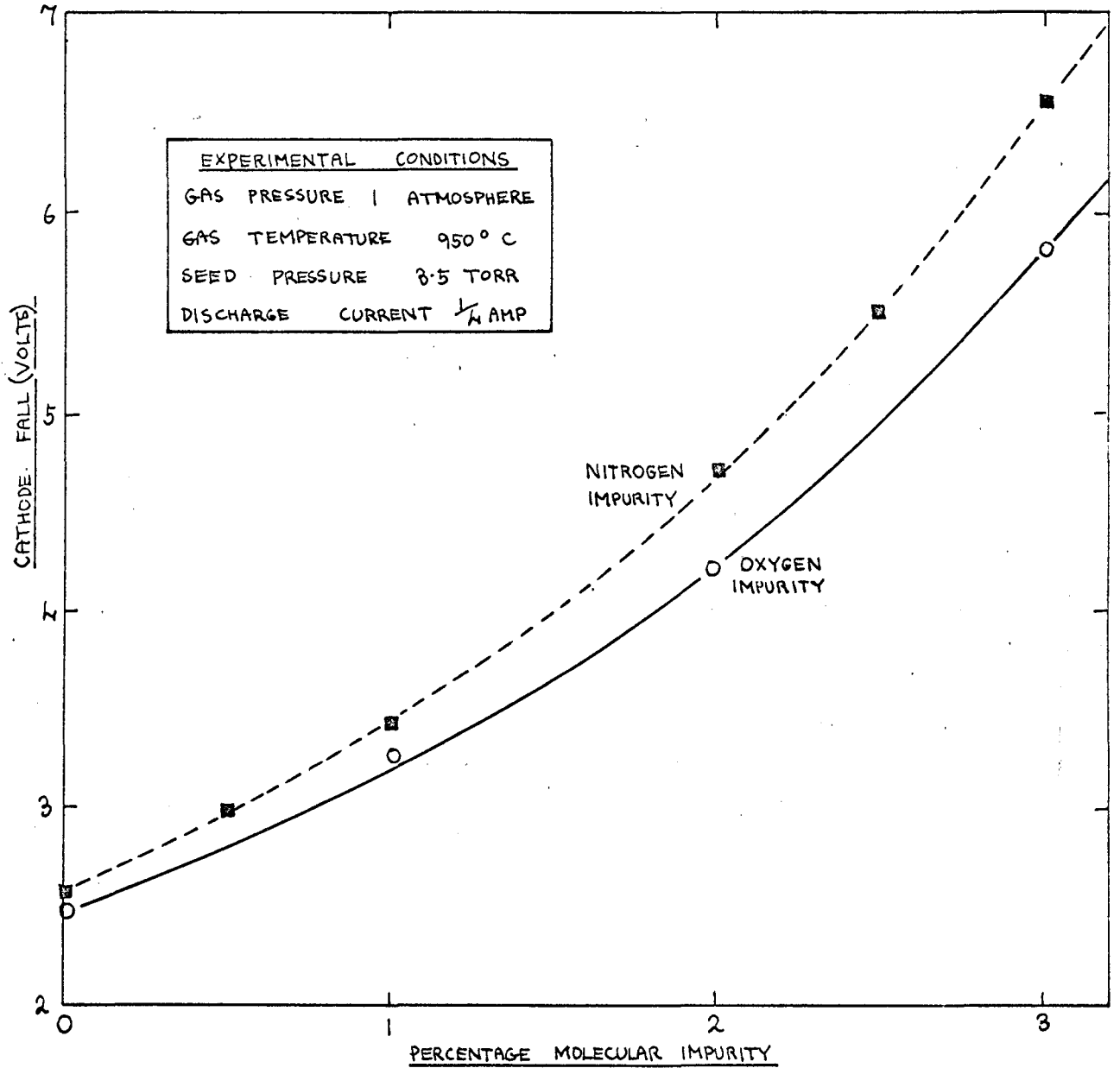
7.7 THE DEPENDENCE OF THE CATHODE FALL ON THE CHOICE OF SEED

It is apparent from most of the figures given in this chapter that the value of the diffuse mode cathode fall depends strongly on the choice of seed metal. In figure 7.1, the mixtures are seen to fall into three distinct groups: those with caesium as seed, which have the lowest cathode fall values throughout the current range studied, those with potassium as seed, which have distinctly higher values, and the mixture with sodium as seed, which has the highest values of all. The same is true for the seed pressure-dependent results. In figure 7.3, it is seen that the two potassium curves lie at higher values than the two caesium curves throughout the seed pressure range investigated, although the difference between the two metals is not great at high seed pressures. Figure 7.4, shows that the sodium results are consistently higher than the potassium and caesium results. The temperature-dependent results given in figures 7.7 and 7.8 also illustrate this difference between the three seeds, and it is seen that the difference becomes greater as the temperature falls to low values.

7.8 THE EFFECT OF ADDED MOLECULAR IMPURITIES ON THE CATHODE FALL.

In section 6.6, it was shown that the addition of a small amount of molecular impurity (oxygen or nitrogen) to a rare gas/alkali metal mixture causes both the positive column field and the cathode fall that are required to support a given current to increase. Figure 7.9 shows the dependence of the cathode fall on the percentage of oxygen and nitrogen in a potassium-argon mixture, the seed pressure, ambient temperature and discharge current being 3.5 torr, 950°C and $\frac{1}{4}$ amp respectively. Three results are evident from this figure. Firstly, it is seen that the cathode fall rises as the amount of impurity increases, the rate of increase being somewhat greater than linear. Secondly, it is seen that comparatively large amounts of impurity can be tolerated, over 2% being needed to double the cathode fall. Thirdly, it is seen that a given quantity of nitrogen appears to have a slightly greater effect on the cathode fall than the same amount of oxygen, but that the difference between the two gases is not great.

PLOTS OF CATHODE FALL AGAINST VOLUME PERCENTAGE OF OXYGEN AND NITROGEN IN POTASSIUM-ARGON



PART II

DISCUSSION OF THE RESULTS

IIA THE BREAKDOWN OF THE GAS

In this section, we will discuss the breakdown voltage results that were given in Part I. In Chapter 8, we will examine the breakdown process in some detail, starting with the low-current discharge that occurs at low applied voltages, and showing how the transition to the high-current discharge takes place. We will then derive a semi-empirical formula for the breakdown voltage in a seeded plasma of the type under study. In Chapter 9, we will show that the theory which we have developed is capable of giving at least a qualitative explanation of most of the features of the experimental breakdown voltage results that were described in Chapter 5.

CHAPTER 8ANALYSIS OF THE BREAKDOWN PROCESS8.1 THE LOW-CURRENT EQUILIBRIUM DISCHARGE.

At temperatures of the order of 1000°C, an atmospheric-pressure rare gas seeded with a few torr of alkali metal vapour contains an electron number density of the order of 10^9 cm^{-3} , and a corresponding ion number density (see Chapter 13). The actual value depends on the nature of the seed and on the gas temperature and seed pressure, being given by the Saha equation. A metal electrode placed in such a plasma becomes covered by a thin layer of the alkali metal, and this greatly reduces the work function of the surface, enabling copious thermionic emission to occur under suitable conditions. If two plane-parallel electrodes are immersed in such a plasma, and a small voltage is applied between them, a small current will flow, its value being limited by space charge effects. Sakuntala (1965) has shown that if one electrode emits electrons and there are no positive ions present in the gas, the current density j is given by

$$j = \frac{9}{32\pi} \cdot K^- \cdot \frac{V^2}{D^3} \quad \text{o.s.u.} \quad \text{-----} \quad 8.1$$

where K^- is the electronic mobility (see Chapter 14),

V is the applied voltage,

D is the electrode separation.

This equation is obtained by substituting for the charge density in Poisson's equation, and integrating twice, since it is the

space-charge field that controls the current.

If electrons are emitted from a cathode and positive ions from an anode, and no ionisation occurs in the gas apart from thermal ionisation, then the current density can be shown to be given by (Sakuntala 1965, Ivey 1954)

$$j = \frac{9}{32\pi} \cdot K^- \cdot \frac{V^2}{D^3} + \left(1 + \frac{K^-}{K^+}\right) j_+ \text{ e.s.u.} \quad \text{--- 8.2}$$

where K^+ is the ionic mobility

and j_+ is the ion current density

The value of j_+ is determined by the ion number density in the plasma, the ionic mobility, and the electric field (see Chapter 14).

Sakuntala has shown that the first term in eqn. 8.2 becomes small compared with the second term as the ion number density rises with increasing gas temperature. For an ion number density of the order of 10^9 cm^{-3} , V about 1 volt and D about 1 cm, the first term is of the order of $10^{-8} \text{ amp cm}^{-2}$, while the second term is about $10^{-5} \text{ amp cm}^{-2}$. Thus, the current that the discharge can carry is limited by the ion number density, and also by the rate at which the ions can move up and neutralise the negative space charge that builds up near the cathode. The electronic mobility is much greater than the ionic mobility (Chapter 14), so the discharge current is virtually all carried by the electrons, but every amp cm^{-2} of electronic current moving from cathode to anode requires an ionic current of $\frac{K^+}{K^-} \text{ amp cm}^{-2}$ and this, in turn, depends on maintaining the ion number density in the plasma. There is no difficulty involved in

obtaining electrons, since the cathode surface is capable of supplying far higher current densities by thermionic emission than are actually carried by the discharge in this low-current equilibrium mode. Indeed, Sakuntala (1964) has shown that a potassium-covered electrode at about 1000°C appears to be capable of supplying a current of the order of amps without the help of secondary emission. Sakuntala (1965) has shown that the theory given above provides an accurate description of the low-current discharge in alkali-metal-seeded rare gases for applied voltages of roughly 10^{-1} to 10 volts (the gap being of the order of several m.m.), and low-current work carried out by the author has proved to be in excellent agreement with Sakuntala's work. Above an applied voltage of the order of 10 volts, the actual value depending on the electrode spacing, the current begins to rise more rapidly than eqn. 8.2 would indicate, and the next stage of the discharge is entered - the transition to the non-equilibrium discharge.

8.2 THE APPROACH TO BREAKDOWN.

In the equilibrium region dealt with above, the ion number density is constant, the linear increase in the current density with rising voltage being brought about by an increase in the drift velocity of the electrons and ions. When the electric field passes a critical value, however, the current/voltage characteristic becomes non-linear, and Sakuntala (1965) has shown that this can only be brought about by an increase in the ion number density due to the onset of primary ionisation. Sakuntala

has also shown that this ionisation occurs in the inter-electrode plasma, where the electrons have a constant mean energy, rather than in the high-field region in front of the cathode. If the electron current density at the cathode end of the discharge is j^- , then the electron current density at a distance x from the cathode is $j^- \exp(\alpha x)$, where α is the first Townsend coefficient (see Chapter 1). This assumes that the cathode fall region is narrow compared with the gap width, an approximation shown by Sakuntala to be valid. If we now assume that the electric field in the plasma is uniform once we have passed through the cathode fall region, an assumption that Sakuntala has shown to be reasonable, it can be shown that the current density j is given by

$$j = \underbrace{j^- \exp(\alpha x)}_{\text{electron current component}} + \underbrace{j^- \left[\exp(\alpha D) - \exp(\alpha x) \right]}_{\text{positive ion current component}} \quad \text{--- 8.3}$$

Sakuntala shows that if this expression for j is used in substituting for the charge density in Poisson's equation and the resulting equation is integrated twice, then the variation of the current density with rising applied voltage is given by

$$j = \frac{9}{32\pi} \cdot K \cdot \frac{V^2}{D^3} \frac{1}{1 - \frac{K j^-}{K+j} \left[\exp(\alpha D) - \frac{3}{\alpha D} (\exp \alpha D - 1) \right]} \quad \text{--- 8.4}$$

As α rises from zero with increasing V , the denominator of this expression decreases, and when αD reaches a value of about 3, it passes through zero. This is more clearly seen if $\exp(-\alpha D)$ is substituted for $\frac{j^-}{j}$ and taken inside the square bracket, when the

denominator becomes

$$1 = \frac{K_-}{K_+} \left[1 - \frac{3}{\alpha D} \frac{(\exp \alpha D - 1)}{\exp(\alpha D)} \right]$$

Since $\frac{K_-}{K_+}$ is of the order of several hundred (see Chapter 14), the denominator vanishes when the second term inside the bracket approaches a value of unity, i.e. when αD approaches a value of , just under 3. Thus, the transition to the high-current discharge should take place when αD reaches this value.

Experimental work carried out by Sakuntala (1965) and the author has shown that the approach to the breakdown of the plasma is characterised by a progressive increase in the slope of the current/voltage characteristic with rising voltage (figure 5.1) the slope becoming infinite at the point of breakdown, and Sakuntala has shown that the theory given above gives a reasonably accurate description of the shape of the characteristic. As we have seen in Chapter 5, the transition itself produces a sudden increase in the discharge current from the order of milliamps or tens of milliamps (the actual value being largely determined by the properties of the plasma) to the order of amps or greater (the actual value being determined not so much by the properties of the plasma as by the values of the external circuit resistance and the total circuit voltage). The increase in current is accompanied by a drop in the electrode voltage from the high value that is needed to bring about the transition to the relatively low value that is required to maintain the high-current discharge. Sakuntala (1965) has shown that the need for a discontinuous transition between the

low- and high-current discharges becomes progressively less as the gas temperature increases, until at temperatures of the order of 2000°K, the discharge makes a smooth transition to the high current discharge. This change in the character of the transition is brought about by the progressive increase in the intrinsic ion number density that takes place as the plasma temperature rises, and has been observed experimentally by Pinchak and Zukoski (1963).

The crux of Sakuntala's theory of the approach to breakdown is that the breakdown voltage depends only on the value of the inter-electrode spacing D and on the first Townsend coefficient α . The problem of deriving a formula for the breakdown voltage is therefore reduced to the somewhat simpler problem of deriving a formula for α . Because of the lack of data on which to base the calculation, it is not possible to give an accurate account of the dependence of α on the applied voltage for the type of plasma under study. What we can do, however, is derive a semi-empirical formula that will give us an idea of how α depends on the different variables, namely, the seed pressure, electronic mean free path, applied voltage and electrode spacing. We shall do this by two methods, the first based on Townsend's classical derivation of α , and the second based on a method given by von Engel. It will be seen that both methods lead to the same formula for α .

8.3 THE CLASSICAL DERIVATION OF THE FIRST TOWNSEND COEFFICIENT.

In the classical derivation of α , as described by von Engel (1965), it is assumed that electrons are drifting through a gas under the influence of an electric field. Since the electrons draw their energy from the field, the least distance l that an electron must travel along the direction of the field in order to be capable of ionising a gas atom is given by

$$l = \frac{V_i}{X} \quad \text{-----} \quad 8.5$$

where V_i is the ionisation potential of the gas

X is the electric field.

If the electronic mean free path is λ , the probability p' of a given free path being greater than l is given by the statistical distribution function, and is

$$p' = \exp\left(-\frac{l}{\lambda}\right) \quad \text{-----} \quad 8.6$$

Since unit length of path along the field direction contains $\frac{1}{\lambda}$ mean free paths, the first Townsend coefficient (the number of ionising collisions per unit length of path) is obviously proportional to $\frac{1}{\lambda} p'$, so that we may write

$$\alpha = \text{const.} \frac{1}{\lambda} \exp\left(-\frac{l}{\lambda}\right) \quad \text{-----} \quad 8.7$$

For a simple gas, we can replace λ by $\frac{\lambda_1}{p}$, where p is the gas pressure and λ_1 is the mean free path at unit pressure.

Combining eqns. 8.5 and 8.7, we see that

$$\frac{\alpha}{p} = \text{const.} \exp\left(-\frac{\text{const}}{\frac{X}{p}}\right) \quad \text{-----} \quad 8.8$$

The first constant is proportional to $\frac{1}{\lambda_1}$ and allows for the fact that not all of the possible ionising collisions actually result

in ionisation. The second constant is proportional to $\frac{V_i}{\lambda}$ and allows for the fact that the effective ionisation potential of the gas is less than V_i , since the classical argument assumes that the electrons start from rest between collisions, whereas this is not in fact the case in an actual discharge.

For the seeded plasmas under study, we can derive a formula for α by essentially the same argument as that which has just been given for a simple, unseeded gas, but we must make two important modifications. In a simple gas, the electronic mean free path λ is inversely proportional to the gas pressure p , whereas this is not the case for a seeded plasma. As we shall see in Chapter 14, the value of λ for a seeded gas is given by

$$\frac{1}{\lambda} = n_s a_s + n_d a_d \quad \text{-----} 8.9$$

where n_s , n_d , a_s and a_d are respectively the number density and mean electron collision cross section of the seed and diluent. It is assumed that the number density of positive ions is not high enough to necessitate the inclusion of an ion-scattering term (see Chapter 14). The other allowance that must be made is for the fact that not all of the possible ionising collisions will occur with seed atoms, the remainder occurring with diluent atoms: the latter have far too high an ionisation potential to allow significant ionisation to take place. Of the possible ionising collision, only $\frac{n_s a_s}{n_s a_s + n_d a_d}$ will occur with seed atoms. If we go through the classical derivation of α making the changes discussed above, we see that

$$\alpha = \text{const.} \frac{n_s a_s}{n_s a_s + n_d a_d} \cdot (n_s a_s + n_d a_d) \exp\left(\frac{-\text{const. Vi}}{X \lambda}\right) \quad \text{--- 8.10}$$

$$\text{so that } \alpha = \text{const. } n_s a_s \cdot \exp\left(-\frac{\text{const. Vi}}{X \lambda}\right) \quad \text{--- 8.11}$$

Since the seed number density n_s is directly proportional to the seed pressure p_s , we can substitute the latter for n_s in the equation. We can also replace the electric field X by $\frac{V}{D}$ (V being the applied voltage), since it seems reasonable to suppose that the electric field will be directly proportional to the applied voltage and inversely proportional to the electrode spacing. The fact that X is not actually equal to $\frac{V}{D}$ will be allowed for by the presence of the empirical constant. Making these substitutions, we see that

$$\alpha = \text{const. } p_s \exp\left(-\frac{\text{const. ViD}}{V \lambda}\right) \quad \text{--- 8.12}$$

8.4 VON ENGEL'S DERIVATION OF THE FIRST TOWNSEND COEFFICIENT.

Von Engel (1965) shows that eqn. 8.8 can also be derived by considering the ionisation efficiency of a swarm of electrons moving through a gas with drift velocity v_d . If the number of ionising collisions per electron per second is Z , and Vd is the distance an electron moves along the field direction in 1 sec, we see that the definition of α as the number of ionising collisions per electron per unit length of path leads to the relationship

$$\alpha = \frac{Z}{v_d} \quad \text{--- 8.13}$$

If the electron temperature is T_e , von Engel shows that Z is approximately proportional to the quantity $p_e^{1/2} \exp\left(-\frac{eVi}{kT_e}\right)$,

where p is the gas pressure and k is Boltzmann's constant. He also shows that the electron temperature is approximately proportional to $\frac{X}{p}$ for the type of situation under study, while the drift velocity v_d is proportional to $\left(\frac{X}{p}\right)^{1/2}$. Substituting in eqn. 8.13, we see that

$$\frac{\alpha}{p} = \text{const.} \exp\left(-\text{const } v_i / \frac{X}{p}\right) \quad \text{-----} \quad 8.14$$

which has exactly the same form as eqn. 8.8.

If we repeat the above argument for a seeded plasma, allowing for the fact that the electronic mean free path is not inversely proportional to the seed pressure p_s , we find that we have to replace the $\frac{X}{p}$ on the right hand side of eqn. 8.14 by $X \lambda$, and if we replace X by $\frac{V}{D}$, we see that

$$\alpha = \text{const.} p_s \exp\left(-\frac{\text{const.} v_i D}{V \lambda}\right) \quad \text{-----} \quad 8.15$$

and this equation has exactly the same form as eqn. 8.12. Let us denote the two empirical constants in the equation by C_1 and C_2 , so that

$$\alpha = C_1 p_s \exp\left(-\frac{C_2 v_i D}{V \lambda}\right) \quad \text{-----} \quad 8.16$$

8.5 CALCULATION OF THE BREAKDOWN VOLTAGE.

Having derived a formula for α , we are now in a position to use Sakuntala's theory to derive a formula for the breakdown voltage V_B . Making use of the above formula for α , we see that Sakuntala's condition for breakdown becomes

$$\alpha D = C_1 p_s D \exp\left(-\frac{C_2 v_i D}{V_B \lambda}\right) = 3 \quad \text{-----} \quad 8.17$$

Taking natural logarithms, we see that

$$\begin{aligned} \log_e (C_1 p_s D) - \frac{C_2 Vi D}{V_B \lambda} &= \log 3 \\ \therefore \frac{1}{V_B} &= \frac{\lambda}{C_2 Vi D} \cdot \log_e \left(\frac{C_1 p_s D}{3} \right) \\ \therefore V_B &= \frac{C_2 Vi D}{\lambda} \cdot \frac{1}{\log_e \left(\frac{C_1 p_s D}{3} \right)} \quad \text{8.18} \end{aligned}$$

where Vi is the ionisation potential of the seed,

D is the electrode spacing,

λ is the electronic mean free path,

p_s is the seed pressure,

C_1 and C_2 are empirical constants.

8.6 THE LIMITATIONS OF THE THEORY.

Before we proceed any further, let us take a critical look at the formula we have just derived, and examine its limitations. Its main weaknesses are that it is only an approximate relation, containing two empirical constants, and that its validity depends on Sakuntala's conclusion that breakdown will occur when E/D reaches a value of about 3. Let us begin with the first of these points, and examine the two empirical constants C_1 and C_2 , since eqn. 8.18 will only be valid throughout the entire range of experimental conditions to be considered if these quantities are in fact constant.

The constant C_2 allows for the fact that the electrons do not start from rest between collisions, but have a fairly high mean energy. This means that they do not have to acquire the full ionisation energy directly from the field during one free path,

so that the effective value of the ionisation potential of the seed is less than V_i . The mean energy of the electrons can be given in terms of the electron temperature T_e , but we must realise that the term "electron temperature" does not have the same meaning when applied to the pre-transition plasmas as it has when applied to the highly-ionised plasmas that will be discussed in Section IIB. If the electron number density were high enough for the electrons to interact among themselves sufficiently strongly to produce a true Maxwellian energy distribution, then we would know that the high-energy tail of the energy distribution was present (see Chapter 12), and could use the value of the electron temperature to calculate the rate of ion production with a fair degree of accuracy. We will see that this can be done in the post-transition plasma, since the electron number density is several orders of magnitude higher than in the pre-transition plasma - high enough for strong electron-electron interaction to take place. If the electron number density were very low, as it is in ordinary gases before breakdown occurs, then the electrons would not interact among themselves at all, but would merely draw energy from the field and collide with the gas atoms. In this case, the electron energy distribution would be a Druyvesteyn distribution (von Engel 1965), and we could again make a reasonably accurate estimate of the rate of ionisation by electron-atom collisions, since the number of electrons having sufficient energy to ionise could be calculated; the number of high-energy electrons would be far lower in a Druyvesteyn distribution than in a Maxwellian

distribution at the same mean energy. In the pre-transition plasma under study, the number density of electrons is high enough to allow some electron-electron interaction to take place, so the electron energy distribution lies somewhere between the Druyvesteyn and Maxwellian cases. It is for this reason that the effective ionisation potential of the seed has to be reduced, but we can see from the above discussion that there is no guarantee that the effective ionisation potential will be constant. Indeed, we can confidently state that it will certainly not remain constant if the plasma conditions are changed by a very large amount. All that we can do in practice is determine its value empirically for a given set of experimental conditions, and then assume that it remains roughly constant if the conditions are varied slightly.

The same sort of argument can be applied to the other empirical constant C_1 . This allows for the fact that the number of free paths in unit distance along the field is greater than $\frac{1}{\lambda}$ because of the random nature of the electronic motion, and also allows for the fact that not all of the possible ionising collisions actually result in ionisation. C_1 will certainly not be a true constant, since the ionising efficiency of electron-atom collisions is known to vary as the electron energy alters (von Engel 1965). The value of C_1 will also be affected by the fact that the electron energy distribution lies somewhere between the Druyvesteyn and Maxwellian cases. As in the case of C_2 , all we can do is determine the empirical value of C_1 for a given set of experimental conditions, and then assume that it remains roughly constant if

the conditions are varied slightly. We see from eqn. 8.18 that the value of the breakdown voltage is not so sensitive to changes in C_1 as it is to changes in C_2 , so that the value of the former can vary by a small amount without greatly affecting the value of V_B .

As we have seen, one of the greatest weaknesses of the formula which we have derived for V_B is that it depends ultimately on a conclusion reached by Sakuntala in her analysis of the pre-breakdown discharge in potassium-argon. We have no guarantee that this result will be valid for other seed-diluent mixtures, or for experimental conditions beyond the limited range investigated by Sakuntala. For this reason, and for the other reasons given above, we would not expect the formula to give anything better than a qualitative description of the dependence of the breakdown voltage on the different variables. Despite these limitations, however, we shall see that the theory which we have developed is capable of explaining most of the results that were given in Chapter 5.

8.7 COMPARISON OF THE BREAKDOWN PROCESS WITH THE CONVENTIONAL SPARK BREAKDOWN OF A GAS.

Let us conclude this analysis of the breakdown process by comparing the type of transition under study with the conventional spark breakdown of a gas, since there are several points of similarity between the two, as well as several important differences. Conventional breakdown of a gas occurs when the value of the second ionisation (or secondary emission) coefficient γ reaches a

sufficiently high value for the relationship

$$\gamma (\exp(\alpha D) - 1) = 1 \quad \text{-----} \quad 8.19$$

to hold (Cobine 1958, von Engel 1965), γ being sometimes called the second Townsend coefficient. The sparking voltage V_S can then be written as

$$V_S = \text{const. } V_i(pD) \frac{1}{\log_e \left(\frac{\text{const. } (pD)}{\log_e \frac{1}{\gamma}} \right)} \quad \text{-----} \quad 8.20$$

and is a function of the product of the gas pressure and the gap width only (Paschen's law). We see that eqns. 8.18 and 8.20 are very similar in form, the main difference being the absence of a secondary coefficient in the former. Another difference between the two is that the electronic mean free path in a seeded plasma is not inversely proportional to the seed pressure, so that Paschen's law does not hold for the variation of the seed pressure p_s , although it does become approximately true at very high seed pressures, when the seed-dependent term dominates the expression for λ . Paschen's law is true for the variation of the total gas pressure, on the other hand, as in the case of a conventional spark breakdown.

There are several other important differences between the transition under study and the conventional breakdown process. In a conventional breakdown process, which normally takes place in the cold, the pre-breakdown current is extremely small (generally in the range 10^{-12} - 10^{-8} amps). The initial current is caused by some external agency (such as U.V. irradiation of the cathode, or production of ions in the gas by some ionising process), and

the current depends for its existence on this external agency, the discharge being non-self-sustaining. In the transition under study, the pre-transition current is not only very much higher than in the conventional case (having a value in the range 10^{-5} - 10^{-2} amps - Sakuntala 1965), but the discharge is also self-sustaining in the sense that a relatively high degree of ionisation is an intrinsic property of the plasma because of its high temperature. Indeed, the ambient temperature of the gas has to be quite high before the breakdown under study can take place, since thermionic emission from the cathode will not occur unless this is so, and we have seen that the transition relies on the fact that the pre-transition plasma has a fairly high degree of ionisation. No such high temperature is necessary for a conventional spark breakdown to occur.

The most important difference between the transition under study and the conventional breakdown process lies in the nature of the breakdown mechanism. In a spark breakdown, the following three stages of the breakdown process can be distinguished. Firstly, there is a region where the current is determined largely by the strength of the external source mentioned above; this is sometimes called the T_0 region. Secondly, as the electric field rises, amplification of the current by direct electron-atom ionisation sets in; this is the T_1 region. Thirdly, more rapid amplification of the current takes place when some secondary ionisation or emission process is called into play (e.g. ionisation by ion-atom collision or production of secondary electrons by positive ion bombardment of the cathode surface); this is the T_2 region, and eventually leads

to the breakdown of the gas. In the present transition, only the first two stages are observed. As we have seen, there is a region where the current/voltage plot is linear and where the current depends largely on the intrinsic degree of ionisation of the seed, and this is followed by a region where the current rises more rapidly than linearly with rising voltage, the degree of ionisation being increased by direct electron-atom collisions. This second region leads directly to the transition, no secondary electron-producing process being required, since a plentiful supply of electrons is readily available from the cathode by means of thermionic emission. As Sakuntala (1965) states, the transition is essentially a "charge neutralisation process", the passage of a large current being made possible only when sufficient positive ions become available to neutralise the space charge that is produced by the flow of electrons from the cathode. In a conventional breakdown process, no such free supply of electrons is available, and the electrons that are needed to carry a large current have to be produced by the actual breakdown mechanism; hence the need for a secondary process to occur.

Because of the above differences, the voltage that is needed to bring about the breakdown under study is far lower than that which would be required to bring about a conventional spark breakdown under similar conditions of electrode spacing and gas pressure. This is mainly because the electric field that is needed to bring about the onset of the primary ionisation process is not nearly so high as that which is needed to bring about the onset of the various

secondary processes. Another factor that makes the transition voltage lower than the value one might expect is the fact that the effective pressure of the seeded plasmas under study is the seed pressure p_s rather than the total gas pressure (one atmosphere in all the cases studied). This is because the low electron collision cross section of the diluent gas makes it a very inefficient scatterer of electrons, so that the plasma has many of the properties of a low-pressure alkali metal vapour.

CHAPTER 9

DISCUSSION OF THE BREAKDOWN VOLTAGE RESULTS

9.1 INTRODUCTION

In the last chapter, we analysed the breakdown process in some detail, and showed why the breakdown voltage values in the plasmas under study are so much lower than conventional sparking voltages for similar conditions of electrode spacing and gas pressure. We shall now determine the extent to which the theory that we have developed is capable of explaining the observed dependence of the breakdown voltage on the different experimental variables. We shall see that it is capable of explaining most of the results that were given in Chapter 5, but that some of the results cannot be explained by the theory in its present form, thus clearly revealing its limitations. The main features of the experimental results are summarised below.

1. The breakdown voltage increases linearly with the electrode spacing over the spacing range investigated (1 - 25 mm), but is not proportional to the spacing, since a plot of breakdown voltage against spacing cuts the voltage axis at a small positive value when extrapolated to zero spacing.
2. At low seed pressures, the breakdown voltage falls fairly slowly as the seed pressure rises, reaches a minimum in the neighbourhood of 1 torr, then increases, eventually rising linearly with increasing seed pressure.

3. The breakdown voltage is roughly constant throughout a fairly wide temperature range, showing no systematic dependence on the temperature between 1000°C (the highest temperature studied) and about 700 or 650°C. Below the latter temperature, the breakdown voltage of potassium-seeded mixtures begins to rise, but no definite rise was observed for caesium-seeded mixtures.
4. The breakdown voltage values for mixtures with helium as the diluent gas are considerably higher than those for mixtures with argon as the diluent for all the experimental conditions investigated. Neon-diluted mixtures occupy an intermediate place.
5. The breakdown voltage does not appear to depend as strongly on the seed metal as on the diluent gas, but it was found that sodium-seeded plasmas required higher breakdown voltages than potassium-seeded plasmas, with caesium-seeded plasmas requiring the lowest voltages of all, under all the experimental conditions studied. For seed pressures of a few torr, however, there was found to be little difference between caesium-seeded plasmas and potassium-seeded plasmas.
6. The addition of a few percent-by-volume of a molecular impurity was found to cause a considerable increase in the breakdown voltage value of a given mixture.

Let us consider these points in turn.

9.2 DEPENDENCE ON ELECTRODE SPACING

Study of eqn. 8.18 shows that the dependence of the breakdown voltage on the electrode spacing should be roughly given by

$$V_B = \text{const} \frac{D}{\text{const} + \log_e D} \quad \text{-----} \quad 9.1$$

It can be shown that the constant in the denominator is large compared with $|\log D|$ for the spacing range under consideration, so that V_B should be very approximately proportional to D . This explains why the breakdown voltage was always observed to rise linearly with increasing electrode spacing, but does not account for the finite zero-spacing voltage intercept that was observed in all the mixtures studied (see figures 5.2, 5.3, 5.4). The reason why eqn. 8.18 does not predict such an intercept is that the theory which was developed in Chapter 8 deals only with effects that occur in the bulk plasma, and does not take into account the cathode mechanism of the breakdown apart from assuming that a plentiful supply of electrons is readily available from the cathode surface. Sakuntala (1965) has shown that the pre-breakdown discharge has a voltage profile that consists of two distinct parts, namely, a uniform voltage gradient stretching from the anode to within a short distance of the cathode, and a much more rapid voltage drop near the cathode surface. The presence of such a cathode fall right up to the moment of breakdown is probably the cause of the voltage intercept under discussion, and we can postulate that the breakdown voltage consists of two components, the first being the voltage necessary to maintain the cathode fall (a constant for given experimental conditions), and the second being the voltage necessary to bring about the breakdown of the bulk plasma (proportional to the electrode spacing). It is the second of

these components that is described by the theory that was developed in the last chapter, the cathode fall component being ignored. Such an approximation can be justified by the fact that the cathode fall component has a value of only a few volts, except at very low temperatures (see figure 5.3), so that it can be neglected in comparison with the bulk plasma component at all but the closest electrode spacings.

Additional experimental evidence for the presence of the cathode fall component is obtained from the high-speed photographic work on the A.C. discharge that was described in Part I. This showed that the breakdown of the bulk plasma in each half cycle was preceded by the build up of a glowing cathode layer, thus demonstrating the importance of the cathode mechanism to the breakdown. It is also interesting to note that the cathode fall component of the breakdown voltage is higher for potassium-seeded plasmas than for caesium-seeded plasmas, and higher still for sodium-seeded plasmas (figure 5.2), and that the cathode fall component falls steadily as the seed pressure rises to very high values (figure 5.4). Study of Chapter 7 shows that the cathode fall of the post-transition discharge behaves in much the same way when the seed is changed or the seed pressure increased.

9.3 DEPENDENCE ON SEED PRESSURE.

In discussing the dependence of the breakdown voltage on the seed pressure, it must always be remembered that Paschen's law does not hold for the variation of the seed pressure (see section 8.7),

so that V_B is not a function of $(p_s D)$ only. This means that no "similarity rules" can be given for the breakdown under study. The dependence of the breakdown voltage on the seed pressure is given in eqn. 8.18, and it is apparent that the effect of a change in p_s is largely going to affect the breakdown voltage through the resulting change in the value of the electronic mean free path λ , since V_B depends linearly on $\frac{1}{\lambda}$ and only logarithmically on p_s itself. The relationship between λ and p_s is given in eqn. 8.9, and is illustrated in figure 9.1, which shows plots of $\frac{1}{\lambda}$ against $\log p_s$ for different mixtures, the values of the electron collision cross sections of the various species that are given in table 14.1 being used in the computation of the curves. At low seed pressures, λ is practically constant with changing p_s , since the seed-dependent term is small compared with the diluent-dependent term. As the pressure rises, the former becomes progressively larger, and eventually dominates the expression for λ , causing the mean free path to fall. If the curves in figure 9.1 were re-plotted on linear graph paper, they would be straight lines, since eqn. 8.9 can be written as

$$\frac{1}{\lambda} = \text{const.} + \text{const. } p_s \quad \text{-----} \quad 9.2$$

It is apparent from eqns. 8.18 and 9.2 that the breakdown voltage should be linearly dependent on the seed pressure at high seed pressures, and should rise as p_s increases. This prediction is in excellent agreement with the experimental results, as is shown in figure 9.2, which shows the breakdown voltage plotted against the seed pressure for a spacing of 5 m.m. in potassium-argon and

FIGURE 9.1

PLOTS OF RECIPROCAL OF ELECTRONIC MEAN FREE PATH
AGAINST SEED PRESSURE FOR DIFFERENT MIXTURES

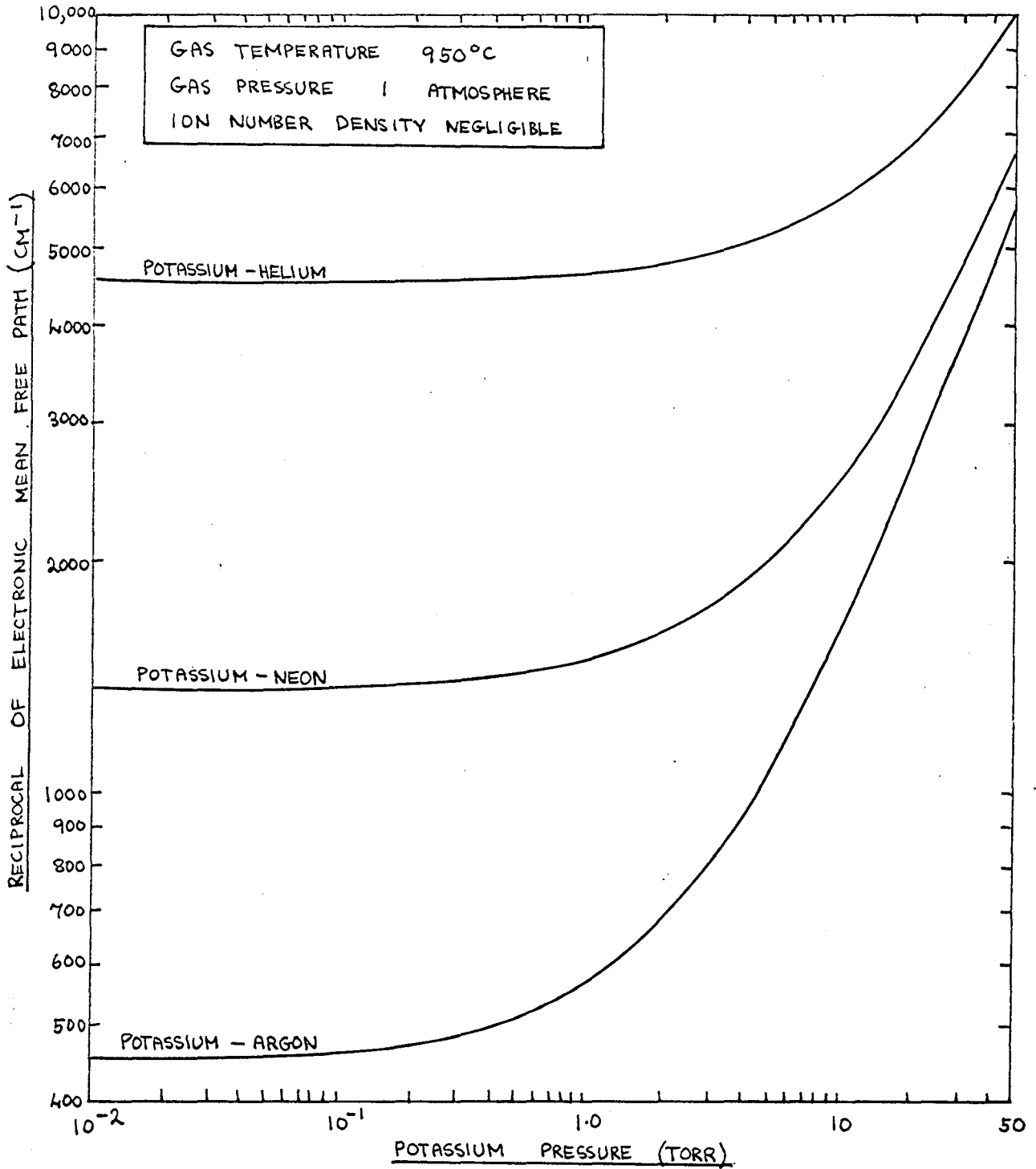
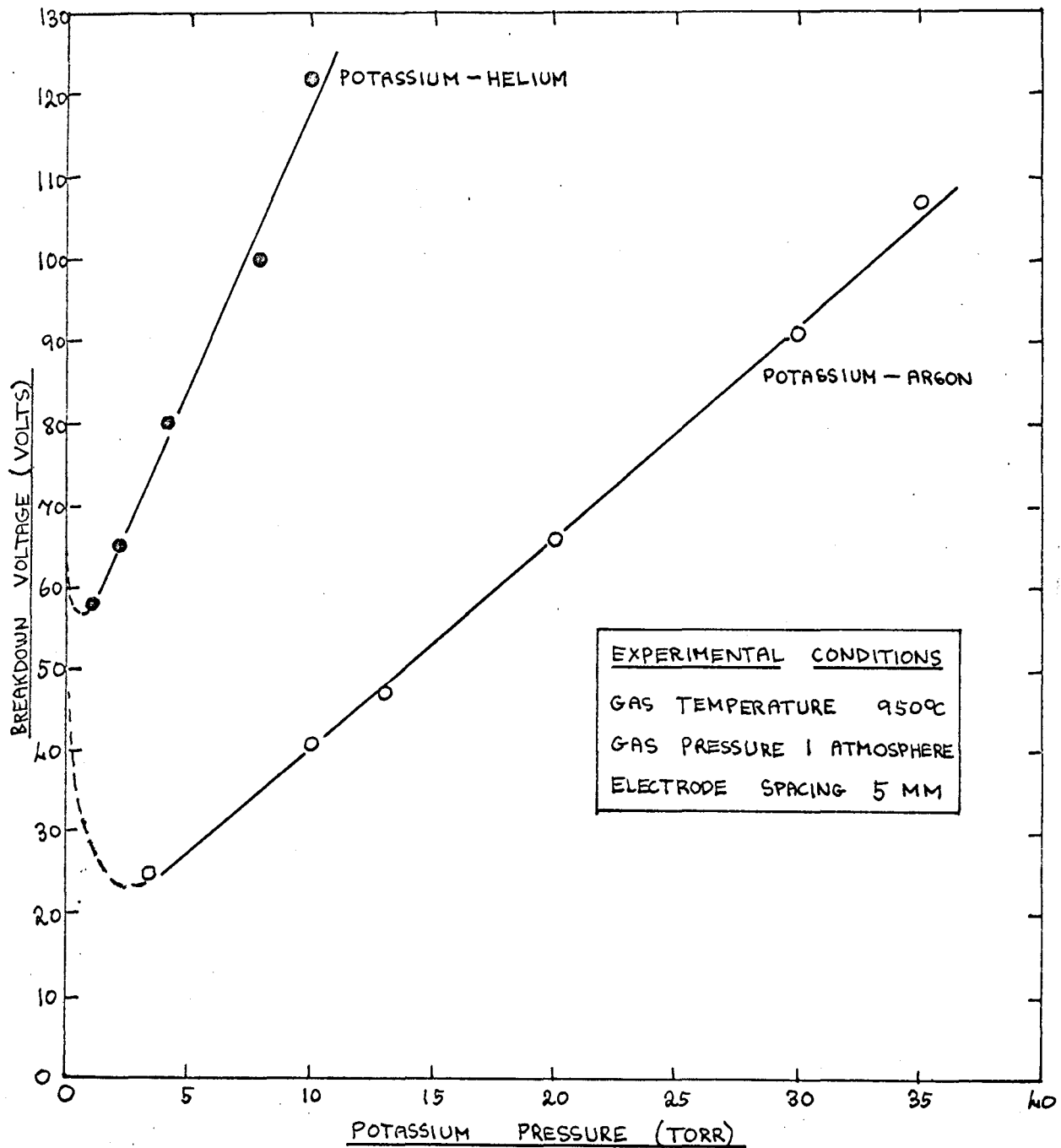


FIGURE 9.2

EXPERIMENTAL PLOTS OF BREAKDOWN VOLTAGE AGAINST
SEED PRESSURE (FIGURE 5.5 RE-PLOTTED ON LINEAR
GRAPH PAPER)



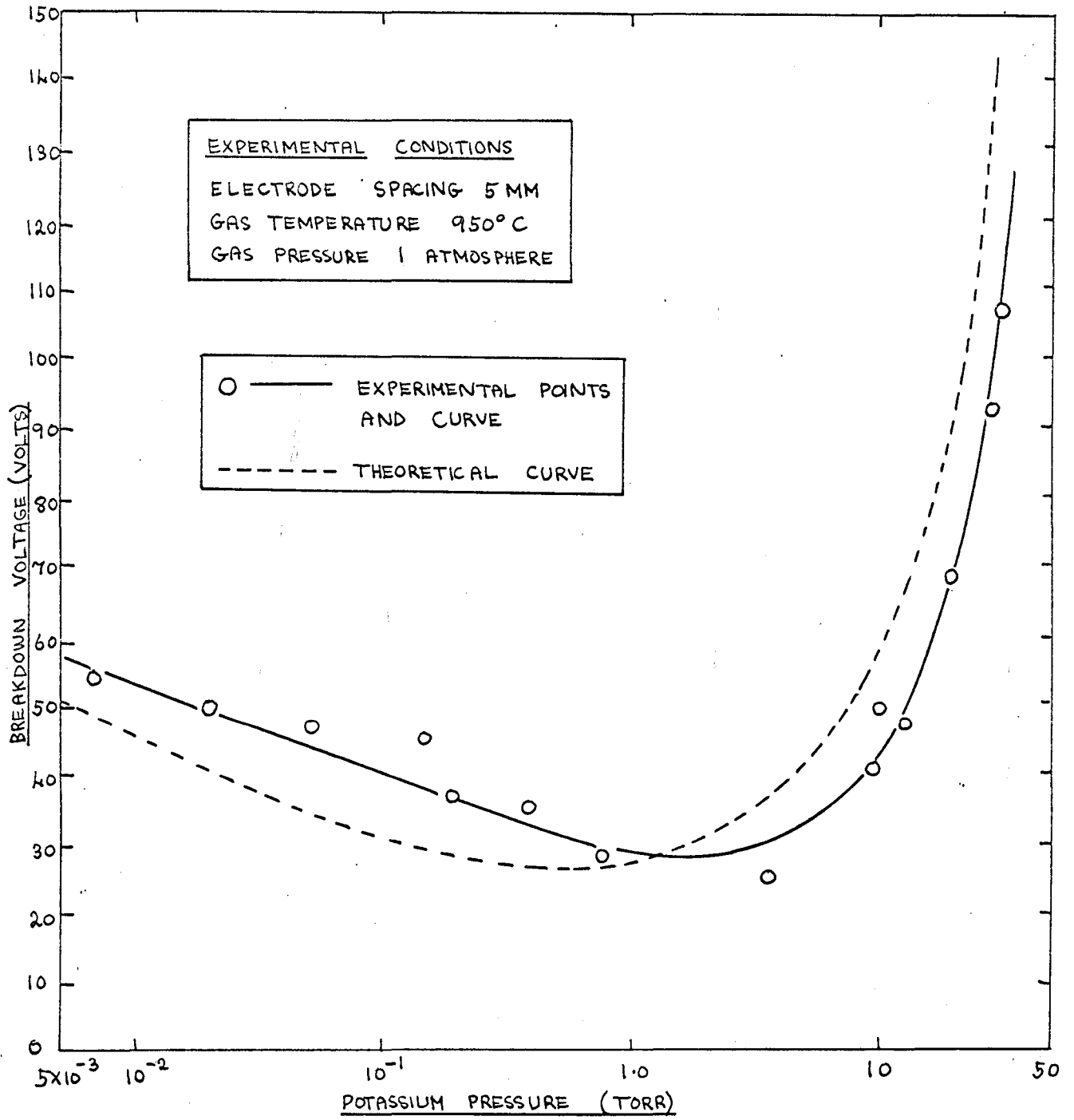
potassium-helium. Figure 9.2 is actually figure 5.5 re-plotted on linear graph paper, and clearly shows the linear relationship that exists between the breakdown voltage and the seed pressure at high seed pressures. At low seed pressures, where λ is virtually independent of p_s , we see from eqn. 8.18 that V_B ought to rise slowly as the seed pressure falls because of the progressive decrease in the value of $\log_{10} \frac{C_1 p_s D}{3}$. Here again, theory and experiment are in qualitative agreement, as is shown by figure 5.5 and also by figure 9.2, both of which show how the breakdown voltage begins to rise when the seed pressure becomes too low to affect the value of the electronic mean free path.

In figure 9.3, eqn. 8.18 has been used to calculate the theoretical dependence of V_B on p_s for one particular case, namely, potassium-argon at 950°C and a spacing of 5 mm. The experimental plot of V_B against p_s that was given for this mixture in figure 5.5 is also shown. The theoretical plot was obtained by estimating the values of the empirical constants C_1 and C_2 from the experimental curve, and then calculating the variation in V_B with changing p_s , the experimental breakdown voltage at $p_s = 1$ torr being taken as a starting point. The equation of the theoretical curve is

$$V_B = \frac{0.432}{\lambda} \cdot \frac{1}{\log_{10} p_s + 9} \quad \text{-----} \quad 9.3$$

where V_B is in volts, λ is in cm., and p_s is in torr, and shows that C_2 has a value of 0.2, so that the effective value of the ionisation potential of the seed is 0.2 of its actual value

THEORETICAL AND EXPERIMENTAL PLOTS OF BREAKDOWN VOLTAGE
AGAINST SEED PRESSURE FOR POTASSIUM-ARGON



(4.32V). This is a perfectly reasonable value, since the effective ionisation potential of the seed can be greatly reduced in the type of plasma under study by the effects that were discussed in Chapter 8. We see that the theoretical curve fits the experimental points as closely as could be expected in view of the approximate nature of the theory. If the potassium-helium curve is calculated in the same way, it is found that it also fits the experimental points reasonably well, although the agreement between the two is not quite as close as in the potassium-argon case.

9.4 DEPENDENCE ON TEMPERATURE.

Over a temperature range that stretches from the highest temperature investigated (1000°C) to around 700°C, the breakdown voltage of the plasmas under study appears to be largely independent of the gas temperature (figures 5.6, 5.7). Examination of eqn. 8.18 shows that this result is at first sight entirely consistent with the theory that we have developed to describe the breakdown, since the temperature does not appear explicitly in the expression for V_B . The situation is not quite as simple as this, however, since two of the terms that appear in eqn. 8.18 do in fact depend on the temperature. As the temperature falls, the number densities of the various species present increase, since the partial pressures remain constant, and this causes the value of the electronic mean free path λ to decrease, λ being roughly proportional to the absolute temperature. The fact that the seed number density depends on the gas temperature also means

that the value of p_s in eqn. 8.18 has to be increased as the temperature falls, since in the course of deriving the equation, we replaced n_s by p_s , making the assumption that the number density is proportional to the seed pressure; this assumption is only true if the temperature is constant. Since V_B depends linearly on $\frac{1}{\lambda}$ and only logarithmically on p_s , we would expect V_B to rise as the temperature falls, and to be roughly inversely proportional to the absolute temperature. We have seen that no such effect is observed experimentally, except possibly in the case of caesium-argon (figure 5.7), and the reason for this discrepancy between theory and experiment is not known.

From the discussion of the breakdown mechanism given in Chapter 8, it is apparent that the temperature range for which the breakdown voltage is roughly constant must be limited, since fundamental changes in the nature of the breakdown process will occur both at very high and at very low temperatures. As we saw in the last chapter, the need for a discontinuous transition between the equilibrium and nonequilibrium discharges becomes progressively smaller as the temperature rises, until at temperatures of the order of 2000°K and higher, the discharge makes a smooth transition to the high-current discharge (Pinchak and Zukoski 1963). This is because the intrinsic degree of ionisation of the plasma is exponentially temperature-dependent, so that the pre-transition current becomes progressively closer to the post-transition current in size as the temperature rises.

As the temperature is lowered, on the other hand, we would certainly not expect the breakdown voltage to remain independent of the temperature indefinitely, since the conditions that allow the transition to take place will eventually cease to prevail. We have seen in the last chapter that the transition relies on there being a ready supply of thermionic electrons available from the cathode surface, and that the breakdown mechanism of the bulk plasma is merely a means whereby this supply of electrons is allowed to pass through the plasma. The current density that can be produced at the cathode by thermionic emission is exponentially temperature-dependent, however, so that below a certain temperature, we would expect the cathode to become incapable of supplying enough electrons to enable the transition to occur without invoking the help of some secondary emission process. For this reason, we would expect the neutralisation breakdown process that was described in the last chapter to give way to a more conventional breakdown process as the temperature falls to very low values, with the various secondary electron-producing processes gradually being brought into play. These will obviously require much higher electric field values than the simple primary ionisation process that leads to the neutralisation breakdown, so the transition zone between the two types of breakdown should be characterised by a considerable rise in the breakdown voltage.

Study of figures 5.3, 5.6 and 5.7 indicates that the change to the spark breakdown process begins to occur at a temperature of

about 700°C for the potassium-seeded plasmas studied, since the breakdown voltage **begins** to rise when the temperature falls below this value, the rate of rise increasing rapidly below 650°C. With caesium-seeded plasmas, on the other hand, no such rise is observed in the temperature range investigated (down to 550°C), **but** it would presumably take place if lower temperatures were investigated. The way in which the breakdown voltage increases as the temperature falls is very interesting, and tends to support the theory given above. Study of figure 5.3 shows that the zero-spacing voltage intercept of the breakdown voltage/electrode spacing plots **begins** to rise when the temperature falls below 700°C and that the slope of the lines also increases (these results are for potassium-argon). This shows that both the cathode fall and the bulk plasma components of the breakdown voltage are increasing, the former probably due to the onset of secondary emission from the cathode surface, and the latter to the onset of secondary ionisation in the bulk plasma. Additional support for the theory that the observed rise in the breakdown voltage at low temperatures is **caused** by a change in the cathode mechanism is given by figure 7.4, which shows plots of cathode fall against ambient temperature for the post-breakdown discharge in potassium-argon. It is seen that the cathode fall rises sharply when the temperature falls below 700°C, indicating that the electron emission process becomes considerably less efficient below this temperature. In caesium-argon, on the other hand, the cathode fall does not start to increase until temperatures of less than

600°C are reached (figure 7.6), and the curve does not rise nearly as steeply as does the potassium curve, indicating that the emission process remains efficient to a lower temperature than in the potassium case. This is the probable reason for the difference between the low-temperature breakdown voltage values in caesium- and potassium-seeded plasmas (figure 5.7).

9.5 THE EFFECT OF CHANGING THE DILUENT GAS

Both Ralph (1962) and the author have observed that helium-diluted mixtures require far higher breakdown voltage values than argon-diluted mixtures, with neon-diluted mixtures occupying an intermediate place. This is in good qualitative agreement with the theory developed in Chapter 8, since eqn. 8.18 predicts that the breakdown voltage of a given mixture should be roughly inversely proportional to the value of the electronic mean free path in the mixture, and we have seen in figure 9.1 how the electronic mean free path in argon-diluted mixtures is several times higher than in helium-diluted mixtures, with neon-diluted mixtures lying between the two. When it comes to giving a quantitative description of the effect on the breakdown voltage of changing the diluent, it is found that the theory is quite accurate at high seed pressures, but that the accuracy decreases as the seed pressure falls. At a potassium pressure of 10 torr, for example, eqn. 8.18 predicts that helium should require breakdown voltages roughly 3.5 times higher than argon, and figure 9.2 shows that the experimental ratio is roughly 3, but

the theory predicts that the ratio should become larger as the seed pressure falls, whereas figures 9.2 and 5.5 show that it remains roughly constant down to a seed pressure of about 2 torr and then becomes smaller.

9.6 THE EFFECT OF CHANGING THE SEED.

To give a qualitative explanation of the effect of the choice of seed on the breakdown voltage, it is only necessary to compare the ionisation potentials of the three seeds used (sodium 5.09V, potassium 4.32V, caesium 3.86V), since eqn. 8.18 shows that the breakdown voltage should rise if the ionisation potential of the seed is increased. For the conditions under which the results given in figures 5.2 and 5.7 were obtained, however, it was found that there was very little difference between caesium-seeded plasmas and potassium-seeded plasmas - certainly less than the difference in the ionisation potentials of the seeds would indicate. To explain this, we must examine the effects of a change of seed in a little more detail.

Replacing potassium by caesium has two effects on the breakdown properties of the plasmas under study. The first effect is to lower the electronic mean free path, since caesium has a larger electron collision cross section than potassium (table 14.1), and this tends to raise the breakdown voltage. The second effect of the change is to reduce the effective value of the ionisation potential of the seed, mainly due to the fact that caesium has a lower ionisation potential than potassium,

but partly because caesium has a higher electron collision cross section, thus increasing the proportion of electron-atom collisions that occur with seed atoms; this reduction in the effective ionisation potential of the seed tends to lower the breakdown voltage. We can therefore explain the observation that potassium-seeded plasmas have very similar breakdown voltage values to caesium-seeded plasmas under certain experimental conditions by inferring that the two effects largely cancel one another out for these particular conditions. Because of the uncertainty in the values of the empirical constants in eqn. 8.18 and the approximate nature of the theory on which the equation is based, however, it is not possible to give an accurate quantitative description of the effects of a change of seed on the breakdown voltage.

9.7 THE EFFECT OF ADDED MOLECULAR IMPURITIES.

As is shown in figure 5.8, the addition of a small amount of a molecular gas such as oxygen or nitrogen to a seeded rare gas causes a marked increase in the breakdown voltage of the mixture. This fact is easily explained, since molecular species not only have high electron collision cross sections, but also have very high collision energy loss factors (see Chapter 12) because of their vibrational and rotational modes, so that they act as highly efficient energy sinks, and tend to prevent the electron temperature from rising. This means that the addition of a molecular impurity to a seeded rare gas reduces the electronic

mean free path, and increases the effective ionisation potential of the seed, and both of these effects cause the breakdown voltage of the mixture to increase, as is seen from eqn. 8.18.

It is not possible to give a quantitative discussion of the effect of a molecular impurity on the breakdown properties of the mixtures under study, however, partly because of the semi-empirical nature of eqn. 8.18, and partly because the electron collision cross sections and collision energy loss factors of the various molecular gases are not known for the electron energy range of interest.

IIB THE POSITIVE COLUMN OF THE DISCHARGE

In this section, we will discuss the positive column of the discharge. In Chapter 10, we will attempt to classify the column, and will then show that four equations, dealing respectively with the energy balance, electron energy balance, ion balance and current continuity, are necessary and sufficient to describe the column. The next four chapters will be devoted to the development of these four equations, Chapter 11 dealing with the energy balance equation, Chapter 12 with the electron energy balance equation, Chapter 13 with the ion balance equation, and Chapter 14 with the arc current equation. In the following three chapters, we will apply the equations to the column. Chapter 15 will deal with the basic properties of the column, Chapter 16 with the dependence of the column properties on the choice of seed metal and on the seed pressure, and Chapter 17 with the dependence of the column properties on the choice of diluent gas and on the diluent pressure. In the course of these three chapters, it will be shown that the theory developed in Chapters 10 - 14 is capable of giving a satisfactory explanation of virtually all the experimental results that are given in Chapter 6.

CHAPTER 10PRELIMINARY DISCUSSION OF THE POSITIVE COLUMN PROPERTIES10.1 CLASSIFICATION OF THE COLUMN.

In this chapter, we will outline the theory that will be used to analyse the positive column of the discharge under study, but before we do so, we will attempt to classify the column. We will see that it appears to be a form of constricted high-pressure arc column, since it has many features in common with other columns of this type, but that we cannot classify it as a conventional thermal arc column because of the nonequilibrium conditions that prevail in the column plasma. The column under study owes its unusual combination of properties to the nature of the gaseous mixture through which the discharge propagates, since this enables it to combine the electrical properties of a low-pressure alkali-metal-vapour column with the thermal properties of a typical high-pressure arc column. Indeed, it combines the most complicated features of these two conventional types of column, namely, an ionisation mechanism based on non-equilibrium effects, and a strongly radially-dependent gas temperature, a fact that makes accurate quantitative analysis of the column mechanisms extremely difficult to carry out, as we shall see later.

It is interesting to compare the properties of the positive column under study with the two standard types of column mentioned above, and this is done in Table 10.1. The first column of the table gives the properties of a typical low-pressure positive

column of the type found in glow discharges or low pressure arcs, and the second column gives the corresponding properties of a typical conventional thermal arc column, the particular case described being a constricted column in atmospheric-pressure argon that was studied by Suits (1939 B). The third column of the table gives the properties of a type of positive column that was recently reported by Massey and Cannon (1965), Massey (1965) and Sugawara (1967) and has properties that are intermediate between those of the type of column under study and those of the conventional thermal arc column that was studied by Suits. The particular column described is in argon at 600 torr, the data being that of Massey and Cannon (1965). The fourth column of the table gives the properties of a typical example of the type of positive column under study, the particular case described being in atmospheric-pressure argon seeded with 3.5 torr of potassium vapour.

TABLE 10.1

<u>1. TYPICAL LOW PRESSURE POSITIVE COLUMN</u>	<u>2. THERMAL COLUMN IN PURE ARGON</u>	<u>3. NONEQUILIBRIUM COLUMN IN PURE ARGON</u>	<u>4. THE COLUMN UNDER STUDY</u>
<u>GAS PRESSURE</u> Generally low- a few torr or less	1 atmosphere	600 torr	argon pressure 1 atmosphere, potassium pressure 3.5 torr
<u>CURRENT RANGE</u> generally in the milliamp range	0.1 amps upwards	0.3 - 1.5 amps observed	0.1 amps upwards
<u>NATURE OF VOLTAGE/CURRENT CHARACTERISTIC</u>			
generally level	negative	negative	negative

TABLE 10.1 (continued)

<u>1. TYPICAL LOW PRESSURE POSITIVE COLUMN</u>	<u>2. THERMAL COLUMN IN PURE ARGON</u>	<u>3. NONEQUILIBRIUM COLUMN IN PURE ARGON</u>	<u>4. THE COLUMN UNDER STUDY</u>
<u>DEPENDENCE OF COLUMN DIAMETER ON CURRENT</u>			
independent of current except at very high currents	diameter increases as current rises	diameter increases as current rises	diameter increases as current rises
<u>COLUMN DIAMETER AT 1 AMP</u>			
_____	about 2 mm	about 4.7 mm	about 5 mm
<u>MEAN COLUMN CURRENT DENSITY AT 1 AMP</u>			
_____	about 32 amps/cm ²	about 6 amps/cm ²	about 5 amps/cm ²
<u>COLUMN VOLTAGE GRADIENT AT 1 AMP</u>			
_____	30 volts/cm	9.4 volts/cm	2.4 volts/cm
<u>POWER DISSIPATED PER UNIT VOLUME OF PLASMA</u>			
generally a few watts per cm ³ or less	extremely high - 960 watts/cm ³ at 1 amp	high - 56 watts/cm ³ at 1 amp	quite high - 12 watts/cm ³ at 1 amp
<u>GAS TEMPERATURE IN COLUMN</u>			
low - generally below 100°C	high - about 8000°K	quite high - 2000 - 3000°K	quite high - 1500 - 2500°K
<u>ELECTRON TEMPERATURE IN COLUMN PLASMA</u>			
very high - several 10 ⁴ °K	same as gas temperature	higher than gas temperature - about 8000 - 10,000°K	higher than gas temperature - about 2500 - 3000°K
<u>NATURE OF IONISATION MECHANISM</u>			
direct ionisation by fast electrons accelerated in field	thermal collisions between atoms	ionisation by electrons in high energy tail of energy distribution	ionisation by electrons in high energy tail of energy distribution
<u>DEGREE OF IONISATION OF GAS</u>			
of the order of 0.001%	in range 0.01 - 100%	about 0.01%	argon unionised, potassium - 1 - 6%
<u>ELECTRON (ION) NUMBER DENSITY IN PLASMA</u>			
of the order of 10 ⁹ cm ⁻³	10 ¹⁴ cm ⁻³ upwards	roughly 10 ¹⁴ cm ⁻³	roughly (1-6) x 10 ¹⁴ cm ⁻³

It is obvious from Table 10.1 that the column under study has far more properties in common with the two high-pressure constricted columns than it has in common with the diffuse low-pressure column that is described in column 1. The three constricted columns have similar gas pressures and currents, all expand as the current rises, and all have negative voltage/current characteristics. The main differences between the three are to be found in their axial voltage gradients, in their energy dissipation rates per unit volume of plasma, and in their electron and gas temperatures, these differences arising because of the different ionisation mechanisms that operate in the three columns. In the thermal argon arc (column 2), the ionisation of the gas is produced by thermal collision processes, and this is a mechanism that requires a very high gas temperature and hence a very high power input per unit volume of plasma. In the nonequilibrium argon arc (column 3), the ionisation of the argon is produced by high-energy electrons, the electron temperature being considerably higher than the gas temperature, and a much smaller energy input per unit volume of plasma is needed to keep the electron temperature high enough to produce nonequilibrium ionisation than is required to keep the gas temperature high enough to produce thermal ionisation. The energy input rate is still fairly high, however, so that the gas temperature is well above the ambient temperature, although it is far too low to produce thermal ionisation. In the seeded nonequilibrium column (column 4) the low ionisation potential of the seed

compared with that of the diluent gas (potassium 4.32 V, argon 15.8 V) means that an even lower power input per unit volume is needed to keep the electron temperature high enough to produce the required degree of ionisation. For this reason, the difference between the column gas temperature and the ambient temperature is considerably less than for the nonequilibrium argon column. The column gas temperature is still quite high, however, because the ambient temperature is high, but is not high enough to produce significant ionisation of either the seed or the diluent gas. The essential difference between the seeded column and the two pure argon columns is that the argon is not ionised to any appreciable extent in the former, and takes no active part in the conduction of electricity, whereas the argon is extensively ionised in the latter two cases, with the entire discharge current being carried by argon ions.

The conclusion to be drawn from the above comparison is that the positive column under study appears to be a form of arc column, so that the five basic relations of Tonks and Langmuir (1929) ought to be necessary and sufficient for a full description of the column properties, since Champion (1951 A) has shown that these relations can be used to describe all types of arc column. The original Tonks-Langmuir theory was only intended to apply to low-pressure columns, but Champion (1952 A) has shown that the theory is valid throughout the pressure range provided that due allowance is made for the changes in the detailed statement and relative importance of the equations that occur as the

pressure rises. Let us now examine the original Tonks-Langmuir theory, and show how it can be adapted to describe high-pressure columns in general and the column under study in particular.

10.2 THE TONKS-LANGMUIR THEORY OF THE LOW-PRESSURE ARC COLUMN.

In 1929, Tonks and Langmuir gave a comprehensive account of the low-pressure arc column in which they showed that there are five basic quantities from which all the other column properties can be derived, and that five equations are necessary and sufficient to determine these quantities. The five basic quantities are:

1. The axial electric field
2. The electron temperature
3. The ion number density
4. The rate of generation of ion pairs
5. The ion current to the containing walls,

and the five basic equations (as named by Champion in 1952) are:

1. The plasma balance equation
2. The ion generation equation
3. The lateral ion current equation
4. The arc current equation
5. The energy balance equation

We assume that the discharge current is determined by the external circuit conditions, so that the current is an independent variable, and that the positive column completely fills the containing tube, so that the column radius is also an independent variable. The

five basic equations describe how the column mechanisms interact to produce a plasma that carries the required current and exactly fills the containing tube, and we assume that the basic variables adjust their values so that such a plasma is produced by the smallest possible axial electric field. Let us now examine the equations in a little more detail, and see how each fits into the general scheme.

In a low-pressure column, the electron temperature is considerably higher than the gas temperature, the ionisation of the gas being produced by collisions between high-energy electrons and gas atoms. The plasma balance equation states "the adjustment of electron temperature to ion generation which just fits the plasma into the space available to it" (Champion 1952 A). This equation and the ion generation equation constitute a pair of simultaneous equations that determine the electron temperature and the degree of ionisation of the gas. The main ion loss process in a low-pressure column is by diffusion of ion pairs to the containing walls where wall recombination occurs, and the rate at which this process takes place is determined by the lateral ion current equation; volume recombination in the body of the plasma is negligible in most low-pressure columns because of the low ion number density. The arc current equation describes the conduction of electricity through the column, and relates the current density in the plasma to the axial electric field and the number densities and mobilities of the various charged particles (electrons and positive ions).

The last of the five equations is the energy balance equation, which relates the rate of dissipation of electrical energy in the plasma to the rate at which energy is removed from the plasma by the various energy loss mechanisms. For a low-pressure column, the rate of power dissipation per unit volume of plasma is generally low, and the energy balance equation is not as important as the other four equations in determining the column properties. A full account of the Tonks-Langmuir theory is given by Cobine (1958).

10.3 EXTENSION OF THE TONKS-LANGMUIR THEORY TO THE HIGH-PRESSURE COLUMN.

As we have seen, the Tonks-Langmuir theory is based on the assumption that the radius of the column is determined entirely by the radius of the containing tube. This assumption is only valid if the tube radius is below a certain critical value, however, since Champion (1952 A) has shown that even a low-pressure column has a "natural arc radius". Champion develops this concept of the natural arc radius by supposing that we start with a low-pressure discharge that fills the available space, with wall recombination the dominant ion loss process, and then make the containing walls progressively more remote. As this is done, the Tonks-Langmuir theory predicts that wall recombination will decrease in importance, with volume recombination showing a corresponding increase in importance until it eventually becomes the main ion loss mechanism.

In addition, the Tonks-Langmuir theory shows that the rate of energy transfer from electrons to gas atoms will increase as the tube radius becomes larger, so that the gas temperature will rise, and the electron temperature will fall. Eventually, the electron temperature will equal the gas temperature and the ion current to the walls will be negligible, so that the properties of the column will be independent of further increases in the containing tube radius, and a "natural arc radius" will have been attained. In a discussion of Champion's theory, Massey (1965) states that a smooth transition to a natural arc radius is extremely unlikely, because the nature of the ionisation and energy loss mechanisms will change during the expansion process, and that a sudden constriction to a thermal column is more likely to occur. Much the same argument as that given by Champion can be given if the gas pressure is increased instead of the containing tube radius, since the effect of an increase in pressure is also to increase the gas temperature and reduce the electron temperature, and to cause the main ion loss process to change from wall recombination to volume recombination. This explains why high-pressure positive columns are nearly all constricted, the column being of smaller cross sectional area than the containing tube unless the radius of the latter is very small. The onset of constriction in positive columns has been discussed by many authors, including Lynch (1967).

As we stated earlier, Champion (1952 A) has shown that the equations of Tonks and Langmuir are valid throughout the pressure range, but that the exact statement and relative importance of the equations changes as the pressure rises. The two most important changes that are required at high pressures are the replacement of the lateral ion current equation by a volume recombination equation, and the elevation of the energy balance equation from a minor to a major role in determining the column properties. As a direct consequence of these two changes, the list of basic dependent variables is different for a high-pressure column than for a low-pressure column, since the ion current to the containing walls must be replaced by the volume recombination rate, and the increase in the importance of thermal energy balance effects means that the gas temperature is no longer independent of the column properties, so that it becomes a dependent variable. From the above argument, it would appear that we now have six basic variables and only five equations, but the situation is simplified by the fact that the volume recombination rate can be dropped from the list of basic variables, since it must be equal to the ion generation rate if equilibrium conditions are to prevail in the plasma. We therefore conclude that the five basic dependent variables from which the properties of a high-pressure column can be completely determined are:

1. The axial electric field
2. The electron temperature
3. The gas temperature

4. The ion number density
5. The rate of generation of ion pairs.

The column radius is not included in the list of basic variables since the value of the column radius can, in theory, be deduced from the five variables listed above. In practice, however, such a calculation is extremely difficult, as we shall see later.

10.4 MODIFICATION OF THE THEORY TO DESCRIBE THE COLUMN UNDER STUDY.

We are now in a position to decide which equations are needed to describe the column under study, and which of the various dependent variables are the basic variables from which the rest of the column properties can be deduced. In theory, the five equations of Tonks and Langmuir (as modified by Champion) are capable of giving a complete description of the column, but in practice, it would prove to be virtually impossible to set up the equations accurately and then solve them simultaneously, since they are not only **intrinsically** complicated, but there is also a considerable degree of uncertainty about the values of many of the basic quantities on which the equations would have to be based (for example, the various ionisation and recombination coefficients). For this reason, the author has decided to use a modified and somewhat simplified version of the Tonks-Langmuir-~~Champion~~ theory in his analysis of the column under study, since this will enable a quantitative description of the column to be attempted, albeit a very approximate one.

The essence of the simplification is the reduction of the number of basic equations to four, with a similar reduction in the number of fundamental variables. This reduction is possible for the type of column under study because we can replace the two equations that determine the ion generation rate and the volume recombination ion loss rate by a single equation which will determine the local value of the ion number density in the plasma in terms of the electron temperature and the other plasma properties. This equation, which we will call the ion balance equation, will be based on statistical thermodynamical considerations, and will be much easier to apply to the column plasma than the two equations that it replaces, since we will no longer need to consider detailed microscopic processes. Because of the above change, we will be able to remove the rate of generation of ion pairs from our list of basic variables.

We will also modify the original theory by replacing the plasma balance equation by an equation that will relate the electron temperature to the local plasma properties; we will call this the electron energy balance equation.

The other two equations that we will employ in our analysis are the same as for the conventional types of column, and are the energy balance equation, which will determine the value of the gas temperature throughout the column, and the arc current equation, which will describe the conduction of electricity through the column.

Our four basic equations are therefore:

1. The energy balance equation
2. The electron energy balance equation
3. The ion balance equation
4. The arc current equation,

and the four basic dependent variables are:

1. The gas temperature
2. The electron temperature
3. The ion number density
4. The axial electric field

As in the case of all the other columns discussed in this chapter, we will assume that the discharge current is determined by the external circuit conditions, so that the discharge current will be an independent variable along with such things as the ambient gas temperature, the seed pressure, and the total gas pressure. The column radius will be a dependent variable, but will not be one of the four basic variables, for the reasons given in the last section.

In the next four chapters, we will develop the four basic equations in more detail, Chapter 11 dealing with the energy balance equation, Chapter 12 with the electron energy balance equation, Chapter 13 with the ion balance equation, and Chapter 14 with the arc current equation. Having developed these equations, we will be in a position to attempt to give a quantitative explanation of the properties of the column that were described in Chapter 6, and this will be done in Chapters 15-17.

CHAPTER 11THE ENERGY BALANCE EQUATION11.1 GENERAL DISCUSSION OF THE ENERGY BALANCE PROCESS

In all steady-state electric discharges, the rate at which energy is dissipated in the positive column plasma by Joule heating must be equalled by the rate at which heat is removed by the various energy loss processes. The amount of heat involved is far greater in the case of the high-pressure arc column than it is for the various low-pressure columns, however, so that the effects of the energy balance process become extremely important at high gas pressures. In this chapter, we will examine the energy balance mechanism of the column under study, and will attempt to develop equations that are capable of describing the rather complicated situation that prevails in and around the column. Because the energy loss mechanisms that operate inside and outside the column are somewhat different, we will find it convenient to discuss the problem in two parts, and will develop one equation to describe the energy balance of the column with respect to its environment (the external energy balance equation), and another to describe the energy balance within the column itself (the internal energy balance equation). Let us briefly examine the two processes before attempting a detailed analysis.

The energy balance of the column and its surroundings.

A positive column which has a diameter that is far less than the bore of its containing tube (as in the case under study) cannot transfer heat directly to the surrounding walls. It must lose the heat that is produced within it through the intervening gas, and will do so partly by direct radiation, and partly by a combination of convection and conduction. In most columns, the latter process is the more important of the two, and necessitates the column boundary being at a higher temperature than the surrounding gas. In the case under study, we shall show that convection/ conduction appears to be the main energy loss process, but that radiation losses must also be considered if an accurate description of the column is to be given.

The internal energy balance of the column.

Whereas convection in the surrounding gas plays a major part in removing the heat from a constricted positive column, it is generally accepted that convection is not important within the actual column plasma, especially if the column diameter is small (as in the present case). The energy that is dissipated in an element of plasma is therefore removed partly by the direct radiation mentioned above, and partly by conduction towards the boundary of the column. This thermal conduction process leads to the production of a negative temperature gradient towards the column boundary, and causes the column to be radially symmetrical.

The core of the column is therefore at a higher temperature than the column boundary, a fact that greatly affects the properties of the column under study, as we shall see in Chapter 15.

The boundary region of the positive column represents a transition zone between the highly-ionised arc plasma and the relatively un-ionised surrounding gas. Because the convection/conduction heat transfer process that prevails outside the column is more efficient than the pure conduction process that prevails inside, the temperature gradient has to be higher on the inside of the boundary than it is on the outside.

Let us now examine the various energy loss processes in more detail. We shall start by considering the rate at which the column loses energy by radiation, and will then attempt to set up the two energy balance equations mentioned above. We shall assume that the column is vertical, cylindrical and radially-symmetrical, and that its length is greater than its diameter, so that only radial losses need be considered. We shall also assume that the column boundary is well-defined, the value of the column radius being small compared with the bore of the containing tube. Finally, we shall assume that the entire discharge current is carried inside the column radius, and that the column electric field (axial voltage gradient) varies neither radially nor axially. All of these assumptions have a sound experimental and theoretical basis.

11.2 THE RADIATION LOSSES FROM THE COLUMN.

In most gaseous arc columns, radiation losses are small or even negligible, especially at low currents (below 10 amps), as has been shown by Holm and Lotz (1934), Hocker and Finkelburg (1946), and several other workers. In arcs of vapours that have strong resonance lines, on the other hand, it has been shown that radiation losses can be important under certain conditions, the vapour atoms being excited by the high-energy electrons present in the plasma (Francis 1946, 1949, Elenbaas 1951, von Engel 1965). In the present case of an arc-type column in alkali-metal-seeded rare gases, we would not expect much radiation loss from the rare gas, since the column temperature is comparatively low, but would expect significant losses from the seed vapour, since the latter has strong resonance lines. This supposition is supported by the work of Lutz (1963), Kerrebrock and Hoffman (1964), Kerrebrock (1964, 1965), Zukoski, Cool and Gibson (1964), and several others, all of whom have observed significant radiation losses from non-equilibrium alkali metal-rare gas plasmas of the type encountered in the column under study. Lutz shows that the resonance radiation of the alkali metal is strongly self-absorbed, but that pressure broadening can cause the energy losses to be significant. Sakuntala (1964) and the author have carried out spectroscopic work on the type of column under study, and have shown that extensive emission occurs in the potassium spectrum for a potassium-argon discharge, whereas the argon

spectrum is very weak. The work of Ben Daniel and Bishop (1963) and Monti and Napolitano (1964B) also shows that radiation losses from the alkali metal vapour can be important for a high-current discharge in a seeded rare gas.

Calculation of the radiative losses from the column under study is extremely difficult. Even for the case of a homogeneous plasma, Kerrebrock (1965) shows that the radiation losses can only be very approximately estimated, the loss rate Q_r from unit volume of plasma "depending on the composition and density of the gas, on the electron temperature, and on the plasma geometry". Lutz (1963) and Zukoski, Cool and Gibson (1964) have computed the radiation energy losses from unit volume of plasma by first calculating the energy flux from a uniform slab of gas, and then dividing by the volume of the slab. In a discussion of their work, Kerrebrock (1965) states that this approximation will break down at large plasma dimensions where the boundaries are more strongly cooled than the centre, but makes use of their theory in calculating a value for Q_r , also referring to the work of Holstein (1951) on a decaying plasma in his calculation, which gives the following result:

$$Q_r = \sum_j G_j h \nu_j n_j A_{j \rightarrow 0} \quad \text{--- 11.1}$$

Here, $h\nu_j$ is the energy of the transition from the j 'th level to the ground state, n_j is the density of the j 'th state, and $A_{j \rightarrow 0}$ is the Einstein spontaneous emission probability. G_j is the resonance escape factor, and depends only on the gas

composition and on the geometry. For the case of dispersion broadening, Kerrebrock uses the following formula for G_j for radiation losses from a cylinder of radius R , again making use of a result derived by Holstein (1951) for a decaying plasma:

$$G_j = 1.115 \frac{2g_0 \sum p \gamma_j^{2/2}}{c^2 n_0 g_j R} \quad 11.2$$

In this formula, g_0 and g_j are the statistical weights of the ground state and the excited state, n_0 is the density of atoms in the ground state, and γ_j and $\sum p$ are the natural and total line widths.

For the alkali metals, where the first line is a doublet, Kerrebrock shows that eqn. 11.1 becomes

$$Q_r = \frac{2\pi e^2 n_0 h}{m_e \lambda^3 \epsilon_1 g_0} \left(G_1 g_1 f_{1 \rightarrow 0} + G_2 g_2 f_{2 \rightarrow 0} \right) \times \exp\left(\frac{-h\nu}{kT_e}\right) \quad 11.3$$

where λ is the wavelength of the doublet, g_1 and g_2 are the statistical weights of the members of the doublet and the ground state, and $f_{1 \rightarrow 0}$ and $f_{2 \rightarrow 0}$ are their emission oscillator strengths. Note that eqns. 11.1 - 3 are given in rationalised MKS units. The values of $g f$ and λ for the alkali metals (Corliss and Bozman 1962) are given in Table 11.1

TABLE 11.1

ATOM	WAVELENGTH (Å)	$g_i f_i \rightarrow 0$
LITHIUM	6707.84	0.80
SODIUM	5889.95	0.95
	5895.92	0.47
POTASSIUM	7664.91	1.4
	7698.98	0.70

...

Table 11.1 (continued.)

ATOM	WAVELENGTH (\AA)	$\epsilon_i f_i \rightarrow 0$
RUBIDIUM	7800.23	2.7
	7946.60	1.2
CAESIUM	8521.10	1.4
	8943.50	0.57

Kerrebrock (1965) has shown that the above theory gives a satisfactory account of the radiation losses from the homogeneous plasmas studied by himself and Hoffman (1964) and by Zukoski, Cool and Gibson (1964). In the column under study, however, the plasma is certainly not homogeneous, since the gas temperature, electron temperature and electron number density all vary radially, so we would not expect the theory to be capable of giving anything more than an approximate value for the radiation losses. Despite this fact, the theory predicts radiation losses that agree fairly well with the values deduced by other methods, and we will therefore use the value of Q_r that is given in eqn. 11.3 in the two energy balance equations that we will now develop.

11.3 THE EXTERNAL ENERGY BALANCE EQUATION.

In an analysis of the energy balance of high-pressure arc columns Suits and Poritsky (1939) have shown that the energy losses by convection/conduction in the surrounding gas can be represented with a fair degree of accuracy by employing the expression that describes such losses for the case of a hot, solid

cylinder immersed in a gas. Suits (1939A) has studied the convection currents that occur in the neighbourhood of arc columns, and has found that the convection velocity has its maximum value at the boundary of the column, falling off as the distance from the column increases. In the case of a solid cylinder, the convection velocity is zero at the actual surface, rising to a maximum quite near the surface, and then falling off as the distance from the surface increases, so the situations are not quite the same, but Suits points out that the discrepancy produced by the different effects at the boundary is small, and can be allowed for by employing an "effective arc diameter" which is slightly smaller than the actual diameter. This effective diameter can be chosen so as to make the arc and solid convection processes correspond extremely closely if a high degree of accuracy is required in the calculation of the heat losses. In the present case, the correction factor is less than the experimental error in the value of the visible diameter, so we will ignore the discrepancy, and will take the effective diameter to be the visible diameter.

Nusselt and Jürges (1928) have shown that the rate of heat loss from a solid cylinder immersed in a gas in which free convection can occur is given by the dimensionless relation

$$\frac{hD}{k} = f \left(\frac{D^3 \beta_0 \rho^2 g \Delta T}{\eta^2}, \frac{C_p \eta}{K} \right) \quad \text{---11.4}$$

where h is the coefficient of heat transfer in $\text{cal. sec}^{-1} \text{cm}^{-2} \text{deg K}^{-1}$

D is the diameter of the cylinder in cm,

k is the thermal conductivity of the gas in $\text{cal. sec}^{-1} \text{cm}^{-1} \text{deg. K}^{-1}$

β_0 is the temperature coefficient of volume expansion in deg. K^{-1}

g is the acceleration of gravity in cm sec^{-2}

η is the viscosity of the gas in $\text{gm sec}^{-1} \text{cm}^{-1}$.

C_p is the specific heat at constant pressure in $\text{cal. gm}^{-1} \text{deg. K}^{-1}$

ΔT is the difference between the temperature of the body and ambient temperature.

The quantities $\frac{hD}{k}$, $\frac{D^3 \beta_0^2 g \Delta T}{\eta^2}$ and $\frac{C_p \eta}{k}$ are respectively known as the "Nusselt", "Grashoff" and "Prandtl" numbers, and

Cobine (1958) states that the experimental evidence shows the Nusselt number to depend only on the product of the Grashoff and Prandtl numbers. He also states that the product $\frac{C_p \eta}{k}$ has the value 0.67 for monatomic gases such as the rare gases, while

for perfect gases, $\beta_0 = \frac{1}{T}$ and $\eta = \frac{Mp}{RT}$,

where M is the molecular weight of the gas,

p is the pressure in gm cm^{-2}

T is the temperature in deg. K ,

R is the gas constant in cm deg. K^{-1}

It therefore follows that

$$\frac{hD}{k} = \text{const.} \frac{D^3 M^2 p^2 g \Delta T}{\eta^2 R T^3} \quad 11.5$$

where the constant in the equation may vary, and η varies between 0.04 and 0.25. Cobine (1958) states that it is customary to evaluate the gas constants at a temperature half way between that of the boundary of the column and the ambient gas temperature in order to avoid the difficulty arising from

the temperature variation that occurs as we leave the column.

If we replace h by

$$\frac{\Delta E_c}{4.18\pi D \Delta T} \quad \text{-----} \quad 11.6$$

where ΔE_c is the energy loss rate per unit length of column by convection/conduction (in watts) it can be shown (Champion 1951, Cobine 1958) that

$$\Delta E_c = (\pi k_f \Delta T) \cdot \text{const.} \left(\frac{D^3 M^2 p^2 g \Delta T}{\eta^2 R^2 T^3} \right)^\alpha \quad \text{-----} \quad 11.7$$

Here, k_f is the value of k at the mean temperature mentioned above.

In order to obtain the energy balance equation for the column and its surroundings, we must equate the total power dissipated in unit length of column with the sum of the energy losses by convection/conduction and radiation. If Q_r is the local energy loss rate by radiation per unit volume of plasma (eqn. 11.3), we can write the total energy loss rate by radiation from unit length of column as

$$\Delta E_R = \int_0^R 2\pi r Q_r dr \quad \text{-----} \quad 11.8$$

where $2\pi r Q_r dr$ is the net loss rate from an annulus of radius r and thickness dr . Since the power dissipated in unit length of column is equal to the product of the discharge current i and the column voltage gradient X , the external energy balance equation can be written

$$Xi = \int_0^R 2\pi r Q_r dr + \text{const.} (k_f \Delta T) \left(\frac{D^3 M^2 p^2 g \Delta T}{\eta^2 R^2 T^3} \right)^\alpha \quad \text{-----} \quad 11.9$$

For the case of a typical high-pressure thermal arc column where radiation losses are small compared with convection/

conduction losses and where the boundary temperature is independent of the current, Cobine (1958) shows that eqn. 11.9 reduces to

$$Xi = \text{const. } D^{3\alpha} \quad \text{11.10}$$

If the current i is now written as

$$i = \text{const. } XD^2 \quad \text{11.11}$$

an approximation that is only valid if T is roughly constant inside the column as i varies, D can be eliminated between 11.11 and 11.10, so that

$$\frac{i}{X} = \text{const. } (Xi)^{2/3\alpha} \quad \text{11.12}$$

and it can be shown that

$$X = \text{const. } i^{-n} \quad \text{11.13}$$

where

$$n = \frac{2 - 3\alpha}{2 + 3\alpha} \quad \text{11.14}$$

and varies from 0.45 to 0.89 as α varies from 0.25 to 0.04.

We would not expect these last two equations to be capable of giving an accurate description of the column under study, partly because of the fact that radiation losses cannot be ignored in the present case, and partly because of the fact that not all of the assumptions that were made in deriving equations 11.13 and 11.14 from eqn. 11.9 are strictly valid for nonequilibrium columns. Nevertheless, the author has found that the observed relationship between X and i is in good qualitative agreement with eqn. 11.13 provided that the current is not too high, as is seen from figure 6.1, which shows experimental plots of X against i for the different mixtures studied by the author. The plots are all seen to be

fairly good straight lines over a wide current range, and since they are plotted on log-log paper, this shows that the relationship between X and i must be of the form

$$X = \text{const. } i^{-m} \quad \text{11.15}$$

throughout this linear region. This indicates that convection-conduction is the main process responsible for removing energy from the type of column under study, since the relationship between X and i would not be of this form if resonance radiation were the main energy loss process (von Engel 1965). The slopes of the log-log graphs give the values of m for the different mixtures, and vary from -0.13 for caesium-helium to -0.23 for potassium-neon and potassium-argon. The experimental values of m are therefore rather lower than the values that are observed in conventional thermal columns, which, as we have seen, generally fall in the range from 0.45 to 0.89 (Cobine 1958).

11.4 THE INTERNAL ENERGY BALANCE EQUATION.

We will now set up the energy balance equation for the region inside the positive column, and will do so by considering the energy losses from an annulus of unit length, radius r , and thickness dr . The total power dissipated in such an annulus is equal to

$$2\pi r^2 \sigma dr \quad \text{11.16}$$

where σ is the local value of the electrical conductivity, and is a radially-varying quantity. Of this energy, a certain amount is lost by radiation. If Q_r is the local value of the radiation

loss rate from unit volume of plasma (see eqn. 11.3), the net radiation loss from the annulus will be equal to $2\pi r Q_r dr$.

The heat that passes through the outer wall of the annulus by thermal conduction is equal to the total heat that is produced inside the outer boundary of the annulus minus the heat that is lost by radiation. Thus, the conduction losses may be written as

$$\int_0^r 2\pi r x^2 \epsilon dr - \int_0^r 2\pi r Q_r dr \quad \text{11.17}$$

Applying Fourier's heat flow equation, we see that

$$\int_0^r 2\pi r x^2 \epsilon dr - \int_0^r 2\pi r Q_r dr = - 2\pi r k_r \frac{\partial T}{\partial r} \quad \text{11.18}$$

where k_r is the local value of the thermal conductivity, and $\frac{\partial T}{\partial r}$ is the radial temperature gradient. Following Francis (1946), ter Horst et. al. (1935), and Edels and Fenlon (1964), the energy balance equation can also be written in the form

$$x^2 \epsilon - Q_r = - \frac{1}{r} \frac{\partial}{\partial r} (2\pi r k_r \frac{\partial T}{\partial r}) \quad \text{11.19}$$

In arc columns in molecular gases or vapours, where molecular dissociation can occur, the thermal conductivity of the gas can vary enormously throughout the column, but in the present case of a seeded rare gas, k_r can be assumed to be approximately constant throughout the column, its value being that corresponding to the mean temperature in the column. In this case, the most useful form of the energy balance equation is eqn. 11.18, and this is the form that will be used in the analysis of the column that will be given in Chapter 15.

CHAPTER 12THE ELECTRON ENERGY BALANCE EQUATION12.1 GENERAL DISCUSSION OF THE ELECTRON ENERGY BALANCE
PROCESS

In the last chapter, we discussed the energy balance of the positive column, and showed how the rate of heat production must everywhere equal the rate of heat loss if steady-state conditions are to be maintained. In our analysis, we treated the problem from a macroscopic point of view, regarding heat as a fluid, and employing the conventional laws of heat transfer. In this chapter, we will examine the local energy balance of the plasma from a microscopic point of view. In particular, we will discuss the various mechanisms by which the electrons lose the energy that they acquire from the applied field, and will show how a "two-temperature" plasma can be produced under suitable conditions.

At pressures of the order of a few torr or less, the electronic mobility in a gas is generally high, since collisions between electrons and gas atoms are relatively infrequent. For this reason, an elevated electron temperature can easily be produced in a low-pressure gas when an electric field is applied across it, and such an elevated electron temperature exists in the positive columns of all low-pressure arc and glow discharges. As the pressure of a gas rises, however, the electronic mobility falls (Chapter 14), and by the time most gases reach atmospheric pressure, significant elevation of the electron temperature is impossible, so that the electron temperature is equal to the gas

temperature in the positive columns of most high-pressure discharges. The inert gases are exceptions to this general rule, partly because of their extremely low electron collision cross sections, and partly because their monatomic structure precludes the possibility of the absorption of energy by rotational and vibrational modes, so that collisions between electrons and rare gas atoms are not only relatively infrequent, but are also perfectly elastic except at very high electron energies. This means that an atmospheric-pressure rare gas is equivalent to a low-pressure gas from the point of view of the elevation of the electron temperature, a fact that has been demonstrated experimentally by Massey and Cannon (1965), who have observed extremely high electron temperatures in the positive columns of high-pressure arc discharges in argon and neon (see Table 10.1). The addition of a small amount of alkali metal vapour to an atmospheric-pressure rare gas does not greatly reduce the ability of the gas to support an elevated electron temperature, and, as we have seen in Chapter 2, such a procedure is found to greatly enhance the electrical conductivity of the rare gas, since the seed has a **far** lower ionisation potential than the rare gas, and can therefore be ionised much more easily. We will now examine the process by which the degree of elevation of the electron temperature in such a plasma is determined, and will derive the equation that describes the process - the electron energy balance equation.

12.2 THE VALUE OF THE ELECTRON TEMPERATURE.

When no electric field is present in a gas, any free electrons are maintained in thermal equilibrium with the gas atoms by means of collisions, so that the electron temperature is equal to the gas temperature. When an electric field is applied across or induced within a gas, on the other hand, the electrons acquire additional energy from the field, so that they tend to have a higher mean energy than the gas atoms, and an equilibrium situation is produced when the rate at which the electrons receive energy from the field equals the rate at which they pass on this energy to the gas atoms. In most high-pressure gases, they lose their energy quickly, so that their mean energy is not much higher than that of the gas atoms, but in high-pressure rare gases (seeded or unseeded) they can not only maintain a mean energy that is far higher than that of the gas atoms, but can even have a separate Maxwellian energy distribution under certain conditions.

The rate at which the electrons in unit volume of plasma acquire energy from an electric field is equal to the electrical power dissipated per unit volume of plasma, i.e.

$$\text{electron energy input rate} = j X \text{ ----- } 12.1$$

where j is the current density,

and X is the field.

We shall see in Chapter 14 that the current density in a plasma is related to the plasma properties by the equation

$$j = \frac{0.85 n_e e^2 t_{eo} X}{m_e} \quad \text{12.2}$$

where n_e is the electron number density in the plasma,

e is the electronic charge,

t_{eo} is the mean electron-atom collision time,

m_e is the electronic mass.

We may therefore write eqn. 12.1 as

$$\begin{array}{l} \text{electron energy} \\ \text{input rate} \end{array} = \frac{0.85 n_e e^2 t_{eo} X^2}{m_e} \quad \text{12.3}$$

The electrons pass most of this energy on to the gas atoms by means of elastic collisions, but some is lost by inelastic collisions, and Kerrebrock (1965) has shown that both types of collision must be considered if an accurate value of the electron temperature is to be obtained. Let us examine them in turn.

Energy loss rate by elastic collisions

It can easily be shown (Kerrebrock 1962) that the rate of energy transfer from the electrons to the gas atoms by elastic collisions is given by the equation

elastic collision energy loss rate per unit volume of plasma = number density of electrons \times collision frequency \times fractional energy loss per collision

$$\times \frac{3}{2} k (T_e - T_g) \quad \text{12.4}$$

where k is Boltzmann's constant

T_e is the electron temperature in $^{\circ}\text{K}$

T_g is the gas temperature in $^{\circ}\text{K}$.

and where the collision frequency is equal to the reciprocal of the electron-atom collision time t_{eo} . The fractional energy loss per collision can be calculated by means of elementary dynamics, and can be shown to have the value $\delta \frac{m_e}{M}$ for collisions between electrons and atoms of mass M . δ is the so-called "collision loss factor", and Kerrebrock (1965) states that it has a value of 2 for elastic collisions of the type under consideration.

(Kerrebrock obtains this value from the work of Champion and Cowling (1958), who show that δ has a value of 2 for collisions governed by a Maxwellian force law, compared with a value of 1.88 for hard sphere collisions). When calculating the fractional energy loss per collision for a composite gas, it is necessary to consider collisions with all the species present, and if these have different atomic weights, a mean value for $\delta \frac{m_e}{M}$ must be computed, taking into account the different electron collision cross sections of the various species present. This will be discussed in greater detail in Chapter 17, when it will be shown that the fractional energy loss factor for a mixture is equal to

$$\frac{\delta m_e \sum_i n_i a_i}{\sum_i n_i a_i M_i} \quad \text{12.5}$$

where n_i , a_i , and M_i are respectively the number density, electron collision cross section and mass of the i 'th species present.

Eqn. 12.4 may therefore be written as

$$\begin{array}{l} \text{elastic collision} \\ \text{energy loss rate} \\ \text{per unit volume} \\ \text{of plasma} \end{array} = \frac{n_e}{t_{eo}} \cdot \frac{\delta m_e}{M_a} \cdot \frac{3}{2} k (T_e - T_g) \quad \text{12.6}$$

where M_a is the average heavy body mass defined by eqn. 12.5.

Energy loss rate by inelastic collisions.

The inelastic collisions that occur in a plasma of the type under consideration can be divided into two groups - collisions with atoms, and collisions with molecules. In a discussion of the former, Kerrebrock (1964) shows that inelastic collisions between free electrons and atoms take the form of interactions between the free electrons and the valence electrons of the atoms, and states that "it is convenient to think of the valence and free electrons together comprising a single gas". He also shows that such collisions "do not constitute a loss of energy from the electron gas unless a photon escapes in the process". In a later paper (1965) Kerrebrock shows that the loss of such photons from the plasma can be an important energy loss process, since "every photo-de-excitation in which a photon escapes implies an excitation by a free electron", so that "the energy of the emergent photon is taken indirectly from the free electron gas". Now the rate at which a plasma of the type under consideration loses energy by radiation has been discussed in detail in section 11.2, the value of Q_r (the net radiative energy loss rate from unit volume of plasma) being given by eqn. 11.3. We must therefore add Q_r to the elastic collision energy loss rate when calculating the total rate of energy loss from the electron gas.

Collisions between free electrons and molecules are not important in the plasmas under study, since the rare gas is entirely monatomic, and the alkali metal is mainly monatomic. When molecular species are present in a gas, the rotational and

vibrational modes of the molecules are easily excited by electrons of comparatively low energy, so that such molecules represent a very efficient energy sink, and tend to prevent the electron temperature from rising above the gas temperature. In a discussion of inelastic collisions with molecules, Kerrebrock (1964) states that it is best to represent such energy losses by regarding the collision loss factor δ as an "empirically determined parameter", and shows that the effective value of δ can be as high as 50 in some molecular gases.

We are now in a position to set up the electron energy balance equation, since we can equate the rate at which unit volume of the electron gas gains energy from the electric field with the rate at which it loses this energy. If this is done, we see that

$$\frac{0.85 n_e e^2 t_{eo} X^2}{m_e} = \frac{n_e}{t_{eo}} \cdot \frac{\delta m_e}{M_a} \cdot \frac{3}{2} k (T_e - T_g) + Q_r \quad \text{--- 12.7}$$

which is very similar to the radiation - corrected electron energy balance equation that was given by Kerrebrock in 1965. From this equation, we see that the degree of elevation of the electron

temperature ΔT_e is given by

$$\Delta T_e = T_e - T_g = \frac{1.7 e^2 t_{eo}^2 M_a X^2}{3 k m_e^2 \delta} \quad \text{---} \quad \frac{2 M_a t_{eo} Q_r}{3 k n_e m_e \delta} \quad \text{--- 12.8}$$

and this is the form of the electron energy balance equation that we shall use in our analysis of the positive column.

12.3 THE CONDITIONS FOR THE ELECTRON ENERGY DISTRIBUTION
TO BE MAXWELLIAN

We have now demonstrated how the mean electron energy can be raised above the mean gas atom energy in the type of plasma under study, but we have not shown that the electron energy distribution thus produced is properly Maxwellian, and this must now be done, otherwise we will not be justified in using the electron temperature to calculate the degree of ionisation of the seed. We must show that the electron energy distribution contains the requisite proportion of high-energy electrons consistent with a Maxwellian distribution, for it is this high-energy tail that produces ionisation, and if the tail is absent or depleted, the ionisation process will be stopped or slowed down. The work of Margenau and Hartman (1948), Cahn (1949) and Kerrebrock (1962) shows that an elevated electron energy distribution can be Maxwellian under certain conditions, the high-energy tail being present only if the electrons interact among themselves more strongly than with the various heavy bodies present. Ben Daniel and Tamor (1962), Kerrebrock (1964) and Massey and Cannon (1965) give the following criterion for the presence of a fully-populated tail. The tail will be present provided that the average rate of energy transfer from an electron to other electrons is well in excess of the rate of transfer to heavy bodies. If the average electron energy is E_e , and the electron-electron and electron-heavy body collision times are t_{ee} and t_{eo} , then the rate of energy transfer from an electron to other electrons will be

equal to $\frac{E}{t_{ee}}$ (assuming that δ has a value of unity for electron-electron collisions - Massey and Cannon 1965), while we have seen in the last section that the rate of energy transfer from an electron to atoms has a value of $\frac{E_e \delta m_e}{t_{eo} M_a}$. If we define the parameter w to be the ratio of these two quantities, i.e.

$$w = \frac{E_e}{t_{ee}} \cdot \frac{t_{eo} M_a}{E_e 2 m_e} = \frac{t_{eo} M_a}{2 t_{ee} m_e} \quad \text{--- 12.9}$$

then the value of w will determine the deviation of the energy distribution from the Maxwellian case (Massey and Cannon 1965). Even with w equal to about 50, the tail deviates quite substantially from the ideal case, and the tail will only contain the correct number of electrons up to an energy E'_e provided that

$$w > \left(\frac{E'_e}{E_e} \right)^2 \quad \text{--- 12.10}$$

(Massey and Cannon 1965).

If we put E'_e equal to the energy of an electron that is capable of producing ionisation of a seed atom by direct collision (i.e. $E'_e = eV_i$, where V_i is the ionisation potential of the seed), and E_e equal to the mean energy kT_e , then we can use this criterion to determine whether or not a Maxwellian distribution exists in the plasmas under study by determining whether or not

$$\frac{t_{eo} M_a}{2 t_{ee} m_e} > \left(\frac{eV_i}{kT_e} \right)^2 \quad \text{--- 12.11}$$

For a potassium-argon plasma, $\frac{M_a}{m_e}$ is of the order of 7×10^4 . Also, the values of t_{ee} and t_{eo} are of the same order of magnitude provided that the electron number density is high - as it is in

all the plasmas under study. The ratio $\frac{t_{eo}}{t_{ee}}$ is roughly given by

$$\frac{t_{eo}}{t_{ee}} = \frac{n_e a_+}{\sum_i n_i a_i} \quad \text{12.12}$$

Here, a_+ is the electron collision cross section of any singly-charged particle (ion or electron); its value will be discussed in Chapter 14. For a typical plasma (3.5 torr of potassium in atmospheric-pressure argon), $\frac{t_{eo}}{t_{ee}}$ has a value of about $\frac{1}{3}$, making the value of w approximately 10^4 . If we take T_e as about 3000°K , then $\frac{eVi}{kT_e}$ is about 17 for a potassium-seeded plasma, making $\left(\frac{eVi}{kT_e}\right)^2$ approximately 300. Thus, we see that the criterion is satisfied for the above plasma (in which the electron number density is of the order of $3 \times 10^{14} \text{ cm}^{-3}$ or over - see Chapter 15). If the electron number density falls below about 10^{13} cm^{-3} , we see that the value of w approaches the critical value, and so we cannot assume that the distribution is Maxwellian for plasmas where the electron number density is much less than 10^{13} cm^{-3} . This agrees with the value given by Massey and Cannon (1965) for pure argon, and also with the value quoted by Kerrebrock (1964), who states that "all the available evidence suggests that the two-temperature conductivity theory (to be given in the next chapter) is valid for plasmas where the electron number density is greater than about 10^{13} cm^{-3} ". Indeed, Kerrebrock's own experimental results show a marked departure from the two-temperature theory when the value of n_e falls below this value (Kerrebrock and Hoffman 1964). In the positive columns under study in the

present thesis, it can be shown that the electron number density is always greater than 10^{13} cm^{-3} , having a value of about 10^{14} cm^{-3} , so that we are justified in assuming that the electron energy distribution is properly Maxwellian in the present case.

Another obvious condition that must be satisfied if Maxwellisation of the electrons is to occur is that the residence time of the electrons in the plasma must be sufficiently long for the electrons to interact among themselves and produce a Maxwellian distribution. Electrons are lost from the plasma in two ways, namely by passing through the plasma to the anode, and by being removed by volume recombination with positive ions. We must therefore show that the time taken for an electron to cross the inter-electrode gap and the average life of an electron are both large compared with the electron-electron collision time t_{ee} . Since the gap widths used are all of the order of m.m. or more, and the electron drift velocities are of the order of 10^5 cm sec^{-1} (as can be shown from the formula given in Chapter 14), we see that the residence time is much greater than the electron-electron collision time, which has a value of about 10^{-11} sec . With regard to the second criterion, Sakuntala (1964) has shown that each free electron undergoes roughly 10^3 ionising collisions per second in the type of plasma under study, and since the ionisation rate must equal the volume recombination ion loss rate, it therefore follows that the average life of an electron is of the order of 10^{-3} sec , which is again several orders of magnitude greater than t_{ee} .

12.4 THE VALUE OF THE ION TEMPERATURE IN THE PLASMA

So far in this chapter, we have tacitly assumed that the gas temperature T_g is also the temperature of the positive ions (T_i). This is not a strictly valid assumption (Dunn 1967 priv. comm.), since the ions will tend to have a higher mean energy than the gas atoms. This is because the ions have a much higher electron collision cross section than the atoms, so that the ions will receive energy from the electrons at a faster rate than the atoms. We will now show that T_i can be assumed to be equal to T_g in the present case, however, since the difference between the two temperatures is very small.

The ion temperature will exceed the gas temperature in a plasma where the rate at which an ion receives energy from the electrons and from the field is significantly greater than the rate at which a gas atom receives energy from the electrons. The ions will then be able to pass on their excess energy to the gas atoms by thermal collision processes in much the same way as the electrons lose their energy to the various heavy bodies present, the difference between the ion and gas temperatures being determined by equating the rate at which an ion gains energy with the rate at which it loses it.

In the plasmas under study, the ions receive energy directly from the electric field, and also by collisions with the electrons. The rate at which they receive energy from the field is equal to the product of the ion current density and the field strength, so that the energy input per ion is equal to

$$\frac{1}{n_e} \cdot j \cdot \frac{K_+}{K_a} \quad \text{X} \quad \text{-----} \quad 12.13$$

(see Chapter 14). The rate at which the ions receive energy from the electrons is merely the share of the electron energy loss rate that goes to the ions, and is approximately equal to

$$j X \frac{n_+ a_+}{\sum_i n_i a_i} \quad \text{-----} \quad 12.14$$

(see Chapter 14), so that the energy input per ion is

$$\frac{1}{n_e} \cdot j X \cdot \frac{n_+ a_+}{\sum_i n_i a_i} \quad \text{-----} \quad 12.15$$

But $\frac{n_+ a_+}{\sum_i n_i a_i}$ has a typical value of the order of $\frac{1}{3}$ in the type of plasma under consideration, while $\frac{K_+}{K_-}$ has a value that is about two orders of magnitude less than this (see Chapter 14), so that we can neglect the energy input from the field and consider only the energy input from the electrons. If we now calculate the rate at which a gas atom receives energy from the electrons, we see that it is roughly given by

$$\frac{1}{n_g} \cdot j X \frac{\sum_i n_i a_i - n_+ a_+}{\sum_i n_i a_i} \quad \text{-----} \quad 12.16$$

where n_g is the total number of gas atoms present in unit volume. Since n_g is roughly four orders of magnitude greater than n_+ , it is obvious that the rate at which an ion receives energy is considerably greater than the rate at which a gas atom receives energy, so we would certainly expect T_i to be greater than T_g .

Let us now estimate the difference between T_i and T_g by equating the energy input and energy output rates for an ion. If we only consider elastic collision processes within the plasma, we see that

$$\frac{1}{t_{ei}} \cdot \delta \frac{n_e}{M_+} \cdot \frac{3}{2} k (T_e - T_i) = \frac{1}{t_{io}} \cdot \frac{3}{2} k (T_i - T_g) \quad \text{-----} \quad 12.17$$

where t_{ei} and t_{io} are the electron-ion and ion-neutral atom collision times, and it is assumed that the ion mass equals the average heavy body mass (this is exactly true for potassium-argon, but only approximately true for the other mixtures studied).

We also assume that the value of the collision loss factor for ion-atom collisions is unity. From eqn. 12.17, we see that

$$\frac{2}{t_{ei}} \cdot \frac{m_e}{M_+} (T_e - T_i) = \frac{1}{t_{io}} (T_i - T_g) \quad \text{12.18}$$

so that $T_i - T_g = \frac{2 t_{io}}{t_{ei}} \cdot \frac{m_e}{M_+} (T_e - T_i) \quad \text{12.19}$

For a typical potassium-argon plasma, we can easily show that t_{ei} is of the order of 5×10^{-11} sec, while $\frac{m_e}{M_+}$ is of the order of 10^{-5} . We can estimate t_{io} , the ion-gas atom collision time, by taking it to be equal to the atom-atom collision time. This can be calculated for argon at atmospheric pressure and a temperature of about 1500°K by using eqn. 14.10, and dividing the mean free path by the average thermal velocity; this gives a value of roughly 5×10^{-10} sec. Substituting these values in eqn. 12.19, we see that

$$T_i - T_g = 2 \times 10^{-4} (T_e - T_i) \quad \text{12.20}$$

so that the difference between the ion temperature and the gas temperature is clearly negligible, and we are justified in assuming T_i to be equal to T_g . Thus, the only temperatures that we need consider in our analysis of the plasma that exists in the positive column under study are the gas temperature T_g and the electron temperature T_e .

CHAPTER 13THE ION BALANCE EQUATION13.1 THE DEGREE OF IONISATION IN EQUILIBRIUM PLASMAS -
THE SAHA EQUATION

We now come to the most crucial part of the theory of the column - the calculation of the degree of ionisation of the seed. Before dealing with the nonequilibrium plasmas under study, however, we will discuss the equation that determines the degree of ionisation of equilibrium (or thermal) plasmas, as this is of considerable interest in the present case.

It is possible to make any gas highly-conducting by merely raising its temperature to a sufficiently high value. At any temperature, a certain number of the atoms of a gas are ionised, as can be shown by statistical-thermodynamical arguments, the best known of which is that given by Lindemann (1919) and Saha (1920), the conclusion of which is known as the Saha equation. This has the following form:

$$\frac{x^2}{1-x} = \frac{2.40 \times 10^{-4}}{p} \cdot T_g^{5/2} \cdot \exp\left(-\frac{eV_i}{kT_g}\right) \quad \text{----- 13.1}$$

where x is the degree of ionisation of the gas,

T_g is the gas temperature,

p is the gas pressure in torr,

V_i is the ionisation potential of the gas,

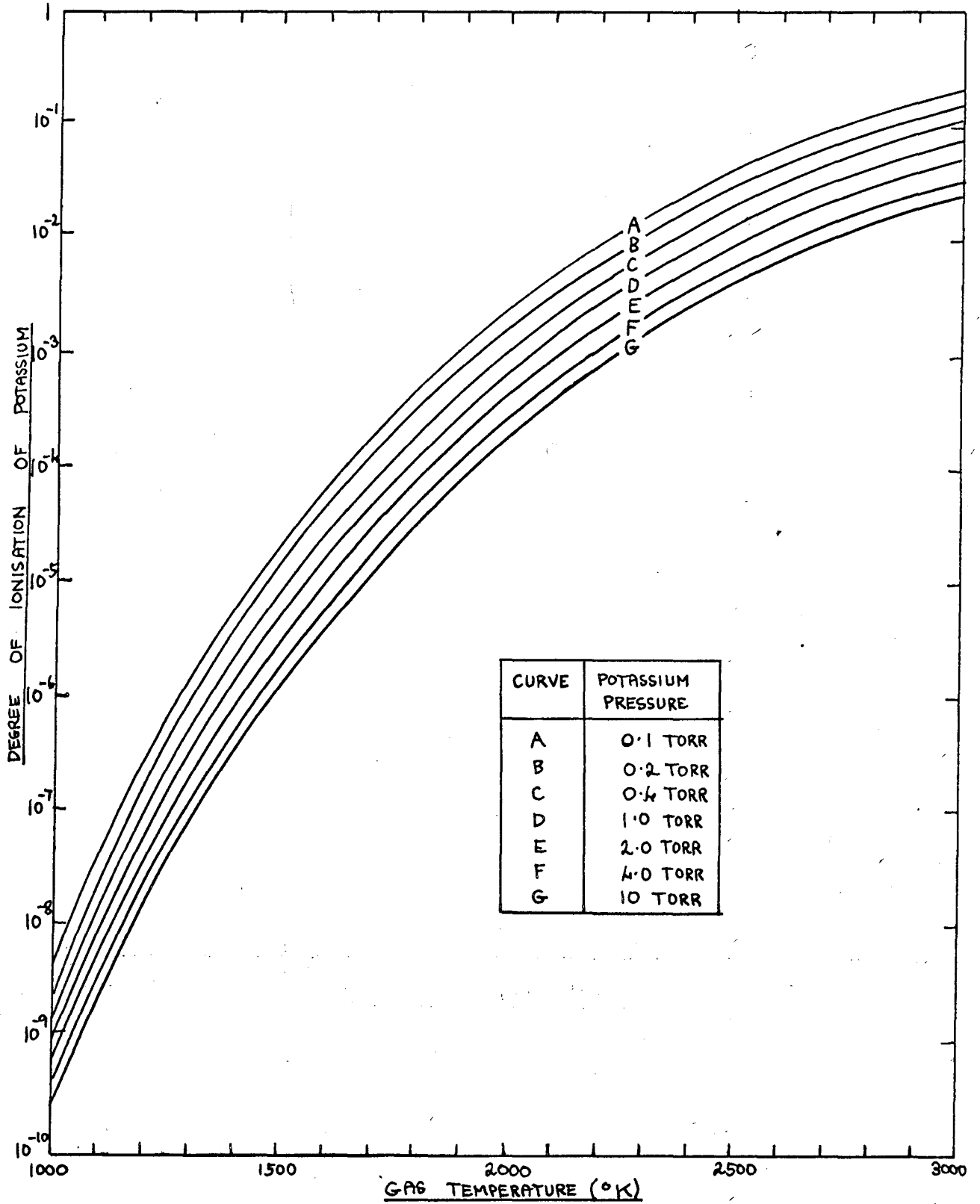
k is Boltzmann's constant

and e is the electronic charge.

For a seeded gas where only the seed is ionised, p is replaced by the seed pressure p_s . At normal room temperatures, the intrinsic degree of ionisation of a gas is small, since x depends exponentially on the ratio of the ionisation energy of the gas (eV_i) to the mean thermal energy (kT_g), and at low temperatures, this has a very large value, since V_i is of the order of several volts or higher (ranging from 3.86V for caesium to 24.6V for helium). Thus, it is only when the temperature reaches values of the order of several thousand degrees K that thermal ionisation becomes significant. Such temperatures prevail in the positive columns of thermal arcs, which have temperatures up to 10,000°K in some cases, and where ionisation by thermal collisions between the atoms is the dominant ionisation process. Figure 13.1 shows plots of the degree of ionisation of the seed in typical plasmas against the gas temperature, results being shown for different potassium pressures in atmospheric-pressure argon. It is seen that the degree of ionisation does not become significant until the temperature reaches a value of the order of 2500°K; with pure argon, a similar degree of ionisation would not be reached until the temperature was over 8000°K. In the positive column under study, however, we have seen that the gas temperature is not high enough for extensive thermal ionisation of the seed to occur, and that nonequilibrium ionisation becomes important. Let us now examine the nonequilibrium ionisation process in more detail.

FIGURE 13.1

PLOTS OF DEGREE OF IONISATION OF SEED AGAINST GAS TEMPERATURE FOR DIFFERENT PRESSURES OF POTASSIUM IN ARGON



13.2 THE DEGREE OF IONISATION OF THE SEED IN NONEQUILIBRIUM PLASMAS.

It is a well-established fact that the ionisation in certain types of discharge plasma occurs because the electron temperature is elevated, with a high degree of ionisation being produced by the interaction of the electron gas with the outer electrons of the atoms. The first person to apply this concept to alkali-metal-seeded rare gases was Kerrebrock (1962), who postulated that it is the electron temperature that determines the degree of ionisation of the seed in such plasmas, and that it should therefore be possible to calculate the degree of ionisation of the seed by substituting the electron temperature for the gas temperature in the Saha equation, provided, of course, that the electron energy distribution is properly Maxwellian. This is the crux of Kerrebrock's two-temperature theory, a theory that has succeeded in explaining the high degree of ionisation (of the order of a few percent) that has been observed in alkali-metal-seeded rare gases by Kerrebrock (1962), Ralph (1962), Robben (1962), Ben Daniel and Bishop (1963), Zukoski, Cool and Gibson (1963), Sheindlin, Latenin and Azinovsky (1964), Kerrebrock and Hoffman (1964), Labois and Lemaire (1964), Sakuntala (1964), and many later workers, including the author. The two-temperature conductivity theory has now been generally accepted by those studying the electrical properties of seeded rare gases, since it has been fairly conclusively demonstrated that (a) the electron temperature in such mixtures can be

considerably higher than the gas temperature under suitable conditions, (b) use of the electron temperature (as calculated by means of the electron energy balance equation) in the Saha equation predicts the correct value of the plasma conductivity, provided that the electron number density is sufficiently high for the electron energy distribution to be Maxwellian.

Direct experimental evidence for the elevation in electron temperature in seeded rare gas plasmas has been obtained by several workers. Kerrebrock and Hoffman (1964) measured the electron temperature in a high-current discharge in potassium-argon by means of the sodium line reversal technique, and showed that the experimental electron temperature was of the same order as the theoretical value. Sakuntala (1965 B, 1966) has shown experimentally that considerable elevation of the electron temperature occurs both in the high-current discharge under study and in the low-current range just before transition to the high-current regime. The best direct experimental evidence for the elevation in the electron temperature and the validity of the Saha equation is the work of Sheindlin, Batenin and Azinovsky (1964). By observing the intensity of the $4s \frac{2}{2} S_{1/2} - 5p \frac{2}{2} P_{1/2}$ transitions in potassium, they measured the electron temperature in flowing argon-potassium plasmas produced by an arc. The conductivity calculated from the measured electron temperature was compared with the measured conductivity, and excellent agreement was obtained. This result is corroborated by the work of Zukoski, Cool and Gibson (1963),

who compared the variation of the electron temperature (as deduced from the variation of the intensity of the resonance lines) with the variation of the electron temperature calculated from the measured conductivities. Good agreement between the two was obtained, especially above an electron temperature of 3000°K. Kerrebrock himself (1965) has applied the two-temperature theory to the results of Kerrebrock and Hoffman (1964) and Zukoski, Cool and Gibson (1963), and has shown that use of the value of the electron temperature calculated by the radiation - corrected electron energy balance equation (see Chapter 12) in the Saha equation predicts electrical conductivity values that agree closely with the measured values of the conductivity throughout the current density range 0.1 - 50 amps/cm². The work of Ben Daniel and Bishop (1963) and Chu and Gottslich (1968) also provides evidence for the validity of the two-temperature theory.

Monit and Napolitano (1964 A, B) have shown that while direct substitution of the electron temperature for the gas temperature in the Saha equation (eqn. 13.1) is empirically justified by the results it produces, it is not strictly correct from a formal thermodynamical point of view. They have produced a modified form of the Saha equation for use with two-temperature plasmas - the so-called "generalised Saha equation". For the plasmas under study, this has the form

$$\left(\frac{x^{\beta} + 1}{1 - x}\right)^{1/\beta} \cdot \frac{1}{1 + x\beta} \cdot \left(\frac{1}{2}\right)^{\frac{\beta - 1}{\beta}}$$

$$= \frac{2.40 \times 10^{-4}}{p_s} \cdot T_g \cdot T_e^{3/2} \cdot \exp\left(-\frac{eV_i}{kT_e}\right) \quad \text{----- 13.2}$$

$$\text{where } \beta = \frac{T_e}{T_g} \quad \text{----- 13.3}$$

This generalised equation is seen to reduce to the ordinary Saha equation when $T_e = T_g$, that is, under equilibrium conditions. The difference between the two equations is that eqn. 13.2 predicts a slightly lower value of x than eqn. 13.1 for the same experimental conditions. In the high-conductivity range of interest in the column under study, however, use of this modified and much more complicated form of the Saha equation is not found to produce any significant improvement in the agreement between theory and experiment, which, as we have seen, is already very good with the conventional equation. For this reason, we shall use the conventional form of the Saha equation as our ion balance equation, as has been done by most of the workers cited above.

13.3 EVIDENCE FOR THE VALIDITY OF THE ION BALANCE EQUATION IN THE COLUMN UNDER STUDY

In using the ion balance equation to calculate the equilibrium ion number density in the plasma of the positive column under study, we are assuming that the ion production rate in the plasma equals the ion loss rate by volume recombination, so that we can replace the two equations that determine the ion production and ion loss rates by a single equation. It will now be shown that this is a reasonable procedure, and that the ion loss rate by volume recombination does in fact equal the ion production rate by electron-atom collisions.

Let us first attempt to evaluate the ion production rate in the plasma. As has already been shown, the ions are produced mainly by direct collisions between fast electrons and seed atoms,

and von Engel (1965) gives a formula for the ion production rate in such a case, namely,

$$Z = 10^8 a_1 P_s \exp\left(\frac{eV_i}{kT_e}\right) \cdot \left(\frac{kT_e}{e}\right)^{1/2} V_i \quad \text{-----} \quad 13.4$$

Here, Z is the number of ion pairs produced per electron per second, and a_1 is a constant expressed in ion pairs per cm. per torr per volt per primary electron. For a potassium-argon plasma where the seed pressure is about 1 torr and the electron temperature is roughly 3000°K (roughly the conditions in the column under study), Sakuntala (1964) has used eqn. 13.4 to show that Z has a value of the order of 10^3 . Thus, since the electron number density is of the order of $3 \times 10^{14} \text{ cm}^{-3}$, we see that the rate of production of ion pairs in the plasma is of the order of 3×10^{17} per second per cm^3 .

Let us now attempt to evaluate the ion loss rate by volume recombination, as this should equal the ion production rate if equilibrium conditions are to prevail. The main volume ion loss processes will be electron-ion recombination by radiative recombination and double excitation recombination (von Engel 1965). The rate of disappearance of ion pairs by volume recombination is proportional to the square of the electron number density n_e , and is given by

$$\frac{dn_e}{dt} = -\rho n_e^2 \quad \text{-----} \quad 13.5$$

where ρ is defined as the recombination coefficient. In the present case, ρ will equal the sum of the recombination coefficients of all the individual processes. In the first process,

radiative recombination, an electron is captured by an ion with the simultaneous emission of a photon, and von Engel gives the recombination coefficient as about $10^{-13} \text{ cm}^3 \text{ sec}^{-1}$. In the second process, an electron is captured by an ion, and enters an excited state, raising another electron to a second excited state; both excited electrons later fall back to their respective ground states with the emission of photons. This second process is more probable than the first, and von Engel estimates the recombination coefficient to be roughly $10^{-12} \text{ cm}^3 \text{ sec}^{-1}$. Other possible recombination processes include the various three-body processes, where electrons and ions recombine in the presence of atoms or other electrons. The recombination coefficients for these processes are very difficult to estimate, but ought to be less than those quoted above. Let us therefore estimate the total recombination coefficient to be of the order of $10^{-12} \text{ cm}^3 \text{ sec}^{-1}$. Thus, for an electron number density of the order of $3 \times 10^{14} \text{ cm}^{-3}$, we see that the ion loss rate by volume recombination is of the order of 10^{17} per second per cm^3 , which is of the same order of magnitude as the ion production rate.

13.4 JUSTIFICATION FOR IGNORING RADIAL ION LOSSES IN THE COLUMN UNDER STUDY

As we have seen in Chapter 10, one of the major assumptions that we make in using the ion balance equation to determine the ion number density throughout the column plasma is that the ion loss rate by diffusion through the column boundary is negligible compared with the ion loss rate by volume recombination. Let us

now calculate the value of the lateral ion current, and show that our assumption is justified. To do so, we need to know the thickness of the column boundary and the drop in the electron number density that occurs across the boundary. The boundary thickness can be calculated using the energy balance equation, since we have seen in Chapter 11 that the rate of flow of heat out of unit length of the column by conduction through the column boundary is given by

$$\Delta E_c = 2\pi R K_R \left(\frac{\partial T}{\partial r} \right)_R \quad \text{-----} \quad 13.6$$

where R is the column radius,

K_R is the thermal conductivity of the gas in the boundary

and $\left(\frac{\partial T}{\partial r} \right)_R$ is the temperature gradient at the column boundary.

Since K_R has a value of roughly 6×10^4 c.g.s.u. for a potassium-argon column, we can roughly estimate the thickness of the boundary by means of this equation. Taking the experimental values of ΔE_c and R for a current of 1 amp through potassium-argon, we see that $\left(\frac{\partial T}{\partial r} \right)_R$ is of the order of 5×10^3 °K cm⁻¹. It will be shown in Chapter 15 that the temperature drop across the column boundary appears to be of the order of several hundred degrees K, so we see that the column boundary thickness must have a value of the order of 1 m.m. This conclusion is fully supported by the available visual and photographic evidence, and we will see in Chapter 15 how the existence of a transition zone of the order of 1 m.m. thick between the column plasma and the

surrounding gas helps to explain certain features of the column properties. The fall in the electron and ion number densities across the boundary can be estimated from the fact that the electron number density just inside the column is between 10^{13} and 10^{14} cm^{-3} , while the value outside the column is between 10^7 and 10^{11} cm^{-3} , depending on the gas temperature. A fall of about 10^5 cm^{-3} across the boundary would be a typical value.

Loeb (1955) shows that the force on a particle of the i 'th species due to diffusion effects is given by

$$f_i = \frac{1}{n_i} \frac{\partial p_i}{\partial x} \quad \text{-----} \quad 13.7$$

where n_i is the number density and p_i the partial pressure of the i 'th species, so that $\frac{\partial p_i}{\partial x}$ is the pressure gradient. Since p_i is equal to $n_i k T_i$, where k is Boltzmann's constant, and T_i is the temperature of the i 'th species, we see that the force on a particle is given by

$$f_i = \frac{k T_i}{n_i} \cdot \frac{\partial n_i}{\partial x} \quad \text{-----} \quad 13.8$$

Now the ion number density equals the electron number density, and the electron and gas temperatures are of the same order of magnitude, so that the diffusion forces on ions and electrons are of the same order of magnitude, the force on the electrons being slightly greater, since the electron temperature is greater than the gas temperature. But the actual diffusion rate that is produced by the diffusion force depends not only on the strength of the force, but also on the mobility of the type of particle, so that the electrons will tend to diffuse faster than the much-heavier

ions. In practice, this will not occur, for as soon as the electrons start to outstrip the ions, they will create a space charge that will tend to pull the electrons back and speed up the ions. This is the well-known effect of ambipolar diffusion, and has the net result of causing the ions and electrons to diffuse at a common rate, a rate that is only slightly greater than the natural diffusion rate of the ions. Loeb (1955) in fact shows that the common ambipolar diffusion rate is equal to the natural electronic diffusion rate multiplied by $\frac{K_+}{K_-}$, the ratio of the ionic and electronic mobilities.

Let us suppose that the number density of ions and electrons inside the column is n_1 , and that the number density outside the column is n_2 ; the number density will thus fall from n_1 to n_2 over a distance a , the boundary thickness. Let us further suppose that we can treat the boundary as a thin-walled cylinder. If we apply the continuity equation, stating that the net flux of ion pairs must be constant across the boundary, we can say that the total loss rate F of ions by diffusion from unit length of the column is given by

$$F = 2\pi R n_e V_D \quad \text{-----} \quad 13.9$$

where n_e is the electron number density

R is the column radius

V_D is the diffusion velocity

Both n_e and V_D will vary across the boundary, but since we are assuming that R does not change greatly as we cross the boundary, we can say that $n_e V_D$ is constant across the boundary.

Now the diffusion force on an electron is $-\frac{kT_e}{n_e} \cdot \frac{\partial n_e}{\partial x}$, and the net force on an electron after allowing for ambipolar diffusion effects will be $\frac{K_+}{K_e} \cdot \frac{kT_e}{n_e} \cdot \frac{\partial n_e}{\partial x}$, so that the value of the electric field X_D that would produce an equal force is given by

$$X_D e = \frac{K_+}{K_e} \cdot \frac{kT_e}{n_e} \cdot \frac{\partial n_e}{\partial x} \quad \text{13.10}$$

Since a field X_D produces a drift velocity equal to $K_e X_D$, we see that the diffusion velocity is given by

$$\begin{aligned} V_D &= \frac{K_+}{K_e} \cdot K_e \cdot \frac{kT_e}{en_e} \cdot \frac{\partial n_e}{\partial x} \\ \therefore V_D &= \frac{K_+ kT_e}{en_e} \cdot \frac{\partial n_e}{\partial x} \quad \text{13.11} \end{aligned}$$

Hence, the total flux F is given by

$$F = \frac{2\pi R K_+ kT_e}{e} \cdot \frac{\partial n_e}{\partial x} \quad \text{13.12}$$

If we now say that F is constant across the boundary, we see that $\frac{\partial n_e}{\partial x}$ must also be constant across the boundary, and must therefore have the value $\frac{n_1 - n_2}{a}$. Thus, the total loss rate of ion pairs from unit length of column by ambipolar diffusion is given by

$$F = \frac{2\pi R K_+ kT_e}{e a} (n_1 - n_2) \quad \text{13.13}$$

If we evaluate F for a current of 1 amp in a potassium-argon column, where $K = 0.25$ cm, $T_e = 3000^\circ\text{K}$ approximately, $K_+ = 4 \times 10^{-4}$ cm sec^{-1} per e.s.u. approximately, a is of the order of 0.1 cm, and $(n_1 - n_2)$ is of the order of 10^5 cm^{-3} , we see that F is of the order of 10^8 sec^{-1} for unit length of column. This is clearly negligible compared with the ion loss rate by volume recombination (see last section), so our use of the ion balance equation has now been completely justified.

The above discussion also shows that the energy loss rate from the column by ambipolar diffusion is negligible compared with the other loss rates (conduction and radiation). Each ion pair that leaves the column carries roughly $1.6 \times 10^{-12} V_i$ ergs of ionisation energy with it, so that the energy loss rate per unit length of column is of the order of 10^{-3} ergs per sec. This is completely negligible compared with the energy input rate per unit length of column (of the order of $10^7 - 10^8$ ergs per sec).

CHAPTER 14THE ARC CURRENT EQUATION14.1 THE CONDUCTION OF ELECTRICITY THROUGH A GAS

In this chapter, we will discuss the relationship that exists between the electrical conductivity of a plasma and the microscopic plasma properties. The equation that describes this relationship is the arc current equation, and is the last of the fundamental equations that we need in order to describe the positive column under study.

Electric currents are carried through gases by free electrons and ions, the latter being in general positively charged. In the plasma of the positive column under study, the axial electric field is uniform, varying neither axially nor radially, and this leads us to conclude (from Poisson's equation) that the number densities of electrons and positive ions are everywhere equal, since there can be no net space charge present. The ions and electrons that are present in the column plasma have random thermal velocities, and the presence of the axial electric field causes a relatively small drift velocity to be added to these thermal velocities, so that the electrons and ions move in opposite directions, thus causing an electric current to flow through the plasma. Suppose that the ionic and electronic mean collision times with heavy bodies (neutral atoms and positive ions) are t_+ and t_{e0} respectively. Then if the electric field is X , the electronic drift velocity v_e can be shown by a statistical

argument first given by Langevin (1905) to be approximately given by

$$v_e = \frac{X e t_{eo}}{m_e} \quad \text{14.1}$$

where m_e is the electronic mass,

and e is the electronic charge.

The electronic mobility K_e (the ratio of the electronic drift velocity to the electric field) is therefore given by

$$K_e = \frac{e t_{eo}}{m_e} \quad \text{14.2}$$

and the corresponding ionic mobility K_+ is given by

$$K_+ = \frac{e t_+}{m_+} \quad \text{14.3}$$

where m_+ is the mass of a positive ion.

Compton (1927) has shown that the total current density j in a plasma is equal to the sum of the electronic and ionic current densities, and, for an electrically-neutral plasma, is given by

$$j = \underbrace{n_e e K_e X}_{\text{electron current}} + \underbrace{n_e e K_+ X}_{\text{ion current}} \quad \text{14.4}$$

From the expressions for the electronic and ionic mobility, we would suspect that the electronic current density would be very much greater than the ionic current density because of the huge difference between m_e and m_+ . In fact, it can be shown that the ratio of the ionic mobility to the electronic mobility is roughly given by $\sqrt{\frac{m_e}{m_+}}$ (von Engel 1965), and the reciprocal of this quantity has a value of several hundred, the exact value depending on the atomic weight of the seed used. We are therefore justified

in neglecting the ionic contribution to the discharge current, and will henceforth only consider the electronic current. It must be remembered, however, that an ionic current does exist, and that every amp of electronic current flowing from cathode to anode is accompanied by a few milliamps of ionic current flowing from anode to cathode.

Applying eqn. 14.2 to Compton's mobility equation and neglecting the ion current term, we see that

$$j = \frac{n_e e^2 t_{eo} X}{n_e} \quad \text{-----} \quad 14.5$$

Now the electrical conductivity σ is defined as the ratio of the current density to the electric field, so that σ is equal to

$$\frac{n_e e^2 t_{eo}}{n_e} \quad \text{-----} \quad 14.6$$

Compton and Langmuir (1930) have shown by a slightly more sophisticated argument that the electrical conductivity is more accurately given by

$$\sigma = \frac{0.85 n_e e^2 t_{eo}}{n_e} \quad \text{-----} \quad 14.7$$

so that the mobility K_e is given by

$$K_e = \frac{0.85 e t_{eo}}{n_e} \quad \text{-----} \quad 14.8$$

An alternative statement of eqn. 14.7 is

$$\sigma = n_e e K_e \quad \text{-----} \quad 14.9$$

which is essentially Compton's mobility equation with the ion current term removed. Eqn. 14.9 states that the electrical conductivity is proportional to the product of the electron

number density and the electronic mobility, and is a very useful form of the arc current equation. The method of calculating the electron number density has already been discussed (Chapter 13), so the rest of this chapter will deal with the evaluation of the electronic mobility.

14.2 THE VALUE OF THE ELECTRONIC MOBILITY

Equation 14.8 shows us that the value of the electronic mobility in a plasma depends only on the electron-heavy body collision time t_{eo} . The latter is easily evaluated, since we can equate it to the average distance that an electron travels between collisions divided by the average thermal velocity of the electrons. It therefore follows that

$$t_{eo} = \frac{\lambda}{\bar{c}} \quad \text{-----} \quad 14.10$$

where λ is the electronic mean free path

\bar{c} is the average electronic thermal velocity.

From the Maxwellian distribution law, it can easily be shown (Cobine 1958) that

$$\bar{c} = \left(\frac{8 kT_e}{\pi n_e} \right)^{1/2} \quad \text{-----} \quad 14.11$$

where k is Boltzmann's constant

and T_e is the electron temperature.

The value of the electronic mean free path can be shown by an extension of the argument first given by Clausius (1889) to be given by

$$\frac{1}{\lambda} = \sum_i n_i a_i \quad \text{-----} \quad 14.12$$

Here, n_i and a_i are respectively the number density and electron collision cross section of the i 'th species present in the gas. The collision cross section of an atom or ion is the effective target area presented to an electron, and is a function of the electron energy. The collision cross sections of the various rare gases and alkali metals are not accurately known for the electron energy range of interest, but a search of the literature by Ralph (1963 priv. comm.) has shown that the values given in Table 14.1 are at least approximately correct.

TABLE 14.1

<u>DILUENT GASES</u>	<u>ELECTRON COLLISION CROSS SECTION</u>
HELIUM	$6A^{\circ 2}$
NEON	$1.8A^{\circ 2}$
ARGON	$0.6A^{\circ 2}$
<u>SEED METALS</u>	<u>ELECTRON COLLISION CROSS SECTION</u>
SODIUM	$130A^{\circ 2}$
POTASSIUM	$200A^{\circ 2}$
CAESIUM	$300A^{\circ 2}$

The uncertainty in the absolute values of the cross sections given in Table 14.1 is quite large - $\pm 25\%$ at least - but the author is confident that the relative values of the cross sections are fairly accurate. Although the cross sections of the various atomic species present in the plasma are not

accurately known, the same is not true for the positive ions, since Spitzer and Härn (1953) and Lin, Resler and Kantrowitz (1955) have shown that

$$a_+ = (8.1 B_0^2 + \log_{10} \frac{h}{B_0}) \text{ cm}^2 \quad \text{--- 14.13}$$

where a_+ is the electron collision cross section of a positive ion,

$$B_0 = \frac{5.569 \times 10^{-4}}{T_e} \quad \text{--- 14.14}$$

$$\text{and } \frac{h}{B_0} = 1.239 \times 10^{-4} \left(\frac{T_e}{n_e} \right)^{3.1/2} \quad \text{--- 14.15}$$

Here, h is the Debye length. We see that a_+ is strongly dependent on the electron temperature, falling as T_e rises. In figure 14.1, a_+ is shown as a function of T_e for a typical plasma - 0.9 torr of potassium in atmospheric-pressure argon. It is seen that a_+ has a value of about 10^4 \AA^2 for the electron temperature range of interest.

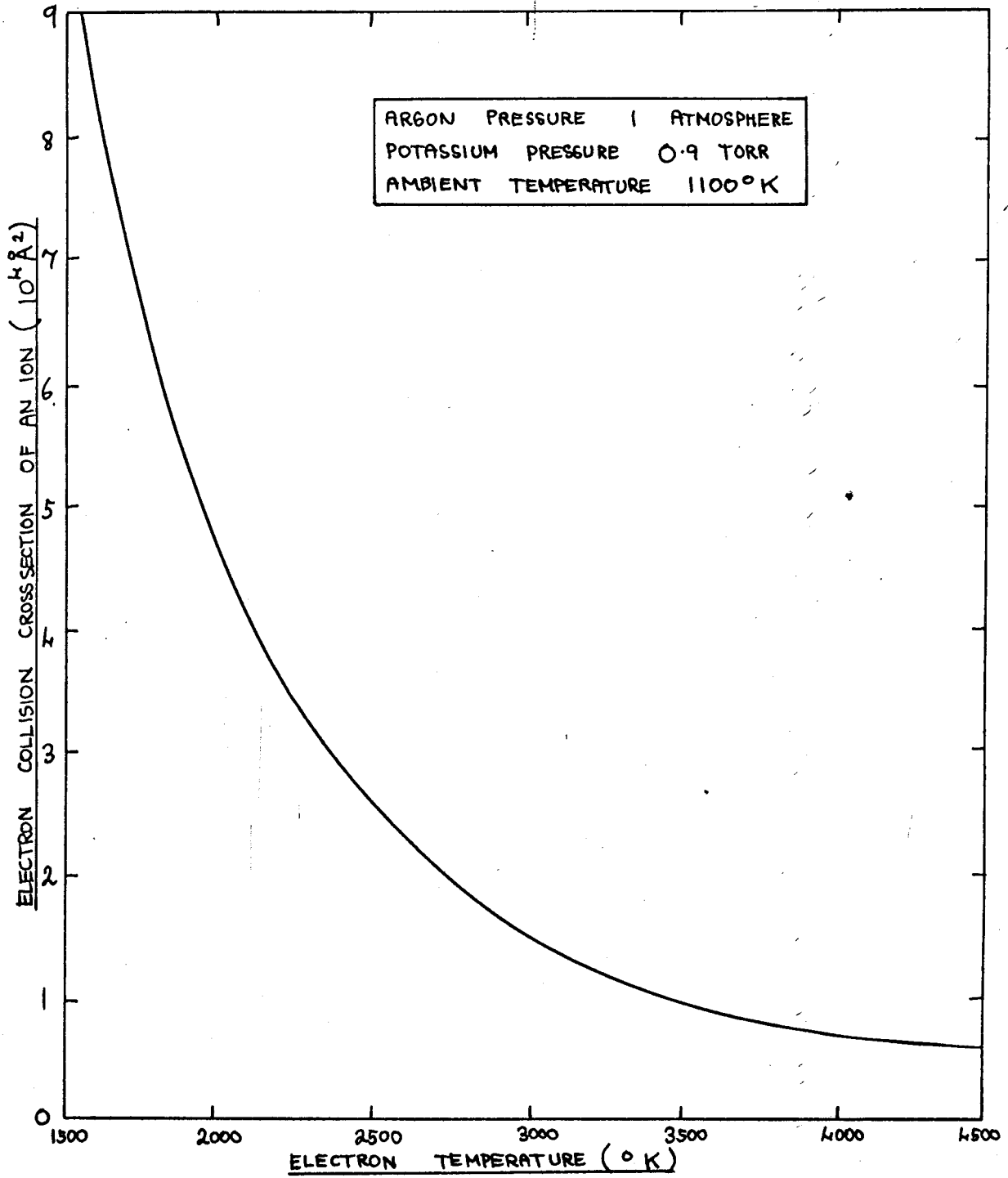
In the positive column under study, the expression for λ contains three terms, namely, a diluent-dependent term, a seed-dependent term and an ion-dependent term, eqn. 14.12 becoming

$$\frac{1}{\lambda} = n_d a_d + n_s (1 - x) a_s + n_+ a_+ \quad \text{--- 14.16}$$

Here, n_d , $n_s(1 - x)$ and n_+ are the number densities of diluent atoms, neutral seed atoms, and ionised seed atoms, the presence of ionised diluent atoms being neglected. a_d , a_s and a_+ are the electron collision cross sections of diluent atoms, seed atoms and positive ions, and x is the degree of ionisation of the seed. In a typical column plasma, n_s is of the order of 1% of n_d , while n_+ , in turn, is generally a few percent of n_s .

FIGURE 14.1

PLOT OF IONIC ELECTRON COLLISION CROSS SECTION
AGAINST ELECTRON TEMPERATURE FOR A TYPICAL PLASMA



The three terms in eqn. 14.16 are of the same order of magnitude, however, since $a_+ \gg a_s \gg a_d$.

The values of n_d and n_s in eqn. 14.16 are easily calculated from the gas laws, the number density of the i 'th species being given by

$$p_i = n_i kT_g \quad \text{-----} \quad 14.17$$

where p_i is the partial pressure of the i 'th species

and T_g is the gas temperature.

$$\text{Hence, } n_i = \frac{p_i}{kT_g} \quad \text{-----} \quad 14.18$$

If p_i is measured in torr and T_g in degrees K, the equation becomes

$$n_i = 9.66 \times 10^{18} \frac{p_i}{T_g} \quad \text{-----} \quad 14.19$$

From the theory developed in this chapter, it is seen that the arc current equation can be set up with a fair degree of accuracy. Its accuracy is limited in practice, however, by the uncertainty in the values of the various quantities involved in the equation. The value of the electronic mobility can be calculated reasonably accurately, but there is a large uncertainty in the value of the electron number density if we attempt to calculate this from the plasma properties using the ion balance equation discussed in the last chapter. For this reason, it is found that the arc current equation proves to be of greater use as a means of computing the electron number density in the plasma, using the electrical conductivity value in the plasma as a starting point, rather than the other way round. It will be used in this manner in Chapters 15 - 17.

CHAPTER 15THE BASIC PROPERTIES OF THE COLUMN15.1 THE CONSTRICTION OF THE COLUMN - MAGNETIC CONSTRICTION

In this chapter, we will discuss the basic properties of the column, and will show that the observed dependence of the column properties on the discharge current is consistent with the theory that we have developed in the last five chapters. Before we carry out a quantitative analysis of the column, however, we will discuss the constriction of the column, and will try to explain why the column does not spread out and fill the space available to it with a corresponding fall in the plasma current density. The constriction of a positive column can generally be explained by one of two distinct types of theory, classified by Massey (1965) as "magnetic" and "thermal", so we will examine them in turn, and see which is relevant in the present case.

Magnetic constriction of a positive column can be caused by a properly-applied magnetic field, or by the self-field of the discharge itself. The former can be disregarded in the case under study due to the absence of an external magnetic field, but the possibility of the column being constricted by what is sometimes called a "Z pinch" cannot be so disregarded, however, as the form of the magnetic field due to the current in the column will certainly cause Lorentz forces that will act radially inwards. This type of constriction occurs when the circular magnetic field produced by the movement of a linear stream of charged

particles is strong enough to produce "pinching" of the particle stream, and generally only becomes important when the discharge current is very large. Let us attempt to evaluate the radial Lorentz forces that occur around the column under study.

To facilitate the calculation, imagine the column to have a definite radius R , and a uniform current density j_m within the column plasma. Application of Ampere's law then shows that the scalar strength of the magnetic field H at a distance r from the column axis is given by

$$H = \frac{2\pi r^2 j_m}{r}$$

$$= 2\pi r j_m, \text{ for } r \leq R.$$

H will reach a maximum value when $r = R$, and will then equal $2\pi R j_m$, or $\frac{2i}{R}$, where i is the total current. For $r > R$, H will fall off as $\frac{1}{r}$, as in the case of the field round an ordinary conductor.

The Lorentz force f_L on an electron will be given by

$$f_L = \frac{e}{c} v_d H$$

Here, v_d is the electronic drift velocity, and is at right angles to the magnetic field, e is the electronic charge, and c is the velocity of light. We assume the permeability of the plasma to be unity.

Since the electronic drift velocity is several hundred times greater than the ionic drift velocity, we can neglect the Lorentz force on the ions compared with that on the electrons. We see that f_L will increase as we leave the column axis, reaching its

maximum value at the column boundary. If we evaluate f_L at the boundary of a typical column, we find that it is of the order of 10^{-15} dynes. This is comparatively small, and while the Lorentz forces will definitely tend to hold the column together, the author believes that they are not strong enough to play a significant part in determining the size of the column. This can be demonstrated by comparing the work that would be done by the magnetic constricting forces in causing a given reduction in the size of the column with the increase in the column energy input rate that such a reduction in the column size would necessitate. Consider a typical column - one carrying a current of 1 amp. in argon seeded with 3.5 torr of potassium. The diameter of this column is roughly 5 mm, and it will be shown later on in this chapter that the mean electron number density in the column plasma is about $4 \times 10^{14} \text{ cm}^{-3}$, so that unit length of column contains roughly 8×10^{13} electrons. Suppose that the constricting forces cause the column diameter to decrease by 1 mm. If we make the very rough approximation that all the electrons in the column move radially inwards by 0.5 mm under a force equal to the Lorentz force at the column boundary, we see that the work done is of the order of 4×10^{-3} ergs. Now the reduction of the column diameter from 5 to 4 mm would cause the mean current density to increase from roughly 5 amps/cm^2 to roughly 8 amps/cm^2 , which would cause the electron number density in the column and the degree of ionisation of the seed to increase to approximately twice their former values. This, in turn, would require the electron temperature to increase from roughly 2800°K

to roughly 3000°K , and we can make use of the energy balance and electron energy balance equations to show that this would require an increase in the column electric field of the order of 0.2 volts/cm. Thus, the energy input rate per unit length of column would have to increase by roughly 0.2 watts, ~~an~~ amount that is many orders of magnitude greater than the energy that is associated with the magnetic constricting forces, so that the magnetic forces are clearly too small to have any significant effect on the size of the column. This conclusion is supported by the work of Massey (1965), who rules out the possibility of constriction by self-field in the case of the pure argon discharge studied by himself and Cannon (1965), a discharge in which the value of the Lorentz force is in fact greater than it is in the column under study. We must therefore turn to the "thermal" type of theory in order to seek the basic reason for the constriction of the column under study.

15.2 THE CONSTRICTION OF THE COLUMN - THERMAL CONSTRICTION

Thermal constriction is generally associated with high-current, high-pressure arc columns. It occurs in the case of conventional thermal arcs because a constricted column carrying a high current density requires a lower energy input per unit length to support a given current than a more diffuse column with a lower current density. This is because a thermal arc column has to operate at a very high temperature in order to ionise the gas, and a high plasma temperature can only be produced if the current density and energy input per unit volume of plasma are high (see Chapter 10).

For this reason, a constricted thermal column is intrinsically more stable than a more diffuse column would be. The fact that the gas temperature falls off as we leave the axis of such a column means that the degree of ionisation and current density also fall as we leave the column axis, and Champion (1952 A) shows that this leads to a fairly well-defined column boundary, the current density and temperature on the outside of the boundary being much lower than on the inside. Von Engel (1965) shows that another factor which tends to increase the degree of constriction of thermal arc columns is the presence of convection currents in the gas surrounding the column. As we have seen in Chapter 11, these are necessary in order to carry off the heat that passes through the column wall by conduction, and their influence on the size of a conventional arc column can best be demonstrated by effecting their removal by some means. Von Engel shows that if this is done, (for example, by allowing the apparatus containing the discharge to fall freely, thus eliminating gravity), then the column of a high-pressure, thermal arc will expand considerably.

The author believes that the constriction of the column under study is brought about by effects that are similar to those described above. Forces caused by convection currents are probably present, and these will have some constricting effect on the column, although their importance is very difficult to estimate. The author does not believe that they are the primary cause of the constriction, however. The main reason for the constriction appears to be that it is an intrinsic property of the type of nonequilibrium column

under study that the current density must be high for the column to exist at all, so that the constriction is not really imposed on the column by external forces, but is a natural consequence of the nature of the processes that enable the column to exist. Let us discuss this in more detail. The discharge current is determined by the external circuit conditions, namely, the external resistance and the total applied voltage, so that the column is given a definite current to carry. This necessitates the production of a highly-conducting plasma, and it has been shown in Chapter 12 that such a plasma can only be produced under non-equilibrium conditions of the type found in the column under study when the electron number density is high enough for the high-energy tail of the electron energy distribution to be present. This means that the electron number density must be of the order of 10^{14} cm^{-3} or more; if it falls below about 10^{13} cm^{-3} , the high-energy tail becomes depleted, causing a reduction in the rate of ion production, so that the electron number density falls still further. For this reason, a constricted column is more stable than a more diffuse column with a lower current density and a lower electron number density would be, as the latter would require a higher energy input rate per unit length of column to support a given current.

Another question must be answered at this point: if the ionisation process becomes progressively more efficient as the electron number density increases, why is the electron number density in the column limited to a value that generally corresponds

to a degree of ionisation of only a few percent? Why does the column not constrict to an even smaller size, causing the degree of ionisation of the seed and the electron number density to rise to much higher values? We have seen in Chapter 13 that the degree of ionisation of the seed is largely controlled by the electron temperature in the plasma, and it has been shown in Chapter 12 that the value of the electron temperature depends strongly on the electronic mean free path. The lower the value of the latter, the higher is the electric field that must be applied across the plasma in order to produce a given elevation in the electron temperature. The author believes that it is this factor that limits the electron number density in the column plasma, and hence the degree of constriction of the column. As the electron number density rises, the electronic mean free path falls because of the increase in the amount of scattering of electrons by positive ions, and as the electron number density becomes very large, the value of the mean free path is eventually controlled by the ion scattering term (see Chapter 14). The ion scattering term becomes comparable in size to the other terms in the expression for the mean free path when the electron number density reaches a value of between 10^{14} and 10^{15} cm^{-3} , so this explains why the electron number density in the column lies in this range. A column with a higher electron number density than this would require a higher power input per unit length in order to support a given current. For this reason, it would be less stable than the column that is in fact observed.

We can therefore conclude from the arguments given in this section that the size of the column at a given current is determined by minimum energy considerations, the stable size being that at which the lowest axial electric field is required. This explains why the column accommodates current changes by altering its size so as to keep the current density roughly constant rather than by remaining the same size and altering the current density: the column adjusts its size so as to keep the electron number density at the optimum value. Further evidence in support of this theory will be given in the next chapter, when the effect on the column properties of varying the seed pressure will be discussed (section 16.4).

15.3 THE BOUNDARY OF THE COLUMN.

Having seen why the current density and electron number density in the column have to be high, but not too high, for the column to exist in its observed form, let us now try to explain why the boundary of the column should be so well-defined. A well-defined boundary appears to be a general property of high-pressure arc columns (Suits 1939 C, Cobine 1958), the temperature of the surrounding gas departing very little from the ambient value up to a distance of a few m.m. from the luminous region of such columns. In the column under study, the presence of a fairly sharp lateral boundary appears to be a consequence of the fall in ionisation efficiency that occurs as the electron number density decreases. The electron-temperature that is required to produce an electron number density of the order of 10^{14} cm^{-3} in potassium-seeded plasmas

is of the order of 2500°K (see figure 13.1), so the local value of the gas temperature plus the elevation in the electron temperature must equal this value if such an electron number density is to be maintained. The elevation in the electron temperature is determined mainly by the electric field in the plasma (Chapter 12), and the latter is constant across the column, so that the elevation in the electron temperature should not vary greatly as we cross the column. But we have seen in Chapter 11 that the gas temperature falls as we leave the column axis, so the electron temperature will also fall, causing a progressive drop in the values of the degree of ionisation of the seed and the electron number density as we move radially outwards. As we have seen, the efficiency of the ionisation process falls drastically when the electron number density falls below about 10^{13} cm^{-3} (Chapter 12), so the effective boundary of the column may be taken to be the place where the electron number density falls from above about 10^{13} cm^{-3} to below about 10^{13} cm^{-3} , as the electron number density and current density will fall off sharply beyond this point. The visible boundary of the column, which, as we have seen, is fairly well-defined, appears to correspond to this postulated boundary. This is because the light output of the column is produced almost entirely by the decay of excited seed atoms, and the number density of the latter will fall off sharply when the electron number density falls below about 10^{13} cm^{-3} for the same reasons that the number density of ionised atoms falls.

Another experimental observation that can be explained by the above picture of the column boundary is the fact that there appears to be a minimum current (whose value depends on the nature of the mixture) below which the column under study cannot exist. We have seen how the column depends for its stability on maintaining a much higher electron number density in its interior than that which is found in the gas surrounding it. We have also seen in section 13.4 how this requires the existence of a transition region between the column plasma and the surrounding plasma - the column boundary - and how this column boundary is of the order of 1 mm thick because of heat transfer and ionisation effects. It follows that if the column contracts to a diameter smaller than twice the column boundary thickness, then the interior of the column cannot possibly maintain the required electron number density, so that the limiting value of the column diameter ought to be of the order of twice the column boundary thickness, namely, about 2 mm. Study of Table 6.1 shows that this is in excellent agreement with the experimental facts, since the minimum column diameter was found to be about 2 mm in all the mixtures studied.

15.4 ANALYSIS OF THE CURRENT-DEPENDENT EXPERIMENTAL RESULTS: PRELIMINARY CONSIDERATIONS.

Having given a qualitative explanation of why the column is constricted and why it has such a well-defined boundary, we shall now attempt the much-more-difficult task of giving a quantitative explanation of the current-dependent results that were given in

Chapter 6. In particular, we shall attempt to explain why the mean electrical conductivity of the column plasma rises as the discharge current increases despite the fact that the column electric field falls as the current increases, since this fact is at first sight inconsistent with the two-temperature conductivity theory that has been developed in the preceding chapters. Use of the ion balance and arc current equations shows that an increase in the plasma conductivity must be accompanied by a rise in the electron temperature, and the electron energy balance equation shows that such an increase in the electron temperature should be accompanied by a rise in the plasma electric field, since it is the value of the electric field that determines the degree of elevation of the electron temperature. Kerrebrock and Hoffman (1964) and other workers already mentioned in earlier chapters have shown experimentally that the electric field across homogeneous two-temperature plasmas does in fact increase as the electrical conductivity rises, and Kerrebrock (1965) has shown that the experimental results are in excellent quantitative agreement with the two-temperature conductivity theory, so the results that are given in figures 6.1 - 6.4 appear to be in complete disagreement with the theory, since they appear to show the opposite effect. In this chapter, we shall show that this **apparent** anomaly can be explained by allowing for the fact that the positive column under study is not a homogeneous plasma of the type studied by Kerrebrock et al., and also for the fact that the ionisation and energy balance mechanisms that operate in the column are

strongly inter-dependent. We have seen in Chapter 11 how the column energy balance processes cause the interior of the column to be considerably hotter than the exterior, and we shall show later on in this chapter that the mean effective value of the gas temperature in the column increases steadily as the discharge current rises. It is the author's contention that this rise in the effective temperature of the column is more than enough to offset the fall in the elevation of the electron temperature that occurs as the current rises because of the fall in the value of the column field, and that the mean effective value of the electron temperature in the column does in fact show a gradual increase as the discharge current increases. The above argument explains why the mean plasma conductivity rises as the current increases despite the fact that the column field falls, and forms the crux of the theory that is given in the remainder of this chapter.

An accurate quantitative analysis of the column under study is rendered extremely difficult by the fact that most of the column parameters are strongly radially-dependent. As we approach the axis of the column, we see from the internal energy balance equation that the value of the gas temperature increases. Since we can assume that the degree of elevation of the electron temperature remains roughly constant as we cross the column, we see that this will cause the electron temperature and the degree of ionisation of the seed to increase as we approach the axis, with the latter depending exponentially on the former. This,

in turn, means that the electrical conductivity and current density increase as we approach the axis, a fact that will affect the energy balance situation, since it means that most of the electrical power will be dissipated at the column core. Thus, we see that the various mechanisms that operate in the column are strongly inter-dependent, so that the four equations that describe these mechanisms (the arc current, energy balance, electron energy balance and ion balance equations) are also strongly inter-dependent. This inter-dependence, combined with the fact that the equations themselves are extremely complicated and difficult to set up accurately, means that it would prove to be extremely difficult to solve the four equations simultaneously and obtain an exact description of the column properties; indeed, Champion (1952) and Massey (1965) have shown that such a procedure is virtually impossible even for the much simpler case of a thermal arc column in which the electron and gas temperatures are equal. For this reason, the author has decided to adopt a somewhat simplified approach to the problem, and will only attempt to give a very approximate description of the column properties. For the purpose of applying the arc current and ion balance equations, we shall make use of the simplest possible model of the column - the so-called "channel model" (ter Horst and Pflanz 1967, Uhlenbusch 1962). As its name suggests, this treats the column as a uniform channel in which the gas temperature, electron temperature, plasma conductivity, etc. are independent of the distance from the column axis. This model will enable us to use the

experimental values of the discharge current, column diameter and column field that were given in Chapter 6 to calculate the mean effective values of the electron number density, the degree of ionisation of the seed, and the electron temperature in the column. Having done this, we will examine the column from an energy balance point of view, and will make use of the energy balance and electron energy balance equations to calculate how the values of the gas temperature and electron temperature vary across the column. Having obtained these temperature profiles of the column, we will attempt to calculate the value of the mean effective electron temperature from the electron temperature profile. The main object of the calculations will be to show that the theory that we have developed to describe the column is self-consistent, and that the values of the various parameters that are obtained from the application of the equations are reasonable. In particular, we will attempt to show that the values of the mean effective electron temperature that are obtained by the two methods outlined above are in agreement.

15.5 APPLICATION OF THE "CHANNEL MODEL" TO THE COLUMN.

In Tables 15.1, 15.2 and 15.3, the results of the first of the calculations that were discussed in the last section are shown. The three tables are for potassium-helium, potassium-neon and potassium-argon, the seed pressure and ambient gas temperature being respectively 3.5 torr and 950°C in all cases. The tables begin by giving the values of the discharge current at which

TABLE 15.1

TOTAL PRESSURE 1 ATMOSPHERE

AMBIENT TEMPERATURE 950°C

DILUENT : HELIUM

SEED : POTASSIUM

SEED PRESSURE 3.5 TORR

1. DISCHARGE CURRENT (AMPS)	$\frac{1}{4}$	$\frac{1}{2}$	1	2	4
2. POSITIVE COLUMN DIAMETER (MM)	2.0	3.0	4.0	6.0	8.5
3. MEAN CURRENT DENSITY (AMPS/CM ²)	7.3	7.3	7.3	7.3	7.3
4. COLUMN ELECTRIC FIELD (VOLTS/CM)	24	21	18	16	14
5. POWER INPUT PER UNIT LENGTH OF COLUMN (WATTS)	6.0	10.5	18	32	56
6. MEAN POWER INPUT PER UNIT VOLUME OF PLASMA (WATTS/CM ³)	175	153	132	117	102
7. MEAN ELECTRICAL CONDUCTIVITY (MHOS/CM)	0.3	0.35	0.4	0.46	0.52
8. MEAN ELECTRON NUMBER DENSITY ($\times 10^{14}$ CM ⁻³)	2.5	2.9	3.4	3.9	4.4
9. DEGREE OF IONISATION OF SEED(%)	1.1	1.3	1.5	1.7	2.0
10. MEAN EFFECTIVE ELECTRON TEMPERATURE (°K)	2650	2700	2730	2750	2780

TABLE 15.2

TOTAL PRESSURE 1 ATMOSPHERE					
AMBIENT TEMPERATURE 950°C					
DILUENT : NEON					
SEED : POTASSIUM					
SEED PRESSURE 3.5 TORR					
1. DISCHARGE CURRENT (AMPS)	$\frac{1}{4}$	$\frac{1}{2}$	1	2	4
2. POSITIVE COLUMN DIAMETER (MM)	2.0	3.0	4.0	5.0	7.0
3. MEAN CURRENT DENSITY (AMPS/CM ²)	7.0	7.0	7.0	7.0	7.0
4. COLUMN ELECTRIC FIELD (VOLTS/CM)	7.6	6.5	5.5	4.8	3.8
5. POWER INPUT PER UNIT LENGTH OF COLUMN (WATTS)	1.9	3.75	5.5	9.6	15.2
6. MEAN POWER INPUT PER UNIT VOLUME OF PLASMA (WATTS/CM ³)	54	46	39	34	27
7. MEAN ELECTRICAL CONDUCTIVITY (MHOS/CM)	0.92	1.06	1.22	1.45	1.84
8. MEAN ELECTRON NUMBER DENSITY (x 10 ¹⁴ CM ⁻³)	3.06	3.55	4.25	4.9	6.1
9. DEGREE OF IONISATION OF SEED(%)	1.03	1.55	1.85	2.13	2.64
10. MEAN EFFECTIVE ELECTRON TEMPERATURE (°K)	2700	2740	2770	2830	2890

TABLE 15.3

TOTAL PRESSURE 1 ATMOSPHERE

AMBIENT TEMPERATURE 950°C

DILUENT : ARGON

SEED : POTASSIUM

SEED PRESSURE 3.5 TORR

1. DISCHARGE CURRENT (AMPS)	$\frac{1}{4}$	$\frac{1}{2}$	1	.2	4
2. POSITIVE COLUMN DIAMETER (MM)	2.5	3.5	5.0	7.0	9.0
3. MEAN CURRENT DENSITY (AMPS/CM ²)	5.0	5.0	5.0	5.0	5.5
4. COLUMN ELECTRIC FIELD (VOLTS/CM)	3.6	2.8	2.5	2.0	1.7
5. POWER INPUT PER UNIT LENGTH OF COLUMN (WATTS)	0.72	1.4	2.5	4.0	6.8
6. MEAN POWER INPUT PER UNIT VOLUME OF PLASMA (WATTS/CM ³)	18	14	12.5	10	8.5
7. MEAN ELECTRICAL CONDUCTIVITY (MHOS/CM)	1.4	1.7	2.0	2.5	2.9
8. MEAN ELECTRON NUMBER DENSITY ($\times 10^{14}$ CM ⁻³)	3.0	3.6	4.1	5.2	6.1
9. DEGREE OF IONISATION OF SEED(%)	1.3	1.6	1.8	2.3	2.7
10. MEAN EFFECTIVE ELECTRON TEMPERATURE (°K)	2700	2740	2770	2840	2890

the calculation of the mean effective electron temperature is to be carried out (row 1), and then give the measured values of the column diameter (row 2) and the mean values of the column current density (row 3). Row 4 then gives the measured values of the column electric field. The next two rows (5 and 6) give the values of the electrical power input per unit length of column, and the mean values of the rate of energy input per unit volume of plasma. It is seen that the former increases as the current rises, but that the latter decreases due to the steady fall in the value of the column electric field. Row 7 gives the mean values of the plasma electrical conductivity that are obtained by dividing the current density by the electric field. The values of the electron number density that are required to produce these values of the electrical conductivity are shown in the next row (row 8). These values were calculated using the arc current equation (Chapter 14), and were obtained by first evaluating the electronic mobility. This required the knowledge of the ion number density in the plasma (equal to the electron number density), so the calculation was cyclical, and had to be carried out as a series of converging approximations. The next row (row 9) gives the values of the degree of ionisation of the seed that are required to produce these values of the electron number density. The final row (row 10) gives the values of the electron temperature that are required to produce these degrees of ionisation, and were calculated using the ion balance equation (eqn. 13.1). Because of the intractable nature of eqn. 13.1 (the Saha equation),

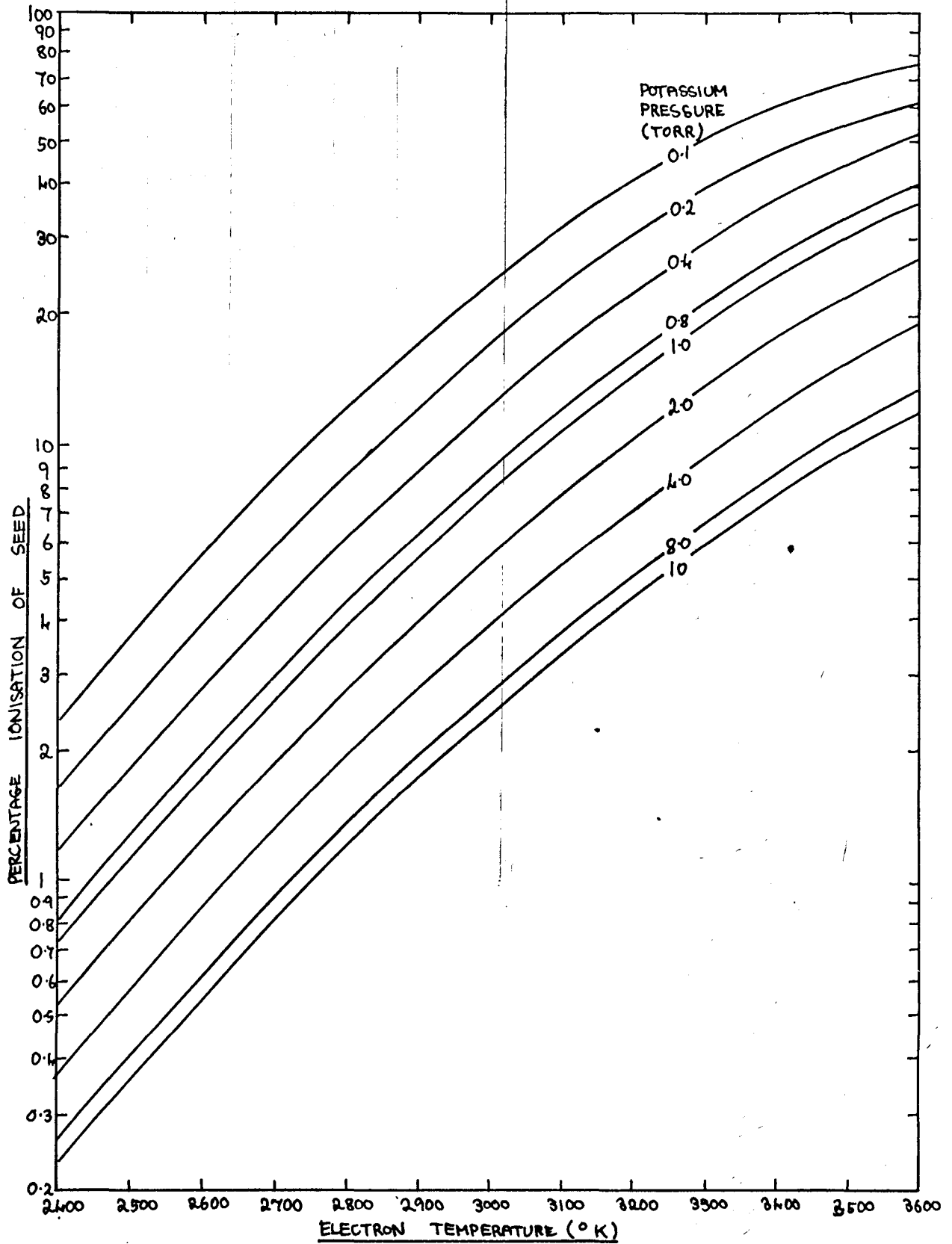
the author had a set of results calculated by computer. These gave the values of the degree of ionisation in potassium at nine different pressures (0.1, 0.2, 0.4, 0.8, 1, 2, 4, 8 and 10 torr) at temperatures rising from 800°K to 5000°K by 100°K intervals, and enabled rapid calculation of the degree of ionisation at intermediate seed pressures and electron temperatures to be carried out by extrapolation. Some of the results are shown in figure 13.1, which shows plots of ionisation against temperature throughout the temperature range 1000 - 3000°K, and a more accurate plot of the results in the temperature range of interest in the present calculations (roughly 2400 - 3600°K) is shown in figure 15.1. It must again be stressed that the results shown in Tables 15.1 - 15.3 are very approximate indeed, and are the mean values of the various quantities that are obtained by employing a greatly simplified model of the column. It is estimated that the degree of uncertainty in the values of the electron number density and the degree of ionisation of the seed is of the order of $\pm 75\%$, so that the error in the electron temperature value is of the order of $\pm 150^\circ\text{K}$.

15.6 THE TEMPERATURE PROFILE OF THE COLUMN.

The positive columns of arc discharges can have a variety of temperature profiles, the nature of the profile depending mainly on the nature and importance of the energy balance processes that are active within the column. If energy balance effects are unimportant, as in a low-pressure column, the temperature will be

FIGURE 15.1

LOTS OF DEGREE OF IONISATION OF SEED AGAINST ELECTRON TEMPERATURE FOR DIFFERENT PRESSURES OF POTASSIUM



roughly constant as we cross the column, but in columns where a large amount of energy is generated within the column plasma, and is removed from the column by conduction, the temperature will increase as we approach the column axis. The simplest model that can be used to describe the latter type of column is the so-called "parabola model" (Uhlenbusch 1962, ter Horst and Pflanz 1967). As in the channel model used in the last section, this assumes that the plasma conductivity and current density are constant within the column, but differs from the channel model in allowing for the fact that the gas temperature rises as the column axis is approached. If we apply the internal energy balance equation (eqn. 11.18) to such a column, taking the current density j to equal the mean current density j_m throughout the column, we see that the net conduction heat losses from a cylindrical element of column of unit length and radius r are equal to

$$- 2\pi r k \frac{\partial T_r}{\partial r} \quad \text{-----} \quad 15.1$$

where k is the mean thermal conductivity of the column plasma and T_r is the gas temperature at radius r

If we now make the assumption that a fraction A of the energy that is generated within the cylinder is removed by conduction through the cylinder walls, the rest being lost by radiation, the internal energy balance equation can be written as

$$A \times j_m \pi r^2 = - 2\pi r k \frac{\partial T_r}{\partial r} \quad \text{-----} \quad 15.2$$

$$\text{so that } \frac{\partial T_r}{\partial r} = - \frac{A \times j_m r}{2k} \quad \text{-----} \quad 15.3$$

If we integrate this equation, and use the fact that $T_r = T_0$ (the axis temperature) at $r = 0$ to evaluate the constant of integration, we see that T_r is given by

$$T_r = T_0 - \frac{A \times j_m r^2}{4k} \quad \text{-----} \quad 15.4$$

so that the axis temperature T_0 is given by

$$T_0 = T_R + \frac{A i X}{4\pi k} \quad \text{-----} \quad 15.5$$

where T_R is the boundary temperature, and $\pi R^2 j_m$ is the discharge current i . We see from eqn. 15.4 why the parabola model is so called, since the gas temperature is shown to fall off parabolically as we leave the column axis.

Application of the parabola model to the column under study would give us a rough idea of the value of the axis temperature, but we can greatly improve the accuracy of our analysis by allowing for the fact that the current density in the column is not constant, but is a function of the distance from the axis. In the column under study, we know that the current density j has its maximum value j_0 at $r = 0$, and falls to zero as we reach the outer boundary of the column, and we can also assume that $\frac{\partial j}{\partial r}$ is equal to zero at $r = 0$, so that any model that we employ must satisfy these boundary conditions. Ter Horst and Pflanz (1967) have shown that the shape of the temperature profile of a positive column does not depend strongly on the way in which the current density varies within the column, but that the difference between the axis temperature and the boundary temperature does depend on

the way in which the current is distributed throughout the column. For this reason, the author has decided to calculate the axis temperature of the column under study by first setting up a simple model of the current density profile that satisfies the above boundary conditions and gives a reasonably accurate representation of the actual current density profile of the column at a current of about 1 amp, and then applying corrections to allow for the fact that the current distribution in the column varies as the current changes. The basic model that we will use is based on the assumption that

$$j_r = j_0 \left(1 - \frac{r^2}{R^2}\right) \quad \text{-----} \quad 15.6$$

where j_r is the current density at a distance r from the axis, j_0 is the current density at $r = 0$, and R is the column radius.

Before we can discuss the nature of the temperature profile that results from this current distribution, we must obtain two preliminary results. To begin with, we must determine the relationship that exists between the maximum current density j_0 and the mean current density j_m , the latter being the quotient of the discharge current and the column cross sectional area. If the discharge current i is written as $j_m \pi R^2$, we see that j_0 and j_m are related by the equation

$$\int_0^R 2 \pi r j_0 \left(1 - \frac{r^2}{R^2}\right) dr = j_m \pi R^2 \quad \text{-----} \quad 15.7$$

so that $2 \pi j_0 \left(\frac{R^2}{2} - \frac{R^4}{4}\right) = j_m \pi R^2$

and $j_0 = 2 j_m \quad \text{-----} \quad 15.8$

This shows us that the value of the current density at the axis of the column is twice the mean value, a result that only holds for currents of about 1 amp, and which will be discussed in detail later. We must also determine the value of the current i_r that is carried within a cylinder of radius r . This is given by

$$i_r = \int_0^r 2 \pi r j_r dr \quad \text{-----} \quad 15.9$$

so that $i_r = \int_0^r 2 \pi r \cdot 2j_m \left(1 - \frac{r^2}{R^2}\right) dr$

$$= 4 \pi j_m \left(\frac{r^2}{2} - \frac{r^4}{4R^2}\right) \quad \text{-----} \quad 15.10$$

We are now in a position to obtain an expression for the temperature profile of the column. If we again make the assumption that a fraction A of the heat that is produced within a cylinder of radius r is carried out of the cylinder by conduction, the rest being lost by radiation, we can use eqn. 11.8 to show that

$$4 \pi A j_m X \left(\frac{r^2}{2} - \frac{r^4}{4R^2}\right) = -2 \pi r k \frac{\partial T_r}{\partial r} \quad \text{-----} \quad 15.11$$

It follows that $\frac{\partial T_r}{\partial r} = \frac{-2 A j_m X}{k} \left(\frac{r}{2} - \frac{r^3}{4R^2}\right)$

so that $T_r = B - \frac{2 A j_m X}{k} \left(\frac{r^2}{4} - \frac{r^4}{16R^2}\right) \quad \text{-----} \quad 15.12$

Using the boundary condition that $T_r = T_R$ (the boundary temperature) when $r = R$, we see that

$$B = T_R + \frac{3 A j_m X R^2}{8k}$$

so that $T_r = T_R + \frac{3 A j_m X R^2}{8k} - \frac{A j_m X}{k} \left(\frac{r^2}{2} - \frac{r^4}{8R^2}\right) \quad \text{-----} \quad 15.13$

and the axis temperature T_o is therefore given by

$$T_o = T_R + \frac{3 A j_m X R^2}{8k} \quad \text{-----} \quad 15.14$$

If we again substitute i for $\pi j_m R^2$, we see that

$$T_o = T_R + \frac{3 A i \bar{x}}{8 \pi k} \quad \text{-----} \quad 15.15$$

In order to use eqns. 15.13 and 15.15 to calculate the temperature profile of the column under study, we need to know the values of the thermal conductivity of the gas (k), the boundary temperature (T_R), and the fraction of the total energy input that is carried out of the column by thermal conduction (A). Comprehensive data on the value of the thermal conductivity of the rare gases has recently been given by Svehla (1962), and his measured values of k for helium, neon and argon throughout the temperature range 1000 - 3000°K are shown in Table 15.4. It is not quite so easy to obtain accurate estimates of the values of T_R and A , however, so we will carry out our calculations on the assumption that T_R is equal to the ambient temperature T_A , and A is equal to unity. The first assumption means that the temperature drop that occurs at the column boundary in order to maintain the convection heat loss process (see section 11.3) is incorporated in the temperature drop that occurs in order to maintain the flow of heat to the column boundary. With regard to the second assumption, we have seen in Chapter 11 that the nature of the voltage/current characteristic of the column indicates that radiation losses are not as important as conduction losses, so we would expect the value of A to be quite close to unity; the fact that radiation losses are present means that the actual difference between the axis temperature and the boundary temperature will be slightly smaller than the value predicted by eqn. 15.15. We shall discuss the radiation losses in more detail in the next section.

TABLE 15.4

THE THERMAL CONDUCTIVITY OF THE RARE GASES AT ATMOSPHERIC PRESSURE (SVEHLA 1962)

TEMPERATURE(°K)	THERMAL CONDUCTIVITY (JOULES/CM.SEC.DEG.K)		
	HELIUM	NEON	ARGON
1000	3.46×10^{-3}	1.07×10^{-3}	4.10×10^{-4}
1100	3.68×10^{-3}	1.15×10^{-3}	4.36×10^{-4}
1200	3.89×10^{-3}	1.20×10^{-3}	4.60×10^{-4}
1300	4.09×10^{-3}	1.29×10^{-3}	4.85×10^{-4}
1400	4.29×10^{-3}	1.32×10^{-3}	5.09×10^{-4}
1500	4.49×10^{-3}	1.38×10^{-3}	5.33×10^{-4}
1600	4.67×10^{-3}	1.44×10^{-3}	5.56×10^{-4}
1700	4.86×10^{-3}	1.49×10^{-3}	5.73×10^{-4}
1800	5.04×10^{-3}	1.55×10^{-3}	6.00×10^{-4}
1900	5.22×10^{-3}	1.61×10^{-3}	6.22×10^{-4}
2000	5.40×10^{-3}	1.66×10^{-3}	6.43×10^{-4}
2100	5.57×10^{-3}	1.71×10^{-3}	6.64×10^{-4}
2200	5.74×10^{-3}	1.77×10^{-3}	6.85×10^{-4}
2300	5.91×10^{-3}	1.82×10^{-3}	7.05×10^{-4}
2400	6.07×10^{-3}	1.87×10^{-3}	7.24×10^{-4}
2500	6.34×10^{-3}	1.92×10^{-3}	7.43×10^{-4}
2600	6.40×10^{-3}	1.97×10^{-3}	7.62×10^{-4}
2700	6.56×10^{-3}	2.02×10^{-3}	7.82×10^{-4}
2800	6.72×10^{-3}	2.07×10^{-3}	8.00×10^{-4}
2900	6.87×10^{-3}	2.11×10^{-3}	8.20×10^{-4}
3000	7.02×10^{-3}	2.16×10^{-3}	8.36×10^{-4}

As we have already pointed out, the picture of the temperature profile of the column that we have built up in this section is only valid for currents of about 1 amp, since it is based on a model in which the current density falls off as we leave the column axis according to eqn. 15.6, and in which the peak current density j_0 is equal to twice the mean current density j_m . For currents below 1 amp, the current density does not fall off as rapidly as eqn. 15.6 would indicate, and the peak current density is equal to less than twice the mean current density, the ratio $\frac{j_0}{j_m}$ becoming progressively closer to unity as the current falls towards its minimum value. This change in the current density profile results from the fact that the difference between the boundary temperature and the axis temperature decreases as the current falls, thus causing the difference between the boundary values of the electron temperature and degree of ionisation of the seed and the axial values of these quantities to decrease as the current falls. This is easily understood when we recall that the elevation in the electron temperature remains roughly constant as we cross the column, so that the electron temperature profile (on which the current density profile depends) has the same shape as the gas temperature profile. As the current rises above 1 amp, the above argument can be applied in reverse. The difference between the boundary temperature and the axis temperature becomes greater as the current rises, so that the difference between the boundary and axis current densities also becomes greater. This has the effect of concentrating a progressively larger proportion

of the column current into the core of the column, so that the axial value of the current density j_o becomes progressively greater as the current rises, until at a current of about 4 amps, it can be shown to have a value roughly equal to four times the mean current density j_m . Ter Horst and Pflanz (1967) have shown that the effect on the temperature profile of a positive column of concentrating more and more of the current into the column core is to increase the difference between the boundary temperature and the axis temperature, a result that is illustrated by comparing eqns. 15.5 and 15.15. The first of these equations, based on a model in which $j_o = j_m$, shows that $T_o - T_R = \frac{1}{4} \frac{AiX}{\pi k}$, whereas the second, based on a model in which $j_o = 2 j_m$, shows that $T_o - T_R = \frac{3}{8} \frac{AiX}{\pi k}$ - an increase of 50%. This argument shows us that the values of $T_o - T_R$ predicted by eqn. 15.15 will be too large for currents below 1 amp, and too small for currents above 1 amp, so we will obtain more accurate values for $T_o - T_R$ if we apply a correction to eqn. 15.15 in order to allow for the effects discussed above. This has been done in Tables 15.5, 15.6 and 15.7, which show how the axis temperatures of the three columns described in Tables 15.1, 15.2 and 15.3 depend on the discharge current. The first row of each table gives the currents at which the calculation is to be carried out, and the second row gives the values of $T_o - T_R$ that are obtained by substituting the experimental values of the discharge current i and the column electric field X in eqn. 15.15. The value of k was taken to be the thermal conductivity of the diluent gas at a temperature half way between T_R and T_o , thus making the

assumption that the thermal conductivity of a seeded rare gas is simply that of the unseeded rare gas at the same temperature and pressure. The third row gives the values of $T_o - T_R$ that are obtained by allowing for the changing nature of the current density profile. The fourth row gives the values of the axis gas temperature that are obtained by adding the corrected values of $T_o - T_R$ to the boundary temperature, the latter being taken to be equal to the ambient gas temperature (1225°K in all cases). The uncertainty in the final values of $T_o - T_R$ is estimated to be of the order of $\pm 25\%$, and the uncertainty in the value of the axis temperature is estimated to increase from roughly $\pm 100^\circ\text{K}$ at $\frac{1}{4}$ amp to roughly $\pm 400^\circ\text{K}$ at 4 amps.

TABLE 15.5 POTASSIUM-HELIUM

DISCHARGE CURRENT (AMPS)	$\frac{1}{4}$	$\frac{1}{2}$	1	2	4
$T_o - T_R$ (°K) UNCORRECTED	175	280	460	760	1250
$T_o - T_R$ (°K) CORRECTED	140	220	460	880	1500
AXIS GAS TEMPERATURE (°K)	1365	1450	1685	2105	2725

TABLE 15.6 POTASSIUM-NEON

DISCHARGE CURRENT (AMPS)	$\frac{1}{4}$	$\frac{1}{2}$	1	2	4
$T_o - T_R$ ($^{\circ}$ K) UNCORRECTED	170	340	450	740	1100
$T_o - T_R$ ($^{\circ}$ K) CORRECTED	140	280	450	860	1350
AXIS GAS TEMPERATURE ($^{\circ}$ K)	1365	1505	1675	2085	2575

TABLE 15.7 POTASSIUM-ARGON

DISCHARGE CURRENT (AMPS)	$\frac{1}{4}$	$\frac{1}{2}$	1	2	4
$T_o - T_R$ ($^{\circ}$ K) UNCORRECTED	150	250	500	740	1150
$T_o - T_R$ ($^{\circ}$ K) CORRECTED	110	200	500	860	1400
AXIS GAS TEMPERATURE ($^{\circ}$ K)	1335	1425	1725	2085	2625

15.7 THE ELECTRON TEMPERATURE PROFILE OF THE COLUMN.

We are now in a position to discuss the nature of the electron temperature profile of the column under study, and to determine how it depends on the discharge current. To describe the electron temperature profile of the column completely, we need to know two things, namely, the value of the electron temperature at the axis of the column, and the way in which the electron temperature falls off as we leave the axis. Knowledge of the latter can easily be obtained by use of the theory that was developed in the last section, since the fact that the difference between the electron temperature and the gas temperature remains fairly constant as we cross the column means that the shape of the electron temperature profile can be inferred from the shape of the gas temperature profile, so it only remains for us to determine the absolute position of the electron temperature profile, and we will now show that this can also be deduced from results that were obtained in the last section. In section 15.5, we showed that the mean effective value of the electron temperature can be calculated by applying the arc current and ion balance equations to the experimental conductivity results. This entails making the simplifying assumption that the current density, electrical conductivity, degree of seed ionisation and electron temperature are constant within the column, however, and we have seen in the last section that this "channel model" only gives a very approximate picture of the actual conditions inside the column, since the current density has a far higher value at the centre of the column than it has in the peripheral regions.

We have also seen how the value of the axis current density j_0 is higher than the mean current density j_m , the value of the ratio $\frac{j_0}{j_m}$ increasing from just over unity at the lowest currents studied to a value of about 4 at a current of 4 amps. We shall now show that we can use the value of this ratio to estimate the value of the electron temperature at the column axis, since we can use it to deduce the amount by which the degree of seed ionisation at the column core exceeds the mean effective degree of seed ionisation that is obtained by use of the channel model, and having done so, can use the ion balance equation to estimate the amount by which the electron temperature at the column core must exceed the mean effective electron temperature. Study of figure 15.1 shows us that a rise in the electron temperature of roughly 200°K is required to double the degree of seed ionisation in the plasmas under study, so we can infer that the difference between the axis electron temperature T_{eo} and the mean effective electron temperature T_{em} is very approximately given by

$$T_{eo} - T_{em} = 200 \frac{j_0}{j_m} \text{ } ^\circ\text{K} \text{ ----- } 15.16$$

We can therefore obtain an approximate value for the axis electron temperature in a given column by adding the value of $T_{eo} - T_{em}$ that is given by this equation to the value of the mean effective electron temperature that can be deduced by the application of the channel model to the column. The results of this calculation are given in Tables 15.8, 15.9 and 15.10, which respectively describe the potassium-helium, -neon and -argon columns that have previously been

described in Tables 15.1 and 5, 15.2 and 6, and 15.3 and 7. Row 1 of each table gives the values of the current at which the calculation is to be carried out, and Row 2 gives the values of the mean effective electron temperature that were calculated in section 15.5; Row 3 then gives the values of the axis electron temperature that are obtained by the argument given above. It is seen that both the mean effective electron temperature and the axis electron temperature rise as the current increases, but that the latter increase much more rapidly.

TABLE 15.8 POTASSIUM-HELIUM

DISCHARGE CURRENT (AMPS)	$\frac{1}{4}$	$\frac{1}{2}$	1	2	4
MEAN EFFECTIVE ELECTRON TEMPERATURE T_{em} ($^{\circ}$ K)	2650	2700	2730	2750	2780
AXIS ELECTRON TEMPERATURE T_{eo} ($^{\circ}$ K)	2700	2850	2930	3050	3230

TABLE 15.9 POTASSIUM-NEON

DISCHARGE CURRENT (AMPS)	$\frac{1}{4}$	$\frac{1}{2}$	1	2	4
MEAN EFFECTIVE ELECTRON TEMPERATURE T_{em} ($^{\circ}$ K)	2700	2740	2770	2830	2890
AXIS ELECTRON TEMPERATURE T_{eo} ($^{\circ}$ K)	2800	2890	2970	3130	3340

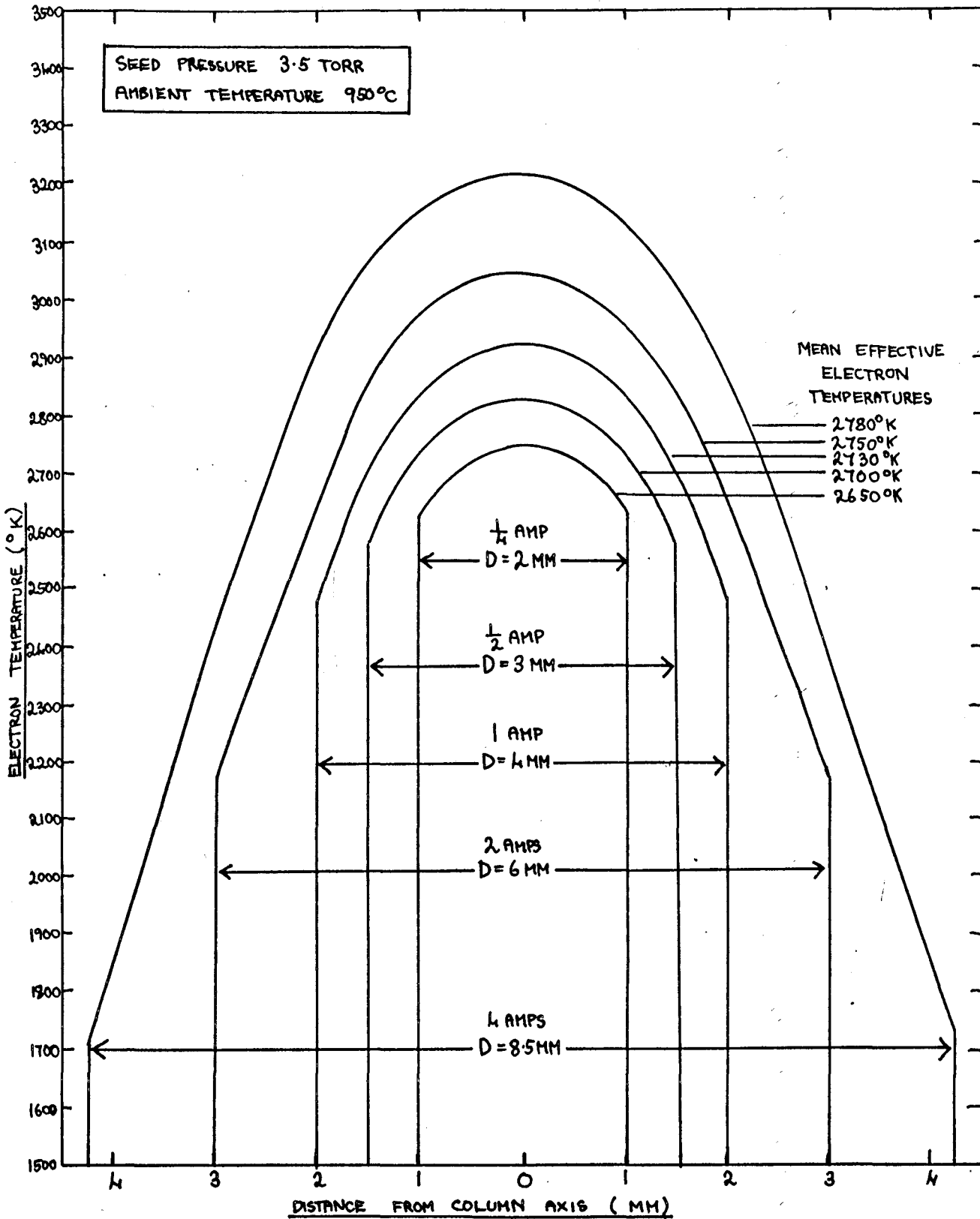
TABLE 15.10 POTASSIUM-ARGON

DISCHARGE CURRENT (AMPS)	$\frac{1}{4}$	$\frac{1}{2}$	1	2	4
MEAN EFFECTIVE ELECTRON TEMPERATURE T_{em} ($^{\circ}$ K)	2700	2740	2770	2840	2890
AXIS ELECTRON TEMPERATURE T_{co} ($^{\circ}$ K)	2800	2890	2970	3140	3340

The potassium-helium results that are given in Table 15.8 are illustrated graphically in Figure 15.2, which shows how the shape of the electron temperature profile depends on the discharge current. In this figure, plots of electron temperature against distance from the column axis are given for currents of $\frac{1}{4}$, $\frac{1}{2}$, 1, 2 and 4 amps, and it is clearly seen how the degree of inhomogeneity of the column increases as the current rises. At a current of $\frac{1}{4}$ amp, the radial variation of the electron temperature is comparatively small, so the conditions in the column approximate to those given by the channel model, with the ratio $\frac{j_o}{j_m}$ being very close to unity. As the current rises and the column expands, however, the difference between the conditions at the core of the column and those in the peripheral regions becomes progressively greater, with the core electron temperature rising well above the mean effective value, and the peripheral electron temperature falling well below the mean effective value. It is clear from this figure why the ratio $\frac{j_o}{j_m}$ increases as the current rises, since a progressively larger proportion of the discharge current has to be carried by the

FIGURE 15.2

ELECTRON TEMPERATURE PROFILES FOR DIFFERENT CURRENTS IN POTASSIUM-HELIUM



column core as the current increases.

Now that we have discussed the nature of the gas temperature and electron temperature profiles of the column, we are in a position to attempt an explanation of one of the most surprising features of the column properties - the fact that the column electric field appears to be virtually independent of the ambient temperature over the temperature range studied (see figures 6.8, 6.9). The results derived in the last two sections show that such an explanation is fairly easy to give for columns where the current is high, since we have seen that most of the current is carried at the core of such columns, and that the core is effectively insulated from the ambient conditions by the peripheral layers of cooler plasma. At very low currents, on the other hand, this explanation is not valid, since the column is thought to become fairly homogeneous in its properties as the minimum current is approached, and we would therefore expect a drop in the ambient temperature to be counteracted by a rise in the column field sufficient to produce a corresponding rise in the elevation of the electron temperature. No such rise is in fact observed until very low temperatures are reached, so we can only postulate that the conducting part of the column plasma is effectively insulated from the ambient conditions even at low current values, or that the tendency for the field to rise slightly is counteracted or masked by other effects that take place as the ambient temperature falls - effects that are not accounted for by the rather approximate analysis that has been carried out in this thesis.

15.8 THE VALUE OF THE DEGREE OF ELEVATION OF THE ELECTRON TEMPERATURE.

To bring this discussion of the basic properties of the column to a satisfactory conclusion, we must now show that the values of the degree of elevation of the electron temperature that are obtained by subtracting the values of the axis gas temperature given in Tables 15.5 - 7 from the values of the axis electron temperature given in Tables 15.8 - 10 are in agreement with the values that are predicted by the electron energy balance equation. Application of the electron energy balance equation (eqn. 12.8) to the column under study is by no means an easy task, however, for although the energy losses from the electron gas by elastic collisions are comparatively easy to calculate, the same is certainly not true for the radiation losses. As has been shown in Chapter 12, the qualitative effect of the latter is to depress the value of the electron temperature by increasing the rate at which the electron gas loses energy to the atoms and ions, but it is extremely difficult even to give a rough estimate of the amount by which they do so. This is partly because the theory that describes the radiation losses is intrinsically very complicated, since it requires a detailed knowledge of the line widths of the various spectral lines (see Section 11.2), but mainly because the theory was developed to describe homogeneous plasmas, and, as we have stressed throughout this discussion, the column under study is certainly not homogeneous. Because of this uncertainty, we cannot use the electron energy balance equation to calculate accurate values for the elevation

of the electron temperature ΔT_e . What we can do, however, is calculate what the value of ΔT_e would be if there were no radiation losses, so that we can regard this as being the upper limit to the value of ΔT_e . Tables 15.11, 12 and 13 show the results of this calculation, respectively dealing with the potassium-helium, -neon and -argon columns that have been discussed throughout this chapter. Row 1 of each table gives the currents at which the calculation is carried out, and Row 2 gives the value of ΔT_e that is obtained by employing eqn. 12.8 and neglecting the radiation loss term. Row 3 of each table then gives the values of the elevation of the electron temperature that are obtained by subtracting the values of the axis gas temperature T_0 (Tables 15.5 - 7) from the values of the axis electron temperature T_{e0} (Tables 15.8 - 10). The uncertainty in the values of $T_{e0} - T_0$ is estimated to be of the order of $\pm 250^\circ\text{K}$, while that in the values of ΔT_e is estimated to be of the order of $\pm 25\%$, not counting the systematic error due to neglecting radiation losses.

TABLE 15.11 POTASSIUM-HELIUM

DISCHARGE CURRENT (AMPS)	$\frac{1}{4}$	$\frac{1}{2}$	1	2	4
ELEVATION IN ELECTRON TEMPERATURE ΔT_e ($^\circ\text{K}$)	1800	1370	1000	770	610
$T_{e0} - T_0$ ($^\circ\text{K}$)	1405	1400	1245	945	505

TABLE 15.12 POTASSIUM-NEON

DISCHARGE CURRENT (AMPS)	$\frac{1}{4}$	$\frac{1}{2}$	1	2	4
ELEVATION IN ELECTRON TEMPERATURE ΔT_e ($^{\circ}$ K)	2600	1900	1350	1000	650
$T_{eo} - T_o$ ($^{\circ}$ K)	1435	1385	1295	1045	765

TABLE 15.13 POTASSIUM-ARGON

DISCHARGE CURRENT (AMPS)	$\frac{1}{4}$	$\frac{1}{2}$	1	2	4
ELEVATION IN ELECTRON TEMPERATURE ΔT_e ($^{\circ}$ K)	2600	1600	1250	950	580
$T_{eo} - T_o$ ($^{\circ}$ K)	1465	1375	1245	1055	615

It is seen that rows 2 and 3 of the tables are in good qualitative agreement in that the values of ΔT_e and $T_{eo} - T_o$ both fall as the discharge current rises. It is also seen that the two sets of values are in quite good quantitative agreement at currents of 1 amp and over, but that the value of ΔT_e becomes considerably higher than the value of $T_{eo} - T_o$ as the current falls to very low values. This suggests that radiation energy losses from the electron gas are quite important at low currents, but that they become progressively less important in comparison with the collision losses as the current rises. This could be due to the fact that the current becomes more and more concentrated in the

column core as the current rises, so that the core becomes insulated from the ambient conditions by layers of cooler plasma as the current rises. The hypothesis that radiation losses are significant at low discharge currents is supported by the fact that the discrepancy between the low-current values of ΔT_e and $T_{co} - T_o$ appears to be considerably smaller for potassium-helium than for the other two mixtures studied. This is to be expected, since the rate of energy transfer from electrons to helium atoms is considerably greater than the rate of energy transfer to argon or neon atoms (see Chapter 17 for more details), so we would expect the proportion of the total electron energy loss rate that takes place by radiation to be less for helium-diluted plasmas than for argon- or neon-diluted plasmas. As we stated earlier in this section, it is virtually impossible to calculate an accurate value for the radiation losses from the electron gas of the column under study, but it can be shown by means of the theory given in Section 11.2 that the radiation losses from the low-current plasmas (which are reasonably homogeneous) are of the correct order of magnitude to explain the discrepancies discussed above. We can therefore conclude that the theory which we have developed in Chapters 10 - 14 is self-consistent, and is capable of explaining the basic features of the column under study within the limits of theoretical and experimental error. We shall now show that the theory is also capable of explaining the effects on the column properties that are produced by changing the nature and proportion of the constituents of the seed-diluent mixture through which the discharge propagates. Chapter 16 will

discuss the dependence of the column properties on the nature and pressure of the seed, and Chapter 17 will discuss their dependence on the nature and pressure of the diluent gas.

CHAPTER 16THE DEPENDENCE OF THE COLUMN PROPERTIES ON THE NATURE
AND PRESSURE OF THE SEED16.1 THE EFFECT ON THE COLUMN PROPERTIES OF CHANGING
THE SEED

We have seen in Chapter 6 that the most obvious effect on the properties of the positive column under study of changing the seed metal is to alter the visible diameter of the column. This indicates that the mean current density in the column undergoes a significant change when the seed is changed. We have also seen that the axial electric field in the column does not appear to depend strongly on the seed metal (figures 6.6, 6.7, 6.9), indicating that this change in the current density must be brought about by a change in the mean electrical conductivity of the column plasma. An idea of how the above quantities depend on the seed metal is given by Table 16.1, which gives typical results for potassium, sodium and caesium in argon, and for potassium and caesium in helium. The seed pressure and gas temperature are respectively 3.5 torr and 950°C in all cases, the argon results being for a current of $\frac{1}{4}$ amp (this being the highest current for which the sodium-seeded discharge was stable), and the helium results being for a current of $\frac{1}{2}$ amp (this being the lowest current for which the caesium-helium discharge was stable).

TABLE 16.1

	COLUMN CROSS SECTIONAL AREA (CM ²)	CURRENT DENSITY (AMPS/CM ²)	AXIAL ELECTRIC FIELDS (VOLTS/CM)	PLASMA ELECTRICAL CONDUCTIVITY (MHOS/CM)
CAESIUM- ARGON	0.02	12	5.5	2.3
POTASSIUM- ARGON	0.05	5	3.4	1.3
SODIUM- ARGON	0.15	1.7	4.9	0.34
CAESIUM- HELIUM	0.04	25	24	1.0
POTASSIUM- HELIUM	0.13	7.5	21	0.36

The experimental error in the conductivity values is high - of the order of $\pm 25\%$ - because of the large absolute error in the positive column diameter values, but the author is confident that the relative values for different mixtures are fairly accurate. We see that caesium-seeded plasmas have a considerably higher electrical conductivity than potassium-seeded plasmas, with sodium-seeded plasmas occupying the lowest place. Let us now see whether this fact is consistent with the theory that we have developed to describe the column.

Equation 14.9 shows that the electrical conductivity of a given mixture is proportional to the product of the electron number density and the electronic mobility, so that both of the

latter quantities must be examined if we are to compare the electrical conductivities of different mixtures. Let us compare the caesium-, potassium-, and sodium-argon columns that are described in Table 16.1. The value of the electronic mobility is proportional to the value of the electronic mean free path λ in the particular mixture, and the value of λ can be calculated using eqn. 14.12, which shows how $\frac{1}{\lambda}$ equals the total electron collision cross section of unit volume of plasma. The contributions to the value of $\frac{1}{\lambda}$ in the three columns under study from diluent atoms, seed atoms and positive ions are shown in Table 16.2, as are the actual values of $\frac{1}{\lambda}$ and λ . Also shown in the table are the values of the electron-heavy body collision time and the electronic mobility for the three mixtures.

TABLE 16.2

	SODIUM- ARGON	POTASSIUM- ARGON	CAESIUM- ARGON
$\frac{1}{\lambda}$ DUE TO DILUENT ATOMS (CM ⁻¹)	450	450	450
$\frac{1}{\lambda}$ DUE TO SEED ATOMS (CM ⁻¹)	250	400	600
$\frac{1}{\lambda}$ DUE TO POSITIVE IONS (CM ⁻¹)	100	400	700
TOTAL $\frac{1}{\lambda}$ (CM ⁻¹)	800	1250	1750
ELECTRONIC MEAN FREE PATH λ (CM)	1.25×10^{-3}	8.0×10^{-4}	5.7×10^{-4}

TABLE 16.2 (continued).

	SODIUM - ARGON	POTASSIUM- ARGON	CAESIUM- ARGON
ELECTRON - HEAVY BODY COLLISION TIME (SEC)	3.3×10^{-11}	2.1×10^{-11}	1.5×10^{-11}
ELECTRONIC MOBILITY CM SEC ⁻¹ /VOLT CM ⁻¹	5.8×10^4	3.7×10^4	2.6×10^4

From the table, we see that the mobilities in the three mixtures are in the ratio

$$\begin{array}{ccc} \text{Na/Ar} & & \text{K/Ar} & & \text{Cs/Ar} \\ 1.56 & : & 1 & : & 0.71 \end{array}$$

Let us now calculate the difference between the mean electron number density values in the three mixtures. Using the theory developed in Chapters 10 - 14, we can show that the electron temperature in the column plasma depends mainly on the discharge current and seed pressure, and is practically independent of the choice of seed. We have seen that the positive column field that is needed to support a given current does not depend strongly on the seed chosen (see Chapter 6), so it follows that the degree of elevation of the electron temperature (calculated using the electron energy balance equation) is also virtually independent of the seed. The observation that the column field values with caesium as seed are all slightly higher than the corresponding values with potassium as seed (see figures in Chapter 6) is explained by the fact that the electronic mobility is lower with caesium than with potassium, thus necessitating a slightly higher

electric field to produce a given elevation in the electron temperature. Since we can also show that the gas temperature in the column is practically independent of the seed chosen, it follows that the mean electron temperature does not change much if the seed is changed. It is apparent, however, that the degree of ionisation of the seed that is produced by this electron temperature does depend on the choice of seed, this being a consequence of the fact that the three seeds used have different ionisation potentials. We see from eqn. 13.1 that the values of the degree of ionisation of the seed and the electron number density in the three mixtures should be roughly proportional to the values of the quantity $\exp\left(-\frac{eV_i}{2kT_e}\right)$ for the three mixtures, e , V_i , k and T_e being respectively the electronic charge, the ionisation potential of the seed, Boltzmann's constant, and the electron temperature. Now the values of V_i for the three seeds are as follows.

Na	K	Cs
5.09V	4.32V	3.86V

If we take T_e to be roughly 2700°K in all cases, we see that the values of $\frac{eV_i}{2kT_e}$ are as follows:

Na/Ar	K/Ar	Cs/Ar
11.0	9.3	8.3

Thus, the electron number densities in the three mixtures should be in the ratio

Na/Ar	:	K/Ar	:	Cs/Ar
0.19	:	1	:	2.6

From the above electron number density ratios and from the mobility ratios given earlier, we see that the electrical conductivity values in the three mixtures should be in the ratio

$$\begin{array}{ccc} \text{Na/Ar} & & \text{K/Ar} & & \text{Cs/Ar} \\ 0.29 & : & 1 & : & 1.85 \end{array}$$

while study of Table 16.1 shows that the measured conductivity values are in fact in the ratio

$$\begin{array}{ccc} \text{Na/Ar} & & \text{K/Ar} & & \text{Cs/Ar} \\ 0.26 & : & 1 & : & 1.77 \end{array}$$

Thus, we see that agreement between theory and experiment is good - certainly well within the limits of experimental and theoretical error, both of which are of the order of $\pm 25\%$. The same good agreement between theory and experiment can be shown for caesium and potassium in helium, when repetition of the above argument leads to the following result for a positive column carrying $\frac{1}{2}$ amp:

Theoretical ratio of electrical conductivities

$$\begin{array}{ccc} \text{K/He} & & \text{Cs/He} \\ 1 & : & 2.6 \end{array}$$

Experimental ratio of electrical conductivities

$$\begin{array}{ccc} \text{K/He} & & \text{Cs/He} \\ 1 & : & 2.75 \end{array}$$

We can therefore conclude that the theory which we have developed to describe the column is capable of giving a satisfactory explanation of the changes that occur when the seed metal is changed. We shall now see whether the theory can also explain the experimental seed pressure - dependent results that were given in Chapter 6, but before we give a detailed discussion

of the column under study, we shall examine the concept of the "optimum seeding fraction" as applied to seeded plasmas, and will try to determine why such an optimum seeding fraction should exist.

16.2 THE OPTIMUM SEEDING FRACTION IN EQUILIBRIUM PLASMAS

If M.H.D. generators employing alkali-metal-seeded rare gases as the working fluid ever became economically feasible, then the cost of the seed metal is likely to constitute a significant proportion of the total running cost. For this reason, it will be essential to operate at the lowest seed pressure consistent with the required plasma conductivity, so that knowledge of the optimum seeding fraction is likely to be of practical importance as well as being of intrinsic scientific interest. The optimum seeding fraction of an alkali-metal-seeded plasma is defined as the ratio of seed pressure to diluent pressure that produces the maximum value of the electrical conductivity of the plasma. If the total pressure is fixed and the seed pressure is small compared with the diluent pressure, as it is in all the cases studied, the optimum seeding fraction is often expressed as an optimum seed pressure, since it is the seed pressure which is in fact varied. Calculation of the optimum seeding fraction of the type of non-equilibrium plasma under study is a very difficult task, but the calculation is relatively straightforward for an equilibrium plasma for which the degree of ionisation is low. Let us derive the formula for the optimum seeding fraction in such a plasma, and then see how the argument has to be modified to deal with the more complicated case of a nonequilibrium plasma.

We have seen in Chapter 14 how the electrical conductivity of a plasma is proportional to the product of the electron number density and the electronic mobility. The basic reason for the existence of an optimum seed pressure in a seeded plasma is that the electron number density tends to increase as the seed pressure rises, while the electronic mobility tends to decrease, so that the electrical conductivity passes through a maximum value at the seed pressure at which these conflicting tendencies cancel one another out and produce a turning point in the plot of conductivity against seed pressure p_s . In an equilibrium plasma, the electron temperature is equal to the gas temperature, and if the latter remains constant, the degree of ionisation of the seed is proportional to $\frac{1}{p_s}^{1/2}$ (see eqn. 13.1). Since the electron number density is proportional to the product of the seed pressure and the degree of ionisation of the seed, it follows that the electron number density in the plasma is proportional to $p_s^{1/2}$, and increases as the seed pressure rises. The electronic mobility, on the other hand, is proportional to the electronic mean free path (see eqns. 14.8, 14.10), and is inversely proportional to the sum of the various electron scattering terms (see eqn. 14.12). In an equilibrium plasma where the electron number density is low enough for the ion-scattering term in eqn. 14.12 to be small compared with the other two terms, we see that the electronic mobility is proportional to $\frac{1}{p_s a_s + p_d a_d}$, where p_s , p_d , a_s and a_d are respectively the pressures and electron collision cross sections of seed and diluent. Taking the product of the electron

number density and the electronic mobility, we see that the conductivity σ is proportional to

$$\frac{p_s^{1/2}}{p_s^{a_s} + p_d^{a_d}} \quad \text{-----} \quad 16.1$$

To obtain the optimum seed pressure, we differentiate this expression with respect to p_s , and equate the result to zero (Zimin and Popov 1964, Rosa 1961, Frost 1961). If this is done, we see that

$$\frac{(p_s^{a_s} + p_d^{a_d}) \frac{1}{2p_s^{1/2}} - a_s p_s^{1/2}}{(p_s^{a_s} + p_d^{a_d})^2} = 0$$

$$\therefore \frac{(p_s^{a_s} + p_d^{a_d}) - 2 p_s^{a_s}}{(p_s^{a_s} + p_d^{a_d})^2} = 0$$

We see that the optimum seed pressure is obtained when the numerator of this expression vanishes, i.e. when

$$p_s^{a_s} = p_d^{a_d} \quad \text{-----} \quad 16.2$$

Thus, the optimum seeding fraction for equilibrium plasmas where the electron number density is small is given by

$$\frac{p_s}{p_d} = \frac{a_d}{a_s} \quad \text{-----} \quad 16.3$$

and the optimum seed pressure is given by

$$p_s \text{ opt.} = p_d \cdot \frac{a_d}{a_s} \quad \text{-----} \quad 16.4$$

It must be noted that this equation is only valid for situations where the electron number density in the plasma is low enough for the ion scattering term in eqn. 14.12 to be small compared with

the other terms, and for such plasmas, it has been verified experimentally by Harris (1963 A,B). When the ion scattering term does become comparable with the other terms in eqn. 14.12, its effect will be to increase the optimum seed pressure, since the seed pressure will have to reach a higher value before the seed-dependent term in the expression for the electron mean free path becomes equal to the sum of the other terms. This effect is discussed in greater detail by Smith and Shair (1966).

16.3 THE OPTIMUM SEEDING FRACTION IN NONEQUILIBRIUM PLASMAS

Until a few years ago, it was generally believed that the simple equilibrium formula for the optimum seeding fraction (eqn. 16.3) would also be valid for nonequilibrium plasmas, or that the formula would at least be approximately true. When experimental investigations of the effect on the properties of nonequilibrium plasmas of varying the seed pressure were carried out, however, it was found that the formula was not even approximately valid, and that the optimum seed pressure values in nonequilibrium plasmas were about an order of magnitude below the corresponding equilibrium values. The first experimental results to show this effect were published by the author (Ellington 1965 A,B,C), and corroborative results by Labois and Ricateau (1965) and Evans (1967) soon followed. The optimum seed pressures observed by the author in the various atmospheric-pressure mixtures studied by him are given in Table 16.3, the caesium-argon result given in the table being in good agreement with that produced by the other workers

cited above (who only studied caesium-argon plasmas). The equilibrium optimum seed pressures that are obtained from eqn. 16.2 are also shown in the table

TABLE 16.3

MIXTURE	EXPERIMENTAL OPTIMUM SEED PRESSURE MEASURED BY AUTHOR (TORR)	THEORETICAL OPTIMUM SEED PRESSURE FOR EQUILIBRIUM PLASMAS (TORR)
CAESIUM-ARGON	$0.15 \pm 50\%$	$1.5 \pm 25\%$
POTASSIUM-ARGON	$0.2 \pm 50\%$	$2.3 \pm 25\%$
CAESIUM-HELIUM	$1.5 \pm 50\%$	$15 \pm 25\%$
POTASSIUM-HELIUM	$2.0 \pm 50\%$	$23 \pm 25\%$

Let us now attempt to explain the discrepancy between the two sets of figures given in Table 16.3. The basic reason for the difference between the equilibrium and nonequilibrium cases is that the degree of seed ionisation in an equilibrium plasma depends on the gas temperature, which is independent of the seed pressure, whereas the degree of seed ionisation in a nonequilibrium plasma depends on the electron temperature, which does depend on the seed pressure, tending to fall as the seed pressure reaches high values. The fact that the degree of ionisation of the seed depends exponentially on the electron temperature means that the conductivity will be far more sensitive to changes in the electronic mean free path than in the equilibrium case. As the value of the electronic mean free path falls with rising seed pressure, the value of the plasma electric field required to maintain a

given electron temperature will tend to rise (see Chapter 12), and the effect of this additional factor will be to lower the pressure at which the drop in electronic mean free path with increasing seed pressure begins to affect the conductivity. This will tend to lower the optimum seed pressure in nonequilibrium plasmas compared with that in equilibrium plasmas. An idea of the dependence of the electronic mean free path on the seed pressure can be obtained from figure 9.1, which shows the reciprocal of the electronic mean free path plotted against seed pressure for potassium in helium, neon and argon. The curves in this figure were computed for zero ion number density, only the seed- and diluent- scattering terms in eqn. 14.12 being used, but the addition of the ion-scattering term does not greatly alter the nature of the curves, merely increasing the value of $\frac{1}{\lambda}$ slightly. We see that $\frac{1}{\lambda}$ is virtually independent of the seed pressure at low seed pressures, but rises sharply at high seed pressures. In addition, we see that the seed pressure begins to affect the value of λ at a much lower pressure with argon as diluent than with helium as diluent, neon occupying an intermediate position. This gives a qualitative explanation of why the optimum seed pressure is lower with argon as the diluent gas than it is with helium as the diluent gas, and it is seen that the optimum seed pressures given in Table 16.3 for potassium-seeded plasmas correspond roughly to the pressures at which the value of λ begins to be noticeably affected by the rising seed pressure.

Shortly after the author published the results given in Table 16.3, Smith and Shair (1966) developed a theory that succeeded in giving a quantitative explanation of the difference between the optimum seeding fractions of equilibrium and nonequilibrium plasmas - a theory that proved to be in excellent agreement with the author's results. They repeated the argument given in section 16.2, allowing for the fact that the degree of ionisation of the seed is exponentially dependent on the electron temperature and also for the fact that the latter tends to fall as the seed pressure rises, and showed that the simple equilibrium formula for the optimum seeding fraction has to be modified when non-equilibrium conditions prevail. For plasmas where the ion number density is not high enough for the ion-scattering term in eqn. 14.12 to dominate the expression for the electronic mean free path, they showed that the expression for the optimum seeding fraction becomes approximately

$$\frac{P_s}{P_d} = \frac{a_d}{a_s} \cdot \frac{2 - \frac{T_g}{T_e}}{1 + 2\left(1 - \frac{T_g}{T_e}\right) \left(1 + \frac{eV_i}{kT_e}\right)} \quad \text{--- 16.5}$$

where T_g and T_e are the electron and gas temperatures, eV_i is the ionisation energy of the seed, and k is Boltzmann's constant. It is seen that eqn. 16.5 reduces to eqn. 16.3 when $T_e = T_g$, i.e., under equilibrium conditions. Eqn. 16.5 has been used to calculate the theoretical optimum seed pressures for the four mixtures described in figure 6.6 and Table 16.3, and the results of the calculation are compared with the author's experimental

optimum seed pressures in Table 16.4. The electron temperature was taken to be 2700°K in all cases, and the ratio $\frac{T_g}{T_e}$ was taken to be $\frac{1}{2}$. It is seen that the theoretical values of the optimum seed pressure are in excellent agreement with the experimental values. The 50% error in the theoretical figures is made up of a 25% error in the ratio $\frac{a_d}{a_s}$ (due to uncertainty in the electron collision cross section values), and an estimated 25% error in the multiplying factor derived by Smith and Shair.

TABLE 16.4

MIXTURE	EXPERIMENTAL OPTIMUM SEED PRESSURE MEASURED BY AUTHOR (TORR)	THEORETICAL OPTIMUM SEED PRESSURE FOR NONEQUILIBRIUM PLASMAS (TORR)
CAESIUM-ARGON	0.15 ± 50%	0.12 ± 50%
POTASSIUM-ARGON	0.2 ± 50%	0.17 ± 50%
CAESIUM-HELIUM	1.5 ± 50%	1.2 ± 50%
POTASSIUM-HELIUM	2.0 ± 50%	1.7 ± 50%

16.4 THE EFFECTS ON THE COLUMN PROPERTIES OF VARYING THE SEED PRESSURE.

Having shown why an optimum seed pressure exists in seeded plasmas and why the optimum seed pressures in homogeneous non-equilibrium plasmas are lower than those in equilibrium plasmas, let us now attempt to perform a quantitative analysis of some of the seed pressure-dependent results that were given in Chapter 6, namely, the potassium-argon and potassium-helium results that are shown in figure 6.6. We have seen that there are two fundamental

results that are observed when the seed pressure is raised from very low to very high values. The first is that the column electric field required to support a given current passes through a minimum value, while the second is that the column cross sectional area needed to carry a given current does not appear to vary greatly. Two further results follow from these basic observations, namely, that the minimum column field mentioned above corresponds to a maximum value of the plasma conductivity, and that the degree of ionisation of the seed must vary considerably over the seed pressure range studied. We have shown in the last section that the values of the optimum seed pressure that have been observed experimentally are in agreement with the values that are predicted by the latest theory, and we will now show that the observed dependence of the electrical conductivity on the seed pressure is consistent with the theory that we have developed to describe the column under study.

We shall begin our analysis by calculating the values of the mean electron number density and the degree of ionisation of the seed throughout the pressure range studied. The results of this calculation are shown in Tables 16.5 and 16.6 for the potassium-argon and potassium-helium results given in figure 6.6, the discharge current being $\frac{1}{2}$ amp in both cases. Each table begins by giving the seed pressure values at which the calculation is to be carried out (column 1), followed by the electrical conductivity values (column 2), the latter being calculated from the measured values of the mean current density and column field. Columns

3 and 4 give the values of the reciprocal of the electronic mean free path and the electronic mobility, calculated using the theory given in Chapter 14. Column 5 gives the values of the mean electron number density in the plasma, these being calculated from the conductivity and mobility values using the arc current equation (eqn. 14.9). From the electron number density values and the seed pressure values, the degree of ionisation of the seed can immediately be deduced, and is given in column 6. The results of this calculation are extremely interesting. In the potassium-argon case, the electron number density varies from roughly $1.6 \times 10^{14} \text{ cm}^{-3}$ at 0.02 torr to roughly $7 \times 10^{14} \text{ cm}^{-3}$ at 40 torr, so that the electron number density has only increased by a factor of about 4 while the seed pressure has increased by a factor of 2000. This, of course, means that the degree of ionisation of the seed has to vary by an enormous amount, varying from almost 100% at the lowest seed pressures studied to roughly 0.3% at the highest. With potassium-helium, the same is true, the electron number density increasing from roughly $2.4 \times 10^{14} \text{ cm}^{-3}$ to roughly $3.7 \times 10^{14} \text{ cm}^{-3}$ while the seed pressure increases by a factor of 400 from 0.1 to 40 torr; this means that the degree of ionisation varies from roughly 40% to roughly 0.2%. We see from these results that the column accommodates changes in the seed pressure by varying the degree of ionisation of the seed and keeping the column size roughly the same rather than by varying the column size and keeping the degree of ionisation roughly constant. This is a fundamental result, and the author believes that it can be

explained by employing the theory that was developed in Chapter 15 to explain the constriction of the column. In that chapter, it was shown that the column adjusts its size so that the electron number density is at the optimum value for the particular mixture, current and conditions, the optimum value of the electron number density being that at which the column electric field needed to maintain the discharge is a minimum. Furthermore, it was shown that the optimum electron number density and current density appear to occur when the rate of electron scattering by positive ions becomes roughly comparable with the rate at which electrons are scattered by the other species present (seed and diluent atoms). As a consequence of this, the optimum electron number density occurs in the range $10^{14} - 10^{15} \text{ cm}^{-3}$, the actual value depending on the mixture and the current. This explains why the electron number density does not change much throughout the seed pressure range investigated, since it appears that the stable configuration of the column is determined by the value of the electron number density rather than by the degree of ionisation of the seed. The fact that the electron number density does show a slow systematic increase with rising seed pressure is entirely consistent with the theory given above: as the seed pressure rises and the value of $\frac{1}{\lambda}$ increases, the value of the electron number density needed to make the ion-scattering term in the expression for $\frac{1}{\lambda}$ comparable in size with the sum of the other terms will also rise. It must be stressed at this point that the values of the various quantities shown in Tables 16.5 and 16.6 are very approximate indeed, since

the experimental and theoretical errors are quite high, but they do give a clear indication of how the column properties depend on the seed pressure.

Having calculated how the degree of ionisation of the seed varies with changing seed pressure, we can now use the ion balance equation to calculate the value of the electron temperature at the various pressures. The results of this calculation are shown in Column 7 of the tables. It is seen that the electron temperature is very high at low seed pressures, but that it falls steadily as the seed pressure rises, levelling out at about 2500°K. Study of the variation of the electron temperature and the electronic mobility throughout the pressure range shows why a minimum value of the column field occurs. As the seed pressure reaches very low values, the fairly rapid rate of increase of the electron temperature means that the field has to increase in order to produce the required elevation in the electron temperature. As the pressure reaches very high values, on the other hand, the fact that the electronic mobility falls fairly rapidly means that the field has again got to rise in order to produce the required elevation in the electron temperature. Use of the electron energy balance equation to give a quantitative prediction of how the column field should vary throughout the seed pressure range of interest is rendered impracticable by the high degree of uncertainty in the various quantities involved in the calculation, however. All that can be concluded from such a calculation (which was attempted by the author) is that the observed

variation of the column field with changing seed pressure is qualitatively in agreement with the theory, and that the seed pressures at which the minimum values of the calculated field occur are in good agreement with the experimental optimum seed pressures and the theoretical optimum seed pressures calculated using the theory of Smith and Shair (see Table 16.4).

TABLE 16.5

TOTAL PRESSURE 1 ATMOSPHERE

DILUENT : ARGON

SEED : POTASSIUM

DISCHARGE CURRENT 0.5 AMPS

<u>COLUMN 1</u>	SEED PRESSURE (TORR)
<u>COLUMN 2</u>	EXPERIMENTAL ELECTRICAL CONDUCTIVITY (MHOS/CM)
<u>COLUMN 3</u>	RECIPROCAL OF ELECTRONIC MEAN FREE PATH (CM ⁻¹)
<u>COLUMN 4</u>	ELECTRONIC MOBILITY (CM SEC ⁻¹ /VOLT CM ⁻¹)
<u>COLUMN 5</u>	ELECTRON NUMBER DENSITY (CM ⁻³)
<u>COLUMN 6</u>	DEGREE OF IONISATION OF SEED
<u>COLUMN 7</u>	ELECTRON TEMPERATURE (°K)

<u>1.</u>	<u>2.</u>	<u>3.</u>	<u>4.</u>	<u>5.</u>	<u>6.</u>	<u>7.</u>
0.02	1.5	680	6.8 x 10 ⁴	1.6 x 10 ¹⁴	98%	3500
0.04	1.85	740	6.2 x 10 ⁴	2.2 x 10 ¹⁴	87%	3300
0.1	2.25	800	5.8 x 10 ⁴	2.4 x 10 ¹⁴	38%	3200
0.2	2.5	870	5.4 x 10 ⁴	3.1 x 10 ¹⁴	24%	3100
0.4	2.5	900	5.2 x 10 ⁴	3.6 x 10 ¹⁴	14%	3000
0.8	2.25	950	4.9 x 10 ⁴	3.6 x 10 ¹⁴	6.8%	2900
1.6	2.1	1050	4.4 x 10 ⁴	3.6 x 10 ¹⁴	3.2%	2800
3.5	1.8	1250	3.7 x 10 ⁴	3.6 x 10 ¹⁴	1.6%	2700
7	1.35	1650	2.8 x 10 ⁴	3.6 x 10 ¹⁴	0.8%	2630
14	1.18	2500	1.8 x 10 ⁴	4.6 x 10 ¹⁴	0.5%	2550
28	0.86	4250	1.1 x 10 ⁴	5.9 x 10 ¹⁴	0.33%	2500
40	0.76	5900	0.8 x 10 ⁴	7.1 x 10 ¹⁴	0.28%	2500

TABLE 16.6

TOTAL PRESSURE 1 ATMOSPHERE

DILUENT : HELIUM

SEED : POTASSIUM

DISCHARGE CURRENT 0.5 AMPS

<u>COLUMN 1</u>	SEED PRESSURE (TORR)
<u>COLUMN 2</u>	EXPERIMENTAL ELECTRICAL CONDUCTIVITY (MHOS/CM)
<u>COLUMN 3</u>	RECIPROCAL OF ELECTRONIC MEAN FREE PATH (CM ⁻¹)
<u>COLUMN 4</u>	ELECTRONIC MOBILITY (CM SEC ⁻¹ /VOLT CM ⁻¹)
<u>COLUMN 5</u>	ELECTRON NUMBER DENSITY (CM ⁻³)
<u>COLUMN 6</u>	DEGREE OF IONISATION OF SEED
<u>COLUMN 7</u>	ELECTRON TEMPERATURE (°K)

<u>1.</u>	<u>2.</u>	<u>3.</u>	<u>4.</u>	<u>5.</u>	<u>6.</u>	<u>7.</u>
0.1	0.27	4910	9.4 x 10 ⁴	2.4	43%	3200
0.2	0.3	4920	9.4 x 10 ⁴	2.7	24%	3100
0.4	0.33	4940	9.4 x 10 ⁴	3.1	14%	3000
0.8	0.35	4980	9.35 x 10 ⁴	3.1	7%	2870
1	0.35	5000	9.3 x 10 ⁴	2.74	5%	2800
2	0.355	5100	9.1 x 10 ⁴	2.84	2.5%	2720
4	0.35	5300	8.7 x 10 ⁴	2.9	1.3%	2650
8	0.33	5700	8.2 x 10 ⁴	2.94	0.66%	2530
10	0.325	5900	7.9 x 10 ⁴	3.0	0.54%	2550
20	0.3	6900	6.7 x 10 ⁴	3.25	0.29%	2500
40	0.27	8900	5.2 x 10 ⁴	3.75	0.2%	2450

CHAPTER 17THE DEPENDENCE OF THE COLUMN PROPERTIES ON THE
NATURE AND PRESSURE OF THE DILUENT GAS17.1 THE EFFECT OF THE CHOICE OF DILUENT ON THE COLUMN
PROPERTIES : PRELIMINARY DISCUSSION.

One of the most striking features of the experimental results that are described in Chapter 6 is the strong dependence of the positive column electric field on the choice of diluent gas. When neon or helium replace argon as the diluent, the other experimental conditions being kept constant, the general appearance and size of the column do not appear to alter greatly, but the value of the column field that is required to support a given current rises by a considerable amount. This is illustrated in Table 17.1, which shows how the column diameter, mean current density, column field, and mean plasma conductivity depend on the diluent gas for a current of 1 amp and a seed pressure of 3.5 torr in potassium-helium, -neon and -argon.

TABLE 17.1

	COLUMN CROSS SECTIONAL AREA (CM ²)	MEAN CURRENT DENSITY (AMPS/CM ²)	COLUMN ELECTRIC FIELD (VOLTS/CM)	MEAN PLASMA CONDUCTIVITY (MHOS/CM)
POTASSIUM- HELIUM	4.0	7.3	18.0	0.4
POTASSIUM- NEON	4.0	7.0	5.5	1.2
POTASSIUM- ARGON	5.0	5.0	2.5	2.0

We see that a far higher energy input rate is required to support a given current in potassium-helium than in potassium-neon, which in turn requires a higher input rate than potassium-argon, and we must now determine whether or not this result is consistent with the theory that has been developed to describe the column.

The basic reason why helium- and neon-diluted plasmas require a higher energy input rate to support a given current than argon-diluted plasmas is that it is considerably more difficult to produce a high electron temperature in these mixtures, and we have seen in Chapters 12, 13 and 15 that a mean effective electron temperature of at least 2500°K is required before the existence of a nonequilibrium column of the type under study becomes possible. Below this temperature, the electron number density becomes too low for the electron gas to have a proper Maxwellian energy distribution, and the nonequilibrium ionisation mechanism becomes ineffective because of the lack of high-energy electrons. It follows from this argument that the mean electron temperature in the column plasma must not be allowed to fall below 2500°K when helium or neon replace argon as the diluent gas. Now we have seen that the electron temperature in the column under study is considerably higher than the gas temperature, and that the difference between the two is determined by balancing the rate at which the electron gas receives energy from the applied field with the rate at which it loses this energy to the atomic gas by collisions. But helium and neon have higher electron collision

cross sections than argon (see Table 14.1), and also have lower atomic weights, so that an electron has a greater probability of hitting a helium or a neon atom than an argon atom, and loses more energy when it does so, since the efficiency of energy transfer in an elastic electron-atom collision increases as the mass of the atom involved falls. For this reason, helium- and neon-diluted plasmas require a higher energy input rate to maintain a given elevation of the electron temperature than argon-diluted plasmas, and the fact that helium and neon have higher thermal conductivities than argon (see Table 15.4) means that the column can support this higher energy input rate without an increase in the gas temperature. Let us discuss this in more detail.

17.2 THE EFFECT ON THE ELECTRON ENERGY BALANCE PROCESS OF CHANGING THE DILUENT.

If we neglect radiation losses, the electron energy balance equation (eqn. 12.8) shows us that the degree of elevation of the electron temperature in the type of plasma under study is roughly proportional to

$$X^2 / \lambda^2 M \quad \text{-----} \quad 17.1$$

where X is the electric field, λ is the electronic mean free path, and M is the average mass of the atoms encountered by electrons. The value of λ is given by eqn. 14.12, and is easily calculated from the number densities and electron collision cross sections of the various species present, and we shall now show that the value of M can also be deduced from these values. If pr_i is the

probability of a given electron-atom collision being with a member of the i 'th species, the average mass M is clearly given by

$$M = \sum_i M_i pr_i \quad \text{-----} \quad 17.2$$

where M_i is the mass of the i 'th species. But pr_i is obviously equal to the fraction of collisions that occur with members of the i 'th species, so that

$$pr_i = \frac{n_i a_i}{\sum_i n_i a_i} \quad \text{-----} \quad 17.3$$

where n_i and a_i are the number density and electron collision cross section of the i 'th species. Thus, we conclude that

$$M = \frac{\sum_i n_i a_i M_i}{\sum_i n_i a_i} \quad \text{-----} \quad 17.4$$

Having obtained this result, we are in a position to attempt a quantitative explanation of the differences between the three columns that were described in Table 17.1. As in our discussion of the effect of changing the seed metal (section 16.1), we shall begin by comparing the microscopic properties of the plasmas in the three columns, since this will enable us to compare the values of the electronic mobility in the columns. This is done in Table 17.2, which shows the contributions to the value of $\frac{1}{\lambda}$ in the three columns under study from diluent atoms, seed atoms and positive ions, and then gives the actual values of $\frac{1}{\lambda}$ and λ . The next two rows give the values of the electron-heavy body collision time and the electronic mobility, and the last row gives the values of the average heavy body mass M that are given by eqn. 17.4.

TABLE 17.2

	POTASSIUM- HELIUM	POTASSIUM- NEON	POTASSIUM- ARGON
$\frac{1}{\lambda}$ DUE TO DILUENT ATOMS (CM^{-1})	4500	1350	450
$\frac{1}{\lambda}$ DUE TO SEED ATOMS (CM^{-1})	400	400	400
$\frac{1}{\lambda}$ DUE TO POSITIVE IONS (CM^{-1})	400	400	400
TOTAL $\frac{1}{\lambda}$ (CM^{-1})	5300	2150	1250
ELECTRONIC MEAN FREE PATH (CM)	1.89×10^{-4}	4.65×10^{-4}	8.0×10^{-4}
ELECTRON - HEAVY BODY COLLISION TIME (SEC)	4.95×10^{-12}	1.22×10^{-11}	2.1×10^{-11}
ELECTRONIC MOBILITY $\text{CM} \cdot \text{SEC}^{-1} / \text{VOLT} \cdot \text{CM}^{-1}$	8.75×10^3	2.15×10^4	3.7×10^4
AVERAGE HEAVY BODY MASS M (A.M.U.)	9.4	27.5	40

Examination of the table shows that the electronic mobility is about four times as high in potassium-argon as in potassium-helium, and about twice as high as in potassium-neon. If we now compare the experimental plots of mean plasma electrical conductivity against

discharge current that were given for the three mixtures in Figure 6.4, we see that the value of the electrical conductivity at a given current in potassium-argon is about four times as high as in potassium-helium and about twice as high as in potassium-neon throughout the current range studied. Thus, making use of the form of the arc current equation which states that the conductivity is proportional to the product of the electronic mobility and the electron number density, we can infer that the electron number density at a given current has approximately the same value for all three mixtures (this is illustrated in Tables 15.1, 2 and 3). Since the seed pressure is the same in all three cases, we can deduce that the degree of ionisation is also the same, and can therefore conclude (via the ion balance equation) that the mean effective electron temperature is virtually the same for a given current in each of the three mixtures (again see Tables 15.1, 2 and 3). But we can use the energy balance equation to show that the gas temperature profile of the column is also practically independent of the nature of the diluent (see Tables 15.5, 6 and 7), so we can infer that the degree of elevation of the electron temperature remains roughly constant when we change the diluent, and can therefore conclude that the value of the function $X^2 \lambda^2 M$ must also remain constant. It follows from this argument that the value of the electric field required to support a given current should be roughly inversely proportional to the value of $\lambda \sqrt{M}$ for the particular mixture. Let us see whether this is in fact the case for the mixtures under study.

Using the data given in Table 17.2, we see that the values of $\frac{1}{\lambda\sqrt{M}}$ in the three mixtures studied are in the ratio

$$\begin{array}{ccc} \text{K/Ar} & & \text{K/Ne} & & \text{K/He} \\ 1 & : & 2.1 & : & 8.4 \end{array}$$

while study of Figure 6.1 shows that the average ratios of the experimental column fields in the three mixtures are

$$\begin{array}{ccc} \text{K/Ar} & & \text{K/Ne} & & \text{K/He} \\ 1 & : & 2.2 & : & 7.4 \end{array}$$

The uncertainty in both the above sets of ratios is estimated to be of the order of $\pm 20\%$, so we see that there appears to be excellent agreement between theory and experiment over the matter of changing the diluent. If the same comparison is made for the caesium-argon and caesium-helium results that are described in Figures 6.1 - 6.4, we again find that good agreement between theory and experiment is obtained. In this case, the values of $\frac{1}{\lambda\sqrt{M}}$ are in the ratio

$$\begin{array}{ccc} \text{Cs/Ar} & & \text{Cs/He} \\ 1 & : & 6.5 \end{array}$$

while Figure 6.1 shows that the average experiment ratio of the column fields is

$$\begin{array}{ccc} \text{Cs/Ar} & & \text{Cs/He} \\ 1 & : & 5.7 \end{array}$$

17.3 THE DEPENDENCE OF $\frac{\chi_{\text{He}}}{\chi_{\text{Ar}}}$ ON THE SEED PRESSURE.

So far, we have considered the effect of changing the diluent at a single seed pressure, namely, 3.5 torr. Reference to the seed pressure-dependent results given in Figure 6.6, however, shows

that the ratio of the electric field needed to support a given current in a helium-diluted mixture to that needed to support the same current in an argon-diluted mixture ($\frac{\lambda_{He}}{\lambda_{Ar}}$) varies considerably over the seed pressure range studied. This is because the values of both the electronic mean free path and the average heavy body mass vary considerably throughout the seed pressure range studied.

In an attempt to explain the difference between the potassium-helium and potassium-argon results that are shown in Figure 6.6, the values of $\lambda\sqrt{M}$ for the two mixtures have been computed throughout the seed pressure range 0.1 to 28 torr, the various steps in the calculation being shown in Tables 17.3 and 17.4. Table 17.3 deals with potassium-argon, and Table 17.4 with potassium-helium.

TABLE 17.3

SEED PRESSURE (TORR)	$\frac{1}{\lambda}$ (CM ⁻¹)	AVERAGE HEAVY BODY MASS M (A.M.U.)	\sqrt{M}	$\lambda\sqrt{M}$
0.1	863	40	6.3	7.3 x 10 ⁻³
0.2	875	40	6.3	7.2 x 10 ⁻³
0.4	900	40	6.3	7.0 x 10 ⁻³
0.8	950	40	6.3	6.6 x 10 ⁻³
1.6	1050	40	6.3	6.0 x 10 ⁻³
3.5	1250	40	6.3	5.0 x 10 ⁻³
7	1650	40	6.3	3.8 x 10 ⁻³
14	2400	40	6.3	2.6 x 10 ⁻³
28	4050	40	6.3	1.6 x 10 ⁻³

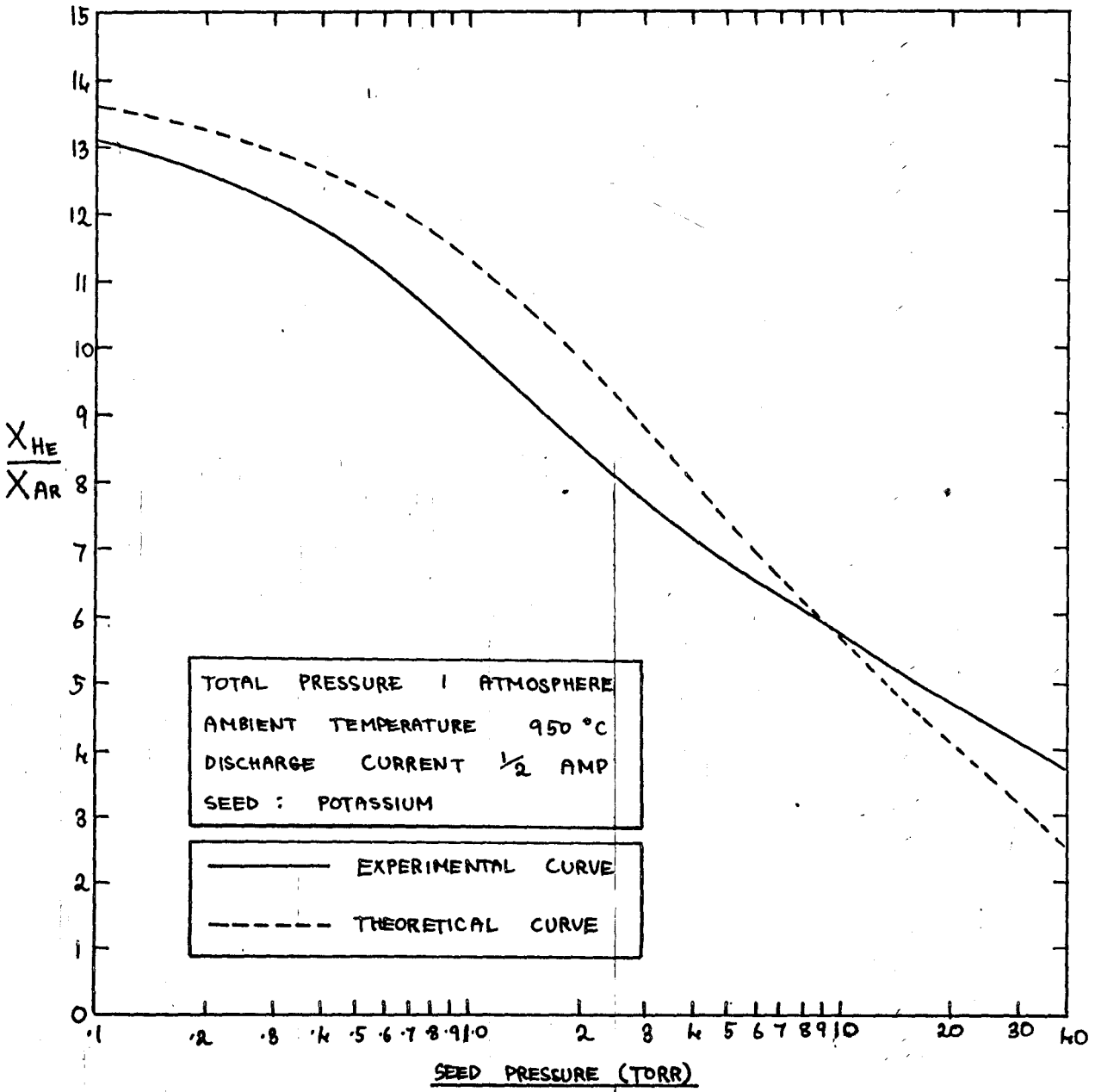
TABLE 17.4

SEED PRESSURE (TORR)	$\frac{1}{\lambda}$ (CM ⁻¹)	AVERAGE HEAVY BODY MASS (A.M.U.)	\sqrt{M}	$\lambda\sqrt{M}$
0.1	4913	7.1	2.66	5.5×10^{-4}
0.2	4925	7.2	2.68	5.5×10^{-4}
0.4	4950	7.3	2.7	5.5×10^{-4}
0.8	5000	7.8	2.76	5.5×10^{-4}
1.6	5100	8.1	2.84	5.6×10^{-4}
3.5	5300	9.4	3.06	5.8×10^{-4}
7	5700	11.6	3.4	5.9×10^{-4}
14	6500	14.8	3.84	5.9×10^{-4}
28	8100	19	4.36	5.3×10^{-4}

As in the case of the results that were discussed in the last section, we can show that the mean electron temperature required to support a given current is practically independent of the nature of the diluent, and can use the energy balance equation to show that the mean gas temperature in the column is also practically independent of the choice of diluent, so we can again infer that the value of the column electric field that is required to support a given current should be roughly inversely proportional to the value of $\lambda\sqrt{M}$ in the column plasma. In Figure 17.1, this theory is tested by comparing the experimental plot of $\frac{X_{He}}{X_{Ar}}$ against seed pressure that is obtained from the potassium-argon and potassium-helium results shown in Figure 6.6 with the theoretical plot of

FIGURE 17.1

THEORETICAL AND EXPERIMENTAL PLOTS OF $\frac{X_{HE}}{X_{AR}}$ AGAINST SEED PRESSURE



$\frac{X_{He}}{X_{Ar}}$ against seed pressure that can be calculated from the values of $\lambda \sqrt{M}$ given in Tables 17.3 and 17.4. It is seen that the two curves are in good agreement - certainly well within the limits of experimental error. A similar result is obtained if the theory is applied to the seed-pressure-dependent caesium-argon and caesium-helium results that are shown in Figure 6.6.

17.4 THE EFFECT ON THE COLUMN PROPERTIES OF CHANGING THE DILUENT PRESSURE.

From the point of view of MHD power generation, the dependence of the properties of the type of nonequilibrium discharge under study on the total gas pressure is very important. A commercial MHD generator would have to operate at several atmospheres pressure in order to be efficient, especially if it were used in conjunction with a nuclear reactor, as suggested in Part I. No experimental data on the dependence of the electrical properties of seeded nonequilibrium plasmas on the diluent pressure has yet been given, however, so a theoretical discussion of the probable effects of raising the diluent pressure will now be attempted. Before dealing with the column under study, we will discuss the somewhat simpler case of a homogeneous two-temperature plasma in which the gas temperature is constant - the type of plasma studied by most of the workers mentioned in Chapter 2, and the type likely to be found in an MHD generator duct. Having done this, we will extend the discussion to the inhomogeneous plasma that is found in the positive column of the discharge under study - a plasma in which the gas temperature is a function of

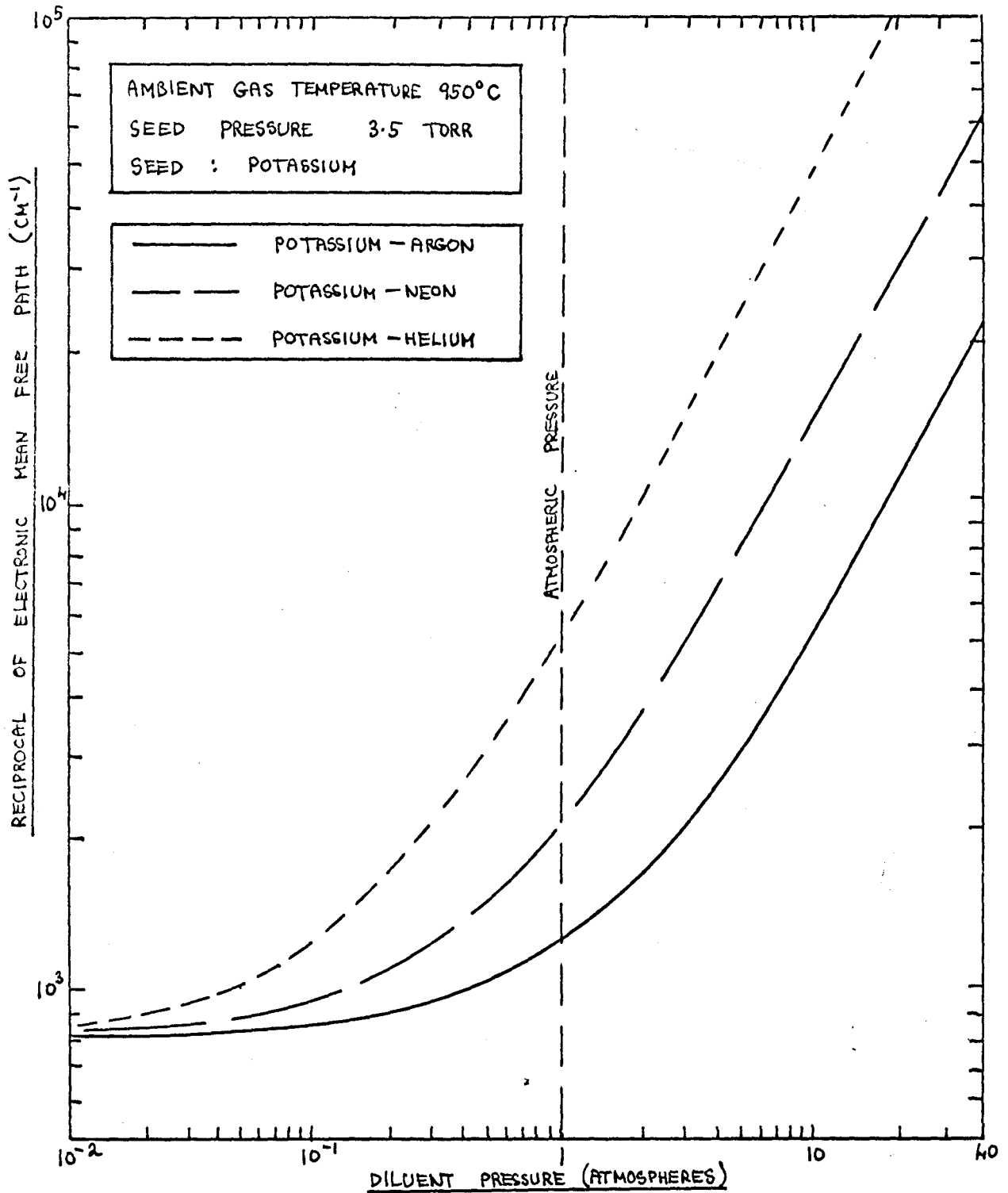
both the discharge current and the distance from the column axis.

It has been fairly conclusively demonstrated that the diluent gas takes no active part in the conduction of electricity through the type of nonequilibrium plasma under study. The diluent merely serves as an elastic scatterer of the electrons, as a sink for their energy, and as a means of removing that energy from the discharge. It has also been shown that the effects on the properties of a nonequilibrium discharge of changing the diluent gas are to leave the electron temperature and electron number density in the plasma virtually unchanged, but to bring about a significant change in the electric field that is needed to support the discharge. In sections 17.1 and 17.2, it was shown that the above facts can be satisfactorily explained by considering the expressions for the electronic mean free path λ (eqn. 14.12), and the average heavy body mass M (eqn. 17.4). If the diluent is changed from argon to neon or helium, both λ and M decrease in value, and if the degree of elevation of the electron temperature is to be kept constant, we see from eqn. 12.8 (the electron energy balance equation) that the electric field has to be increased so as to keep the value of the function $X^2 \lambda^2 M$ constant. This theory has been shown to give a satisfactory explanation of the author's diluent-dependent results (sections 17.1 - 17.3), and the author has found that it is also capable of giving a satisfactory explanation of the diluent-dependent results of Morgulis and Polushkin (1966), who studied a pulsed discharge in caesium- and potassium-seeded helium and

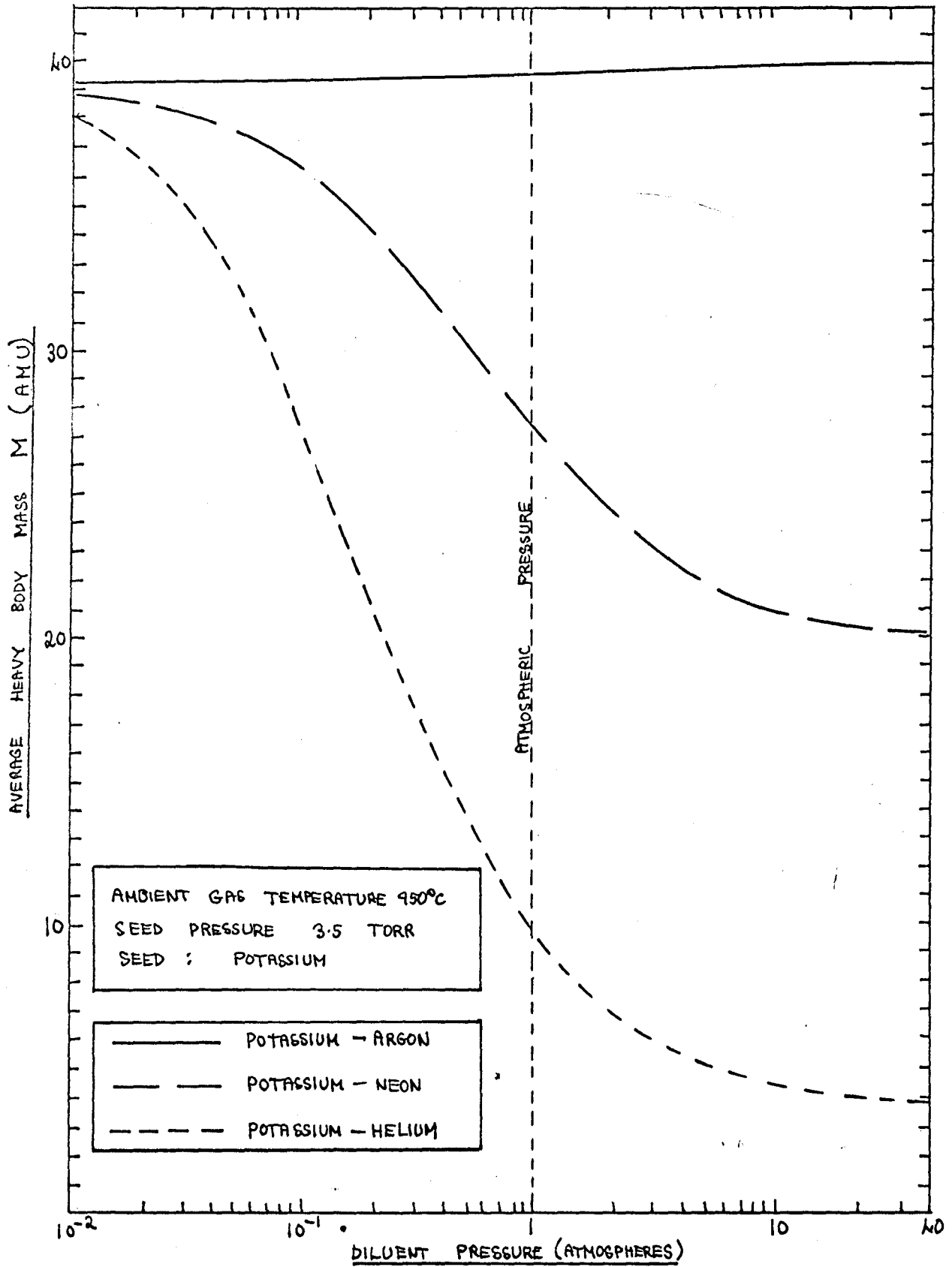
argon at 60 torr total pressure. Morgulis and Polushkin found that the electric fields that are needed to support a given current density in caesium- and potassium-helium are higher than the fields that are required to support the same current density in caesium- and potassium-argon by factors of roughly 8:1 and 9:1 respectively, ratios that are in good agreement with those that are predicted by the theory (7.7:1 and 8.3:1).

Suppose now that instead of changing the diluent gas, we merely change the diluent pressure. The effect on the electron energy balance process will be much the same as that produced by changing from one diluent to another, and if we want to keep the degree of elevation of the electron temperature constant, we will have to adjust the value of the electric field so as to keep the value of $X^2 \lambda^2 M$ constant. This means that in a homogeneous non-equilibrium plasma in which the gas temperature is kept constant either by using a continuous flow system or by employing a pulse technique (see section 2.5), the electric field that is needed to maintain a given electron temperature will be roughly proportional to the value of $\frac{1}{\lambda \sqrt{M}}$ in the mixture. Let us consider plasmas consisting of 3.5 torr potassium in helium, neon and argon, and having an electron number density of the order of $3 \times 10^{14} \text{ cm}^{-3}$ (a typical value for the column under study). In figures 17.2, 17.3 and 17.4, the values of $\frac{1}{\lambda}$, M and $\frac{1}{\lambda \sqrt{M}}$ in these three mixtures are shown plotted against diluent pressure throughout the pressure range 0.01 to 40 atmospheres. In figure 17.2, we see that the three mixtures have virtually the same value of λ

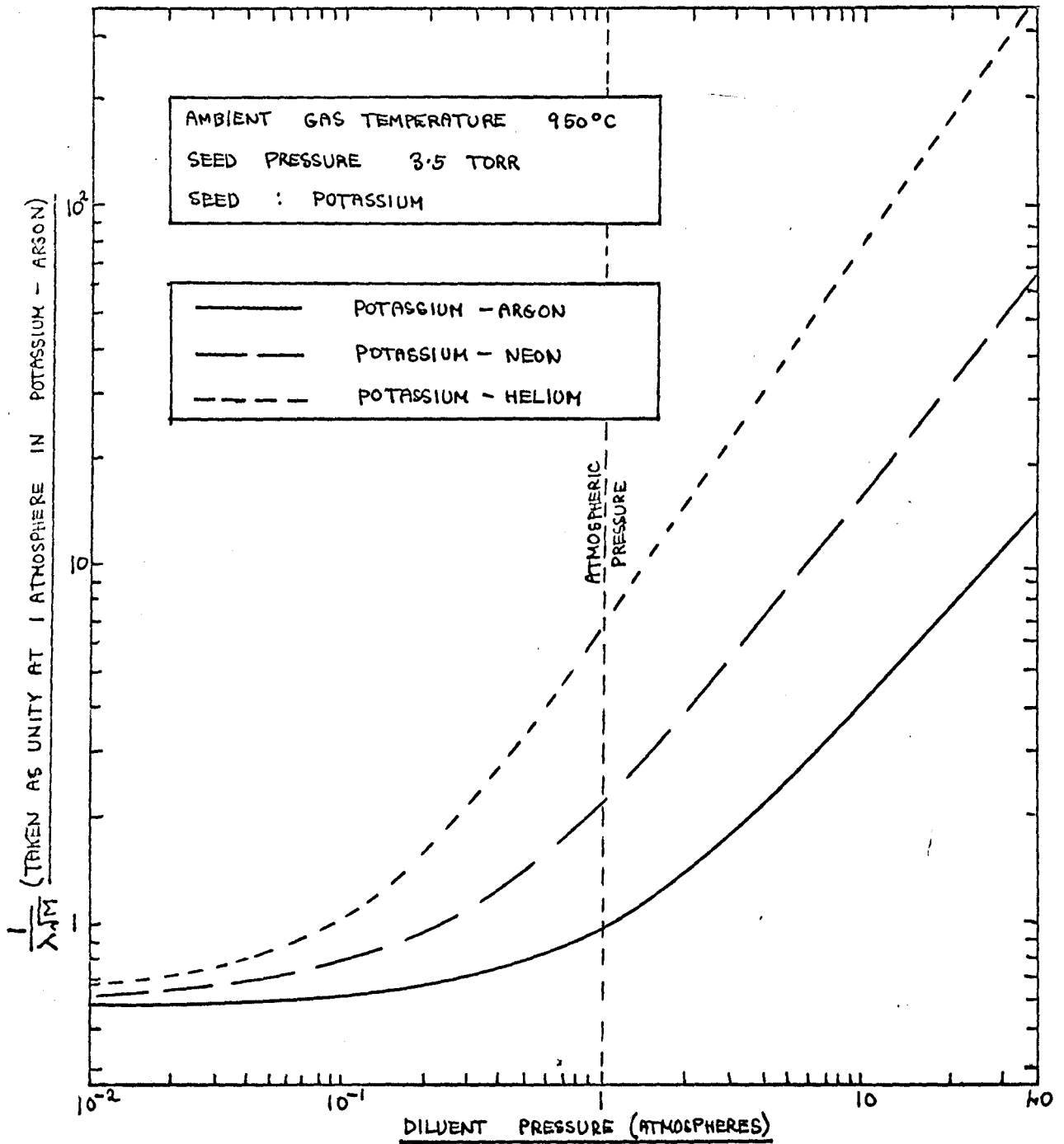
RECIPROCAL OF ELECTRONIC MEAN FREE PATH PLOTTED
AGAINST DILUENT PRESSURE



AVERAGE HEAVY BODY MASS PLOTTED AGAINST DILUENT PRESSURE



PLOTS OF $\frac{1}{\lambda \sqrt{M}}$ AGAINST DILUENT PRESSURE



at low diluent pressures, and that the value of $\frac{1}{\lambda}$ in each mixture increases as the pressure rises. We also see that the differences between the three mixtures become progressively more pronounced as the pressure rises. Figure 17.3 shows that the values of M in the three mixtures are also virtually the same at low diluent pressures, having the value corresponding to the atomic weight of the seed (potassium in this case), but as the seed pressure rises, the curves are again seen to diverge. The potassium-argon curve remains almost level, since potassium and argon have virtually the same atomic weight, but the potassium-neon and potassium-helium curves fall, eventually levelling out at the atomic weights of neon and helium. The plots of $\frac{1}{\lambda\sqrt{M}}$ against diluent pressure shown in figure 17.4 are particularly interesting. It is seen that the three curves converge and level out at low pressures, but that the values of $\frac{1}{\lambda\sqrt{M}}$ increase rapidly as the pressure rises above atmospheric pressure, with the difference between the mixtures again becoming more pronounced as the pressure rises to high values. From this figure, we can infer that the field values that would be required to maintain nonequilibrium conditions in helium-diluted plasmas at high pressures would be very high indeed (of the order of several hundred volts/cm at 10 atmospheres), and the author believes that this could be a vital limiting factor in the design of a reactor-driven MHD system. The author does not envisage any difficulties in operating a high-pressure generator with argon as the diluent gas, however, since the field value required to maintain a given degree of elevation of the

electron temperature in argon at 20 atmospheres is less than the value that is required to maintain the same degree of elevation of the electron temperature in helium at one atmosphere.

Let us now extend the above argument to the plasma of the discharge under study. In this case, the situation is complicated by the fact that the gas temperature in the column will change as the gas pressure and column field increase, thus affecting the degree of elevation of the electron temperature needed to maintain a given electron temperature. This complication does not arise in the case of changing diluent gases, since we have seen that the rise in the thermal conductivity of the plasma that is produced by replacing argon by neon or helium is just sufficient to remove the extra heat that is produced by the increase in the column field without necessitating a rise in the column gas temperature (see sections 15.6 and 17.1). When the diluent pressure is increased, on the other hand, the increase in the energy input rate that is produced by the resulting increase in the column field is not automatically accommodated by an increase in the thermal conductivity of the mixture, since the thermal conductivity of a gas is independent of the gas pressure except at very low or very high pressures. The rise in the column field will thus produce an increase in the gas temperature throughout the column, and the net effect of this increase will be to reduce the degree of elevation of the electron temperature that is needed to maintain the electron temperature at the required level, and hence to reduce the amount by which the

column field has to increase when the diluent pressure is increased by a given amount. The above situation is further complicated by the fact that the degree of dependence of the column properties on the gas temperature profile increases as the discharge current rises (see Chapter 15), so that the effect on the column properties of changing the diluent pressure will depend on the discharge current, being greatest at low currents, and decreasing steadily as the current rises. Let us discuss this in more detail.

At low currents, the column is reasonably homogeneous in its properties, the difference between the axis and boundary temperatures being small (see figure 15.2). At such currents, the value of the gas temperature in the column differs only slightly from the ambient value, and the degree of elevation of the electron temperature is high. For these reasons, we would expect the value of the column field that is needed to support a given current to be determined almost entirely by electron energy balance considerations, and would therefore expect the value of X to be roughly proportional to the value of $\frac{1}{\lambda M}$ in the mixture as the diluent pressure rises. As the discharge current becomes greater, however, we have seen in Chapter 15 that the properties of the column become increasingly dependent on the conditions at the core of the column, while the difference between these conditions and the conditions at the column boundary increase steadily because of thermal energy balance effects. The core gas temperature increases, thus allowing the degree of elevation of the electron temperature to fall, and causing the column to become progressively

closer to a thermal column in its properties. The increasing dependence of the column properties on the value of the gas temperature means that the effect on the column properties of increasing the diluent pressure will decrease as the discharge current rises, since the amount by which the column field has to increase in order to maintain the same mean effective electron temperature will decrease. Let us demonstrate this by considering a specific case. For a current of $\frac{1}{4}$ amp in helium seeded with 3.5 torr potassium, the column field at a total pressure of 1 atmosphere is 24 volts/cm. The axis gas temperature is 1365°K, and the axis electron temperature is 2770°K, so that the degree of elevation of the electron temperature is 1405°K (see Chapter 15). If the diluent pressure is doubled, the value of $\lambda\sqrt{M}$ for the mixture falls to 0.47 of its value at one atmosphere, and the value of the column field that is needed to maintain a degree of elevation of electron temperature of 1405°K increases to roughly 51.5 volts/cm. This increase in the column field causes the core temperature to increase by only 140°K, and has virtually no effect on the mean effective electron temperature in the column. For a current of 4 amps in the same mixture, the column field at a diluent pressure of one atmosphere is 14 volts/cm. The values of T_{g0} , T_{e0} and $T_{e0} - T_{g0}$ are 2725°K, 3230°K and 505°K. Increasing the diluent pressure from one atmosphere to two atmospheres again causes $\lambda\sqrt{M}$ to decrease to 0.47 of its former value, and means that the column field that would be required to keep the degree of elevation of the electron temperature constant

at 505 °K would be 30 volts/cm. Such an increase in the column field would increase T_{go} by 1500°K, however, indicating that the increase in X is far too high. The core electron temperature can in fact be maintained at the same value by increasing X from 14 volts/cm to about 16.2 volts/cm, since this produces a core gas temperature of 2965°K, which, added on to the degree of elevation of the electron temperature (now reduced to about 265°K) produces a core electron temperature of 3230°K. We therefore see that the percentage increase in the column electric field that is needed to keep the current constant when the diluent pressure is increased from one atmosphere to two atmospheres falls from over 100% at a discharge current of $\frac{1}{4}$ amp to approximately 12% at 4 amps. We can therefore conclude that the value of the column field that is needed to support a given discharge current will be strongly dependent on the diluent pressure at low discharge currents, being roughly proportional to the value of $\frac{1}{\lambda\sqrt{M}}$ in the mixture, but that the field will become progressively less dependent on the diluent pressure as the discharge current rises.

IIC THE CATHODE REGIONS OF THE DISCHARGE

In this section, we will discuss the cathode fall results that were given in Chapter 7. We will begin by attempting to classify the cathode mechanism of the diffuse mode of the discharge under study, and will then set up a rough model of the cathode regions of the discharge. Having done this, we will take a detailed look at the emission process, and at the processes that occur in the cathode fall space. Finally, we will attempt to give a qualitative explanation of certain features of the experimental cathode fall results.

CHAPTER 18ANALYSIS OF THE DIFFUSE CATHODE MECHANISM18.1 CLASSIFICATION OF THE DIFFUSE CATHODE MECHANISM.

We have seen in Chapter 7 how the cathode mechanism of the discharge under study can operate in two different modes - named the "constricted" and "diffuse" modes by the author - and how the author has made a detailed experimental study of the properties of the second of these modes. We will now attempt to classify the cathode mechanism of this mode of the discharge, and will then attempt to describe the physical processes that operate in the region of the discharge between the cathode surface and the positive column.

When it was first reported by Ralph in 1962, the diffuse mode of the discharge under study was described as an "abnormal glow". The discharge was later described by Sakuntala (1964) as an "arc discharge with an externally-heated cathode", and it is interesting to note that Ralph and Sakuntala were describing **exactly** the same discharge - a discharge carrying a current of a few amps between plane stainless-steel electrodes immersed in potassium-seeded argon. Sakuntala's classification appears to **be** the more appropriate of the two, since the discharge has **many** properties in common with a conventional hot-cathode arc, but the discharge does also bear a close qualitative resemblance to a high-pressure abnormal glow - especially at low temperatures or seed pressures. A comparison of the properties of the discharge under study with those of the abnormal glow and hot cathode arc are given in Table 18.1.

TABLE 18.1

	THE DIFFUSE MODE OF THE DISCHARGE UNDER STUDY	CONVENTIONAL EXTERNALLY - HEATED HOT CATHODE ARC	CONVENTIONAL HIGH-PRESSURE ABNORMAL GLOW
APPEARANCE	cathode surface covered by glowing sheath, which is separated from a constricted positive column by a dark space.	cathode surface separated from glowing plasma by dark space (normally too narrow to be visible at high pressures).	cathode surface covered by negative glow, which is separated from a constricted positive column by the Faraday dark space
CURRENT	of the order of amps	of the order of amps under suitable conditions.	of the order of amps under suitable conditions.
CATHODE FALL	typically a few volts, rising to a few tens of volts under certain conditions	typically a few volts or tens of volts	of the order of hundreds of volts
DEPENDENCE OF CATHODE FALL ON CURRENT	rises as current rises	rises as current rises	rises as current rises
DEPENDENCE OF CATHODE CURRENT DENSITY ON CURRENT	rises as current rises	rises as current rises	rises as current rises
NATURE OF SPECTRUM	seed metal only - no spectrum of diluent gas or vapour of electrode material.	gas only - no spectrum of vapour of electrode material.	gas only - no spectrum of vapour of electrode material.
TEMPERATURE OF CATHODE SURFACE	has to be high - of the order of 1200 - 1600°K - before discharge can operate	has to be high - of the order of 2500°K - before discharge can operate	may rise to over 1000°K at high currents, but does not have to be high for emission mechanism to operate.

TABLE 18.1 (contd.)

	THE DIFFUSE MODE OF THE DISCHARGE UNDER STUDY	CONVENTIONAL EXTERNALLY - HEATED HOT CATHODE ARC	CONVENTIONAL HIGH-PRESSURE ABNORMAL GLOW
EMISSION MECHANISM	Thermionic emission (en- hanced at low temperatures and seed pressures by bombardment of surface by positive ions and radiation).	thermionic emission.	mainly caused by bombardment of surface by positive ions and radiation.
FACTOR LIMITING CURRENT	current appears to be space charge limited, except at low temperatures and seed pressures, when it is also limited by efficiency of emission process.	current space charge limited.	current limited by efficiency of emission process.
STABILITY	generally stable, but tends to change to ther- mionic arc at low temperatures and seed pressures.	... stable.	cathode must be kept cool to prevent change to thermionic arc.

In the opinion of the author, the discharge under study can best be classified as a form of externally-heated hot cathode arc, since the emission mechanism is essentially that of a hot cathode arc, and the value of the cathode fall is far too low for the discharge to be classified as a glow. Nevertheless, it is

apparent from Table 18.1 that the classification cannot be a rigid one, since the discharge has some features that are more generally associated with a high-pressure glow discharge than with a hot-cathode arc. One such feature is the narrow dark space that separates the positive column from the luminous sheath that covers the cathode surface. This corresponds to the Faraday dark space of the glow discharge, and is a feature that is not normally found in a hot cathode arc, where the space between the boundary of the cathode fall region and the anode is filled by the positive column plasma (Langmuir 1929, von Engel 1965).

18.2 DEVELOPMENT OF A THEORY TO DESCRIBE THE DIFFUSE MODE OF THE DISCHARGE.

In developing a theory to describe the diffuse mode of the discharge under study, we will take as our starting point the theory that was given by Sakuntala in 1964, following her experimental study of the potassium-argon discharge. Sakuntala postulated that the discharge was an arc discharge with an externally-heated cathode, the electrons being emitted from the cathode surface by thermionic emission, and the discharge current (which appeared to be smaller than the maximum possible thermionic emission current, except at low temperatures) being limited by space charge effects in the cathode fall region. She further postulated that the value of the cathode fall was just high enough to produce sufficient ionisation to replace the ions that were lost from the discharge plasma to the cathode, and that the high light output of the sheath that covered the cathode surface was caused

by the excitation of potassium atoms by electrons which had been accelerated by the high electric field in the fall space.

Sakuntala's theory (Sakuntala 1964, 1965B), which attributed to the discharge under study all the features of a conventional hot-cathode arc (see Langmuir 1929 and von Engel 1965), was capable of giving a qualitative explanation of those features of the diffuse mode of the discharge that were known at the time. The experimental work of the author, which was carried out after that of Sakuntala, has revealed several features of the discharge that cannot be accounted for by the conventional theory of the hot cathode arc, however, and we will now attempt to set up a modified form of Sakuntala's theory that is capable of explaining these features.

In the opinion of the author, the diffuse mode of the discharge under study is rather more complicated than a conventional hot cathode arc, and consists of two separate, largely self-sufficient regions, connected by the dark space that was mentioned at the end of the last section. The first of these is the cathode region of the discharge, which the author believes to be a miniature hot cathode arc of the type described by Sakuntala (1964), the plasma of the arc being the luminous sheath that covers the cathode surface. The second region is the positive column, which, as we have seen in Part IIB, serves as a conducting path for the discharge current over the greater part of the inter-electrode distance. Let us examine this theory in more detail.

In common with most other types of arc discharge, the discharge under study has its current determined by external

circuit conditions. Thus, the configuration adopted by the discharge is that which enables the required current to be supported by the smallest possible electrode voltage. This means that the component parts of the discharge all adjust their mechanisms so that they operate at the lowest possible voltages. Now a gas discharge consists essentially of two processes, the first being the process by which electrons are removed from the cathode surface, and the second being the process by which these electrons are transported through the gas that lies between the cathode and the anode. In the case of the discharge under study, the most efficient method of producing a supply of electrons from the cathode surface appears to be for thermionic emission to occur from as large an area of cathode surface as is available. The electrons so produced are allowed to leave the vicinity of the cathode surface because of the presence of a layer of plasma at a short distance from the cathode surface. This acts as a source of positive ions, which move through the plasma towards the cathode, and then flow across the narrow cathode fall space that separates the plasma from the cathode surface, thus permitting the electrons to flow in the opposite direction (Langmuir 1929, von Engel 1965). If such a plasma were not present, the flow of electrons would be severely limited by space charge effects (Child 1911, Cobine 1958), so we see that the cathode mechanism of the discharge under study requires the existence of a layer of plasma that covers the entire emitting region of the cathode. Because of its strong resemblance to the negative glow region of the high-pressure glow discharge, we will henceforth refer to this sheath of plasma as the negative glow.

In the case of the conventional hot cathode arc, which normally operates at low pressure, the plasma that covers the cathode surface extends all the way to the anode surface, serving as a conducting path for the discharge current as well as a source of ions to neutralise the negative space charge that would otherwise build up in the inter-electrode space. In such a discharge, the field in the plasma is very low, being just high enough to maintain the drift motion of the electrons and ions through the plasma, and the ionisation of the gas that is needed to maintain the plasma and replace the ions that are lost to the cathode is produced by the electrons that have been accelerated across the cathode fall space (von Engel 1965). The value of the cathode fall and the thickness of the fall space adjust their values so that a steady state system is produced in which the conduction process is maintained by the smallest possible electrode voltage. In the case of the discharge under study, the plasma that covers the cathode surface does not extend all the way to the anode, but soon gives way (via the dark space) to the constricted plasma of the positive column, since the current can be carried much more efficiently by such a column than by a uniform, homogeneous plasma in the case of a high-pressure discharge (see Part IIB). Furthermore, the ionisation in the positive column is not produced by the electrons that have been accelerated across the cathode fall space, but by the maintenance of nonequilibrium conditions in the column plasma by the column field, the electrons having a Maxwellian energy distribution that corresponds to a much higher temperature

than that of the gas atoms. Thus, we can regard the positive column of the discharge under study as being an independent entity whose properties are largely independent of the processes that occur near the cathode, unlike the case of the conventional hot-cathode arc, where the positive column and cathode regions are strongly inter-dependent (von Engel 1965).

As in the case of the high-pressure glow discharge, the sheath of plasma that covers the cathode surface is connected to the constricted plasma of the positive column by a dark space. In the opinion of the author, the dark space in the discharge under study is a region in which the electrons have a lower mean energy than in either the negative glow or the positive column. The electrons acquire an energy of several electron volts in crossing the cathode fall region, and then give up this energy to the atoms in the negative glow by means of ionising, exciting and elastic collisions with the seed and diluent atoms. The electrons then drift across the dark space, picking up energy from the electric field and interacting among themselves as they do so, and eventually attain the Maxwellian energy distribution that prevails in the positive column, a distribution in which the electrons in the high-energy tail have enough energy to produce ionisation and excitation of the seed atoms. The dark space thus appears to be that region of the discharge where the electrons have lost the energy that they acquired in crossing the cathode fall space, and have not yet interacted among themselves for long enough to produce a high-energy tail. The dark space

thus appears to serve the same function as the Faraday dark space of the glow discharge, being (in the words of von Engel 1965) the "anteroom of the positive column", and we will therefore refer to it as the Faraday dark space from now on.

18.3 THE EMISSION PROCESS OF THE DIFFUSE MODE

We will now take a more detailed look at the various processes that occur between the cathode surface and the positive column, starting with the actual emission process. In 1964, Sakuntala showed that this appeared to be thermionic emission from a surface whose work function was greatly reduced by the presence of a partial covering of alkali metal, and the experimental work of the author has proved to be in good agreement with this theory. Let us examine the thermionic emission process, and see how the presence of an alkali metal covering affects the emission properties of a surface.

The theory of thermionic emission was first given by Richardson in 1901, and was later improved by Dushman (1923, 1930). It is based on the free electron theory of metals, and makes the assumption that the electrons obey the laws of a perfect gas, share in the heat energy of the metal, and have a Maxwellian energy distribution. The derivation (see Cobine 1958) assumes that electrons having velocities in excess of a critical value and directed along the outward normal to the surface will have sufficient energy to escape from the attractive forces that hold them in the metal, and will be emitted from the surface.

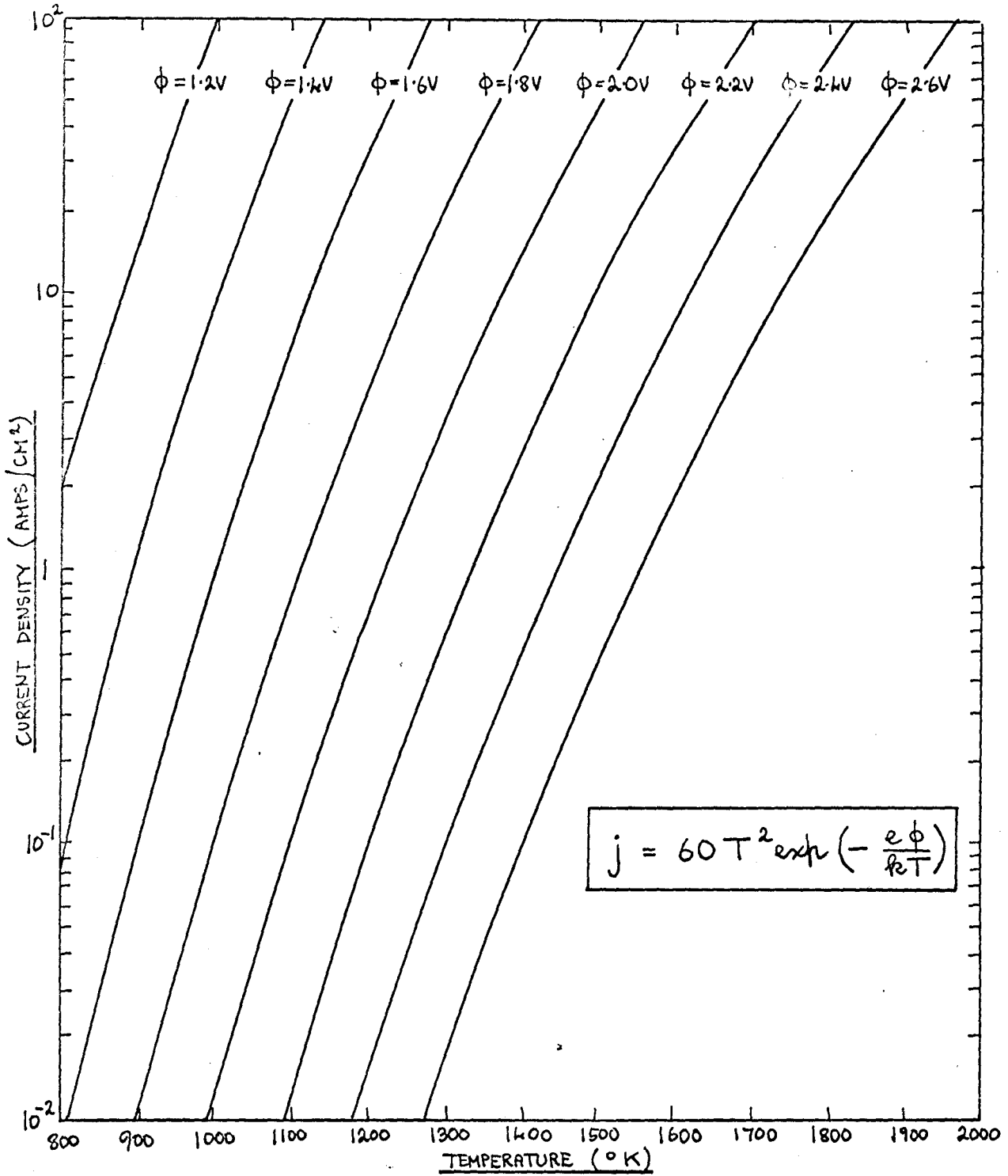
Dushman's form of the thermionic emission equation (which is commonly referred to as the Richardson equation) is

$$j = A T^2 \exp\left(-\frac{e\phi}{kT}\right) \text{-----} 18.1$$

where j is the current density, T is the temperature of the emitting surface, e is the electronic charge, and k is Boltzmann's constant. The constant ϕ is the work function of the surface, $e\phi$ being the work that has to be done to remove an electron from the surface; ϕ is generally given in volts. The constant A is a universal constant whose value is $\frac{2\pi e m k^2}{h^3}$, where m is the electronic mass and h is Planck's constant. It has a value of $60.2 \text{ amp cm}^{-2} \text{ deg}^{-2}$. When the spin of the electron is taken into account, it is found that the value of A has to be doubled, (Cobine 1958), but the theoretical value of 120.4 only holds for pure surfaces of a single crystal face, and it is found that A has a value of about 60 for most metals. Following Sakuntala (1964), we will take A to have the latter value. Using this value of A , eqn. 18.1 has been used to compute a set of current density/temperature curves for different work functions. These curves are shown in figure 18.1, and cover the temperature, current density and work function ranges of interest. It is seen that a small change in either the temperature or the work function produces a large change in the current density.

The main difficulty involved in applying eqn. 18.1 is not the uncertainty in the value of A , but is the uncertainty in the values of the work function and temperature of the emitting surface, since the current density is exponentially-dependent on

PLOTS OF THERMIONIC EMISSION CURRENT DENSITY AGAINST TEMPERATURE FOR DIFFERENT WORK FUNCTIONS



these quantities, and only linearly-dependent on A . The work function is particularly difficult to determine in the present case, for it is a well-known fact that the work function of a metal surface that is partly covered by a metallic film can be considerably lower than the work function of either of the metals involved (Langmuir and Taylor 1939, Gyftopoulos and Levine 1961, Sakuntala 1964). For a refractory metal surface partly covered by an alkali metal film, Langmuir (1933) has shown that the work function of the composite surface depends on the temperature and on the alkali metal vapour pressure. If the logarithm of the emission current density is plotted against the inverse of the temperature, with the alkali metal vapour pressure as a parameter, the so-called "Langmuir S curves" are produced (Langmuir and Taylor 1933, Wilson 1959). In these curves, the current density at first rises steadily as the temperature rises, being exponentially dependent on the temperature, thus indicating that the work function of the surface is constant. At a critical temperature, each curve levels out, passes through a maximum, and then actually falls as the temperature rises higher, passing through a minimum before rising once again. At high temperatures, the current density is again exponentially temperature-dependent, but the work function of the surface now corresponds to that of the pure metal, and is considerably higher than the original work function of the covered surface. The critical temperature at which a given curve starts to level out depends on the vapour pressure of the alkali metal, and rises steadily as the latter increases.

The above effects are produced because the work function of the composite surface depends on the percentage of surface that is covered by the alkali metal, while the degree of covering depends on the temperature and on the alkali metal vapour pressure. At the critical temperature, the alkali metal starts to boil off the surface, thus causing the work function to rise, and causing the current density to decrease as the temperature rises through a certain temperature range.

Although Langmuir's work was carried out using caesium-covered tungsten, we would expect to find a similar effect for caesium, potassium and sodium on stainless steel. No systematic experimental measurements of the dependence of the work function of such surfaces on the experimental conditions have yet been carried out, however, the only available data on such surfaces being that obtained by Sakuntala (1964), who measured the work function of potassium on stainless steel at a seed pressure of a few torr and a temperature of the order of 1000°K . By measuring the current that flowed between two electrodes at very low applied voltages at different temperatures, she found that the effective work function of the surface was of the order of 1.6V , a value that was consistent with her work on the high-current discharge, where she observed current densities of the order of amps/cm^2 at electrode temperatures of the order of 1100°K (see figure 18.1). The experimental work of the author, which will be discussed in section 18.7, tends to confirm that the work function of potassium on stainless steel is of the order of 1.6V at high seed pressures,

but indicates that the work function tends to increase as the seed pressure falls to low values. The author's work also indicates that the work function of caesium on stainless steel is lower than that of potassium on stainless steel, while that of sodium on stainless steel is higher.

As mentioned above, one of the main difficulties involved in applying eqn. 18.1 is in knowing the temperature of the surface. The experimental work of Ralph (unpublished), Sakuntala (1964) and the author has shown that the temperature of the cathode is in fact higher than the ambient temperature, the difference between the two becoming progressively greater as the discharge current rises. This heating is presumably caused partly by positive ion bombardment of the cathode surface, and partly by the flow of heat from the positive column, whose temperature rises well above the ambient temperature at high discharge currents (see section 15.6). Although it is a comparatively simple matter to measure the ambient temperature or the temperature of the cathode as a whole, it is practically impossible to measure the actual surface temperature under the conditions that prevail in the discharge under study, and the author suspects that the surface can be hotter than the rest of the cathode at high currents.

18.4 THE THEORY OF SPACE-CHARGE-RESTRICTED CURRENT FLOW.

Before we attempt to analyse the cathode fall region of the discharge under study, we will discuss the theory of space-charge-restricted current flow. We will deal with the subject

under four headings, namely, (1) the motion of electrons (or ions) under free-fall conditions, (2) the motion of electrons (or ions) under mobility-limited conditions, (3) the motion of electrons and ions under free-fall conditions, and (4) the motion of electrons and ions under mobility-limited conditions. In all cases, we will consider the motion to take place between infinite plane parallel electrodes, so that our equations will be one-dimensional.

(1) The motion of electrons (or ions) under free-fall conditions.

This situation occurs in thermionic valves, in which electrons are emitted from a cathode and collected at an anode, and also occurs when a negative probe is immersed in a low pressure plasma, the charge carriers being positive ions that migrate from the plasma to the probe surface in this case. In both of the above systems, the current is limited by the build-up of a space charge sheath that opposes the motion of the charge carriers; the sheath is negative in the case of the thermionic valve, and positive in the case of the negative probe.

The theory of systems in which current is carried by a single type of charged particle under free-fall conditions was first developed by Child in 1911. The theory, which is fully dealt with by Cobine (1958), involves using the principle of conservation of energy to express the velocity of the charged particles in terms of the potential drop through which they have fallen, expressing the charge density in Poisson's equation in terms of the current density (assumed constant) and particle velocity, and integrating the resulting equation twice. In this way, a formula for the

current density j that flows between electrodes a distance d apart when a potential difference V is applied between them is obtained:

$$j = \left(\frac{1}{9\pi}\right) \left(\frac{2e}{m}\right)^{1/2} \frac{V^{3/2}}{d^2} \quad \text{----- 18.2}$$

In this equation, which is sometimes referred to as Child's law, e is the electronic charge and m is the mass of the particle involved.

(2) The motion of electrons (or ions) under mobility-limited conditions.

Under conditions of high pressure, or in systems where the electrode separation is large compared with the mean free path of the charge-carrying particles, the particles rapidly reach a drift velocity that is determined by their mobility and by the field, unlike the free-fall case, where continuous acceleration of the charged particles occurs. By carrying out the same basic process that was used in the derivation of eqn. 18.2, namely, substituting for the charge density in Poisson's equation and integrating twice, it can be shown (Cobine 1958) that the current density j that flows between electrodes a distance d apart when a potential difference V is applied between them is given by

$$j = \left(\frac{9}{4}\right) \frac{KV^2}{3\pi d^3} \quad \text{----- 18.3}$$

Here, K is the mobility of the particles. In general, the current density that flows between electrodes under mobility-limited conditions is considerably smaller than that which flows through a similar system under free fall conditions. In both

the free-fall and mobility-limited cases, we see that we can greatly increase the current density by reducing the value of d , and this fact is made use of in the design of thermionic power diodes and similar devices (Wilson 1959).

(3) The motion of electrons and ions under free-fall conditions.

Both of the cases studied so far involve the single space charge sheaths that are produced by the motion of a single type of charged particle. In the discharge under study, however, the current is carried by the simultaneous motion of electrons from the cathode to the anode and positive ions from the anode to the cathode, and the situation is correspondingly more complicated.

Langmuir (1929) has carried out a comprehensive study of the influence of space charge on the simultaneous motion of ions and electrons under free-fall conditions, and has shown that the current is limited by the build-up of both negative and positive space charge sheaths. If a cathode emits an unlimited supply of ions, a net positive space charge develops in front of the anode, and a corresponding negative space charge develops in front of the cathode. The ions and electrons move in opposite directions through this double sheath, with the electron current density being given by

$$j_e = \frac{1.85}{9\pi} \left(\frac{2e}{n_e}\right)^{1/2} \frac{V}{d^2} \quad \text{-----} \quad 18.4$$

and the ratio of the ion current to the electron current being given by

$$\frac{j_+}{j_e} = \left(\frac{m_e}{M_+}\right)^{1/2} \quad \text{-----} \quad 18.5$$

Here, m_e and $M+$ are respectively the mass of an electron and the mass of an ion, d is the electrode separation, and V is the potential difference between the electrodes. We see that eqn. 18.4 is very similar to eqn. 18.2, the only difference between the two equations being that the electron current density is increased by a factor of 1.85 when the ion current is present.

Langmuir has also shown that the source of positive ions in a system of the type described above need not be a solid anode, but can also be a plasma. If a thermionic cathode is immersed in a plasma and is maintained at a negative potential with respect to the plasma, the electrons in the plasma are repelled from the cathode, and this, combined with the build-up of negative space charge in front of the cathode, leads to the formation of a double space charge sheath of the type described above, with the plasma corresponding to the anode, and the thickness of the sheath corresponding to the electrode separation. In such a system, which operates in certain types of hot-cathode arc (Langmuir 1929, Malter et. al. 1951, von Engel 1965), the current is determined not by the rate at which the cathode can emit electrons, but by the rate at which positive ions can move up through the plasma to the boundary of the sheath, since the electron current is limited to $\sqrt{\frac{M+}{m_e}}$ times the ion current. The sheath generally adjusts its thickness (and hence its voltage drop, which is given by eqn. 18.4) so that the system operates with the optimum overall efficiency.

(4) The motion of electrons and ions under mobility-limited conditions.

Let us now extend the theory of space-charge-limited current flow to a system where the current is carried by both ions and electrons, and where the motion of the charged particles is mobility-limited. We shall consider a system where a cathode emits electrons and an anode (or plasma) emits positive ions, and where the ions and electrons move through the inter-electrode space in opposite directions. Let the electronic and ionic number densities at a distance x from the cathode be n_e and n_+ , the electronic and ionic mobilities be K_e and K_+ , and the electronic and ionic current densities be j_e and j_+ . Let the potential at distance x from the cathode be V_x . Then

$$j_e = -e n_e K_e \left(\frac{dV_x}{dx} \right) \quad \text{-----} \quad 18.6$$

$$\text{and } j_+ = +e n_+ K_+ \left(\frac{dV_x}{dx} \right) \quad \text{-----} \quad 18.7$$

the electronic mobility being, of course, negative.

Poisson's equation states that

$$\frac{d^2 V_x}{dx^2} = -4\pi\rho \quad \text{-----} \quad 18.8$$

and can be written in the form

$$\frac{d^2 V_x}{dx^2} = -4\pi (e n_+ - e n_e) \quad \text{-----} \quad 18.9$$

Substituting for n_+ and n_e from eqn. 18.6 and 18.7, eqn. 18.9 becomes

$$\frac{d^2V}{dx^2} = -4\pi e \left(\frac{-j_+}{e K_+ \frac{dV}{dx}} - \frac{j_e}{e K_e \frac{dV}{dx}} \right) \quad 18.10$$

so that

$$\frac{dV}{dx} \cdot \frac{d^2V}{dx^2} = 4\pi \left(\frac{j_+}{K_+} + \frac{j_e}{K_e} \right) \quad 18.11$$

It is not possible to give a general solution to this differential equation, but we can integrate it if we make the assumption that no ions or electrons are created or destroyed in the region under consideration. In this case, j_+ and j_e are both independent of x , and since K_+ and K_e are also approximately constant, the RHS of eqn. 18.11 is independent of x . Thus,

$$\frac{1}{2} \left(\frac{dV}{dx} \right)^2 = 4\pi \left(\frac{j_+}{K_+} + \frac{j_e}{K_e} \right) x + C \quad 18.12$$

where C is the constant of integration. This equation has a number of possible solutions. If the ratio of the electronic current to the ionic current is equal to $\left| \frac{K_e}{K_+} \right|$, the net space charge will be zero throughout the region under consideration, and the electric field will be constant, its value being given by eqn. 18.6 or 18.7. This corresponds to the steady-state drift motion of electrons and ions that takes place in a neutral plasma such as the positive column of a gas discharge. If the ratio of the electronic current to the ionic current is not equal to $\left| \frac{K_e}{K_+} \right|$, on the other hand, the net space charge will not be zero throughout the region under consideration, and the situation will

be more complicated. If $\frac{j_e}{j_+} > \left| \frac{K_e}{K_+} \right|$, a net negative space charge will build up in front of the cathode, and this will limit the value of the electronic current. The limiting case will occur when $j_+ = 0$, in which case the value of the electronic current will be given by eqn. 18.3. If $\frac{j_e}{j_+} < \left| \frac{K_e}{K_+} \right|$, the opposite situation will arise, with the positive ion current being limited by the build-up of a positive space charge sheath in front of the anode (or in front of the plasma that serves as the anode). In this case, the limiting case will occur when $j_e = 0$, when the positive ion current will be given by eqn. 18.3.

18.5 APPLICATION OF THE THEORY TO THE CATHODE FALL REGION OF THE DIFFUSE MODE.

We will now apply the theory that was developed in the last section to the cathode fall region of the discharge under study, and will attempt to answer the following five questions.

- (1) What is the thickness of the cathode fall space?
- (2) How do the electric potential and electric field vary across the fall space?
- (3) What is the space charge distribution in the fall space?
- (4) What proportion of the discharge current is carried across the fall space by electrons, and what proportion is carried by positive ions?
- (5) What is the factor that determines the value of the cathode fall?

In seeking the answers to these questions, we will start by considering the theory that was given by Sakuntala in 1964, when she showed that many of the discharge properties could be

qualitatively explained by considering the discharge to be a hot cathode arc of the type described by von Engel (1965). If this theory were valid, we would be able to give a quantitative description of the cathode fall region of the discharge under study by applying Langmuir's theory of the free-fall double space charge sheath (see section 18.4.3). In particular, the relationship between the current density (j), the cathode fall voltage drop (V) and the thickness of the cathode fall space (d) would be given by eqn. 18.4, and the ratio of the electron current (j_e) to the ion current (j_+) would be given by eqn. 18.5. Let us test this theory by applying eqn. 18.4 to the discharge under study, calculating the thickness of the fall space, and seeing if the value thus obtained is a reasonable one.

If we substitute for the various constants in eqn. 18.4, we find that

$$j = 6.73 \times 10^7 \frac{V^{3/2}}{d^2} \quad \text{18.13}$$

where j and V are in e.s.u., and d is in cm. This equation can also be written as

$$j = 4.3 \times 10^{-6} \frac{V^{3/2}}{d^2} \quad \text{18.14}$$

where j is in amps/cm², V is in volts, and d is in cm. Solving for d , we see that

$$d = 2.07 \times 10^{-3} \frac{V^{3/4}}{j^{1/2}} \quad \text{18.15}$$

If we now consider a typical discharge (in potassium-argon at 3.5 torr seed pressure and 950°C ambient temperature), we see from figure 7.1 that V is roughly 6 volts when j is 1 amp/cm². Use of these values in eqn. 18.15 gives a value of the order of 8×10^{-3} cm for d , the thickness of the fall space, a value that is consistent with the experimental work of Sakuntala (1964), Evans (1967), and the author, all of whom have shown that the cathode fall occurs very close to the cathode surface. But we know that the value of the electronic mean free path in the mixture under consideration is roughly an order of magnitude less than this (see table 17.2), and it can be shown that the discrepancy between the value of d given by eqn. 18.15 and the value of the electronic mean free path is even greater if argon is replaced by neon or helium as the diluent gas (see table 17.2). Thus, we see that we cannot apply Langmuir's theory of the free-fall double space charge sheath to the cathode fall region of the discharge under study since one of the basic conditions required for its validity - the existence of free-fall conditions - is clearly not satisfied. This means that the movement of the ions and electrons across the fall space is limited by mobility considerations as well as by space charge, so we must turn to the theory that is given in section 18.4.4 in order to obtain an accurate description of the cathode fall space of the discharge under study.

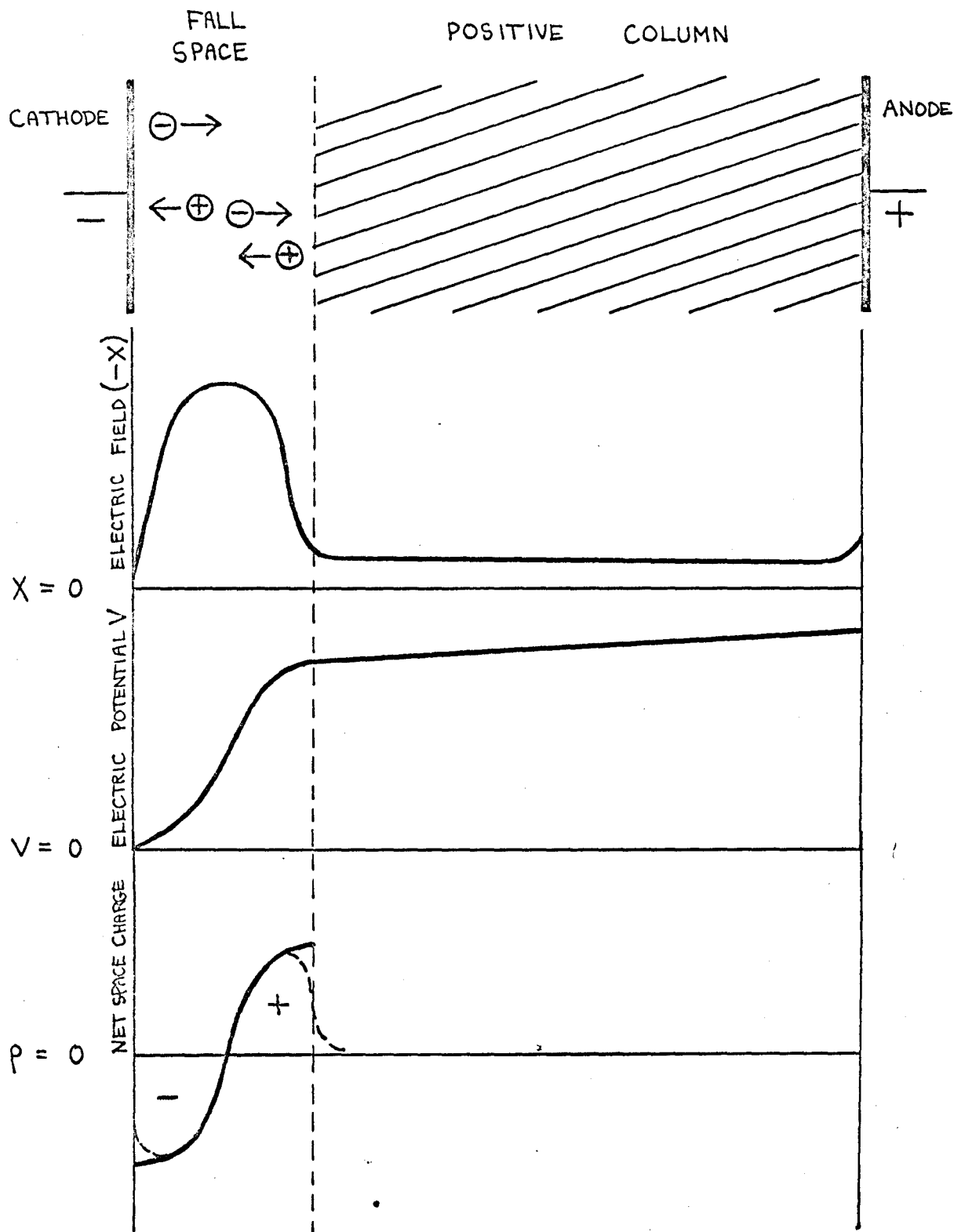
In applying this theory to the discharge under study, we come up against a major difficulty. We know that the region immediately in front of the cathode must have a negative space charge because of the copious emission of electrons that occurs from the cathode surface (Cobine 1958), and that the part of the negative glow plasma nearest the cathode must have a net positive space charge because of the repulsion of the plasma electrons by the cathode (Cobine 1958, von Engel 1965). We also know that the ratio of the electron current leaving the cathode region of the discharge to the ion current approaching the cathode region is given by eqn. 18.5. Now if free-fall conditions existed in the cathode fall space, these facts could be easily explained by applying the theory that is given in section 18.4.3. We know that free-fall conditions do not exist in the present case, however, and our difficulty arises because it can be shown that it is not possible to have a double space charge sheath in which the electron current/ion current ratio is given by eqn. 18.5 under mobility-limited conditions.

To understand why this is the case, we must examine the changes that occur as we cross a free-fall, double-space-charge sheath of the type described by Langmuir (1929). As we cross the fall space from the cathode to the anode, the electron number density n_e falls, but the electron current density is kept constant by the fact that the electronic velocity v_e increases steadily with increasing distance from the cathode in such a way as to keep the product $n_e v_e$ constant. The same is true for

the positive ion number density n_+ and the positive ion velocity v_+ : as we cross from the anode to the cathode, the former falls and the latter rises in such a way as to keep $n_+ v_+$ constant. It is these changes in the relative values of n_e and n_+ that give rise to the double space charge sheath, while the latter, in turn, produces electric potential and electric field profiles of the type shown in figure 18.2. We see that the field is zero at the cathode and at the anode, (or in the plasma that serves as the anode), but rises to a finite value in the fall space.

This situation is made possible by the fact that the values of v_e and v_+ are determined by the distance through which the electrons and ions have fallen, and not by the local value of the electric field, as is the case under mobility-limited conditions. Under mobility-limited conditions, the ratio of j_e to j_+ is always proportional to the ratio of n_e to n_+ , a fact that precludes the possibility of producing a double space charge sheath in which the ratio of j_e to j_+ is everywhere constant. To produce a double space charge sheath under mobility-limited conditions, the ratio of j_e to j_+ must alter as we cross the system, having its greatest value at the point where the net negative space charge is greatest, and its smallest value at the point where the net positive space charge is greatest, and it is difficult to see how such a situation can be brought about, as it does not seem to be possible to satisfy current continuity and particle conservation requirements simultaneously. A possible explanation of this apparent anomaly is that the value of d is not great enough for

THE STRUCTURE OF THE CONVENTIONAL HOT CATHODE ARC (VON ENGEL 1965)



all the ions and electrons to undergo collisions in the actual fall space, so that the conditions in the fall space are in fact somewhere in between true free-fall conditions and true mobility-limited conditions (1 in $\exp \frac{d}{\lambda}$ of the charged particles will have a free path that is greater than d , so that if d has a value of only a few mean free paths, the number of particles crossing the fall space without collision will be quite large). Because of this uncertainty about the conditions that prevail in the fall space, the author has come to the conclusion that it is not possible to give an accurate quantitative description of the mechanisms that operate in the fall space of the discharge under study, or to give definite answers to the questions that are listed at the beginning of this section. The best that we can do is set up a very rough model of the cathode fall region - a model that will at least enable us to give approximate answers to some of the questions - and this will be done in the next section.

18.6 A MODEL OF THE CATHODE FALL REGION OF THE DIFFUSE MODE.

In setting up a model of the cathode fall region of the discharge under study, we will make the following three assumptions. Firstly, we will assume that the fall space is bounded by a plane cathode on one side, and by a neutral plasma on the other. Secondly, we will assume that the fall space is a double space charge sheath in which the total net space charge is zero (the second part of this assumption is based on the fact that the

electric field in the positive column is so much smaller than the field in the fall space that it can be taken to be zero in comparison with the latter, since this is only possible if the net space charge in the fall space is zero). Thirdly, we will assume that the values of the electric field and electric potential can be calculated using Poisson's equation.

Let us suppose that the space charge distribution in the fall space is symmetrical, and that the net space charge ρ is roughly given by

$$\rho = e (n_+ - n_e) = A \sin \left(\frac{\pi x}{d} - \frac{\pi}{2} \right) \quad \text{18.16}$$

where d is the width of the cathode fall region, x is the distance from the cathode, and A is an empirical constant. The net positive charge between $x = \frac{d}{2}$ and $x = d$ is equal to

$$\begin{aligned} & \int_{\frac{d}{2}}^d A \sin \left(\frac{\pi x}{d} - \frac{\pi}{2} \right) dx \\ &= -\frac{d}{\pi} A \cos \left(\frac{\pi}{d} x - \frac{\pi}{2} \right) \Big|_{\frac{d}{2}}^d \\ &= \frac{d}{\pi} A \quad \text{18.17} \end{aligned}$$

and the net negative charge between $x = 0$ and $x = \frac{d}{2}$ clearly has the same numerical value.

The value of the electric field X also varies sinusoidally between $x = 0$ and $x = d$, being equal to zero at both these values of x and rising to a maximum value at $x = \frac{d}{2}$. Using Gauss's law, the maximum value of the field can be shown to be equal to $-4Ad$ e.s.u., with the general value of X being given by

$$X = -4Ad \sin \frac{\pi x}{d} \quad \text{18.18}$$

The electric potential can be found by integrating this equation, so that

$$V = -\frac{4Ad^2}{\pi} \cos \frac{\pi x}{d} + \text{const} \quad 18.19$$

The constant of integration can be evaluated by taking $V = 0$ at $x = 0$, and the resulting equation for V is

$$V = \frac{4Ad^2}{\pi} \left(1 - \cos \frac{\pi x}{d}\right) \quad 18.20$$

Thus, we see that the value of the cathode fall is given by

$$V_c = \frac{8Ad^2}{\pi} \quad 18.21$$

so that

$$A = \frac{\pi V_c}{8d^2} \quad 18.22$$

Before we can use eqn. 18.22 to calculate A , we need to know the values of V_c and d . The former can be directly measured, but it is not possible to determine the value of the latter with any accuracy, since d is too small to be measured experimentally using a probe, and the uncertainty about the conditions that prevail in the cathode fall space precludes our determining its value by theoretical methods. We can, however, set rough upper and lower limits to the value of d by stating that it must be lower than 5×10^{-2} cm (the limiting accuracy of probe measurements) and higher than the value of the electronic mean free path in the particular mixture. Since λ generally has a value of the order of $10^{-4} - 10^{-3}$ cm, we can say that d probably has a value of the order of $10^{-3} - 10^{-2}$ cm. Since V_c generally lies in the range from 1 - 10 volts, we can conclude that A has a value of the order of $4 \times 10^3 - 4 \times 10^6$ e.s.u., so that the maximum value of $|n_+ - n_c|$

is of the order of $3 \times 10^{10} - 3 \times 10^{13} \text{ cm}^{-3}$. This is perfectly feasible, since the values of n_e and n_+ in the positive column are of the order of $10^{14} - 10^{15} \text{ cm}^{-3}$, and we would expect the values in the negative glow plasma to be of the same order. It is interesting to note that if we take d to be of the order of $10^{-3} - 10^{-2} \text{ cm}$, the peak value of the electric field in the cathode fall space turns out to be two or three orders of magnitude greater than the value of the positive column field, thus justifying our neglecting the latter in setting up our model of the fall space.

We see from the above discussion that we have now succeeded in giving answers - albeit very approximate answers - to the first three of the five questions that were listed at the beginning of section 18.5. We have not been able to answer the last two questions at all, however, and the author does not believe that it is possible to do so at the present time, since the theory of the cathode mechanisms of discharges in which the flow of ions and electrons is limited by mobility considerations is still in a relatively primitive state. Indeed, the same can be said for the theory of the cathode mechanisms of most types of gas discharge, including such well-known forms as the low-pressure glow and thermionic arc. This highly unsatisfactory situation is largely due to the fact that we do not fully understand the basic microscopic processes that operate in the cathode regions of gas discharges, and **until** we do so, there is little hope of our developing a satisfactory quantitative theory of the cathode regions of even

the simpler forms of gas discharge, let alone highly complicated discharges like the one that is the subject of this thesis.

18.7 DISCUSSION OF THE EXPERIMENTAL CATHODE FALL RESULTS.

Because of our failure to give a satisfactory theoretical description of the cathode regions of the discharge under study or to derive a formula for the cathode fall voltage drop, it is clearly not possible for us to give a quantitative discussion of the experimental cathode fall results that were given in Chapter 7. We will now give a brief summary of the main features of these results, however, and will then see to what extent they can be qualitatively explained using the rough theory that has been built up in this chapter.

Summary of experimental cathode fall results.

1. For all the seed-diluent mixtures used and for all the experimental conditions studied, the cathode fall increases steadily as the discharge current rises, a log-log plot of cathode fall against current being roughly linear, with a slope of roughly 0.2 - 0.5 (see figure 7.1).
2. With potassium as seed, the cathode fall decreases steadily as the seed pressure rises, reaches a minimum, then rises slowly (see figures 7.2, 7.3, 7.4). With caesium as seed, the minimum is not observed, and the variation of the cathode fall is not nearly so marked as in the potassium case (see figures 7.3, 7.4).
3. The cathode fall is virtually independent of the ambient temperature at high temperatures, but rises sharply when the temperature falls below a critical value that depends on the nature

of the seed-diluent mixture (see figures 7.5 - 7.8).

4. The cathode fall depends strongly on the choice of seed, sodium-seeded mixtures having much higher values than potassium-seeded mixtures, and caesium-seeded mixtures having the lowest values of all (see figures 7.1, 7.3, 7.4, 7.7, 7.8).

5. The cathode fall does not appear to depend strongly on the choice of diluent gas, except at low temperatures and seed pressures, when helium-diluted mixtures have higher values than argon-diluted mixtures (see figures 7.1, 7.3, 7.7).

6. The addition of a small amount of molecular impurity causes the cathode fall to rise, roughly 2% of O_2 or N_2 being needed to double its value (see figure 7.9).

Let us now examine these points in turn.

1. The fact that a log-log plot of cathode fall against current is linear and has a positive slope tells us that the relationship between V_c and i is roughly of the form

$$V_c = \text{const. } i^m \quad \text{-----} \quad 18.23$$

where m has a value of roughly 0.2 - 0.5. We do not know enough about the structure or thickness of the cathode fall region to explain this result, but the general form of the relationship is similar to that which exists in the case of conventional space charge sheaths (see section 18.4). The low value of m suggests that the thickness of the cathode fall space decreases steadily as i rises, but it is not possible to be certain of this.

2. The fact that the cathode fall increases as the seed pressure falls to low values is probably partly due to the fact that the efficiency of the ionisation process in the negative glow plasma decreases as the number density of seed atoms falls, since the probability of an electron hitting a seed atom falls as the seed number density falls. The high cathode fall and low sheath stability that are observed at moderately-low sodium pressures and very low potassium pressures are probably partly due to the fact that the effective work function of the electrode surface is higher than it is at high seed pressures, so that the emission of electrons has to be enhanced by positive ion bombardment of the cathode surface. The high work function is probably due to the fact that the temperature at which the alkali metal coating starts to boil off the electrode surface falls as the seed pressure falls (see section 18.3); if Langmuir S curves were available for the alkali metals on stainless steel, we would be able to discuss this in more detail. The author is unable to offer an explanation of the rise in the cathode fall that occurs at very high potassium pressures.

3. The plots of cathode fall against ambient temperature that are given in figures 7.5 - 7.8 are very interesting indeed, and tend to support the theory of the cathode mechanism that has been built up in this chapter. The fact that the cathode fall is independent of the ambient temperature at high temperatures can be explained by Sakuntala's theory of the cathode mechanism, which postulates that the current density being drawn from the

cathode surface is less than the maximum possible thermionic emission current density at high temperatures, and that the current is limited by space charge effects in the cathode fall space rather than by the efficiency of the emission process (Sakuntala 1964, 1965B). The fact that the cathode fall begins to rise when the ambient temperature falls below a certain critical value can also be explained by Sakuntala's theory, which postulates that the emission process has to be assisted by positive ion bombardment of the cathode surface once the temperature falls below the value at which the thermionic emission current density equals the required current density. The lower the temperature, the greater is the extent to which positive ion bombardment has to assist the emission process, and the greater is the value of the cathode fall. The method by which the positive ion bombardment enhances the emission process is not known for certain, but Sakuntala (1964, 1965B) believes that it is by heating the cathode surface above the ambient value, and the work of the author tends to corroborate this hypothesis.

The above theory is supported by the fact that the critical temperature below which the cathode fall begins to rise corresponds closely to the temperature below which the breakdown voltage begins to rise. This was discussed in section 9.4.

4. One of the most striking features of the author's cathode fall results is the fact that the value of the cathode fall depends strongly on the choice of seed metal. The author believes that this is due to the different ionisation potentials of the

alkali metals (sodium - 5.09V, potassium - 4.32V, caesium - 3.86V). We have seen in section 18.2 that the existence of a highly-ionised plasma that covers the emitting area of the cathode surface appears to be vital for the existence of the discharge, and that the ionisation of the seed atoms in this plasma appears to be produced by high energy electrons that have been accelerated across the cathode fall space. Although the mechanism by which this ionisation process operates is not yet fully understood, it seems reasonable to suggest that the value of the cathode fall voltage drop is partly determined by the ease with which the seed atoms can be ionised, and to explain the fact that sodium-seeded plasmas require higher cathode falls than potassium-seeded plasmas, which, in turn, require higher cathode falls than caesium-seeded plasmas by the fact that the rate at which a given alkali metal can be ionised depends exponentially on the reciprocal of its ionisation potential.

Another striking feature of the cathode fall results is the fact that the critical temperature below which the cathode fall starts to rise depends strongly on the choice of seed (see figure 7.8). We see from this figure, which shows plots of cathode fall against ambient temperature for 3.5 torr seed pressure in atmospheric-pressure argon, that the critical temperature is about 900°C with sodium as seed, about 700°C with potassium as seed, and about 600°C with caesium as seed. These results can be explained by postulating that the effective work function of sodium on stainless steel is considerably higher than that of

potassium on stainless steel, which is itself higher than that of caesium on stainless steel. This hypothesis also explains the fact that the diffuse mode of the discharge is much less stable in sodium-seeded mixtures than in potassium-seeded mixtures, while caesium-seeded mixtures are the most stable of all (see section 7.2).

5. The author is unable to offer an explanation of the fact that the cathode fall appears to be virtually independent of the choice of diluent gas at high temperatures and seed pressures. If the movement of charged particles through the cathode fall space is indeed restricted by mobility considerations as well as by space charge, we would expect helium-diluted mixtures to require higher cathode fall values than argon-diluted mixtures, but this effect is only observed at low temperatures and seed pressures (see figures 7.3, 7.7).

6. The author is unable to explain the significant increase in the cathode fall that is produced by the addition of a small amount of molecular impurity to the seed-diluent mixture.

CONCLUSION.

Having completed our discussion of the experimental results, we will now discuss the significance of the work that is described in this thesis, and will do so from two points of view, namely, from the point of view of its intrinsic scientific interest, and from the point of view of its practical applications in the closed-cycle MHD field. We will then conclude the thesis by suggesting some of the ways in which the work could be extended in the future.

The intrinsic scientific importance of the work.

The author believes that the most significant parts of his work are those which deal with the breakdown of the gas and the positive column of the discharge, with the latter being the more important. In both cases, a large body of original experimental data has been provided, and a theory that is capable of giving a fairly satisfactory explanation of most features of this data has been developed.

In the case of the work on the breakdown of the gas, the author has shown how the breakdown voltage of seeded rare gases depends on the electrode spacing, seed pressure, gas temperature, choice of seed metal and choice of diluent gas, and has also deduced a semi-empirical formula that relates the value of the breakdown voltage to the experimental conditions. This formula, which is based on Sakuntala's theory of the breakdown mechanism (Sakuntala 1965), has been shown to be capable of giving at least

a qualitative explanation of most features of the author's experimental results, thus providing strong evidence for the validity of Sakuntala's theory.

In the case of the work on the positive column of the discharge, a completely new form of column has been brought to light - a column that combines features that are normally only found in low-pressure discharges with properties that are generally associated with high-pressure thermal arcs, and which is therefore of great scientific interest. We have seen how the author has developed experimental techniques for measuring the electric field in the column and for measuring the column diameter, and how he has carried out a systematic investigation of the dependence of the column properties on the discharge current, seed pressure, ambient temperature, choice of seed metal and choice of diluent gas. We have also seen how the author has developed a comprehensive theory of constricted positive columns that combine a radially-varying gas temperature with an elevated electron temperature - a theory that is capable of explaining most features of his own experimental results. The main successes of this theory are its ability to explain the falling voltage-current characteristic of the positive column of the discharge under study, and its ability to give a fairly accurate description of the effect on the column properties of changing the diluent gas or seed metal.

Compared with his work on the breakdown of the gas and on the positive column, the author considers that his work on the cathode regions of the discharge has been a partial failure. A great deal of original experimental data has been obtained - data that shows how the cathode fall of the discharge depends on the current, seed pressure, ambient gas temperature, choice of seed metal and choice of diluent gas - but the author has not succeeded in developing a theory that is capable of giving anything more than a tentative explanation of a few features of this data.

The importance of the work in the closed-cycle MHD field.

The author's work on seeded rare gases had its origins in the search for a suitable gaseous conductor for a reactor-driven MHD generator, and although the research that is described in this thesis has tended to be more pure than applied, several features of the work have proved to be of practical importance in the MHD field.

1. The author's work has shown that caesium is only marginally superior to potassium as a potential seed for a practical MHD generator, a fact that could have considerable economic importance in view of the much lower cost of the latter.
2. The author's experimental results were the first to show that the optimum seed pressure in a nonequilibrium plasma is roughly an order of magnitude lower than the corresponding value for a plasma where the electron temperature equals the gas temperature. This result has proved to be in excellent agreement with the theoretical

work of Smith and Shair (1966), and could lead to further savings in seed costs if MHD ever becomes a practical proposition.

3. The author's work has shown that nonequilibrium discharges can tolerate relatively large amounts of molecular impurity, impurity levels of the order of a few percent being needed to produce any significant change in the discharge properties.

Some workers had thought that much smaller quantities than this might "poison" the discharge.

4. The author's experimental results were the first to show that helium-diluted mixtures require far higher electric fields than argon-diluted mixtures to support nonequilibrium conditions, and the author has shown that it may prove to be impracticable to operate an MHD generator at high helium pressures because of this fact.

5. The author's work provided Evans with the necessary data on which to base his highly-successful experiments on moving gases (Evans 1967), experiments that led to the construction of the first nonequilibrium MHD generator to produce significant power (Evans 1968). This is the most important application of the author's work to date, and is the application that has given the author by far the greatest satisfaction.

Suggestions for future work.

One of the chief drawbacks of the apparatus that was used to obtain the experimental data that is given in this thesis is the fact that it could only operate at atmospheric pressure; this meant that it was not possible to determine the dependence

of the properties of the discharge on the diluent pressure. The author now intends to extend his work to pressures of up to 10 atmospheres, and an apparatus that is capable of operating at such pressures is at present under construction. Using this apparatus, the author intends to determine whether or not his theoretical predictions about the dependence of the positive column properties on the diluent pressure are correct (see section 17.4). He also intends to study the effect on the breakdown voltage of raising the diluent pressure, and to determine whether his formula for the breakdown voltage is consistent with the results.

Other possible extensions of the author's work include the following.

1. The systematic study of the discharge that precedes the breakdown of the gas, and the measurement of the increase in the value of the first Townsend coefficient that takes place as breakdown is approached.
2. The development of spectroscopic techniques to measure the gas temperature and electron temperature in the positive column of the discharge and in the sheath of plasma that covers the cathode surface.
3. The determination of the effect on the positive column properties of varying the size of the tube that contains the electrode system.
4. The systematic study of the dependence on the ambient temperature and vapour pressure of the emission properties of a stainless steel surface that is partly covered by a layer of alkali metal.

5. The study of the effect on the cathode regions of the discharge of using different electrode geometries and different electrode materials.

REFERENCES.

- Ben Daniel, D.J. and Tamor, S., 1962, General Electric Research Lab. Report No. 62-RL-2922E.
- Ben Daniel, D.J. and Bishop, C.M., 1963, Phys. Fluids, vol. 6, no. 2, pp. 300-306.
- Bernard, E., et. al., 1966, Services de Physique Appliquee Report no. PA/1 Gn. RT/441.
- Cahn, J.H., 1949, Phys. Rev., vol. 75, no. 2, pp. 293-300.
- Champion, K.S.W., 1952A, Proc. Phys. Soc., B.65, pp. 329-44.
- Champion, K.S.W., 1952B, Proc. Phys. Soc., B.65, pp. 345-56.
- Chapman, S. and Cowling, T.G., 1958, "The mathematical theory of non-uniform gases" (Cambridge University Press-New York) 2nd ed.
- Child, C.D., 1911, Phys. Rev., vol. 32, p. 492.
- Chu, T.K. and Gottschlich, C.F., 1968, A.I.A.A.J., vol. 6, no. 1, pp. 114-119.
- Clausius, R., 1889, "Die Kinetische Theorie der Gas".
- Cobine, J.D., 1958, "Gaseous Conductors", (Dover Pub. Inc. - New York).
- Cool, T.A. and Zukoski, E.E., 1966, Phys. Fluids, vol. 6, pp. 780-96.
- Coombe, R.A., 1964, "Magnetohydrodynamic Generation of Electric Power", (Chapman and Hall) pp. 1-33.
- Compton, K.T. and Langmuir, I., 1930, Rev. Mod. Phys., vol. 2, no. 2, pp. 123-242.
- Compton, K.T., 1927, A.I.E.E. Trans., vol. 46, pp. 868-83.
- Corliss, C.H. and Bozman, W.R., 1962, Nat. Bureau of Standards Monograph 53.
- Dunn, P.D., et. al., 1962, Proc. I. Mech. Eng., vol. 176, pp. 421-440.
- Dunn, P.D., 1964, "Magnetohydrodynamic Generation of Electric Power", (Chapman and Hall), pp. 176-97.

- Dushman, S., 1923, Phys. Rev., vol. 21, p. 623.
- Dushman, S., 1930, Rev. Mod. Phys., vol. 2, p. 458.
- Elenbaas, W., 1951, "The high-pressure mercury vapour discharge",
(North Holland Pub. Co. - Amsterdam).
- Ellington, H.I., 1964, U.K.A.E.A. Res. Grp. Report no. A.E.R.E. M.1474.
- Ellington, H.I., 1965A, U.K.A.E.A. Res. Grp. Report no. A.E.R.E. M.1545.
- Ellington, H.I., 1965B, U.K.A.E.A. Res. Grp. Report no. A.E.R.E. M.1597.
- Ellington, H.I., 1965C, U.K.A.E.A. Res. Grp. Report no. A.E.R.E. M.1616.
- Ellington, H.I. and Ralph, J.C., 1966, "Electricity from MHD",
(I.A.E.A. - Vienna), pp. 17-27.
- Ellington, H.I., 1967, Brit. J. Appl. Phys., vol. 18, pp.931-37.
- Ellington, H.I., 1968A, Brit. J. Appl. Phys., Series 2, vol. 1,
pp. 49-53.
- Ellington, H.I., 1968B, Brit. J. Appl. Phys., Series 2, vol. 1,
pp. 189-192.
- Ellington, H.I., 1968C, Brit. J. Appl. Phys., Series 2, vol. 1,
pp. 1082-84.
- Ellington, H.I., 1969, Brit. J. Appl. Phys., Series 2, vol. 2,
pp. 65-69.
- von Engel, A., 1965, "Ionised Gases", (Clarendon Press - Oxford),
2nd ed.
- Evans, N.A., 1967, A.I.A.A.J., vol. 5, no. 10, pp. 1908-10.
- Evans, N.A., 1968, A.I.A.A.J., vol. 6, no. 3, pp. 394-400.
- Francis, V.J., 1946, Phil. Mag., vol. 37, pp. 433-53 and 653-73.
- Francis, V.J., 1949, Phil. Mag., vol. 40, pp. 435-48 and 1063.
- Frost, L.S., 1961, J. Appl. Phys., vol. 32, pp. 2029-36.
- George, D.W., 1963, Proc. I.E.E., vol. 110, no. 11, pp. 2063-72.
- George, D.W., 1964, Proc. I.E.E., vol. 111, no. 9, pp. 1619-24.
- George, D.W. 1965, Brit. J. Appl. Phys., vol. 16, pp. 1105-11.

- Gyftopoulos, E.P. and Levine, J.D., 1962, J.A.P., vol. 33, no. 1, pp. 67-73.
- Harris, L.P., 1963A, General Electric Research Lab. Report no. 63-RL-3278G.
- Harris, L.P., 1963B, General Electric Research Lab. Report no. 63-RL-3334G.
- Herbert, R., "New Scientist", 12th April, 1962.
- Höcker, K.H. and Finkelburg, W., 1946, Z. Naturforsch, vol. 1, pp. 305-10.
- Holm, R. and Lotz, A., 1934, Miss Veroff, Siemens, K.XIII, vol. 2, p. 87.
- Holstein, T., 1951, Phys. Rev., vol. 83, pp. 1159-68.
- ter Horst, D.Th.J. and Pflanz, H.M., 1967, Zeitschrift für Physik vol. 198, pp. 508-26.
- Hurwitz, H., Sutton, G.W. and Tamor, S., 1962, A.R.S. Journal, pp. 1237-43.
- Ivey, H.F., 1954, Adv. Electronics, vol. 6, pp. 137-256.
- Karlowitz, et. al., 1940, U.S. Patent 2, 210, 918.
- Kerrebrock, J.L., 1962, "Engineering Aspects of MHD", (Mannell and Mather - Columbia Univ. Press), pp. 327-346.
- Kerrebrock, J.L., 1964, A.I.A.A.J., vol. 2, no. 6, pp. 1072-80.
- Kerrebrock, J.L. and Hoffman, M.A., 1964, A.I.A.A.J., vol. 2, no. 6, pp. 1080-87.
- Kerrebrock, J.L., 1965, A.I.A.A.J., vol. 3, no. 4, pp. 591-601.
- Labois, E. and Lemaire, A., 1964, "Magnetohydrodynamic Electrical Power Generation", Proc. MHD Symp., Paris 1964.
- Labois, E. and Ricateax, P., 1965, Proc. Symp. on Low-Temp. Plasmas, 20th Congress on Theoretical and Applied Chemistry, Moscow.
- Langevin, P., 1905, Ann. de Chim. et de Phys., vol. 5, pp. 245-88.
- Langmuir, I. and Kingdon, K.H., 1923, "Science", vol. 57, p. 58
- Langmuir, I., 1929, Phys. Rev., vol. 33, pp. 954-989.

- Langmuir, I. and Taylor, J., 1933, Phys. Rev., vol. 44, p. 423.
- Linn, I., Resler and Kantrowitz, 1955, J. Appl. Phys., vol. 26, no. 1, pp. 95-109.
- Lindemann, F.A., 1919, Phil. Mag., vol. 38, pp. 669-684.
- Loeb, L.B., 1961, "Basic Processes of Gaseous Electronics", (Univ. of Calif. Press - Berkeley and Los Angeles).
- Lutz, M.A., 1963, Avco-Everett Res. Report, 175, ESD-TDR-64-6.
- Lutz, M.A., 1967, A.I.A.A.J., vol. 5, no. 8, pp. 1416-23.
- Lynch, R.H., 1967, J. Appl. Phys., vol. 38, no. 10, pp. 3965-68.
- Malter, L., Johnson, E.O. and Webster, W.M., 1951, R.C.A. Review, vol. 12, pp. 415-435.
- Margenau, H. and Hartman, L.M., 1948, Phys. Rev., vol. 73, pp. 209-15.
- Massey, J.T. and Cannon, S.M., 1965, J. Appl. Phys., vol. 36, no. 2, pp. 361-72.
- Massey, J.T., 1965, J. Appl. Phys., vol. 36, no. 2, pp. 373-80.
- Monti, R. and Napolitano, L.G., 1964A, Sixth Agard Combustion and Propulsion Colloquium, Cannes, I.A. Report no. 109.
- Monti, R. and Napolitano, L.G., 1964B, Proc. XVth Int. Astronautical Congress (Wersgawa), vol. 3, pp. 57-69.
- Morgulis, N.D. and Polushkin, I.N., 1966, Teplofizika Vysokikh Temperatur, vol. 4, no. 6, pp. 745-52.
- Nusselt, W. and Jürges, W., 1928, Zeit. V.D.J., vol. 72, pp. 597-604.
- Pinchak, A.C. and Zukoski, E.E., 1963, Proc. of 4th Symp. on Eng. Aspects of MHD, pp. 51-57 (Berkeley, California).
- Ralph, J.C., 1962, MHD Symp. Newcastle, later published in Inst. of Elect. Eng. Conf. Report Series no. 4, (Pub. 1963), pp. 115-18.
- Ralph, J.C., 1963, J. Appl. Phys., vol. 34, no. 8, pp. 2499-500.
- Ralph, J.C., 1964, "Magnetohydrodynamic Generation of Electrical Power", (Chapman and Hall), pp. 34-64.
- Ralph, J.C. and Bainton, K.F., 1966, "Electricity from MHD", (I.A.E.A. - Vienna), vol. 2, pp. 457-71.

- Rice, G. and Parsons, M.J., 1966, "Electricity from MHD",
(I.A.E.A. - Vienna), vol. 2, pp. 789-804.
- Rice, G., 1967, U.K.A.E.A. Res. Grp. Report no. A.E.R.E. R5030.
- Robben, F.A., 1962, Bull. Amer. Phys. Soc., vol. 7, no. 4, pp. 371-72.
- Rosa, R.J., 1961, Phys. Fluids, vol. 4, no. 2, pp. 182-194.
- Saha, M.N., 1920, Phil. Mag., vol. 40, pp. 472-488.
- Sakuntala, M., 1964, "Magnetohydrodynamic Electrical Power
Generation", Proc. of MHD Symp., Paris, vol. 1, pp. 263-77.
- Sakuntala, M., 1965A, Brit. J. Appl. Phys., vol. 16, pp. 821-32.
- Sakuntala, M., 1965B, U.K.A.E.A. Res. Grp. Report No. A.E.R.E. R.5107.
- Sakuntala, M., 1966, Brit. J. Appl. Phys., vol. 17, pp. 191-95.
- Shair, F.H., 1963, Proc. of 4th Symp. on Eng. Aspects of MHD,
(Univ. of Calif. - Berkeley), pp. 31-37.
- Shair, F.H., 1964, A.I.A.A.J., vol. 2, no. 11, pp. 1883-85.
- Sheindlin, A.E., Batenin, V.A. and Asinovsky, E.J., 1964,
"Magnetohydrodynamic Electrical Power Generation",
Proc. of MHD Symp., Paris, pp. 453-69.
- Smith, J.M., and Shair, F.H., 1966, Phys. Fluids, vol. 9, pp. 1615-17.
- Spitzer, L. and Härm, R., 1953, Phys. Rev., vol. 89, pp. 977-81.
- Sporn, P. and Kantrowitz., A., 1962, "Power", vol. 103, p. 62.
- Sugawara, M., 1967, Phys. Letters, vol. 25A, no. 2, pp. 154-55.
- Suits, C.G., and Poritsky, H., 1939, Phys. Rev., vol. 55, pp. 1184-91.
- Suits, C.G., 1939A, Phys. Rev. vol. 55, pp. 198-201.
- Suits, C.G., 1939B, Phys. Rev., vol. 55, pp. 561-67.
- Suits, C.G., 1939C, J. Appl. Phys., vol. 10, p. 730.
- Svehla, R.A., 1962, N.A.S.A. Technical Report no. R-132.
- Thring, M.W., 1965, "Survey of MHD Research", Direct Current,
vol. 10, no. 1.
- Tonks, L. and Langmuir, I., 1929, Phys. Rev., vol. 34, pp. 876-922.

- Uhlenbusch, J., 1962, Doctoral Thesis, Univ. of Aachen.
- Westendorp, W.F. et. al., 1961, Phys. Fluids, vol. 4, p. 786.
- Wilson, V.C., 1959, J. Appl. Phys., vol. 30, no. 4, pp. 475-81.
- Zimin, E.P. and Popov, V.A., 1964, "Magnetohydrodynamic Electrical Power Generation", Proc. of MHD Symp., Paris, vol. 1, pp. 319-38.
- Zukoski, E.E., Cool, T.A. and Gibson, E.G., 1963, Karman Lab. of Fluid Mechanics and Jet Prop., Final Report, Grant AR-AROSR-160-63, Calif. Inst. of Tech.